

U.S. Army Coast. Eng. Res. Ctr. TP

TP 77-11

# Forces Exerted by Waves on a Pipeline At or Near the Ocean Bottom

by

George L. Bowie

TECHNICAL PAPER NO. 77-11  
OCTOBER 1977



DAVIDSON CENTER ARCHIVES  
1000 North 3rd Street  
Fort Belvoir, VA 22060

Approved for public release;  
distribution unlimited.

Prepared for  
**U.S. ARMY, CORPS OF ENGINEERS  
COASTAL ENGINEERING  
RESEARCH CENTER**

Kingman Building  
Fort Belvoir, Va. 22060

Q-B  
450  
.74  
no 77-11

Reprint or republication of any of this material shall give appropriate credit to the U.S. Army Coastal Engineering Research Center.

Limited free distribution within the United States of single copies of this publication has been made by this Center. Additional copies are available from:

*National Technical Information Service  
ATTN: Operations Division  
5285 Port Royal Road  
Springfield, Virginia 22151*

Contents of this report are not to be used for advertising, publication, or promotional purposes. Citation of trade names does not constitute an official endorsement or approval of the use of such commercial products.

The findings in this report are not to be construed as an official Department of the Army position unless so designated by other authorized documents.



REPORT DOCUMENTATION PAGE		READ INSTRUCTIONS BEFORE COMPLETING FORM
1. REPORT NUMBER TP 77-11	2. GOVT ACCESSION NO.	3. RECIPIENT'S CATALOG NUMBER
4. TITLE (and Subtitle)  FORCES EXERTED BY WAVES ON A PIPELINE AT OR NEAR THE OCEAN BOTTOM		5. TYPE OF REPORT & PERIOD COVERED Technical Paper
		6. PERFORMING ORG. REPORT NUMBER Technical Report HEL 9-24
7. AUTHOR(s)  George L. Bowie		8. CONTRACT OR GRANT NUMBER(s)  DACW72-74-C-0004
9. PERFORMING ORGANIZATION NAME AND ADDRESS University of California Hydraulic Engineering Laboratory Berkeley, California 94720		10. PROGRAM ELEMENT, PROJECT, TASK AREA & WORK UNIT NUMBERS  F31234
11. CONTROLLING OFFICE NAME AND ADDRESS Department of the Army Coastal Engineering Research Center (CEREN-DE) Kingman Building, Fort Belvoir, Virginia 22060		12. REPORT DATE October 1977
		13. NUMBER OF PAGES 177
14. MONITORING AGENCY NAME & ADDRESS (If different from Controlling Office)		15. SECURITY CLASS. (of this report)  UNCLASSIFIED
		15a. DECLASSIFICATION/DOWNGRADING SCHEDULE
16. DISTRIBUTION STATEMENT (of this Report)  Approved for public release; distribution unlimited.		
17. DISTRIBUTION STATEMENT (of the abstract entered in Block 20, if different from Report)		
18. SUPPLEMENTARY NOTES		
19. KEY WORDS (Continue on reverse side if necessary and identify by block number)  Submarine pipeline Two- and three-dimensional experiments Wave force analysis Wave-induced lift forces		
20. ABSTRACT (Continue on reverse side if necessary and identify by block number)  The wave-induced forces on a submarine pipeline near the ocean floor consist of several components--inertial forces, drag forces, lift forces, and under some conditions, eddy-induced forces. For a pipeline touching the bottom, or at a small clearance above the bottom, the lift force is the predominant force in the vertical direction. This force is generally expressed as $F_L = 1/2 C_L \rho A u^2$ , and is added as a lift term to the Morison equation.  (Continued)		

The experimental results of this investigation, however, show that this steady-flow lift model is inadequate for wave-induced oscillatory flows. For pipelines at small clearances above the bottom, viscous effects near the bottom clearance constriction may result in lift forces acting in both the upward and downward directions during different parts of the wave cycle. In addition, the maximum positive and negative lift forces may not correspond to the positions of maximum horizontal velocities in the wave cycle.

A modified lift force model of the form,  $F_L = 1/2 C_L \rho A u_{\max}^2 [\cos^2(\theta - \phi) - k]$ , is proposed where the parameters,  $C_L$ ,  $\phi$ , and  $k$ , may vary accordingly to allow adequate description of all characteristics of the lift force phenomenon. Quantitative relationships between these unknown lift force parameters and various dimensionless parameters defining the wave and pipe conditions were found. These relationships exhibited good correlation for all wave conditions, bottom clearances, pipe diameters, and orientation angles.

## PREFACE

This report is published to provide coastal engineers with an analysis of wave-induced forces on a submarine pipeline near the ocean floor. The work was carried out under the structural design program of the U.S. Army Coastal Engineering Research Center (CERC).

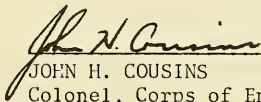
The report was prepared by George L. Bowie, Research Assistant, University of California, Berkeley, under CERC Contract No. DACW72-74-C-0004.

The author acknowledges the help and advice of Professor R.L. Wiegel, Professor J.W. Johnson, and Dr. J.D. Cumming, throughout different stages of the project. Many thanks also go to Dr. M.F. Al-Kazily, J. Allison, and L. Magel for their help in designing and setting up the instrumentation for the experiments, and to W. Krogmoe, E. Parscale, and W. Matthew for their skillful assistance in building the models.

Dr. J.R. Weggel was the CERC contract monitor, under the general supervision of G.M. Watts, Chief, Engineering Development Division.

Comments on this publication are invited.

Approved for publication in accordance with Public Law 166, 79th Congress, approved 31 July 1945, as supplemented by Public Law 172, 88th Congress, approved 7 November 1963.

  
\_\_\_\_\_  
JOHN H. COUSINS  
Colonel, Corps of Engineers  
Commander and Director

CONTENTS

	Page
CONVERSION FACTORS, U.S. CUSTOMARY TO METRIC (SI) . . . . .	9
SYMBOLS AND DEFINITIONS . . . . .	10
I WAVE FORCE ANALYSIS . . . . .	17
1. Wave Force Components on Pipelines	
Near the Bottom . . . . .	17
2. Wave-Induced Lift Forces . . . . .	19
3. Model for Wave-Induced Lift Forces . . . . .	26
4. Extension of Model to Higher Order Theories . . . . .	32
II EXPERIMENTAL INVESTIGATION . . . . .	36
1. Experimental Equipment . . . . .	36
2. Procedure for Two-Dimensional Experiments . . . . .	45
3. Procedure for Three-Dimensional Experiments . . . . .	51
4. Data Reduction . . . . .	53
III RESULTS AND DISCUSSION . . . . .	58
1. Resultant Force Through Wave Cycle . . . . .	58
2. Orientation Angle Considerations . . . . .	75
3. Interrelationships Between $C_L$ , $\phi$ , and $k$ . . . . .	77
4. Relationships Between $\phi$ and $k$ and Parameters	
Defining the Wave and Pipeline Conditions . . . . .	89
5. Relationships Between $\phi$ (clear/Dia) and $k$ (clear/Dia)	
and Parameters Defining the Wave and Pipeline	
Conditions . . . . .	104
6. Relationships Between the Coefficients of Lift and	
Parameters Defining the Wave and Pipeline Conditions . . . . .	109
7. Relationships Between the Lift Forces and Parameters	
Defining the Wave and Pipeline Conditions . . . . .	109
8. Relationships Involving the Vertical Coefficients	
of Mass and Drag and the Vertical Inertial and	
Drag Forces . . . . .	111
9. Relationships Between the Horizontal Coefficient of	
Mass and Parameters Describing the Wave and	
Pipeline Conditions . . . . .	111
10. Relationships Involving the Horizontal Coefficient	
of Drag . . . . .	113
11. Example Problems . . . . .	113
IV CONCLUSIONS . . . . .	117
V RECOMMENDATIONS FOR FURTHER RESEARCH . . . . .	121
LITERATURE CITED . . . . .	123

CONTENTS

APPENDIX	Page
A	LEAST SQUARES ANALYSIS OF EXPERIMENTAL DATA . . . . . 125
B	COMPUTER PROGRAM FOR VERTICAL LEAST SQUARES ANALYSIS (TWO-DIMENSIONAL DATA) . . . . . 140
C	COMPUTER PROGRAM FOR VERTICAL LEAST SQUARES ANALYSIS (THREE-DIMENSIONAL DATA) . . . . . 144
D	COMPUTER PROGRAM FOR HORIZONTAL LEAST SQUARES ANALYSIS (TWO-DIMENSIONAL DATA) . . . . . 149
E	TABULATED VERTICAL FORCE DATA FROM TWO-DIMENSIONAL EXPERIMENTS . . . . . 153
F	TABULATED VERTICAL FORCE DATA FROM THREE-DIMENSIONAL EXPERIMENTS . . . . . 158
G	TABULATED HORIZONTAL FORCE DATA FROM TWO-DIMENSIONAL EXPERIMENTS . . . . . 176

TABLE

Estimated accuracy of experimental measurements . . . . .	59
-----------------------------------------------------------	----

FIGURES

1 Change in lift with increasing velocity . . . . .	21
2 Change in lift force with passing wave crest . . . . .	23
3 Lift force phenomenon . . . . .	25
4 Change in lift force record for increasing bottom clearance . . . . .	27
5 Definition sketch . . . . .	29
6 Definition of lift force parameters . . . . .	31
7 Comparison of linear and Stokes' third-order theories: Simultaneous shift of lift force record as $\phi$ increases from $0^\circ$ to $90^\circ$ and $k$ increases from 0 to 1 with increasing bottom clearance . . . . .	34
8 Comparison of lift force extreme cases for linear and Stokes' third- order theories . . . . .	35
9 Force meter and support . . . . .	38

CONTENTS

FIGURES--Continued

Page

10	Four-inch cylinder mounted in the flume . . . . .	39
11	Test section (force meter) . . . . .	40
12	Test section mounted in position . . . . .	41
13	Test section and force transducer . . . . .	42
14	Schematic of pipeline model . . . . .	43
15	Pipeline model . . . . .	44
16	Brush recording instruments . . . . .	46
17	Digitizer and recording instruments . . . . .	47
18	Calibration method for two-dimensional experiments . . . . .	48
19	Experimental arrangement for two-dimensional tests . . . . .	49
20	Calibration method for three-dimensional experiments . . . . .	52
21	Experimental arrangement for three-dimensional tests . . . . .	54
22	Definition sketch for three-dimensional experiments . . . . .	55
23	Example of data record . . . . .	57
24	Example of computer output for vertical least squares analysis . . . . .	60
25	Example of computer output for horizontal least squares analysis . . . . .	61
26	Resultant force through wave cycle for 0.001-foot clearance, 1.85-second period, and 0.24-foot height . . . . .	62
27	Resultant force through wave cycle for 1/16-inch clearance, 1.86-second period, and 0.24 foot height . . . . .	63
28	Resultant force through wave cycle for 1/8-inch clearance, 1.85-second period, and 0.25-foot height . . . . .	64
29	Resultant force through wave cycle for 3/16-inch clearance, 1.85-second period, and 0.25-foot height . . . . .	65



CONTENTS

FIGURES--Continued

		Page
30	Resultant force through wave cycle for 1/4-inch clearance, 1.86-second period, and 0.25-foot height . . . . .	66
31	Resultant force through wave cycle for 1-inch clearance, 1.86-second period, and 0.24-foot height . . . . .	67
32	Resultant force through wave cycle for 2-inch clearance, 1.86-second period, and 0.25-foot height . . . . .	68
33	Change in resultant force with increasing clearance . . . . .	69
34	Resultant force through wave cycle for 1-inch clearance, 1.23-second period, and 0.3-foot height . . . . .	71
35	Resultant force through wave cycle for 0.001-foot clearance, 0.95-second period, and 0.24-foot height . . . . .	72
36	Resultant force through wave cycle for 1/16-inch clearance, 0.95-second period, and 0.24-foot height . . . . .	73
37	Resultant force through wave cycle for 2-inch clearance, 0.96-second period, and 0.25-foot height . . . . .	74
38	Alternative approaches for handling pipeline orientation angles . .	76
39	$\phi$ versus $k$ . . . . .	78
40	$C_L$ versus $k$ . . . . .	79
41	$C_L$ versus $\phi$ . . . . .	80
42	Effective positive coefficient of lift versus $k$ . . . . .	82
43	Effective positive coefficient of lift versus $\phi$ . . . . .	83
44	Effective negative coefficient of lift versus $k$ . . . . .	84
45	Effective negative coefficient of lift versus $\phi$ . . . . .	85
46	$C_L(1-k)$ or $C_L(k)$ versus $k$ . . . . .	88
47	$\phi$ versus $(\text{clear}/u_{\text{max}}T)$ for 4-inch diameter . . . . .	91
48	$\phi$ versus $(\text{clear}/u_{\text{max}}T)$ for 3-inch diameter . . . . .	92
49	$\phi$ versus $(\text{clear}/u_{\text{max}}T)$ for 2-inch diameter . . . . .	93

CONTENTS

FIGURES--Continued		Page
50	k versus $(\text{clear}/u_{\text{max}}T)$ for 4-inch diameter . . . . .	94
51	k versus $(\text{clear}/u_{\text{max}}T)$ for 3-inch diameter . . . . .	95
52	k versus $(\text{clear}/u_{\text{max}}T)$ for 2-inch diameter . . . . .	96
53	k versus $(u_{\text{max}}T/\text{Dia})$ . . . . .	98
54	$\phi$ versus $(u_{\text{max}}T/\text{Dia})$ . . . . .	99
55	k versus $(u_{\text{max}}\text{clear}/v)$ for 4-inch diameter . . . . .	100
56	$\phi$ versus $(u_{\text{max}}\text{clear}/v)$ for 4-inch diameter . . . . .	101
57	k versus $(\text{clear}/u_{\text{max}}T)(\text{Dia}/u_{\text{max}}T)$ . . . . .	102
58	$\phi$ versus $(\text{clear}/u_{\text{max}}T)(\text{Dia}/u_{\text{max}}T)$ . . . . .	103
59	$k(\text{clear}/\text{Dia})$ versus $(\text{clear}/u_{\text{max}}T)(\text{clear}/\text{Dia})$ . . . . .	105
60	$\phi(\text{clear}/\text{Dia})$ versus $(\text{clear}/u_{\text{max}}T)(\text{clear}/\text{Dia})$ . . . . .	106
61	$k(\text{clear}/\text{Dia})$ versus $\sqrt{\text{Dia}/u_{\text{max}}T}(\text{clear}/u_{\text{max}}T)(\text{clear}/\text{Dia})$ . . . . .	107
62	$\phi(\text{clear}/\text{Dia})$ versus $\sqrt{\text{Dia}/u_{\text{max}}T}(\text{clear}/u_{\text{max}}T)(\text{clear}/\text{Dia})$ . . . . .	108
63	Maximum lift force (positive or negative) versus the Reynolds number . . . . .	110
64	Comparison of the horizontal $C_M$ with potential flow theory for a flow with constant acceleration . . . . .	112
65	Horizontal $C_M$ versus $(\text{clear}/u_{\text{max}}T)$ . . . . .	114

CONVERSION FACTORS, U.S. CUSTOMARY TO METRIC (SI)  
UNITS OF MEASUREMENT

U.S. customary units of measurement used in this report can be converted to metric (SI) units as follows:

Multiply	by	To obtain
inches	25.4	millimeters
	2.54	centimeters
square inches	6.452	square centimeters
cubic inches	16.39	cubic centimeters
feet	30.48	centimeters
	0.3048	meters
square feet	0.0929	square meters
cubic feet	0.0283	cubic meters
yards	0.9144	meters
square yards	0.836	square meters
cubic yards	0.7646	cubic meters
miles	1.6093	kilometers
square miles	259.0	hectares
knots	1.8532	kilometers per hour
acres	0.4047	hectares
foot-pounds	1.3558	newton meters
millibars	$1.0197 \times 10^{-3}$	kilograms per square centimeter
ounces	28.35	grams
pounds	453.6	grams
	0.4536	kilograms
ton, long	1.0160	metric tons
ton, short	0.9072	metric tons
degrees (angle)	0.1745	radians
Fahrenheit degrees	5/9	Celsius degrees or Kelvins <sup>1</sup>

<sup>1</sup>To obtain Celsius (C) temperature readings from Fahrenheit (F) readings, use formula:  $C = (5/9) (F - 32)$ .

To obtain Kelvin (K) readings, use formula:  $K = (5/9) (F - 32) + 273.15$ .

SYMBOLS AND DEFINITIONS

A	projected area of pipe section
ANG	orientation angle with respect to wave crests
$C_D$	coefficient of drag
$C_L$	coefficient of lift
$C'_L$	coefficient of transverse force due to eddy shedding
clear	bottom clearance
$C_M$	coefficient of mass
d	stillwater depth
Dia	pipe diameter
F	total wave-induced force
$F_D$	drag force
$(F_D)_h$	horizontal component of drag force
$(F_D)_v$	vertical component of drag force
$F_h$	horizontal component of total wave force
$F_h(\theta_i)$	calculated horizontal force at position $\theta_i$ in wave cycle
$F_I$	inertial force
$(F_I)_h$	horizontal component of inertial force
$(F_I)_v$	vertical component of inertial force
$F_L$	lift force
$F'_L$	transverse "lift" force due to eddy shedding
$F_{oh}(\theta_i)$	observed horizontal force at position $\theta_i$ in wave cycle
$F_{ov}(\theta_i)$	observed vertical force at position $\theta_i$ in wave cycle
$F_v$	vertical component of total wave force
$F_v(\theta_i)$	calculated vertical force at position $\theta_i$ in wave cycle

SYMBOLS AND DEFINITIONS--Continued

H	wave height
k	negative fraction of lift force cycle
L	wavelength
T	wave period
t	time since last wave crest passed over center of pipe section
u	horizontal component of water particle velocity if pipeline was absent
$u_{max}$	maximum horizontal water particle velocity if pipeline was absent
V	volume of fluid displaced by pipe section
v	vertical component of water particle velocity if pipeline was absent
$v_{max}$	maximum vertical water particle velocity if pipeline was absent
z	vertical distance of center of pipe section above bottom
$\partial u/\partial t$	horizontal component of water particle acceleration if pipeline was absent
$\partial v/\partial t$	vertical component of water particle acceleration if pipeline was absent
$\theta$	$2\pi t/T$ = position of wave cycle over center of pipe section with respect to time
$\nu$	kinematic viscosity of fluid
$\rho$	mass density of fluid
$\phi$	phase shift of maximum lift forces with respect to wave cycle

Computer Programs

Input Parameters:

ANGLE	orientation angle
C	calibration factor for manual digitizer

SYMBOLS AND DEFINITIONS--Continued

CFD	downward force calibration factor
CFU	upward force calibration factor
CL	bottom clearance
DF	downward force calibration factor
DIA	pipe diameter
DN	negative wave (trough) calibration factor
FI(I)	wave force readings
FO	zero point of wave force record
HI(I)	wave surface readings
N	number of wave force readings
T	wave period
UF	upward force calibration factor
UP	positive wave (crest) calibration factor
WO	zero point of wave record
XC	length of pipe test section
XF	amplification factor for force record
XW	amplification factor for wave record
YI(I)	wave surface readings

Program Variables:

ANG	orientation angle (in radians)
ANGLE	orientation angle (in degrees)
CDH	horizontal coefficient of drag
CDV	vertical coefficient of drag
CL	bottom clearance

SYMBOLS AND DEFINITIONS--Continued

CLV	coefficient of lift (calculated using horizontal velocity in direction of wave advance and projected area in plane parallel to the pipeline axis)
CLVA	coefficient of lift (calculated using horizontal velocity in direction of wave advance and projected area in plane normal to the direction of wave advance)
CLVU	coefficient of lift (calculated using the component of the horizontal velocity in the direction perpendicular to the pipeline axis and the projected area in the plane parallel to the pipeline axis)
CMH	horizontal coefficient of mass
CMV	vertical coefficient of mass
D	stillwater depth
DIA	pipe diameter
FDH	$1/2 \rho A u_{\max}^2$
FDV	$1/2 \rho A v_{\max}^2$
FH(I)	calculated horizontal wave force
FI(I)	measured wave force readings (in grams for two-dimensional data; in 10-grams for three-dimensional data)
FLV	$1/2 \rho A u_{\max}^2$
FMAX	maximum positive wave force (measured)
FMH	$\rho V (\partial u / \partial t)_{\max}$
FMIN	maximum negative wave force (measured)
FMV	$\rho V (\partial v / \partial t)_{\max}$
FP(I)	measured wave force readings (in pounds)
FV(I)	calculated vertical wave force
H	wave height
HI(I)	wave surface profile readings

SYMBOLS AND DEFINITIONS--Continued

PHI	phase-shift parameter $\phi$ of modified lift force equation
PI	$\pi$
R	mass density of water
RES(I)	difference between measured wave force and calculated wave force
SF	wave force averaged through wave cycle
T	wave period
U	maximum horizontal water particle velocity
XC	length of pipe section
XK	parameter K of modified lift force equation
XL	wavelength
ZV	vertical distance from bottom to center of pipe section

Tabulated Experimental Data

ANG	orientation angle of pipeline with respect to wave crests
CDH	horizontal coefficient of drag
CDV	vertical coefficient of drag
CLER	bottom clearance
CLV	coefficient of lift (calculated using horizontal velocity in direction of wave advance and projected area in plane parallel to the pipeline axis)
CLVA	coefficient of lift (calculated using horizontal velocity in direction of wave advance and projected area in the plane normal to the direction of wave advance)
CLVU	coefficient of lift (calculated using the component of the horizontal velocity in the direction perpendicular to the pipeline axis and the projected area in the plane parallel to the pipeline axis)
CMH	horizontal coefficient of mass'



CMV	vertical coefficient of mass
DIA	pipe diameter
FAVG	average horizontal force (averaged over complete wave cycle)
H	wave height
K.	parameter k of modified lift force equation
L	wavelength
PHI	phase shift parameter $\phi$ of modified lift force equation
T	wave period
UMAX	maximum horizontal component of water particle velocity at center of pipe section if absent



FORCES EXERTED BY WAVES ON A PIPELINE  
AT OR NEAR THE OCEAN BOTTOM

by  
George L. Bowie

I. WAVE FORCE ANALYSIS

1. Wave Force Components on Pipelines Near the Bottom.

The most common method of analyzing wave forces on pipelines is the application of the Morison equation (Morison, et al., 1950). Using this approach, the total wave-induced force on a pipeline can be broken into several components, depending on whether the components are due to the water particle velocities or accelerations. These force components can, in turn, be separated into horizontal and vertical components by using the horizontal and vertical components of the water particle velocities and accelerations in their respective force equations. Where there is no lift effect and no eddy-induced forces, the vertical component,  $F_v$ , of the total wave force is

$$F_v = (F_I)_v + (F_D)_v = C_M \rho V \frac{\partial v}{\partial t} + 1/2 C_D \rho A v |v| \quad (1)$$

and the horizontal component,  $F_h$ , is

$$F_h = (F_I)_h + (F_D)_h = C_M \rho V \frac{\partial u}{\partial t} + 1/2 C_D \rho A u |u|, \quad (2)$$

where

- $(F_I)_v$  = vertical component of inertial force
- $(F_I)_h$  = horizontal component of inertial force
- $(F_D)_v$  = vertical component of drag force
- $(F_D)_h$  = horizontal component of drag force
- $v$  = vertical component of water particle velocity if pipeline was absent
- $u$  = horizontal component of the water particle velocity if pipeline was absent
- $\frac{\partial v}{\partial t}$  = vertical component of water particle acceleration if pipeline was absent

$\frac{\partial u}{\partial t}$	=	horizontal component of water particle acceleration if pipeline was absent
A	=	projected area of pipe section
V	=	volume of fluid displaced by pipe section
$\rho$	=	mass density of fluid
$C_M$	=	coefficient of mass
$C_D$	=	coefficient of drag

For a pipeline located near the ocean bottom, the water particle orbits are flattened parallel to the boundary. Assuming a horizontal bottom, the vertical motions of the water particles are small in comparison to the horizontal motions, especially in shallow-water depths relative to the wavelength. As a result, the vertical components of the water particle velocities and accelerations are much smaller than the horizontal components, and correspondingly the vertical components of the drag and inertial forces will be smaller than the analogous horizontal forces.

Since the water particles at the bottom are effectively oscillating in a horizontal plane, the vertical excursions of the water particles will generally be less than the diameter of a submarine pipeline lying on or near the bottom. Therefore, the vertical drag forces are generally insignificant, and could probably be neglected from the vertical wave force equation.

Pipelines near the bottom are subject to vertical lift forces. These forces are the result of the asymmetric distortion of the flow field due to the proximity of the bottom boundary, which induces differences in the horizontal flow velocities and corresponding pressure distribution over the top and bottom of the pipeline. Since the water particle velocities near the bottom are at a maximum in the horizontal plane, the lift forces induced by these horizontal motions will generally be the predominant force acting in the vertical direction.

Transverse "lift" forces due to eddy shedding may also be an important component of the vertical wave force, since these forces are also due to the horizontal water particle velocities and excursions which are maximum in the horizontal direction. Certain values of the Keulegan-Carpenter parameter and Reynolds number must be attained for the eddy release phenomenon to occur. The proximity of the bottom boundary will probably have some effect on the formation and release of the eddies, both because it is a solid boundary, and because it affects the orbital motions of the water particles induced by the wave action.

Although the eddy-induced component of the vertical wave force may be significant when compared to the relatively small vertical drag and inertial forces, the experimental results of this investigation show that the eddy-induced lift forces are much smaller than the "Bernoulli-type" lift forces for pipelines located near the bottom. At large clearances above the bottom where the Bernoulli-type lift effect becomes negligible, the transverse lift forces due to eddy shedding may become a significant component of the total vertical force. At the same time, as the pipeline is raised farther from the bottom boundary, the vertical inertial and drag forces also become more significant.

The vertical component of the total wave-induced force acting on a pipeline near the ocean bottom thus consists of four components--the lift force, the inertial force, the drag force, and the transverse lift force due to eddy shedding. Using the Morison approach, the total vertical wave force is expressed as the sum of these components:

$$F_v = F_L + (F_I)_v + (F_D)_v + F_L' \quad (3)$$

where  $F_L$  is the lift force and  $F_L'$  is the transverse lift force due to eddy shedding.

## 2. Wave-Induced Lift Forces.

Consider a pipeline in contact with a horizontal rigid, impervious bottom. Water cannot flow between the pipe and the bottom boundary, so the flow must be diverted over the top of the pipe. The asymmetrical distortion of the flow field results in maximum velocities over the top of the pipe section and minimum velocities over the bottom, with zero velocities at the stagnation point on the upstream side of the pipe bottom at the point of contact with the sea floor. Correspondingly, the associated pressure distribution will induce an upward lift force for any velocity field acting on the pipeline. The stagnation pressure at the bottom of the pipe section will increase with increasing velocity, while simultaneously the pressure distribution over the top of the pipeline will decrease with the increased velocities of the flow diverted over the top of the pipe section. The wave-induced lift forces will thus act in the upward direction throughout the wave cycle, increasing with the horizontal water particle velocities to maximum magnitudes under the crests and troughs of the passing waves, and diminishing to zero at the points of horizontal flow reversal.

In contrast, a pipeline located at a small clearance above the bottom boundary is subject to a more complex type of lift phenomenon. At the phase in the wave cycle where the horizontal component of the water particle velocity reverses direction, the horizontal velocity over the pipeline is approximately zero. As the wave crest or trough begins to approach the pipeline, the wave-induced horizontal velocities are initially low, inducing unrestricted flow at low velocities over both the top and bottom of the pipeline. However, the water flows

faster through the bottom clearance constriction than over the top of the pipeline, so the corresponding differences in the pressure distribution exert a downward (negative lift) force toward the bottom boundary (Fig. 1, a).

At first, the negative lift force will increase with the increasing horizontal water particle velocities of the approaching wave, since the flow velocities increase at a faster rate through the bottom clearance constriction than over the top of the pipeline, thus producing larger differences in the corresponding pressure distributions over the top and bottom of the pipe section (Fig. 1, b).

This continues until viscous effects begin to restrict the flow through the narrow bottom clearance. For a given small clearance and a given amount of energy in the horizontal water particle velocities approaching the pipeline, the velocities and flow rates of a viscous fluid through the bottom clearance constriction can attain only certain maximum values. Thus, a "choking" effect is exerted on the restricted flow through the small bottom clearance, and the remainder of the wave-induced flow is forced to flow over the top of the pipe section. Correspondingly, the stagnation point will shift downward, increasing the pressure on the lower upstream side of the pipeline. The larger the proportion of the flow diverted over the top of the pipe, the lower the stagnation point.

At the same time, the increasing velocities associated with the approaching wave crest cause the restricted flow through the bottom clearance to form a turbulent jet with the generation of eddies behind the jet. The generation of increased turbulence and eddies results in an energy loss in the water flowing through the bottom constriction, decreasing the velocities under the pipe section behind the jet.

The above effects associated with the choking phenomenon limit the maximum flow velocities and minimum pressures under the bottom side of the pipe section. In contrast, the unrestricted flow velocities over the top of the pipeline increase freely with the increasing horizontal velocities of the advancing wave. The increased part of the approaching flow that is diverted over the top of the pipe section due to the shift in stagnation point produces a further increase in the flow velocities over the top. Correspondingly, the pressure distribution over the top side of the pipeline decreases at a faster rate than the associated pressures along the bottom side, so the negative lift force gradually decreases and eventually becomes positive (Fig. 1, c, d, and e).

At this stage, the upward lift force becomes larger as the horizontal velocities acting on the pipeline increase further with the advancing wave crest or trough (Fig. 1, f).

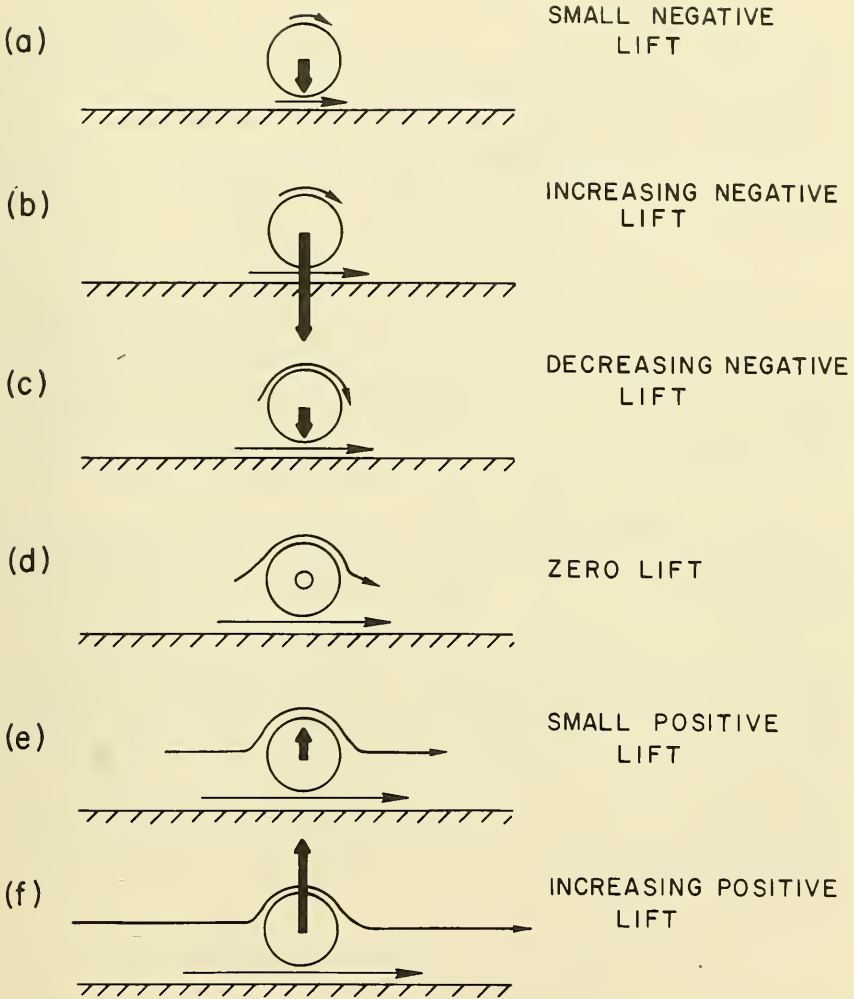


Figure 1. Change in lift with increasing velocity.

As the wave crest or trough passes, this series of steps in the lift force phenomenon is reversed. The horizontal velocities approaching the pipe section begin to decrease, resulting in a decrease in the positive lift force exerted on the pipeline. As the velocities decrease further with the passing wave, the flow under the pipe section begins to become less restricted. The choking effect thus decreases, and the turbulence and eddies near the bottom clearance gradually diminish. As the flow under the pipe section ceases to be restricted, less of the horizontal flow approaching the pipeline is forced to flow over the top of the pipe, so the stagnation point will accordingly shift upward, closer to the center of the pipe section.

The flow velocities decrease simultaneously over the top and bottom of the pipeline as the wave passes, but the rate of decrease is faster over the top of the pipe than in the vicinity of the bottom constriction. The positive lift force decreases until eventually, the flow velocities, location of the stagnation point, and associated pressure distribution are such that the pressure integrated over the pipe section again results in a negative lift force. The downward lift force then increases as the flow through the bottom clearance becomes less restricted with the decreasing velocities of the passing wave.

This lift phenomenon, as shown in Figure 2 for a passing wave crest, is repeated twice during each wave cycle as the direction of the wave-induced horizontal velocities reverses under the crests and troughs of the passing waves.

In reality, the horizontal flow reversal occurs almost instantaneously, so the negative lift force does not return to zero at the point of zero velocity when the flow reverses through the bottom clearance constriction. The instant of zero velocity occurs only at the center of the pipe cross section (the reference point). Since the pipeline has a finite diameter, the wave-induced flow acting on the pipe section at any instant includes the sum of the flow conditions induced by the part of the wave covering the entire diameter of the pipeline. So instead of going to zero with the passing wave crest, and then increasing initially with the approaching trough, the lift force remains negative during the period of minimal velocities as the flow reverses under the pipe section.

In a similar manner, the lift force does not become positive as soon as the choking effect occurs in the bottom clearance constriction. The development of the choking phenomenon involves the formation of a turbulent jet through the constriction, and a downward shift in the stagnation point as more water is diverted over the top of the pipe with increasing restriction of the flow through the clearance. The corresponding changes in the velocities, flow pattern, and associated pressure distribution over the top and bottom of the pipe section produce the transition from negative to positive lift. This process requires some small but finite amount of time. Conversely, the reversal



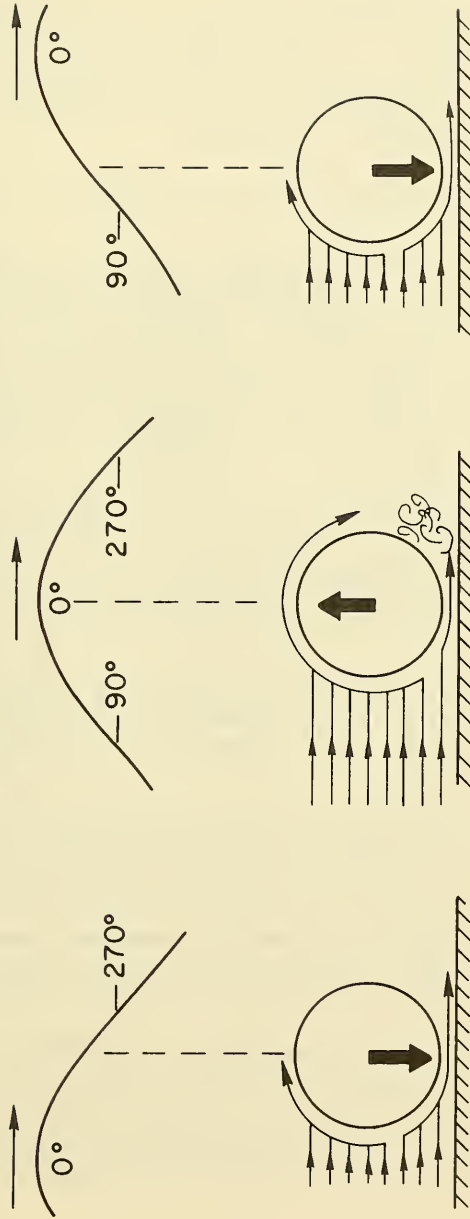


Figure 2. Change in lift force with passing wave crest.

of these processes with the decreasing velocities of the passing wave crest also involves a small but finite amount of time. Thus, there will be a slight timelag in the point of maximum positive lift with reference to the instant of maximum velocity as the wave crest (or trough) passes over the reference point. The smaller the amount of positive lift relative to the amount of negative lift, and the later the positive lift occurs in the wave cycle, the greater the timelag.

An example of the lift force phenomenon over a complete wave cycle for a small bottom clearance is shown in Figure 3.

For a given pipe diameter and wave condition, as the bottom clearance is increased, higher velocities are necessary to produce the choking effect in which the flow becomes restricted through the bottom clearance constriction. Thus, as the bottom clearance is increased, the flow under the pipeline begins to become restricted closer to the approaching wave crest or trough, where the horizontal velocities are at a maximum; this choking effect also diminishes soon after the wave crest or trough has passed. Therefore, as the bottom clearance is increased, the downward lift force occurs during a larger part of the wave cycle.

At the same time, larger clearances permit greater maximum velocities and corresponding lower pressures under the pipe section. Since higher flow rates are possible under the pipe section, less of the wave-induced flow must be diverted over the top of the pipeline. As a result of these changes, the negative lift forces reach a greater magnitude before the choking effect begins, and these maximums are attained later in the wave cycle.

Correspondingly, the upward lift forces occur during a smaller part of the wave cycle, and the maximum magnitude these forces attain decreases with increasing bottom clearance. These maximum values are also reached later in the wave cycle.

If the clearance is increased further, a point is eventually reached at which the clearance is large enough so that the choking effect does not occur. At this stage, the velocities are higher through the bottom clearance constriction than over the top of the pipeline during the entire wave cycle. So the associated pressure distribution results in a negative lift force throughout the wave cycle, with maximum downward forces occurring under the crests and troughs of the passing waves. The negative lift diminishes to zero at the points of horizontal flow reversal.

As the bottom clearance is increased further, the downward lift effect is gradually reduced. The phase of the force cycle relative to the wave cycle remains the same, but the magnitude decreases. Eventually, a point is reached where the bottom clearance no longer acts as a constriction to the wave-induced flow. The flow pattern becomes approximately symmetrical, and the increased velocities of the horizontal flow diverted over the top and bottom of the pipeline, along with the corresponding

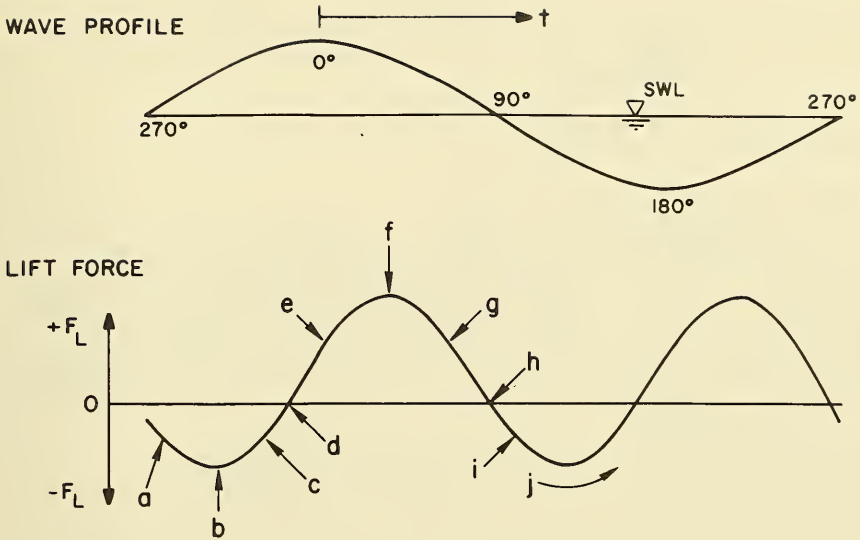


Figure 3. Lift force phenomenon.

- (a) Unrestricted flow through the bottom clearance at low velocities results in downward lift force.
- (b) Unrestricted flow through the bottom clearance at higher velocities increases the negative lift.
- (c) Choking effect begins, so downward lift force decreases.
- (d) Velocities increase and pressures decrease at a faster rate over the top of the pipe section than in the restricted flow through the bottom clearance, so the lift force becomes positive.
- (e) Upward lift force increases with increasing velocities.
- (f) Positive lift reaches a maximum.
- (g) Positive lift force decreases and choking effect diminishes with decreasing velocities of the passing wave crest.
- (h) Lift force again becomes negative as the flow through the bottom clearance becomes less restricted.
- (i) Unrestricted flow through bottom clearance at low velocities results in downward lift force.
- (j) Lift force cycle is repeated as the flow reverses with the approaching wave trough.

pressure distribution, become approximately equal over both sides of the pipe section. At this point, the lift effect is no longer present, and the lift force term may be neglected in calculating the wave-induced forces acting on the pipeline.

The transition in the lift force cycle with increasing bottom clearance is shown in Figure 4.

### 3. Model for Wave-Induced Lift Forces.

The traditional lift force equation, derived for unidirectional steady-flow situations, is expressed as  $F_L = 1/2 C_L \rho A u^2$ , where  $C_L$  is the coefficient of lift. This equation has been applied to wave-induced lift forces, using the horizontal component of the oscillating water particle velocity,  $u$ , in the relationship. The lift force expressed in this way assumes that the force acts in one direction only (either upward or downward) throughout the entire wave cycle.

A pipeline located on the ocean floor with no clearance will experience an upward lift force throughout the entire wave cycle, increasing with the horizontal velocities to reach maximum values under the crests and troughs of the passing waves, and diminishing to zero as the horizontal velocities go to zero at the point of flow reversal. This phenomena is described adequately by the above lift force equation with a positive coefficient of lift  $C_L$ .

A pipeline located at a large enough clearance above the bottom so that the choking effect does not occur will experience a downward lift force throughout the wave cycle, since the flow is always faster through the bottom constriction than over the top of the pipeline. Again, this negative lift force increases with the horizontal water particle velocities, reaching maximum magnitudes under the crests and troughs of the passing waves, and decreasing to zero as the flow reverses. This phenomenon is also suitably expressed by the traditional lift force equation, but using a negative coefficient of lift.

These two situations represent the extreme cases bounding the lift force phenomena. However, the choking phenomenon will occur at any clearance between these two limits, and the traditional lift force equation cannot be used to accurately describe the forces exerted on a pipeline. This equation must be replaced by a model developed specifically for wave-induced lift forces. The experimental results of this investigation demonstrate that the largest wave-induced lift forces occur at these intermediate clearances, where the choking phenomenon does develop.

Since the lift force phenomenon is repeated twice per wave cycle with the reversal of the horizontal flow pattern, the lift force can be described mathematically by a sinusoidal function of twice the frequency of the waves. In addition, the mathematical expression must allow for description of the following lift force properties:

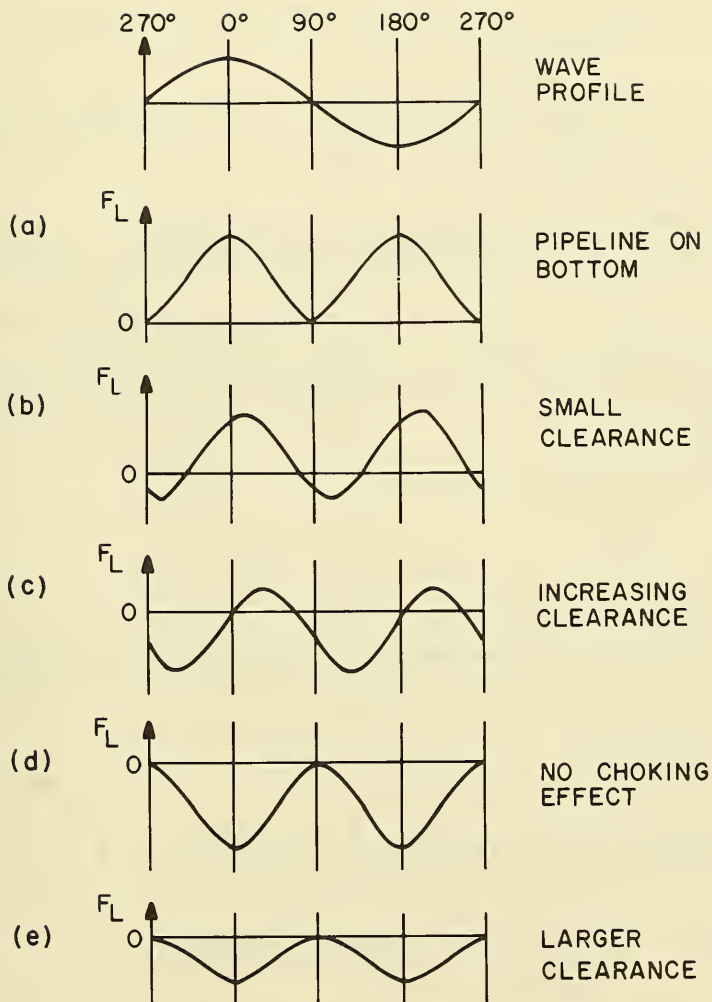


Figure 4. Change in lift force record for increasing bottom clearance.

(a) The lift force may be positive during part of the wave cycle and negative for the rest of the cycle. The proportion of positive lift to negative lift may range from all positive lift to all negative lift.

(b) The positions of the maximum values of both the upward and downward lift forces will shift with respect to the position of the wave cycle as the bottom clearance is increased (for a given pipeline and wave condition).

(c) As the clearance is increased, the maximum value of the upward lift force will decrease, while correspondingly the maximum value of the downward lift force will increase.

(d) When the bottom clearance is increased to a point at which the lift effect is downward throughout the entire wave cycle, further increases in clearance will result in decreases in the maximum magnitude of the downward lift force, but without a shift in the position of the maximum lift force with respect to the position of the wave cycle over the pipeline.

A lift force equation of the form,

$$F_L = 1/2 C_L \rho A u_{\max}^2 [\cos^2 (\theta - \phi) - k], \quad (4)$$

allows an adequate mathematical description of all the above properties of the wave-induced lift force phenomena. This equation fits the experimental data reasonably well over the wide range of conditions tested.

The parameters involved in this modified form of the traditional lift force equation are:

- $C_L$  = coefficient of lift
- $\rho$  = mass density of fluid
- $A$  = projected area of pipe section
- $u_{\max}$  = maximum value of horizontal component of water particle velocity at center of pipe section if pipeline was absent
- $\theta = \frac{2\pi t}{T}$  = position of wave cycle over center of pipe section with respect to time, where  $T$  is the wave period and  $t$  is the time since the last crest passed over the center of the pipe section (see definition sketch in Fig. 5). The wave crest corresponds to  $\theta = 0^\circ$  (0 radians) or  $2\pi t/T = 0$  radians. The wave trough corresponds to  $180^\circ$  ( $\pi$  radians) or  $2\pi t/T = \pi$  radians

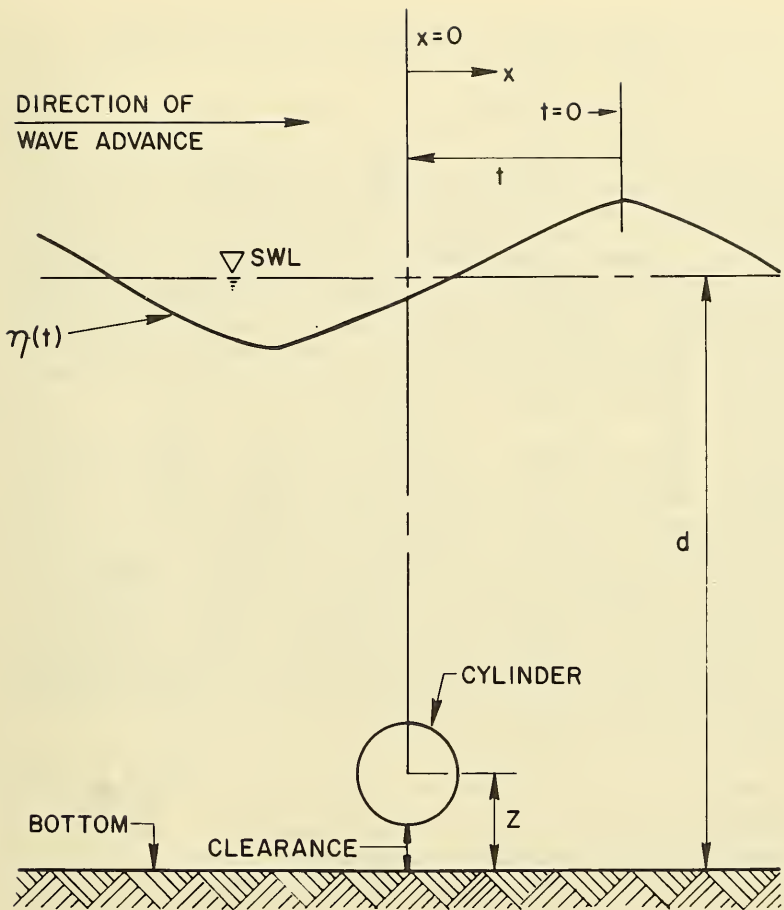


Figure 5. Definition sketch.

$\phi$  = phase shift of maximum lift forces with respect to wave cycle

$k$  = negative fraction of lift force cycle

The parameter,  $k$ , represents the increase in the magnitude and duration of the negative lift forces acting on a pipeline with increasing bottom clearance, and the corresponding decrease in the magnitude and duration of the positive lift forces. The value of  $k$  varies from a minimum of 0 to a maximum value of 1.  $k = 0$  corresponds to the case of a pipeline lying on the bottom with no clearance, in which the lift forces are positive throughout the wave cycle.  $k$  increases with increasing bottom clearance to a maximum value of 1, which corresponds to the case of a pipeline located at a sufficient clearance from the bottom so that the choking phenomenon does not occur, and in which the lift forces are therefore negative throughout the wave cycle.

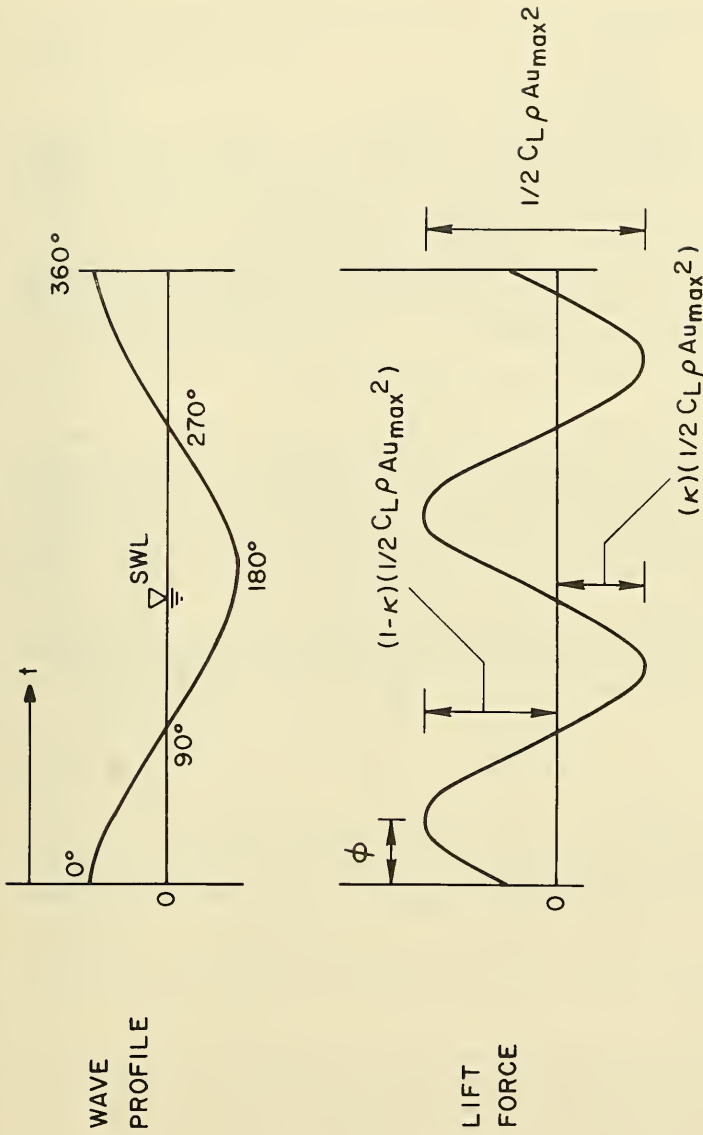
The phase shift parameter,  $\phi$ , represents the shift in the position of the maximum values of both the positive and negative lift forces with respect to the wave cycle as the bottom clearance increases. The value of  $\phi$  may range from  $0^\circ$  to a maximum value of  $90^\circ$ .  $\phi = 0^\circ$  corresponds to the case of a pipeline located on the ocean floor with no bottom clearance, in which the lift forces are positive throughout the wave cycle with maximum forces occurring under the crests and troughs of the passing waves.  $\phi$  increases with increasing bottom clearance to a maximum value of  $90^\circ$ , corresponding to a pipeline located above the bottom at a sufficient clearance so that the choking effect does not occur; the lift forces are negative throughout the wave cycle with maximums occurring under the crests and troughs of the waves. As defined,  $\phi = 0^\circ$  when  $k = 0$ , and  $\phi = 90^\circ$  when  $k = 1$ , or vice versa.

The coefficient of lift,  $C_L$ , in this form of the lift force equation will always have a positive value, since negative values of the lift force are accounted for by the value of the parameter,  $k$ . The lift force equation is shown graphically in Figure 6.

To apply the lift force equation to a practical design situation, values of  $C_L$ ,  $k$ , and  $\phi$  must be determined for a given set of pipeline and wave conditions corresponding to the particular case under consideration. Selection of the appropriate values requires quantitative knowledge of the functional relationships between these parameters and the wave conditions, bottom clearance, and pipeline size and configuration. The development of these relationships was the purpose of the experimental part of this investigation.

In a real situation, a pipeline on the ocean floor is often laid over an irregular bottom, supported by the high points in the bottom topography but probably spanning the depressed areas. In this case, the pipeline must be broken into component sections of the same approximate bottom clearance for a separate analysis of each section. The results of the





analysis will yield the lift force record (both magnitudes and time history) of each separate component pipe section, which may then be integrated in the appropriate manner to determine the maximum wave-induced stresses exerted on the pipeline at any critical section.

This is important because the maximum lift forces may act upward on a bottom-supported section of a pipeline, while acting downward on the adjacent sections of the pipeline spanning the bottom at a small clearance. Maximum values of both the positive and negative lift forces acting in opposite directions could easily occur at the same point in the wave cycle (under the crests and troughs), thus exerting stresses on the pipeline twice as high as would be calculated considering any pipe section alone, or in using some average clearance for a long section of the pipeline.

#### 4. Extension of Model to Higher Order Theories.

The lift force model (eq. 4) is based on linear theory, assuming the lift force phenomenon is identical as either the wave crest or trough passes over the pipeline. Such a symmetrical expression is not flexible enough to consider slightly different kinematics under the wave crests and troughs, which are expressed in higher order theories. These different kinematics would, in reality, produce slightly different lift forces under the crests and troughs of nonlinear waves.

The lift force model described above was derived as a modification of the traditional lift force equation using linear wave theory to express the horizontal water particle velocities. Using linear wave theory, the traditional lift force equation can be expressed as:

$$F_L = 1/2 C_L \rho A u_{\max}^2 \cos^2 (\theta). \quad (5)$$

This equation was modified to make it a suitable expression for wave-induced lift forces by adding the phase shift parameter,  $\phi$ , to account for maximum lift forces occurring in places other than the crest-and-trough in the wave cycle, and by adding the parameter,  $k$ , to account for positive lift forces during part of the wave cycle and negative forces during the rest of the cycle. This modified equation fits the experimental data very well for all conditions tested in this investigation.

The model was developed after thorough inspection of the experimental data. For a given pipe diameter and wave condition, the force record followed a sinusoidal relationship of twice the frequency of the waves. As the clearance increased, the maximum positive forces gradually diminished while continuously shifting to a maximum of  $90^\circ$  from the wave crest as the forces went to zero (Fig. 4). At the same time, the maximum negative forces slowly grew from a minimum value of zero at a position

90° from the wave crest and increased while continuously shifting positions to reach a maximum negative value at a position 180° from the wave crest (Fig. 7, a).

Since a sinusoidal function of twice the frequency of the wave ( $\sin 2\theta$  or  $\cos 2\theta$ ) can be expressed as  $\cos^2\theta$ , using the appropriate trigonometric relationships, and since the lift force is a function of the horizontal velocity squared  $(u_{\max} \cos \theta)^2$ , using linear wave theory, the lift force equation was expressed as  $F_L = 1/2 C_L \rho A u_{\max}^2 [\cos^2(\theta - \phi) - k]$ .

However, it is the symmetrical properties of this equation and linear wave theory that allow this expression to work so well. When higher order wave theories are applied to this relationship, problems due to nonsymmetry are encountered. This is easily seen by graphically comparing the transition from positive to negative lift forces with increasing bottom clearance with this lift model, using both linear and higher order theories.

The horizontal component of the water particle velocity for both Stokes' third-order waves and linear waves is shown in Figure 8, along with the corresponding lift forces on a pipeline for the two extreme cases of: (a) a pipeline on the bottom with no clearance, and (b) a pipeline with a large enough bottom clearance so that the choking phenomenon does not occur. By gradually shifting the linear theory lift force curve for case (a) (no bottom clearance) to the right 90° from the wave crest, while simultaneously lowering it so that the forces become negative, the lift force curve for case (b) is obtained (compare Figs. 7 and 8). This same transformation of the wave force record was observed with increasing bottom clearance in the experimental data.

However, if this procedure is repeated with the Stokes' third-order lift force record, the correct force record for case (b) is not obtained (compare Figs. 7 and 8). In reality, rather than a mere shift of the force record downward and to the right with increasing bottom clearance, a simultaneous transformation of the shape of the lift force record would also occur for highly nonlinear waves. This gradual transformation of the shape occurring simultaneously with the shift would provide a continuous change in the lift force record with increasing clearance between the two limiting cases (a) and (b) (Fig. 8).

However, the lift force phenomenon is not a direct function of the instantaneous water particle velocity acting at the center of the pipe section if the pipeline was absent. Rather, it is a complicated function of the asymmetrical distorted flow pattern and accelerating velocity field acting on the pipeline, which in turn causes the choking phenomenon to occur, with the resulting change in the relative differences in the flow velocities and corresponding pressure distribution over the top and bottom of the pipeline. Boundary layer flow through the bottom constriction, the formation of a turbulent jet and associated eddies, and a cyclic change in the location of the stagnation point with the accelerating velocity field further complicate matters. In addition, the eddies and

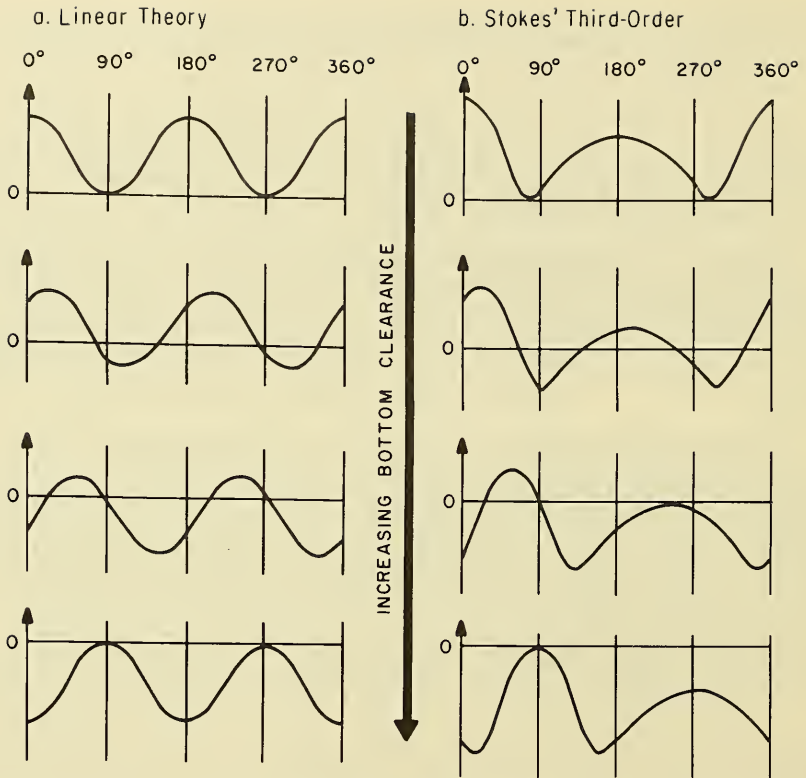


Figure 7. Comparison of linear and Stokes' third-order theories. Simultaneous shift of lift force record as  $\phi$  increases from  $0^\circ$  to  $90^\circ$  and  $\kappa$  increases from 0 to 1 with increasing bottom clearance.

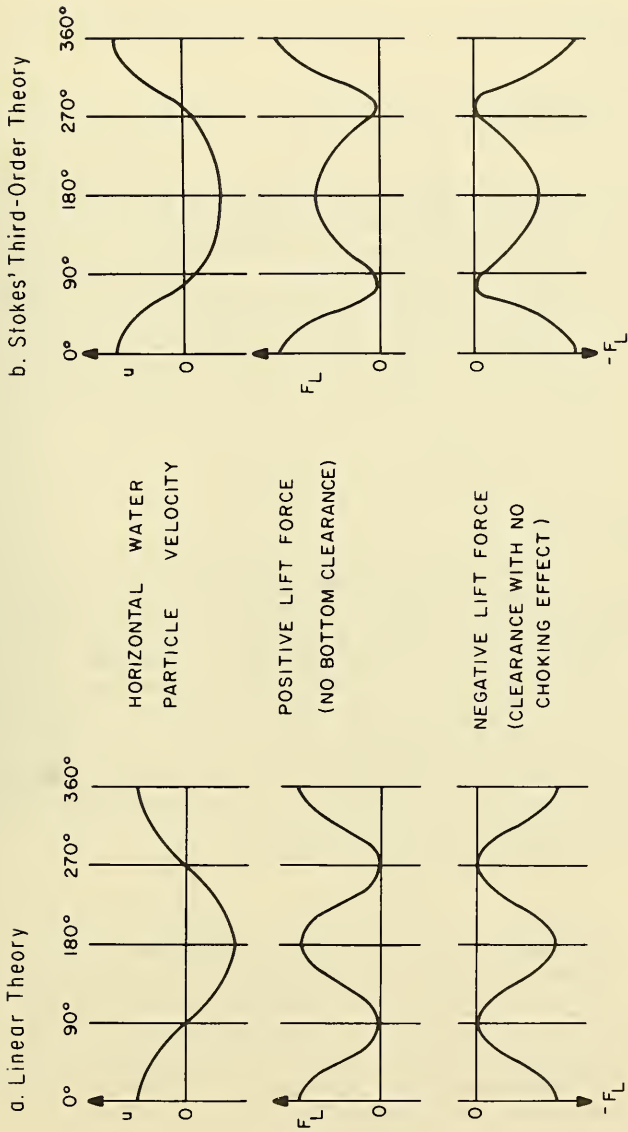


Figure 8. Comparison of lift force extreme cases for linear and Stokes' third-order theories.

increased turbulence generated by the jet may be swept back through the bottom constriction as the flow pattern reverses with the passing waves.

Because of this, development of an accurate mathematical description of the lift force phenomena for nonlinear waves that would cover the complete transformation of the lift force record with increasing bottom clearance, and yet be flexible enough to allow application of any higher order theory, would be a formidable, if not impossible, task. Since the lift force model developed for linear theory seems to fit the experimental data reasonably well, even for waves that were obviously nonlinear, it should provide a useful tool for engineering calculations, even though it may not be flexible enough and theoretically correct to allow the use of higher order wave theories. The value of the maximum horizontal velocity,  $u_{max}$ , can be calculated under the wave crest using any higher order wave theory; this value can then be used in the linear lift force model, possibly giving a better approximation of the lift forces induced by highly nonlinear waves.

## II. EXPERIMENTAL INVESTIGATION

### 1. Experimental Equipment.

Model experiments were performed in three different wave tanks. The two-dimensional tests were done in a 1-foot-wide wave channel in the Hydraulic Engineering Laboratory (HEL) at the University of California, Berkeley. The three-dimensional tests were started in the 8-foot-wide Naval Architecture (NA) tow tank, and then continued in the 8-foot-wide HEL wave tank where the majority of the experiments were conducted, both located at the Richmond Field Station of the University of California. The 1-foot wave channel is 100 feet (30.48 meters) long; the 8-foot HEL wave tank and NA tow tank are 180 and 200 feet (54.86 and 60.96 meters) long, respectively. All tests were conducted at approximately the middle of the tanks. A stillwater depth of 2 feet (60.96 centimeters) was used in the two dimensional tests, and a 3-foot (91.44 centimeters) water depth was used in the three-dimensional experiments.

A flapper-type generator is located at one end of each of the HEL wave tanks; the NA tow tank has a piston-type wave generator. The wave period is controlled by varying the speed of the electric motors which drive the wave generators. A cam mechanism with a variable stroke length is connected between the drive motor and the flapper, and the wave height is varied by changing the stroke length. A wave filter, consisting of a series of vertical screens, was placed in front of the wave generator in the 1-foot-wide wave channel to smooth out any irregularities in the generated waves due to reflections from the flapper. A permeable beach was installed at the opposite end of each of the tanks to absorb the wave energy and minimize the wave reflections from that end of the wave tank.

The wave-induced forces on the model pipe section were measured by a wave force meter designed and built by Al-Kazily (1972). A few modifications were made to make the instrument more suitable for this investigation. The same transducer unit was used in all of the experiments, but fittings of different sizes were made to accommodate test cylinders of various diameters.

The force transducer consists of a strain bar mounted between two supports. The model pipe section is mounted to the strain bar in such a way that forces on the pipe induce bending stresses on the strain bar. These forces are measured by four strain gages mounted to the strain bar at sections of maximum strain, with two gages in compression and the other two in tension. The strain gages are wired in a Wheatstone bridge, which is connected to a carrier amplifier which amplifies the output from the strain gages. The signal is then recorded on a strip-chart recorder.

The original strain gages were Bean-type BAB-13-125DD-120S, and were mounted to the steel strain bar with EPY-150 two-part epoxy, and then coated with Dow Corning Silastic RTV silicon rubber for waterproofing. Shortly after the beginning of the three-dimensional tests, problems were encountered in the operation of the transducer. These problems were caused by the deterioration of the original strain gage adhesive and coating, so new strain gages were installed on the transducer unit. The new gages were Micromasurement-type EA-06-125AD-120, bonded to the strain bar with Micromasurement M-Bond 610 two-part strain gage adhesive, and then coated with Micromasurement M-Coat D and M-Coat G for waterproofing protection. About halfway through the three-dimensional tests, further problems were encountered in the operation of the transducer unit, probably due to water leakage into the waterproof coating. There was also evidence of corrosion on the steel strain bar, so it was decided to build a new force transducer using a stainless-steel strain bar to minimize corrosion, and encapsulated strain gages to minimize problems with water leakage. The new strain gages were Micromasurement-type CEA-06-125UW-120. The same strain gage adhesive and waterproof coatings were used, with Micromasurement M-Coat B along the lead wires to minimize the change of water "wicking" along the lead wires to the inside of the coating materials.

The transducer mounting arrangement was different for the two-dimensional and three-dimensional experiments. The test cylinder and transducer unit for the two-dimensional tests were mounted between two support brackets on each side of the 1-foot wave channel. For the three-dimensional experiments, the test cylinder and transducer unit were mounted between two long dummy pipe sections, which were in turn mounted to a steel base. The force meter and mounting arrangement is shown in Figures 9 and 10 for the two-dimensional tests, and in Figures 11 to 15 for the three-dimensional tests.

A parallel-wire resistance-type wave gage was used to record the waves passing over the model pipe section. The gage was mounted directly over

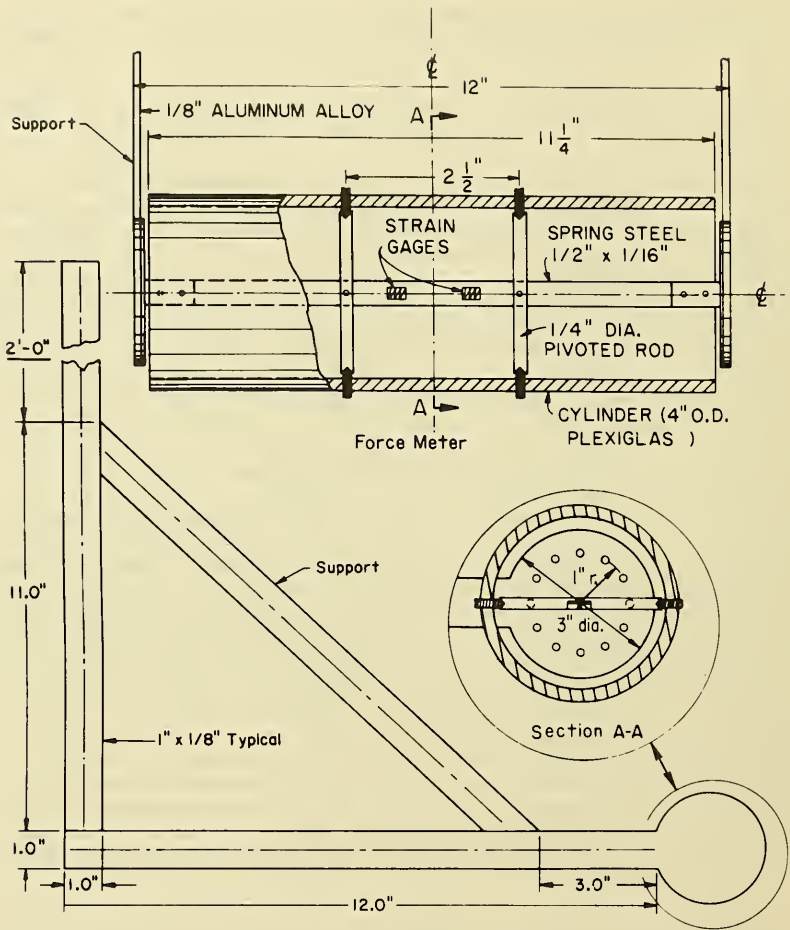


Figure 9. Force meter and support.



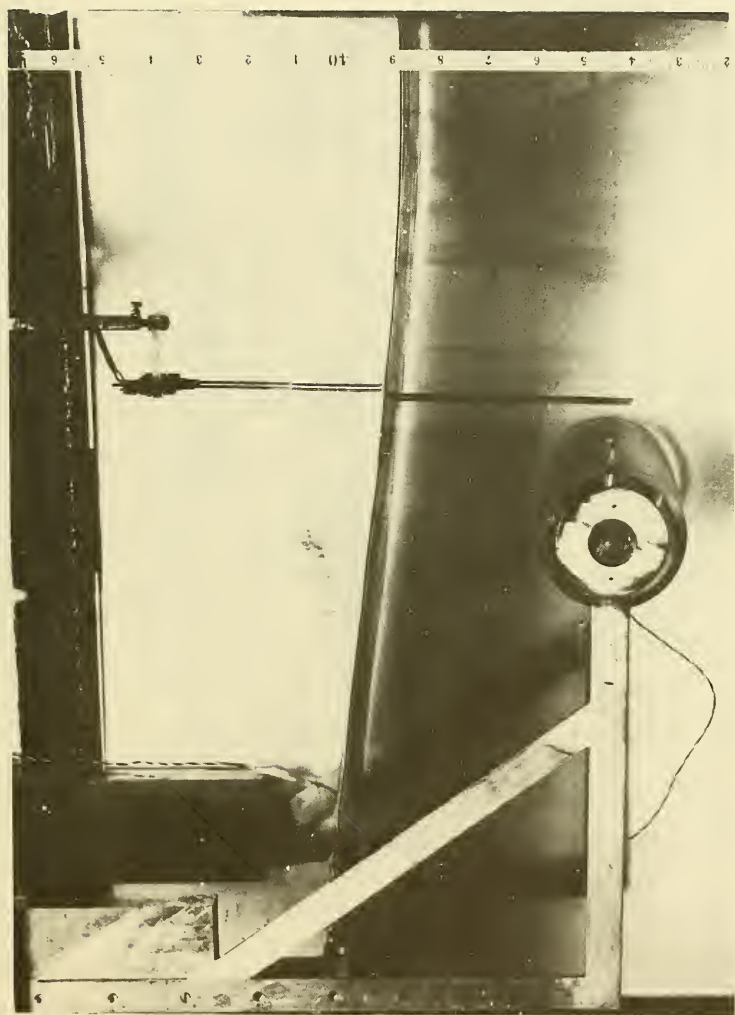


Figure 10. Four-inch cylinder mounted in the flume.

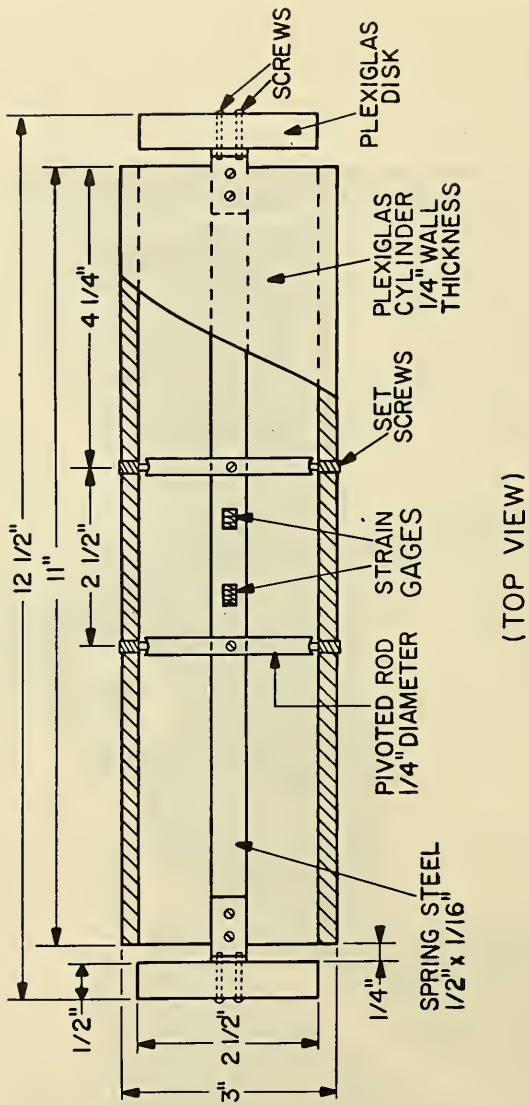


Figure 11. Test section (force meter).

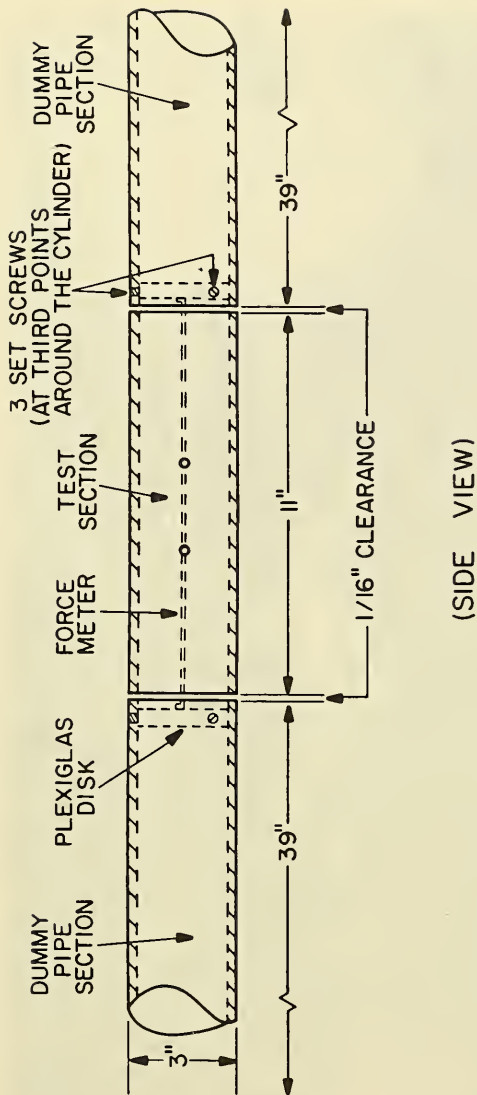


Figure 12. Test section mounted in position.

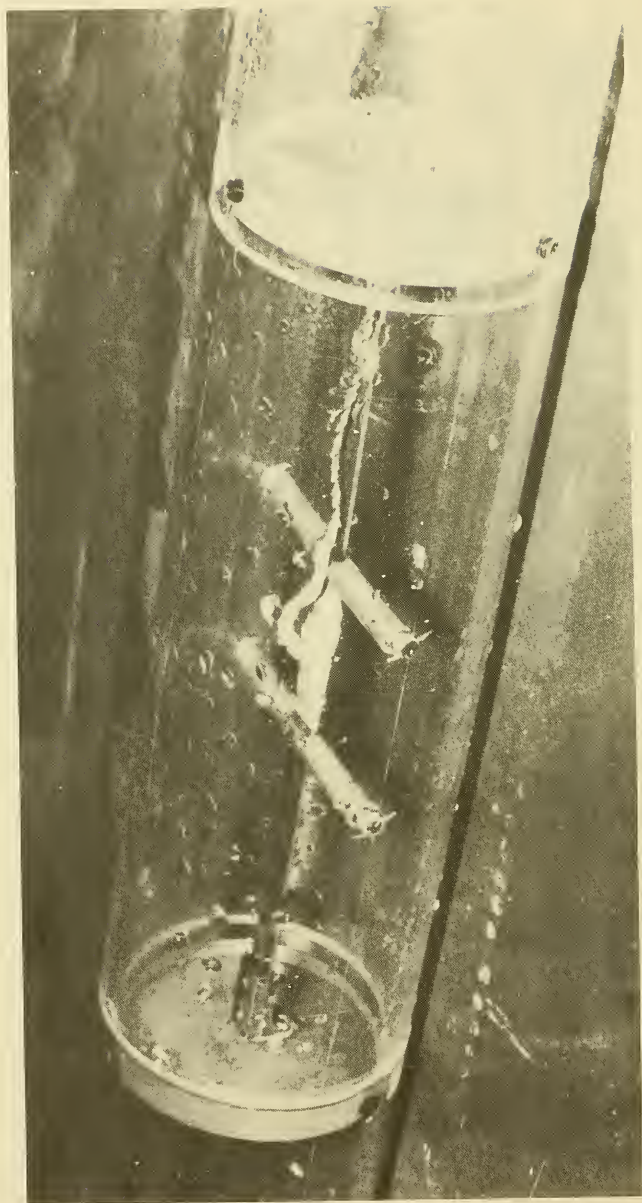


Figure 13. Test section and force transducer.

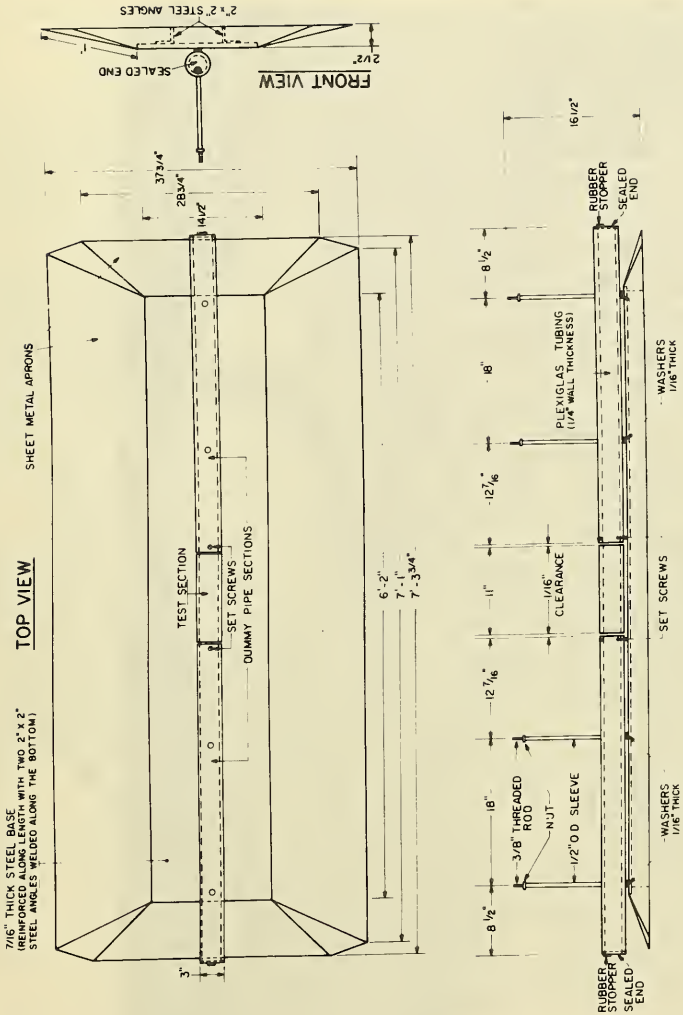


Figure 14. Schematic of pipeline model.

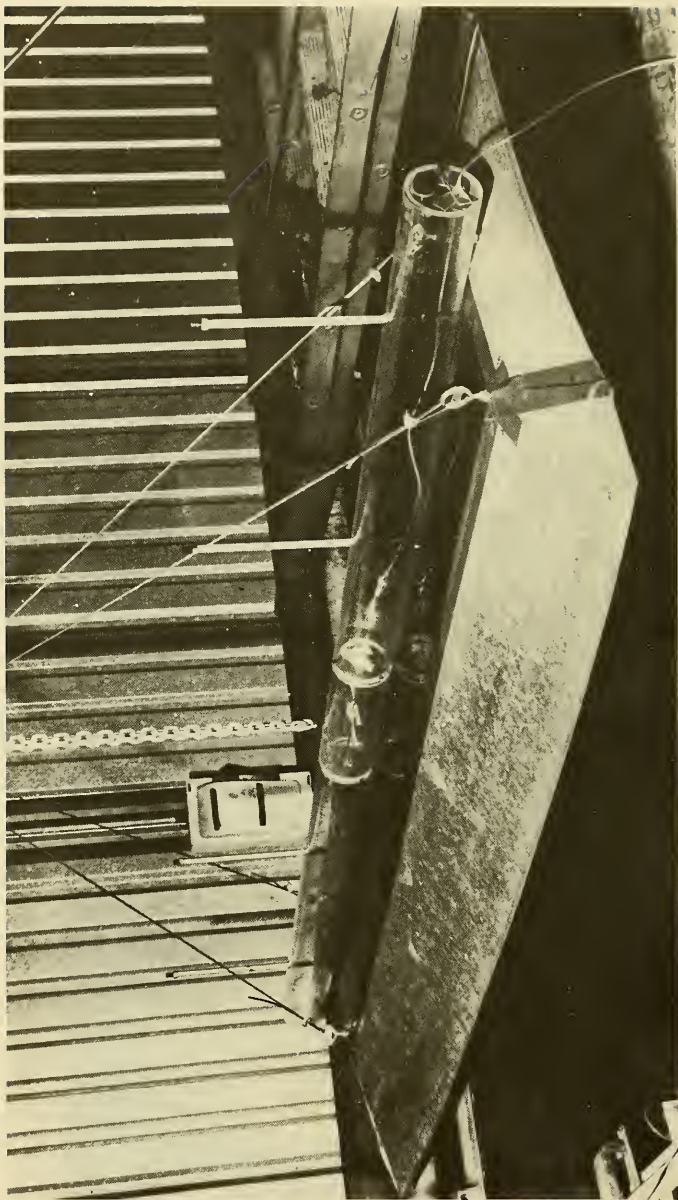


Figure 15. Pipeline model.

the center of the test section, so that the wave records could be correlated directly with the resulting wave-induced force record.

A Brush dual-strain gage amplifier was used in the experiments, with one channel connected to the wave gage, and the other channel connected to the force meter. The amplifier was connected to a Brush two-channel rectilinear writing recorder which continuously recorded the waves and corresponding wave-induced forces on the pipe section (Fig. 16).

An electronic digital data acquisition system (Paulling and Sibul, 1968) was used in the three-dimensional experiments. The digitizer was connected in parallel with the strain gage amplifier to record simultaneously the wave and corresponding force data on magnetic tape, while at the same time the data were being recorded continuously on the strip-chart recorder (Fig. 17). The digitizer sampled alternately from both the wave record and force record at a rate of 100 samples per second, resulting in 50 samples per second from each of the two channels.

## 2. Procedure for Two-Dimensional Experiments.

a. Calibration. Both the wave gage and the force transducer were calibrated before each set of experimental runs. The wave gage was calibrated statically by raising and lowering the gage in increments of 0.05 foot (1.52 centimeters) and recording the output. The force meter was also calibrated statically by hanging weights in increasing equal increments from a system of pulleys connected to the force meter and recording the output on the strip chart. The force transducer was calibrated in both the upward and downward directions by rearranging the pulley system and repeating the above procedure. The calibration method is shown in Figure 18.

b. Procedure. After calibrating the force meter, the model pipe section was lowered and fixed in a horizontal position at the desired clearance above the bottom of the wave channel, with the long axis of the test cylinder parallel to the approaching wave crests. A sliding point gage was mounted to the wave channel above the pipe section and was used to accurately set the model pipe to the desired bottom clearance and align the pipe section parallel to the wave crests. Once the model was in the correct position, the mounting brackets and support struts were clamped to the sides of the wave channel. The force transducer was mounted in such a way that it was sensitive only to forces acting in the vertical direction.

After the model pipe section was mounted in position, the wave gage was lined up directly over the center of the pipe section with a plumb bob and then clamped in position. The wave gage was then calibrated as described above. The experimental arrangement is shown in Figure 19.

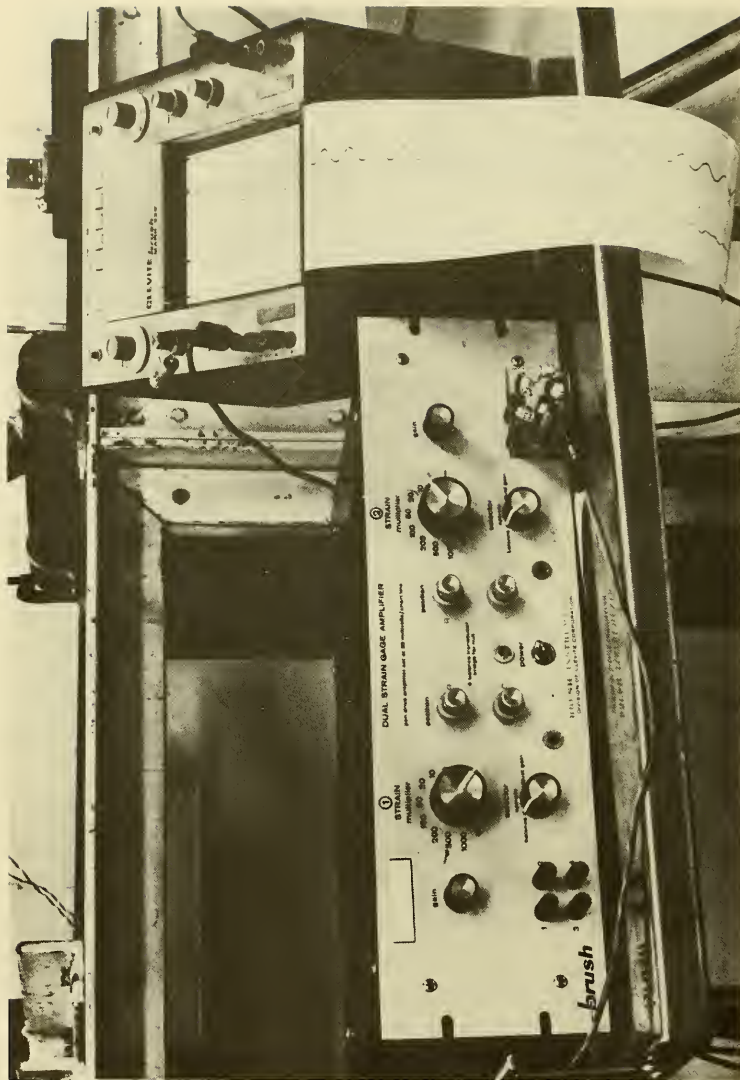


Figure 16. Brush recording instruments.



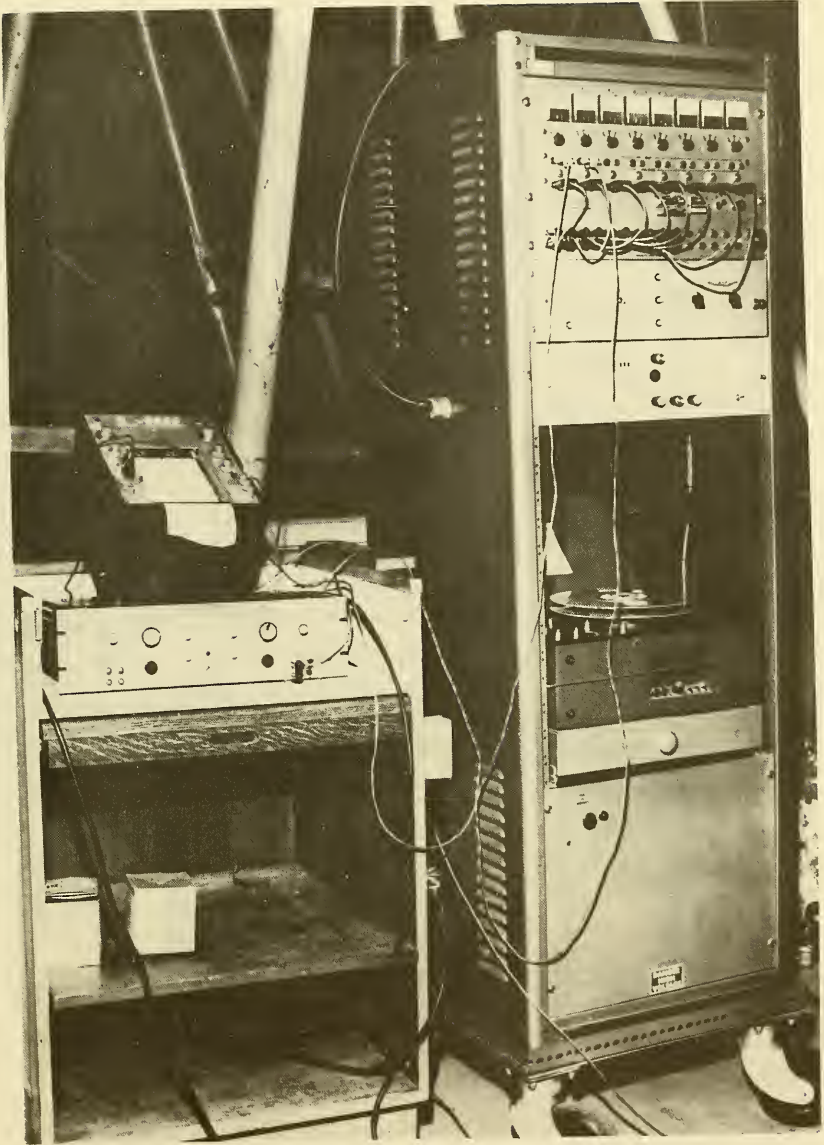


Figure 17. Digitizer and recording instruments.

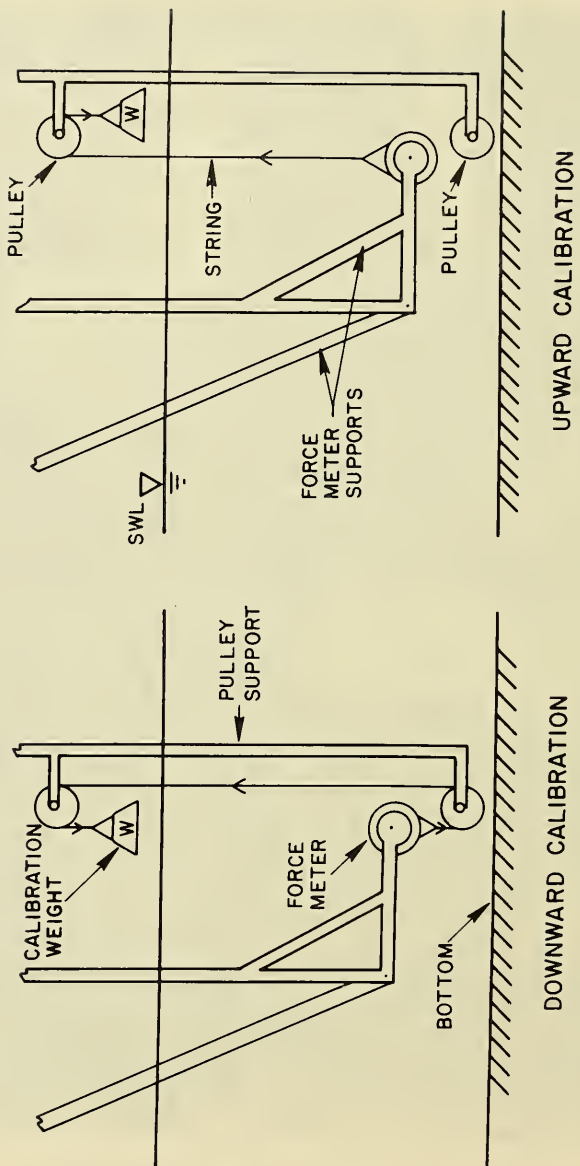


Figure 18. Calibration method for two-dimensional experiments.

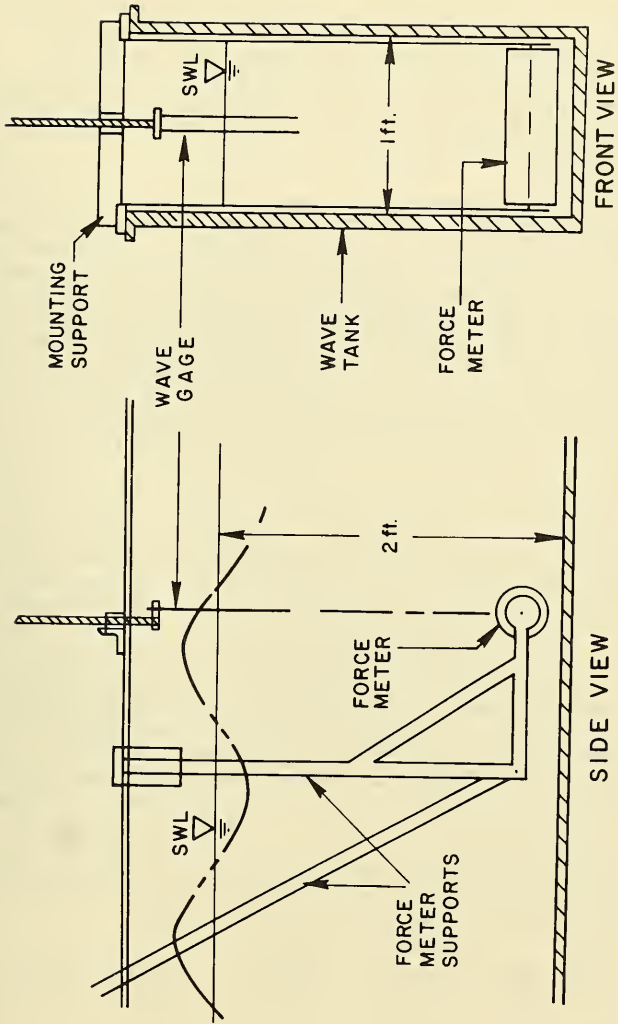


Figure 19. Experimental arrangement for two-dimensional tests.

The pipe model and wave gage were mounted in a glass-walled part of the tank near the middle of the wave channel to facilitate the visual observation of the phenomenon being studied. For each bottom clearance tested, a series of runs was made with waves generated at 19 different wave periods, covering a range of 0.95 to 2.5 seconds. Seven wave heights were generated for each wave period, ranging up to 0.34 foot (10.4 centimeters).

After these runs were completed, the pipeline was set at another bottom clearance, and the procedure was repeated. Seven bottom clearances were tested for each wave condition, ranging from 0.001 foot, 1/16, 1/8, 3/16, 1/4, 1, and 2 inches (0.305, 1.59, 3.18, 4.76, and 6.35 millimeters, 2.54 and 5.08 centimeters), respectively. The minimum clearance tested (0.001 foot) was that which placed the pipe section as close to the bottom as possible without touching the bottom when the waves passed over it. This was necessary to measure any downward forces exerted on the pipe section due to the wave action. The 2-inch bottom clearance placed the pipe section far enough from the bottom so that the vertical lift forces were insignificant.

These experiments were carried out with a 4-inch-diameter (10.16 centimeters) test cylinder. The experiments were repeated with pipe sections of 2-, 2½-, and 3-inch (5.08, 6.35, and 7.62 centimeters) diameters, but only three bottom clearances were tested--0.001 foot, 1/8 inch, and 1/4 inch. The wave conditions covered the same range of wave heights and periods, but were not quite as extensive in number.

In addition to the vertical force measurements, a series of experiments was performed to measure the horizontal forces acting on the pipe section, so that the resultant wave-induced force could be determined throughout the entire wave cycle for several of the experimental conditions tested. Only the 4-inch-diameter test cylinder was used in these experiments, since the corresponding vertical experiments were the most extensive for the 4-inch cylinder. The horizontal forces were measured by rotating the force transducer 90° so that it was sensitive only to forces acting in the horizontal direction. The calibration procedure was the same as described above for the vertical force measurements except that the system of pulleys was rearranged so that the calibration weights exerted forces in the horizontal direction only.

All seven of the bottom clearances used in the vertical experiments were also used in the horizontal tests. The wave periods covered the same range as the vertical experiments, but only 6 of the 19 wave periods were used--0.95, 1.25, 1.5, 1.85, 2.25, and 2.55 seconds. Two of the seven wave heights corresponding to each wave period in the vertical experiments were used in the horizontal tests.

The stillwater depth was held constant at a depth of 2 feet throughout the two-dimensional tests.

### 3. Procedure for Three-Dimensional Experiments.

a. Calibration. The wave gage and force meter were calibrated before each set of experimental runs. The wave gage was calibrated in the same manner as the two-dimensional tests, but 0.1-foot (3.05 centimeters) increments were used rather than 0.05-foot increments, since larger waves were used in these experiments.

The force transducer was calibrated in the upward direction in the same manner as the two-dimensional tests, by hanging weights over a pulley to a string attached to the pipe test section. However, because the three-dimensional model was mounted to a base with a small bottom clearance, it was impossible to calibrate the transducer in the downward direction by using a system of pulleys, since there was no room for a pulley between the pipe section and the base to which it was mounted. Rather, the force meter was calibrated in the downward direction by placing the weights directly on top of the center of the submerged test section and using the submerged weight of the weights in calculating the calibration curve. Weight increments of 50 grams were used in calibrating the transducer. The calibration method is shown in Figure 20.

b. Procedure. An overhead crane was used to lower the pipeline model and base into the wave tank. The assembly was first submerged to a depth of about 1½ feet (45.7 centimeters). The model was tilted at both ends to remove all air bubbles from the system, and the ends of the dummy pipe sections were stoppered to prevent waterflow through the pipeline model. The bottom clearance between the base and the pipe model was adjusted by placing spacers on the support rods between the base and the dummy pipe sections, and then tightening the nuts on the support rods above the dummy pipe sections. The test section was then centered and adjusted carefully to the exact bottom clearance desired with the aid of 10 adjusting screws. The calibration string was attached to the test section, and the assembly was lowered to the bottom of the tank.

The calibration string and pulley system was alined directly over the center of the test section with a plumb bob, and the pulley supports were then clamped to the sides of the wave tank. The transducer was first calibrated in the upward direction, after which the calibration string was removed, and the transducer was calibrated in the downward direction, as described above.

The pipeline model was positioned at the desired angle of orientation on the tank bottom by lining up one of the long edges of the model base parallel to the correct line marked on the bottom of the wave tank. Lines were marked on the tank bottom in 15° increments from 0° to 75°, where 0° corresponds to a pipeline parallel to the approaching wave crests. After the model was calibrated and placed in position, the wave gage was lined up directly over the center of the test section with

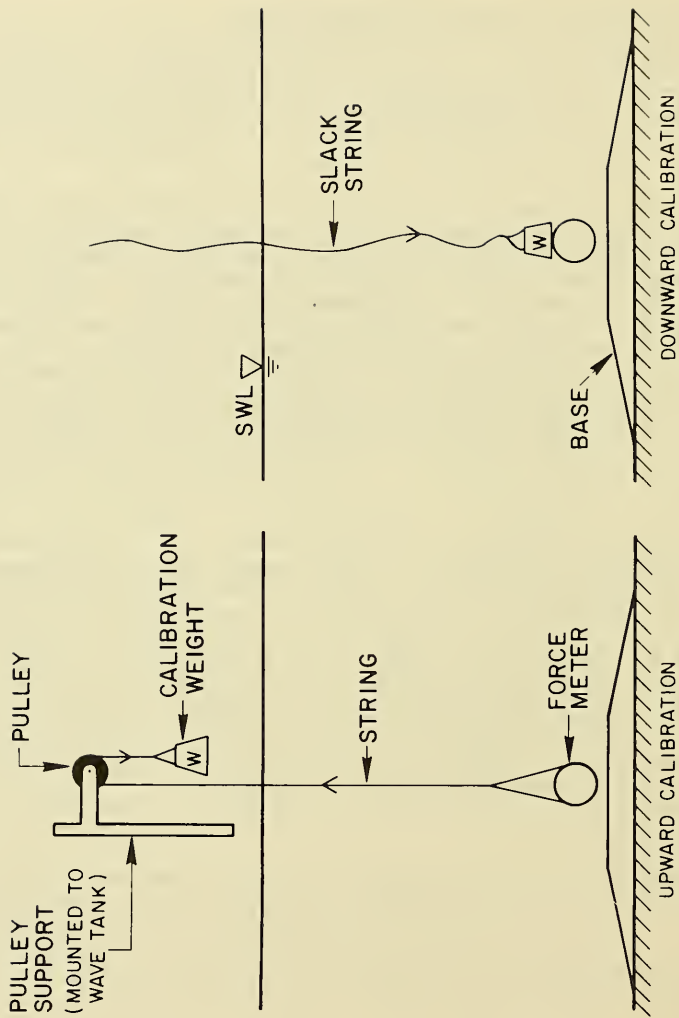


Figure 20. Calibration method for three-dimensional experiments.

a plumb bob, clamped in position, and then calibrated as described above. The experimental arrangement is shown in Figure 21.

For each bottom clearance, six angles of orientation ( $0^\circ$ ,  $15^\circ$ ,  $30^\circ$ ,  $45^\circ$ ,  $60^\circ$ , and  $75^\circ$ ) were tested. Fifteen runs with different wave conditions were made for each bottom clearance and orientation angle. These runs covered four wave periods ranging from 1.4 to 2.6 seconds, with waves generated at four heights for each period, ranging to a maximum of about 0.7 foot (21.3 centimeters). Eight bottom clearances were tested, ranging from 0.001 foot, 1/16 inch, 1/8 inch, 3/16 inch, 1/4 inch, 1/2 inch, 1 inch, and 2 inches.

The above experiments were done using a 3-inch-diameter pipeline model. The tests were then repeated using a 2- and 4-inch-diameter pipeline. The 1- and 2-inch clearances were not tested because the lift forces at these clearances proved insignificant in the previous tests. Also, the tests at an orientation angle of  $75^\circ$  were eliminated, since the previous experiments demonstrated that the vertical forces measured at this angle were insignificant, and too small to be measured with any accuracy. Aside from these changes, the 4-inch-diameter pipeline was tested at the same bottom clearances, orientation angles, and wave conditions as the 3-inch-diameter model. The 2-inch-diameter model was tested at the same bottom clearances and wave conditions, but only three of the five orientation angles ( $0^\circ$ ,  $30^\circ$ , and  $60^\circ$ ) were tested.

The stillwater depth in the wave tank was held constant at 3 feet throughout the three-dimensional experiments, but since the base of the pipeline model was located 2-7/16 inches (6.19 centimeters) above the tank bottom, the effective stillwater depth over the pipeline base was 2.797 feet (85.25 centimeters). The definition sketch for the three-dimensional experiments is shown in Figure 22.

#### 4. Data Reduction.

The wave force data were taken on a two-channel strip-chart recorder with the paper advancing at a speed of 25 centimeters per second. One channel recorded the forces while the other channel simultaneously recorded the wave surface profile directly over the center of the pipeline test section, thus allowing direct correlation of the two records.

The two-dimensional experimental data were digitized manually using a Gerber digital data reduction system connected with a card punch to automatically punch the digitized values on computer cards. Using a variable linear scale, each force record was first divided into 20 equally spaced intervals per wave, each interval representing a time interval of  $T/20$ , where  $T$  is the wave period. Each force record was digitized at these points over an interval of two consecutive waves (beginning at the wave crest), thus giving 40 values for the analysis and averaging the wave forces over two wave cycles.

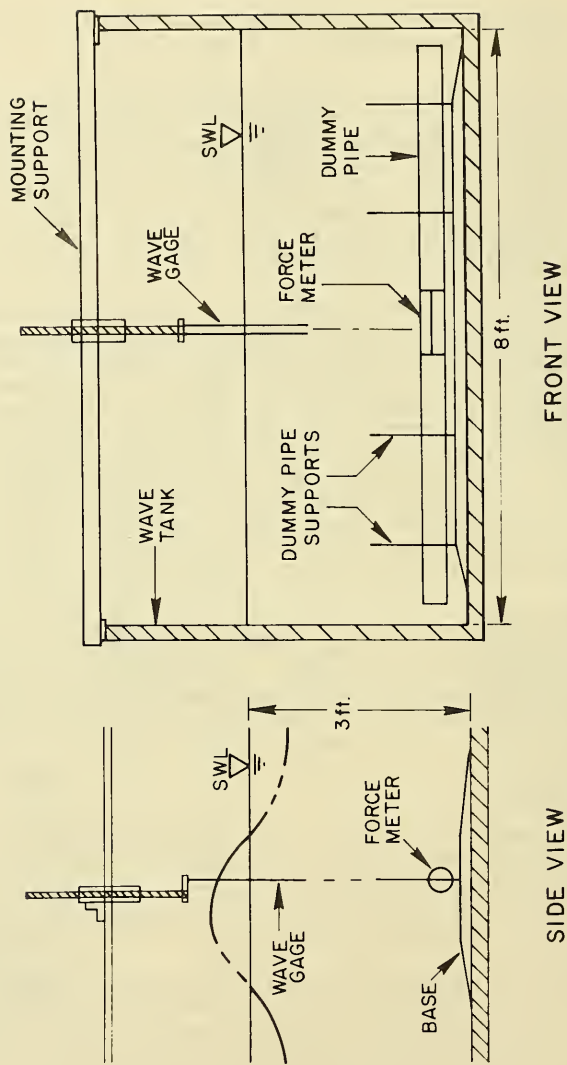


Figure 21. Experimental arrangement for three-dimensional tests.



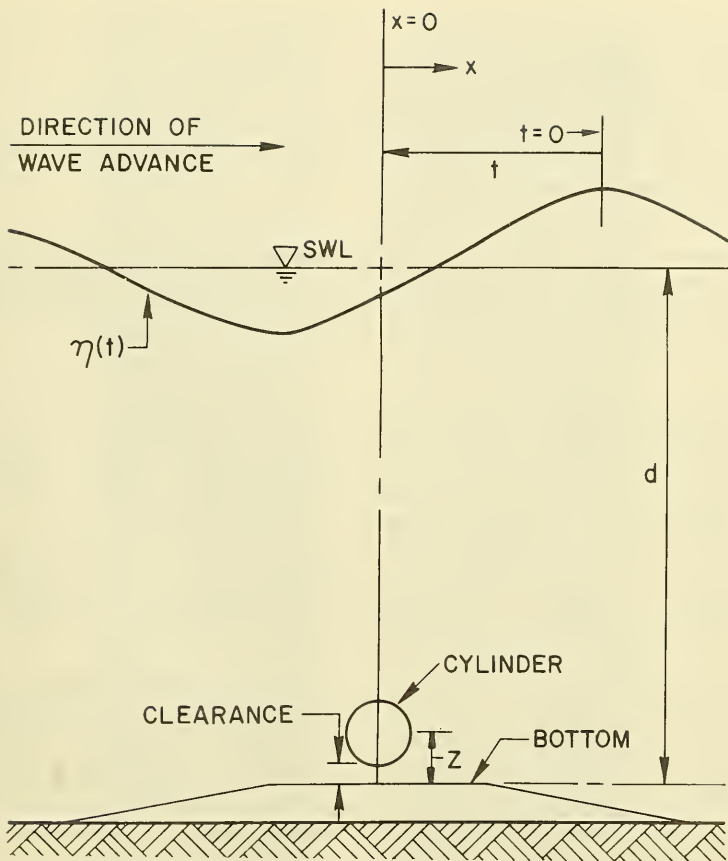


Figure 22. Definition sketch for three-dimensional experiments.

The points in the force records corresponding to the wave crests were chosen as the origin (and end) of the digitized records. These points were determined by averaging the midpoints of three or four horizontal lines drawn through the crests of the wave record at several elevations above the stillwater level (SWL). These midpoints were approximately identical except for some of the larger, longer waves in which the peak of the wave crest did not exactly coincide with the midpoint of the zero crossings of the wave crest. A sample data record is given in Figure 23.

The three-dimensional experimental data were handled differently; the data were recorded on magnetic tape with an electronic digital data acquisition system. This instrument sampled alternately from the two channels (wave and force) at a rate of 100 samples per second, resulting in 50 samples per second from each channel.

The origin at the wave crest and the wave period were determined from the digitized wave records, rather than directly from the strip-chart records. Since positive readings of the wave profile corresponded to the crest and negative readings corresponded to the trough, the point of origin of the wave crest was determined by taking the midpoint of the positive readings between zero crossings on the wave profile. The crest was thus defined as the data point closest to the midpoint of the zero crossings. The wave period was determined from the number of readings between two successive crests, since there was a time interval of  $1/50$  second between each reading. Thus, the wave period was determined to the nearest 0.02 second.

The origin of the force record was taken as the force reading corresponding to the defined origin at the center of the wave crest surface profile. In reality, there was a small timelag of  $1/100$  second between the wave profile readings and the corresponding force readings. This small timelag was ignored in the analysis, since it was felt that the accuracy of the defined origin at the wave crest was only good to the nearest  $1/50$  second, the time interval between successive readings of the wave record.

Only one wave cycle was used for analysis of the electronically digitized data. Since the data were on magnetic tape, it was impossible to determine that two successive waves had exactly the same period and height until after the calculations were completed on the computer. Thus, if the waves had slightly different periods, the time phase correlation of the corresponding force readings would be slightly in error when taken over two wave cycles. In addition, since the accuracy, resolution, and rapid sampling rate of the electronic digitizer allowed more readings per wave cycle than the manual digitizing method, a sufficiently large number of force readings could be obtained in one wave cycle.

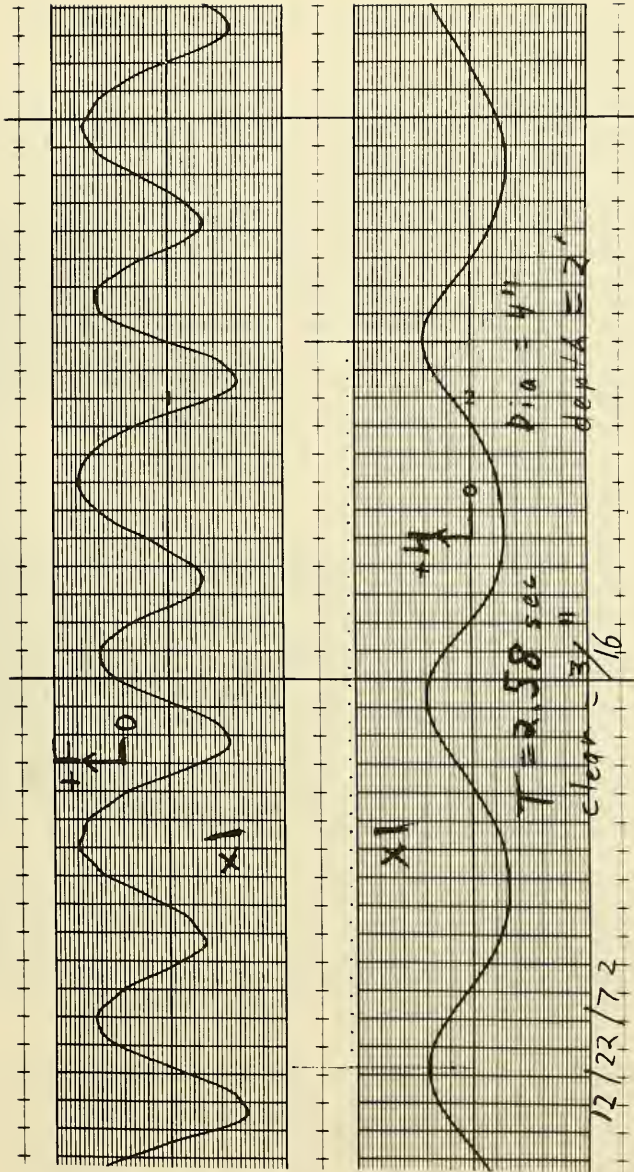


Figure 23. Example of data record.

An estimation of the accuracy of the experimental measurements, along with the sources of error, is tabulated in the Table.

A least squares analysis was performed on the digitized force data to calculate the parameters,  $C_L$ ,  $\phi$ ,  $k$ ,  $C_M$ , and  $C_D$ , of the vertical wave force equation, and the coefficients,  $C_M$  and  $C_D$ , corresponding to the horizontal wave force equation. Using this approach, values of the wave force parameters that best fit the force data throughout the entire wave cycle can be determined. These values were then substituted back into the wave force equation to calculate the force over a complete wave cycle, thus allowing comparison of the results with the original data. The least squares analysis is given in Appendix A. The computer programs used for the analysis are given in Appendixes B, C, and D; the tabulated results of the analysis are in Appendixes E, F, and G. Examples of the computer output showing comparison of the original data with the forces calculated using the results of the least squares analysis are given in Figures 24 and 25.

### III. RESULTS AND DISCUSSION

#### 1. Resultant Force Through Wave Cycle.

Both horizontal and vertical force measurements were made for some test conditions in the two-dimensional experiments using the 4-inch-diameter cylinder. The resultant force throughout the wave cycle could thus be determined for these conditions. Figures 26 to 32 show the resultant force plotted for each bottom clearance under the same wave condition, a period of 1.85 to 1.86 seconds and a wave height of 0.24 to 0.25 foot (7.32 to 7.62 centimeters). Values from the corresponding horizontal and vertical force records were plotted at 20 evenly spaced intervals ( $18^\circ$ ) through each wave cycle. The forces were plotted for two consecutive wave cycles to indicate the degree of scatter in the data. A rectangle was drawn at each plotted point to illustrate the horizontal and vertical range of the force data over the two wave cycles, and an envelope curve was drawn over these points.

Examination of these plots as a group (Fig. 33) shows the transition of the resultant wave-induced force with increasing clearance for the given wave condition ( $T = 1.85$  to  $1.86$  seconds,  $H = 0.24$  to  $0.25$  foot). The vertical component of the wave force is dominated by the lift force, while the horizontal component of the resultant force is due to the inertial and drag forces, with the inertial forces predominating for the experimental conditions tested.

For the smallest clearance (0.001 foot), in which the pipeline is almost in contact with the bottom, the resultant force attains a maximum upward value under the crests and troughs of the passing waves. The total wave force acts in the upward (positive) direction throughout the complete wave cycle, except for small downward forces in the vicinity of  $90^\circ$  and  $270^\circ$ , where the horizontal flow reverses.

Table. Estimated accuracy of experimental measurements.

<u>Variable</u>	<u>Maximum error</u>	<u>Major source of error</u>
Wave height	3 to 5 percent	Stability of amplifier with respect to calibration
Wave period	0.02 seconds (0.8 to 1.4 percent, depending on period)	Accuracy of strip-chart records for two-dimensional experiments; time interval between successive digitizer readings of wave record for three-dimensional experiments
Water depth	1/8 inch (0.5 percent for two-dimensional tests, 0.35 percent for three-dimensional tests)	Direct measurement
Pipe diameter	0.002 foot (0.610 millimeter) (0.6 to 1.2 percent, depending on diameter)	Variations in nominal diameters of tubing from which the models were constructed
Bottom clearance	0.001 foot for two-dimensional tests; 0.0005 foot (0.152 millimeter) for three-dimensional tests	Least count of point gage used to set clearance in two-dimensional tests; accuracy of metal gages used to set clearance in three-dimensional tests
Orientation angle	1.5°	Accuracy of lines marking the angles on the tank bottom, and alignment of pipeline model with the edge of the base to which it was mounted
Wave force	5 percent, except for data taken at largest orientation angles (60° and 75°) in the three-dimensional tests, which are accurate to within 10 percent	Stability of amplifier with respect to force calibration

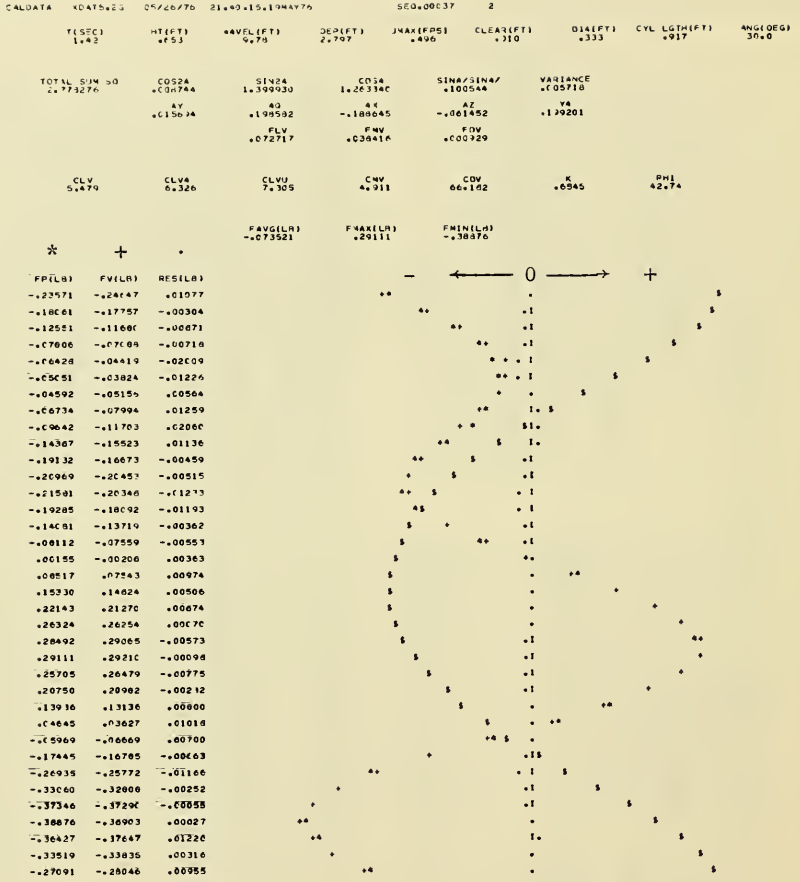
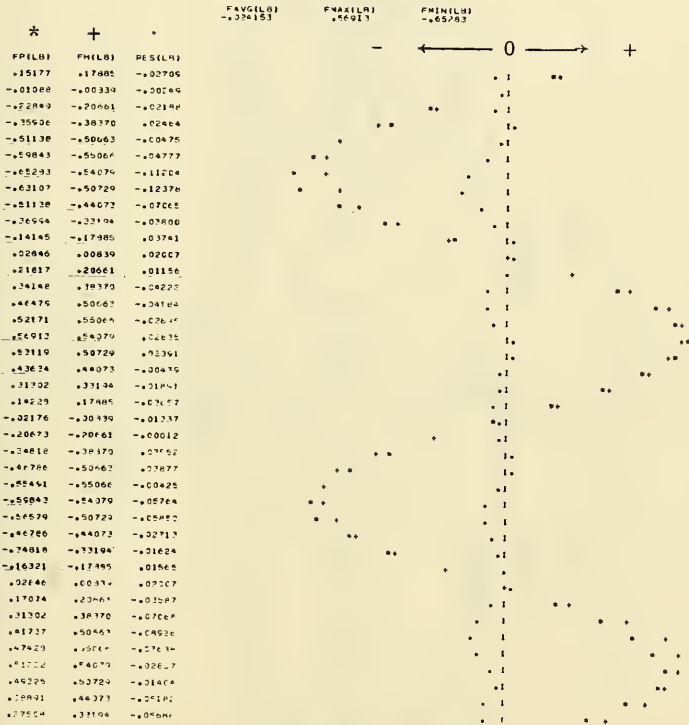


Figure 24. Example of computer output for vertical least squares analysis.

TISEC) 1.53      H(EFT) 2.27      HAV(LIFT) 17.85      DEPRFT) 2.000      JMAX(EFS) 4.359      CLEAR(EFT) 0.010      DIA(F) 3.33      CYL LGTH(F) 1.917      ANGLE(DEG) 0.

TOTAL SUM SQ      SIN      COS/COS/      AD      AZ      FWH      FWH      CMH      CMH  
 6.4670543      6.436509      4.70972      -5.50459      1.79854      1.90450      .039005      2.991      4.706



\* = measured force  
 + = calculated force  
 • = measured force - calculated force

Figure 25. Example of computer output for horizontal least squares analysis.

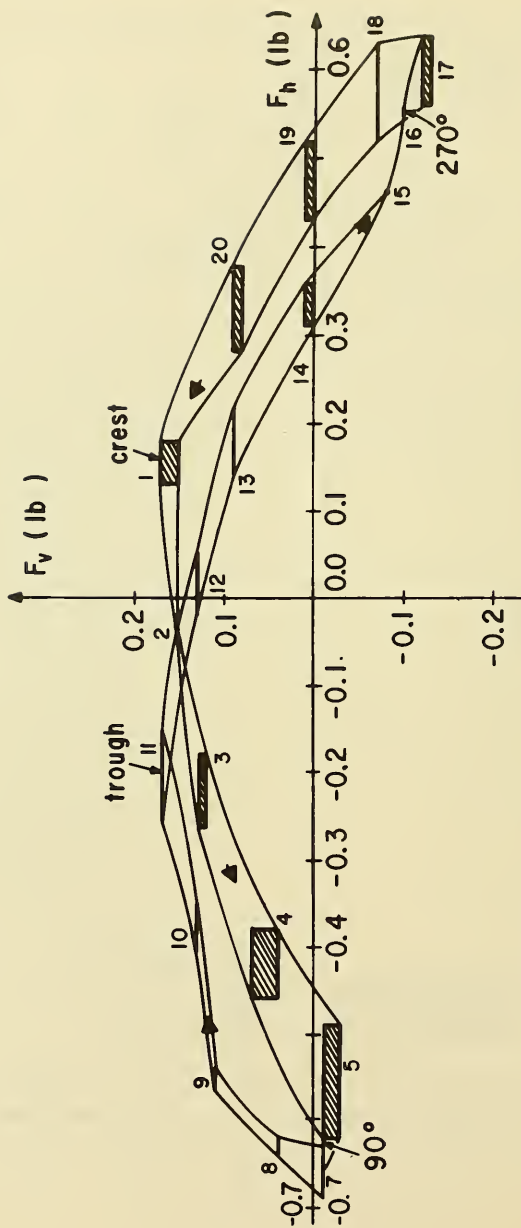


Figure 26. Resultant force through wave cycle for 0.001-foot clearance, 1.85-second period, and 0.24-foot height.



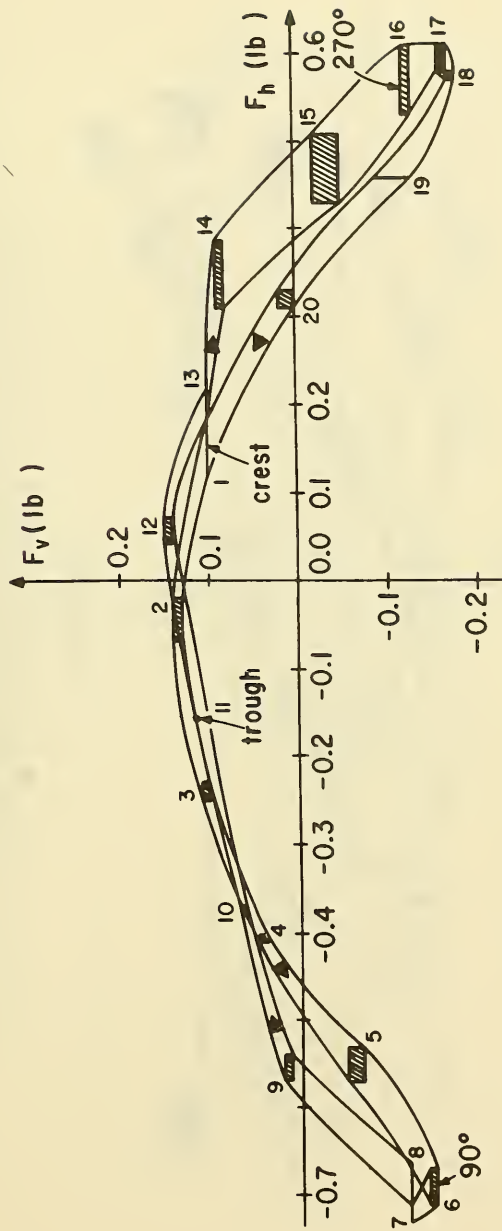


Figure 27. Resultant force through wave cycle for 1/16-inch clearance, 1.86-second period, and 0.24-foot height.

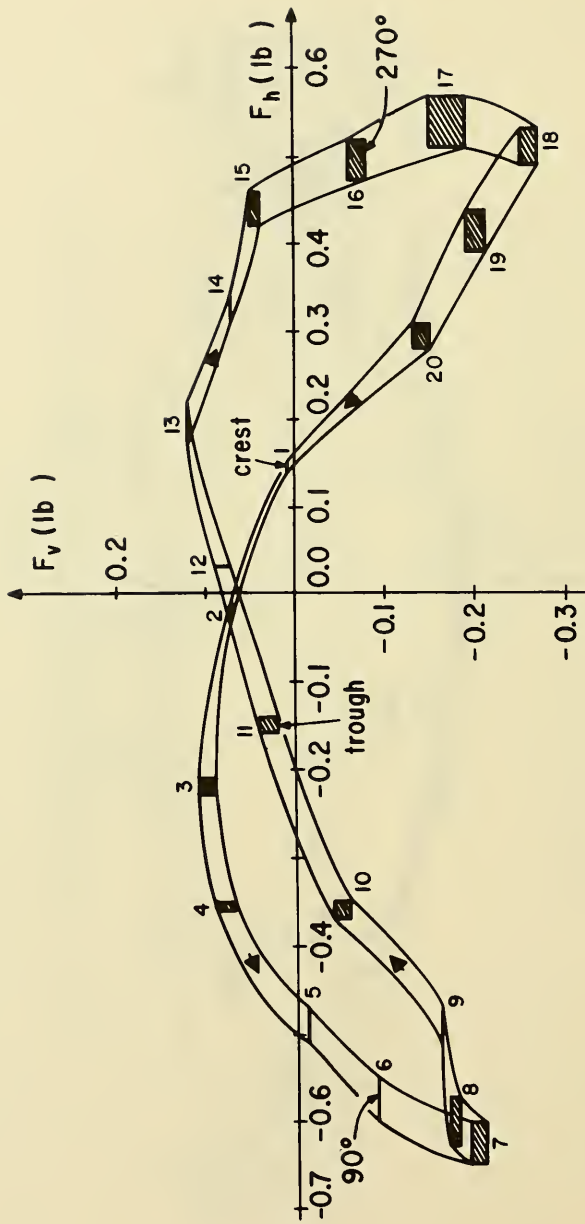


Figure 28. Resultant force through wave cycle for 1/8-inch clearance, 1.85-second period, and 0.25-foot height.

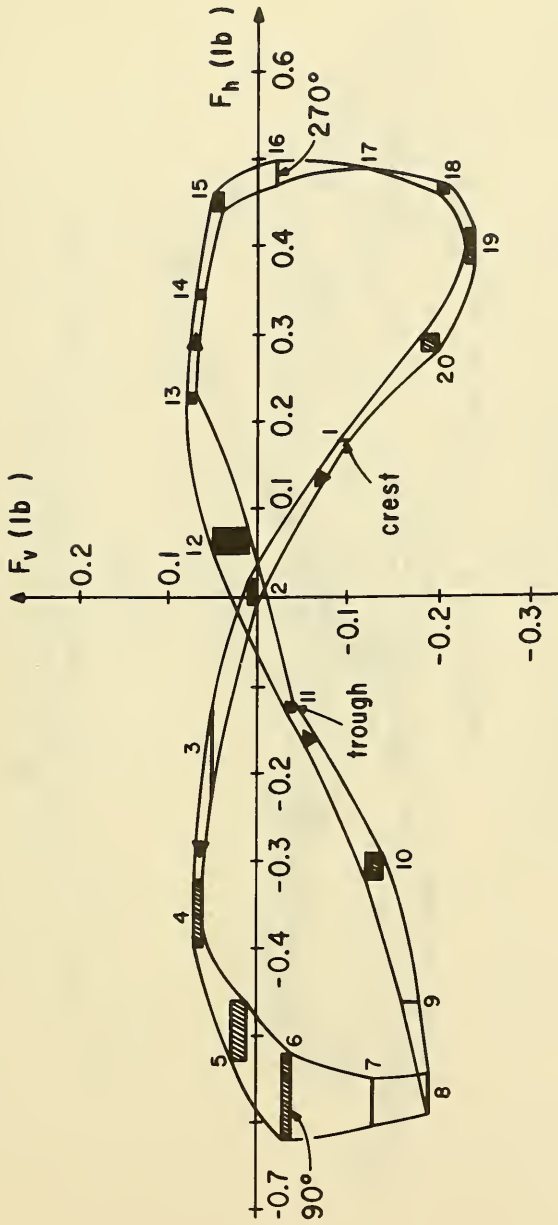


Figure 29. Resultant force through wave cycle for 3/16-inch clearance, 1.85-second period, and 0.25-foot height.

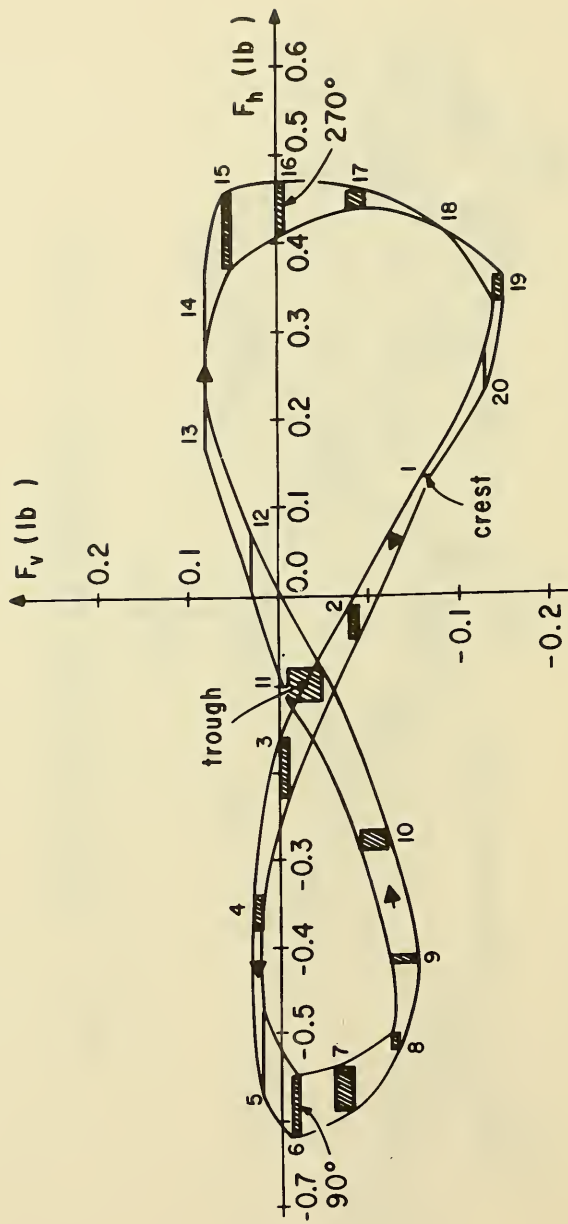


Figure 30. Resultant force through wave cycle for 1/4-inch clearance, 1.86-second period, and 0.25-foot height.

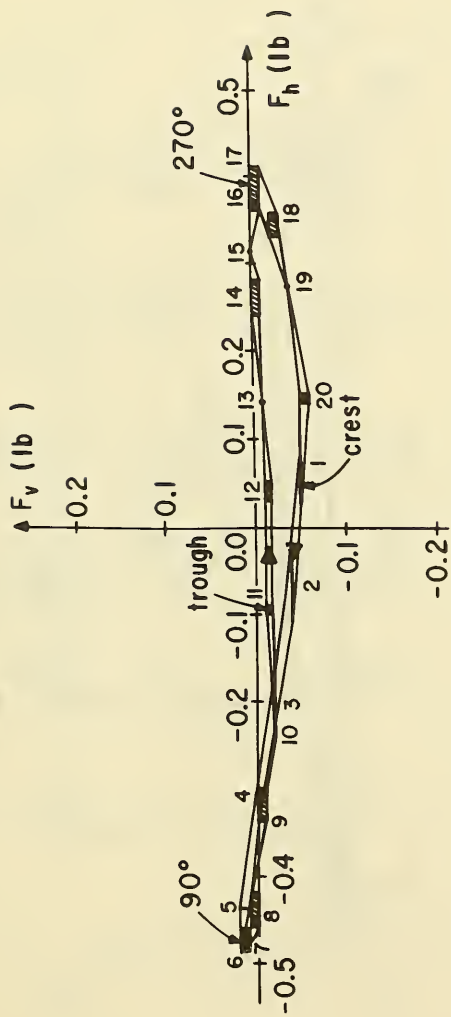


Figure 31. Resultant force through wave cycle for 1-inch clearance, 1.86-second period, and 0.24-foot height.

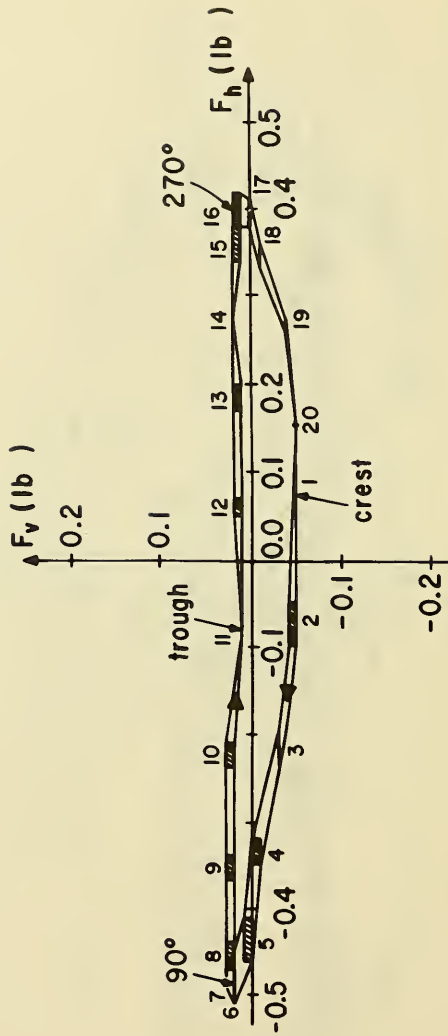


Figure 32. Resultant force through wave cycle for 2-inch clearance, 1.86-second period, and 0.25-foot height.

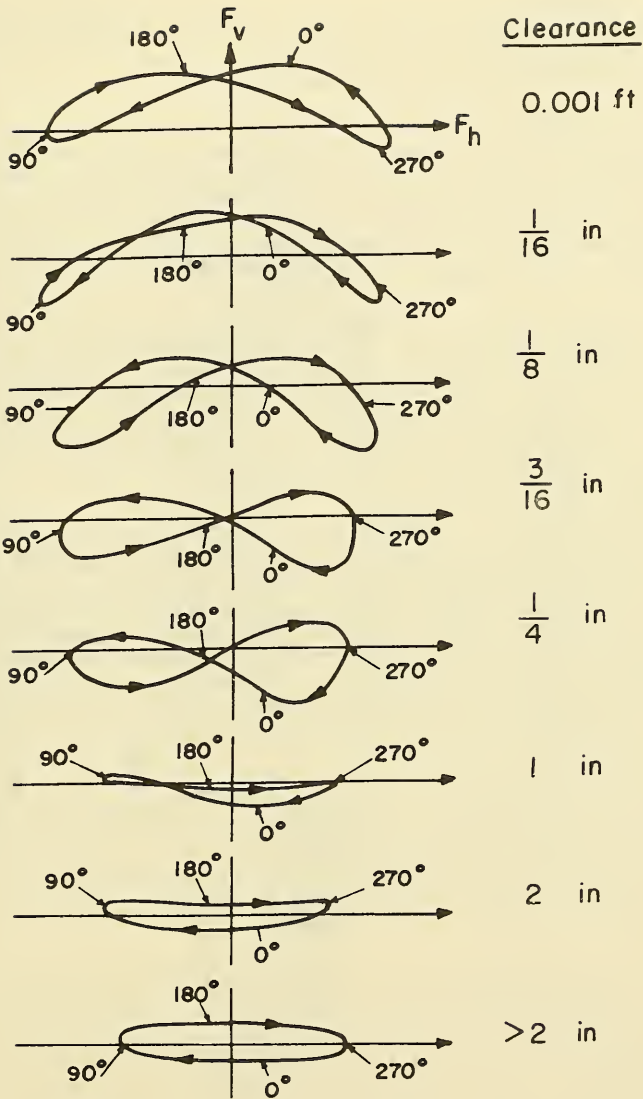


Figure 33. Change in resultant force with increasing clearance.

As the clearance is increased to 1/16 inch, the maximum upward forces decrease in magnitude, and also occur slightly later in the wave cycle. At the same time, the downward forces increase, reaching their maximum values at approximately  $90^\circ$  and  $270^\circ$ .

Further increases in the bottom clearance produce a continuous shift of the positions of both the maximum upward and maximum downward forces later in the wave cycle. Simultaneously, the forces become downward rather than upward for a larger part of the cycle. At the same time, the vertical components of the wave force under the crests and troughs become negative and increase in the downward direction, while the negative forces at  $90^\circ$  and  $270^\circ$  gradually decrease to zero.

At a 1-inch clearance, the resultant force acts downward throughout almost the complete wave cycle, with maximum downward forces occurring under the crests and troughs of the passing waves. The vertical forces are zero at  $90^\circ$  and  $270^\circ$ , the positions of the maximum horizontal inertial forces. However, the lift effect is not very large for the 1-inch clearance. The resultant force plot for the 2-inch clearance shows that the lift effect is still present, but is relatively small, even in comparison to the small vertical inertial forces.

At a slightly larger clearance, the lift effect will disappear, and the vertical forces will be due almost entirely to the inertial forces, since the vertical drag forces are negligible near the bottom. At this clearance, the inertial force will act upward under the trough and downward under the crest, so the resultant force plot will take the form of an approximately symmetrical ellipse. This condition is shown in Figure 34 for a smaller wave period (1.23 seconds), with a 1-inch bottom clearance. The ellipse is distorted slightly, due to the small drag forces acting in the horizontal direction,  $90^\circ$  out of phase with the larger horizontal inertial forces.

The horizontal components of the resultant wave force are also affected by the proximity of the bottom boundary. Although the horizontal water particle velocities and accelerations increase with distance above the bottom, the corresponding horizontal drag and inertial forces are larger when the pipe is close to the bottom than when it is located above at larger clearances.

Figures 35, 36, and 37 show the resultant force plots at both large and small bottom clearances, for a wave with a period of 0.95 to 0.96 second and a height of 0.24 to 0.25 foot. Because the wave period is small, the horizontal excursions of the water particles at the bottom and the duration of the horizontal flow are too small for the lift effect to develop. So the forces acting in both the horizontal and vertical directions are mostly inertial, with a small drag component in the horizontal direction. The resultant force plots therefore take the form of an ellipse.



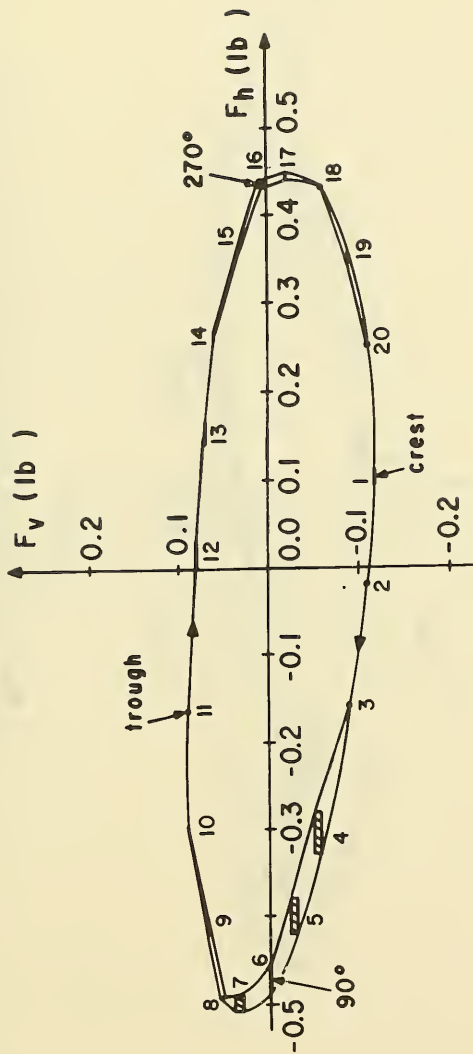


Figure 34. Resultant force through wave cycle for 1-inch clearance, 1.23-second period, and 0.3-foot height.

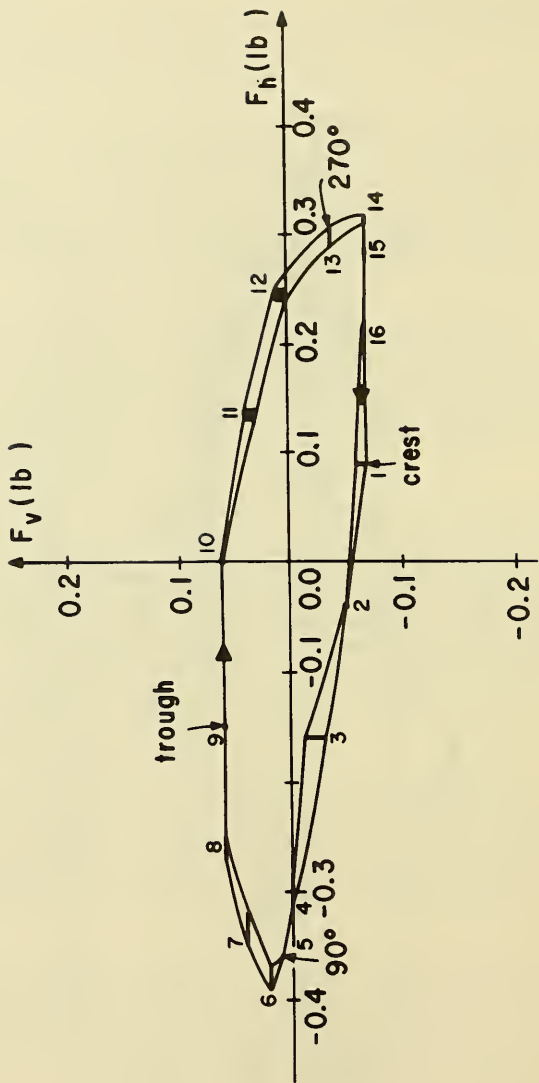


Figure 35. Resultant force through wave cycle for 0.001-foot clearance, 0.95-second period, and 0.24-foot height.

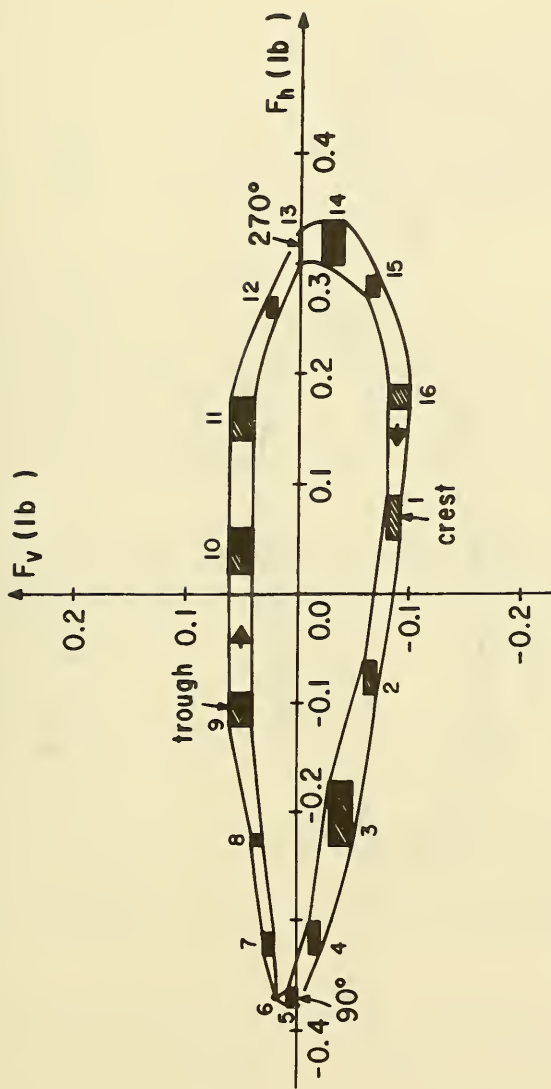


Figure 36. Resultant force through wave cycle for 1/16-inch clearance, 0.95-second period, and 0.24-foot height.

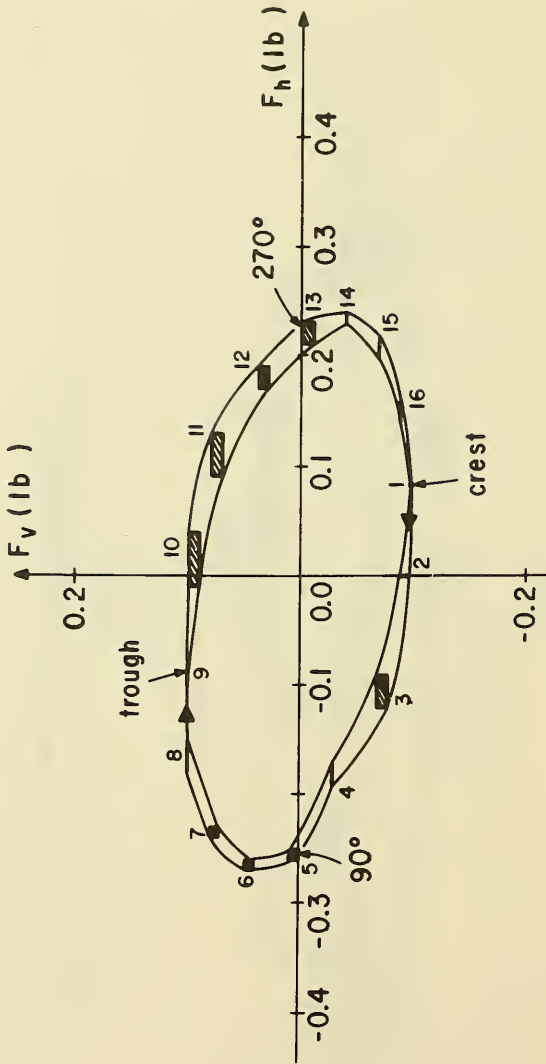


Figure 37. Resultant force through wave cycle for 2-inch clearance, 0.96-second period, and 0.25-foot height.

However, the horizontal components of the resultant forces are larger at the smallest bottom clearances, even though the lift phenomenon is absent. The presence of the bottom boundary produces an asymmetric flow field around the pipeline. The resulting velocities and accelerations of the water particles over the pipe section are thus modified by the presence of the boundary, and the associated horizontal forces are larger than they would be if subject to the same kinematics in the absence of the boundary. The increased horizontal forces on pipelines located close to the bottom are reflected in increased values of the coefficients of mass and drag,  $C_M$  and  $C_D$ .

## 2. Orientation Angle Considerations.

The coefficient of lift calculated in the least squares analysis of the experimental data was computed using two alternative approaches (Fig. 38): (a) the total horizontal water particle velocity in the direction of wave advance, with the projected area of the pipeline in the plane perpendicular to the direction of wave advance; and (b) only the component of the horizontal water particle velocity perpendicular to the pipeline axis, with the projected area in the plane parallel to the pipeline axis.

After tabulating the data from the three-dimensional experiments, it became apparent that the second method gave consistent values of the coefficient of lift for all angles of orientation. In contrast, the values of  $C_L$  obtained using the first method gave values that were low, and which decreased with increasing angles of orientation (where  $0^\circ$  corresponds to a pipeline parallel to the wave crests).

Relationships between the coefficient of lift,  $C_L$ , and the parameters,  $\phi$  and  $k$ , of the lift force equation were the same for all angles of orientation when  $C_L$  was calculated considering only the component of the horizontal velocities perpendicular to the pipeline axis.

In addition, relationships involving any of the parameters of the lift force equation ( $C_L$ ,  $\phi$ , or  $k$ ) and various dimensionless parameters defining the wave and pipeline conditions were consistent for all angles of orientation when the horizontal water particle velocity acting on the pipe section was treated by considering only the component perpendicular to the pipeline, and completely ignoring the parallel component.

Thus, the results of this investigation show that the modified lift force equations presented in this report can be applied to pipelines located at any angle of orientation with respect to the wave crests. However, only the component of the horizontal water particle velocity perpendicular to the pipeline axis should be considered as contributing to the wave-induced lift force acting on the pipeline. Using this approach, the parameters,  $C_L$ ,  $\phi$ , and  $k$ , defining the lift forces exhibit the same quantitative relationships between the various dimensionless parameters defining the wave and pipe conditions, regardless of the angle of orientation.

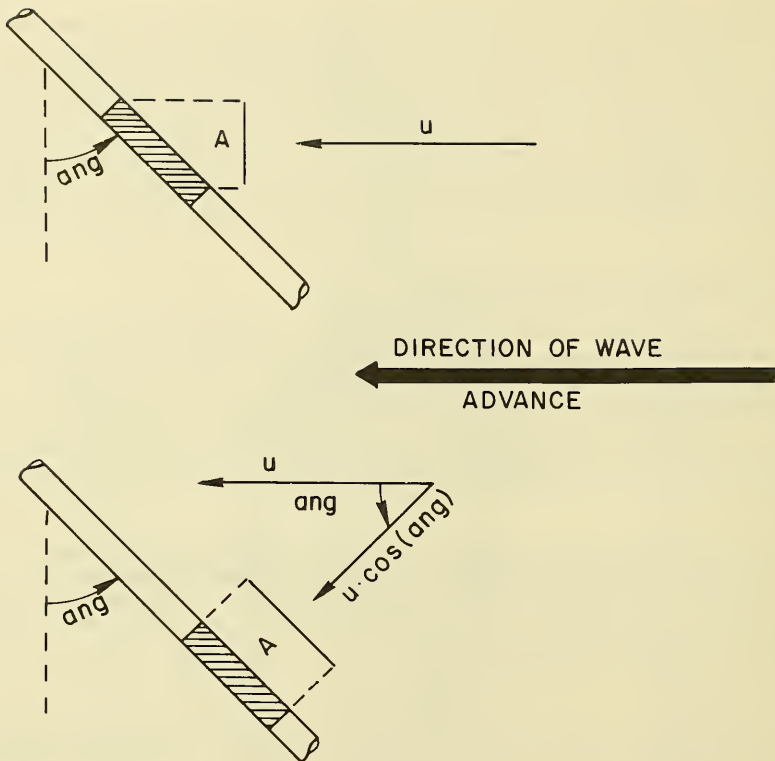


Figure 38. Alternative approaches for handling pipeline orientation angles.

### 3. Interrelationships Between $C_L$ , $\phi$ , and $k$ .

$\phi$  and  $k$  were defined as varying from  $0^\circ$  to  $90^\circ$  and 0 to 1, respectively, with increasing clearance.  $\phi = 0^\circ$  and  $k = 0$  correspond to the case of a pipeline in contact with the bottom (no clearance), while the maximum values of  $\phi = 90^\circ$  and  $k = 1$  correspond to the case of a large enough clearance so that the choking phenomenon does not occur at any time throughout the wave cycle. Since a simultaneous increase of both parameters was noted in the data for increasing clearance between the two limiting cases, it was suspected that a direct relationship may exist between  $\phi$  and  $k$ . Such a relationship was found, as shown in Figure 39. The same relationship held for all three pipe diameters tested, regardless of the orientation angle, indicating that the relationship was independent of these two factors, and was thus valid for any pipeline configuration in which the lift effect was present.

In this plot and the ones that follow, the data for orientation angles from  $0^\circ$  to  $30^\circ$  were plotted for each pipe diameter, without differentiating the data corresponding to each angle. The relationships shown were found to be valid regardless of the angle of orientation, provided the data were handled as discussed above (using the component of the horizontal velocity perpendicular to the pipeline axis). The data corresponding to each pipe diameter are distinguished by using different plot symbols. The same relationships hold for orientation angles of  $45^\circ$ , but these data were not plotted in order to minimize scatter so that differences between the pipe diameters could be detected more easily. In general, the same relationships held for orientation angles up to  $60^\circ$ . But in some cases, the lift effect was negligible at high orientation angles, so the values of the associated parameters ( $C_L$ ,  $\phi$ , and  $k$ ) were less accurate. Thus, plotting all of the data corresponding to the larger orientation angles would introduce additional scatter, obscuring the valid relationships which were consistent when the lift forces were significant.

A relationship was found between the coefficient of lift,  $C_L$ , and the parameters,  $\phi$  and  $k$  (Figs. 40 and 41).  $C_L$  appears to be better correlated with  $k$  than with  $\phi$ . Note that for minimum values of  $k$  and  $\phi$ , corresponding to the case of a pipeline in contact with the bottom, the value of  $C_L$  is approximately 4.5. This value is of interest, since it agrees with the potential flow solution ( $C_L = 4.495$ ) for the value of the coefficient of lift for a circular cylinder in contact with a plane wall, subject to an inviscid steady flow (Yamamoto, Nath, and Slotta, 1973).

Maximum values of  $C_L$  occur at approximately  $k = 1/2$ , corresponding to maximum lift forces that are equal in both the upward and downward directions. The average value of the coefficient of lift at this point is about 9.0, with values extending up to about 10.5. These maximum values of  $C_L$  are attained at approximately  $\phi = 25^\circ$  to  $30^\circ$  in the  $\phi$  versus  $C_L$  plot.

Since the coefficient of lift,  $C_L$ , defines the combined magnitude of both the positive and negative lifts, it can be separated into two parts: (a) the part defining the magnitude of the positive lift,  $C_L(1-k)$ , and

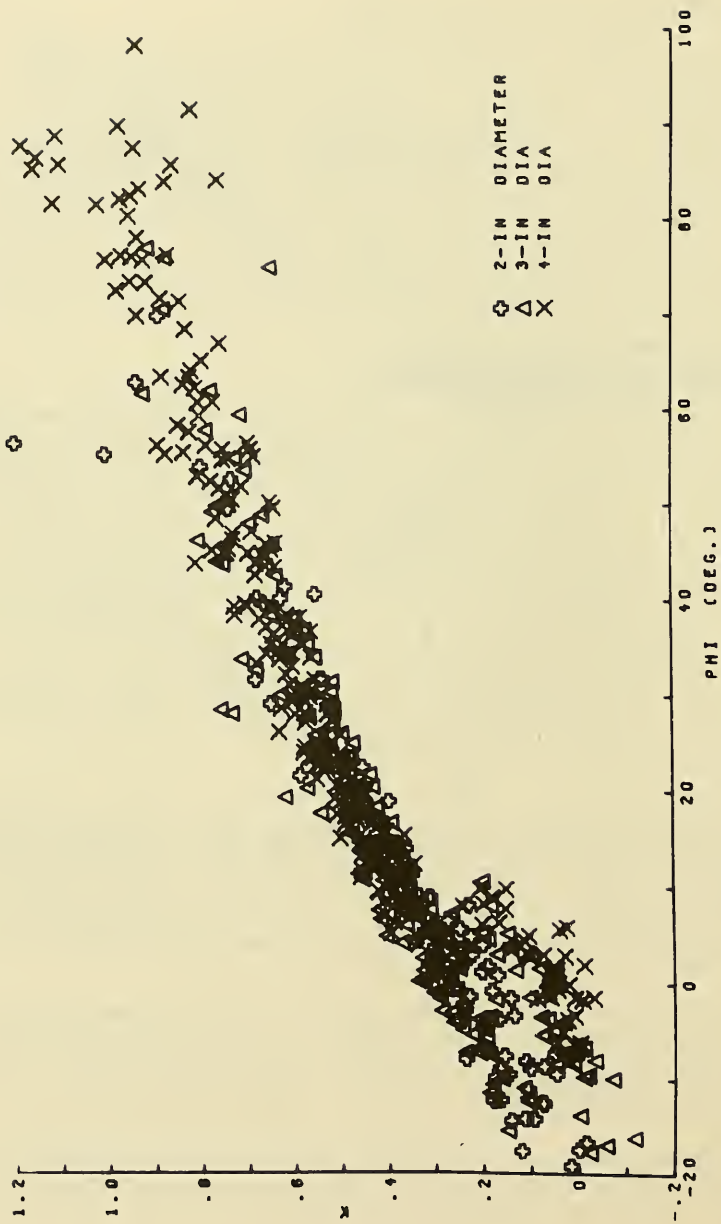


Figure 39.  $\phi$  versus  $k$ .



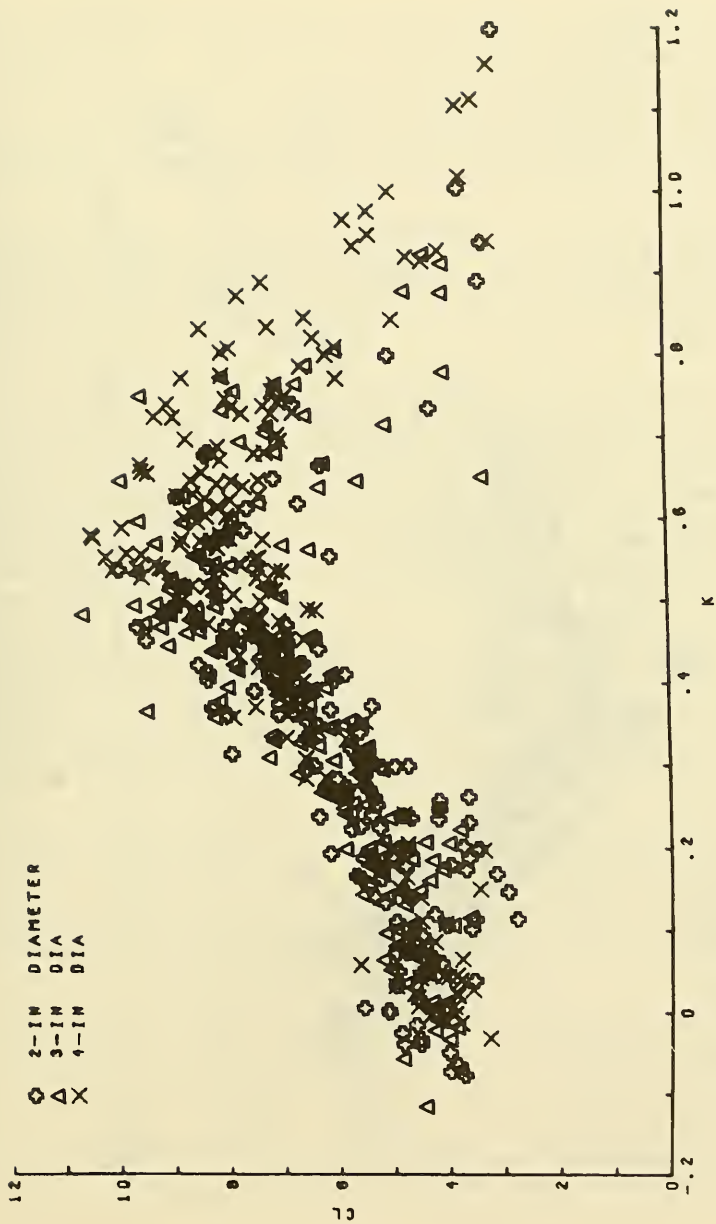


Figure 40.  $C_L$  versus  $k$ .

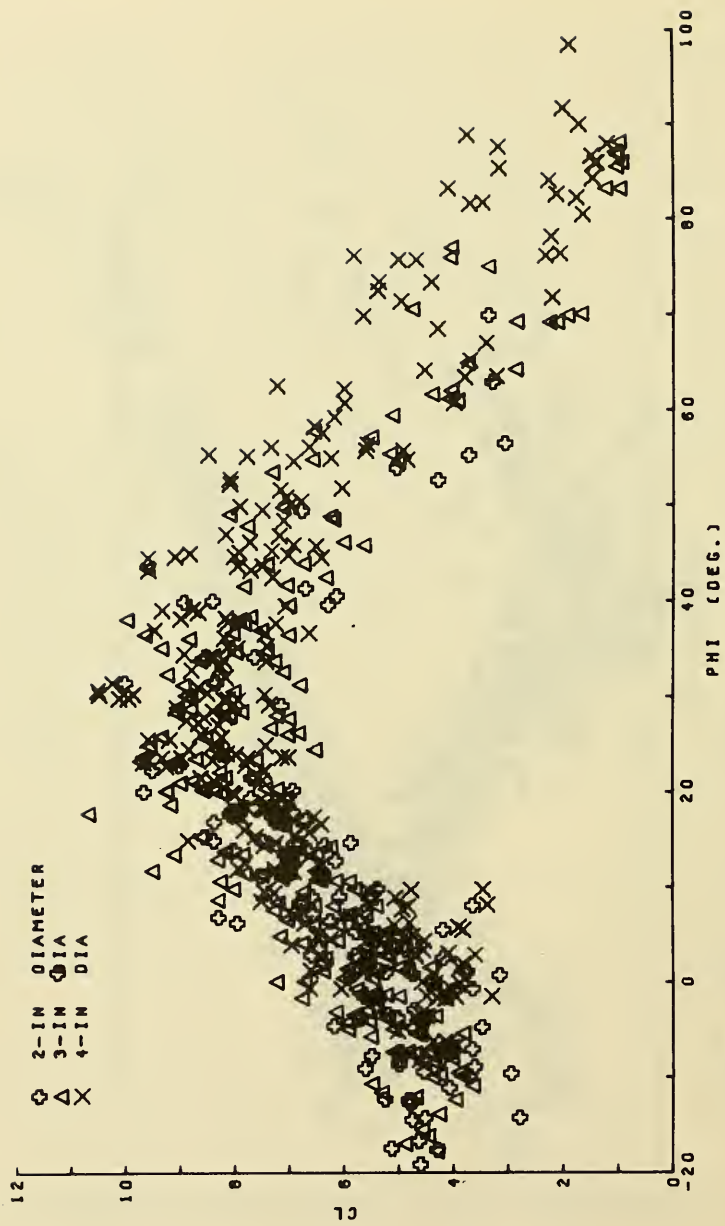


Figure 41.  $C_L$  versus  $\phi$ .

(b) the part defining the magnitude of the negative lift,  $C_L(k)$ . The quantities,  $C_L(1-k)$  and  $C_L(k)$ , can be referred to as the effective positive coefficient of lift and the effective negative coefficient of lift, respectively. Since  $C_L = 9.0$  for  $k = 1/2$ , both  $C_L(1-k)$  and  $C_L(k)$  are equal to 4.5 at this point. This means that the lift forces can reach the same maximum magnitude in both the upward and downward directions as are attained in the upward direction only for the same pipe in contact with the bottom (where  $C_L(1-k) = 4.5$ , but  $C_L(k) = 0$ ).

The effective positive and negative coefficients of lift are plotted versus both  $\phi$  and  $k$  in Figures 42 to 45. Again, the correlations are much better with  $k$  than with  $\phi$ . The average value of  $C_L(1-k)$  drops only slightly from 4.5 at  $k = 0$  and  $k = 1/2$ , but for values of  $k$  greater than  $1/2$ , the effective positive coefficient of lift drops rapidly to a value of 0 when  $k = 1$ .

The average value of  $C_L(k)$  increases with  $k$  until it reaches a maximum value of about 6.0 when  $k = 0.75$ , and then decreases to about 4.5 when  $k = 1$ . Individual maximum values of  $C_L(k)$  attain values slightly greater than 7.0 in the vicinity of  $k = 0.75$ . But even the average maximum value of 6.0 for the effective negative coefficient of lift indicates that the downward lift forces may attain maximum values 33 percent greater than the maximum possible lift forces acting in the upward direction. Maximum values of  $C_L(k)$  corresponds to a value of  $\phi$  of about  $45^\circ$ , which is half way through the phase shift cycle.

The potential flow theory gives a value of  $C_L = 4.495$  for zero bottom clearance, with a discontinuous jump to very high negative values of  $C_L$  for a very small clearance (Yamamoto, Nath, and Slotta, 1973). In the potential flow solution, the value of  $C_L$  depends only on the relative clearance; i.e., the ratio clearance-diameter. The coefficient of lift is negative whenever the pipe is not in contact with the bottom, and its magnitude decreases as the relative clearance is increased.

Although the potential flow solution appears to work reasonably well when a pipeline is touching the bottom, this approach does not work when there is a small clearance. This is because viscous effects are very important for the flow through the narrow bottom clearance constriction. The choking phenomenon limits the maximum flow velocities and corresponding pressure drops on the bottom side of the pipeline, thereby limiting the maximum possible downward lift forces.

The results of this investigation indicate that the effective negative coefficient of lift,  $C_L(k)$ , can attain a maximum value of only 7.0. This is much less than the values of  $C_L$  suggested for small relative clearances by potential flow theory. The coefficient of lift is obviously not a simple function of relative clearance, since for a given clearance and diameter, both the lift effect and the coefficient of lift will vary with the wave-induced flow conditions. For the smallest relative clearances, the positive lift forces were larger than the negative lift forces, especially where the horizontal water particle velocities and excursions were high.

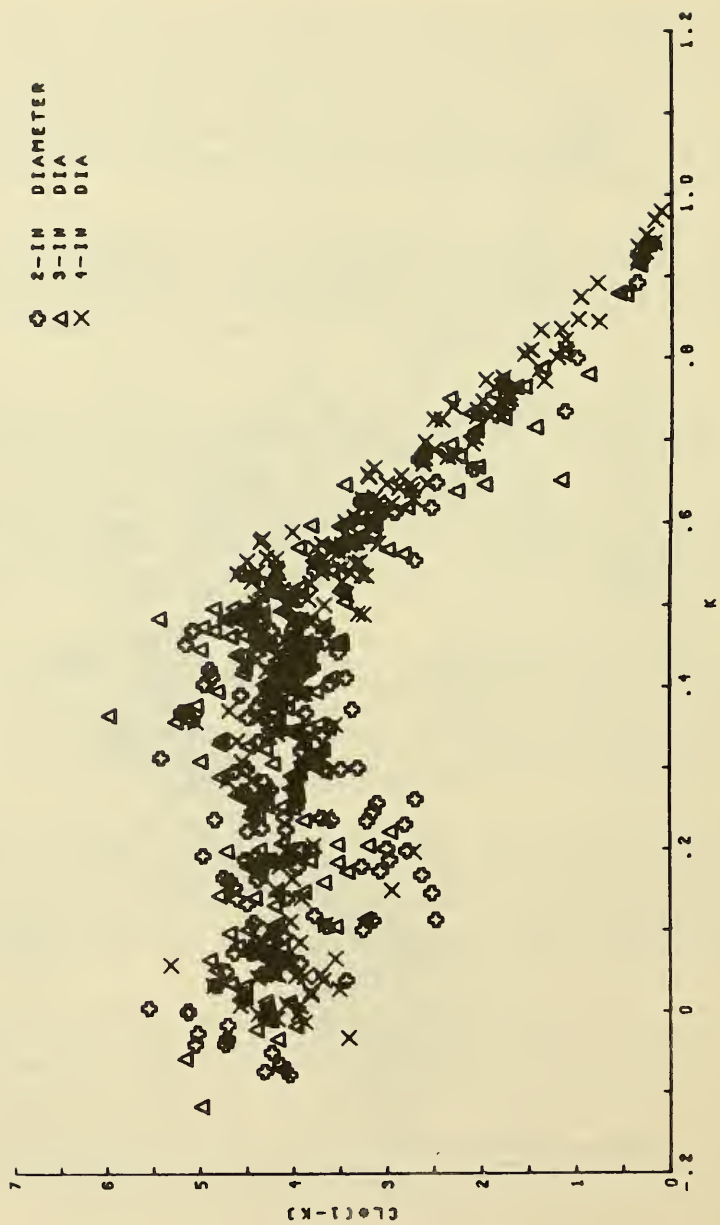


Figure 42. Effective positive coefficient of lift versus  $k$ .

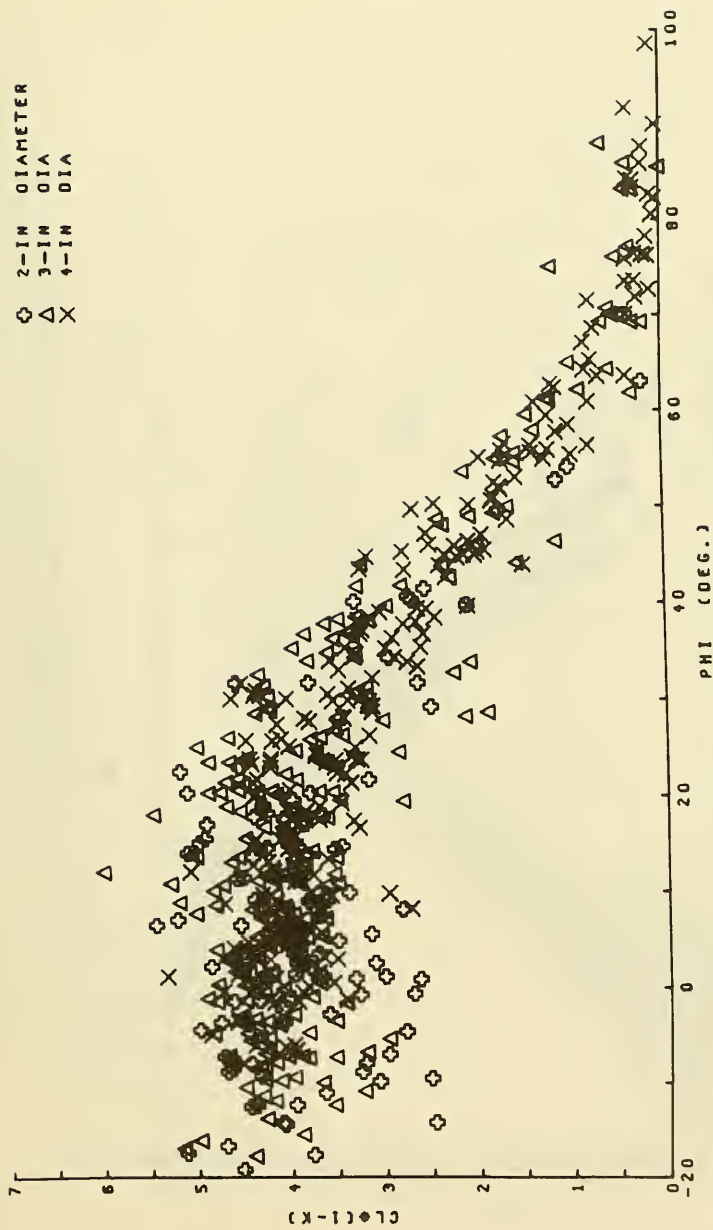


Figure 43. Effective positive coefficient of lift versus  $\phi$ .

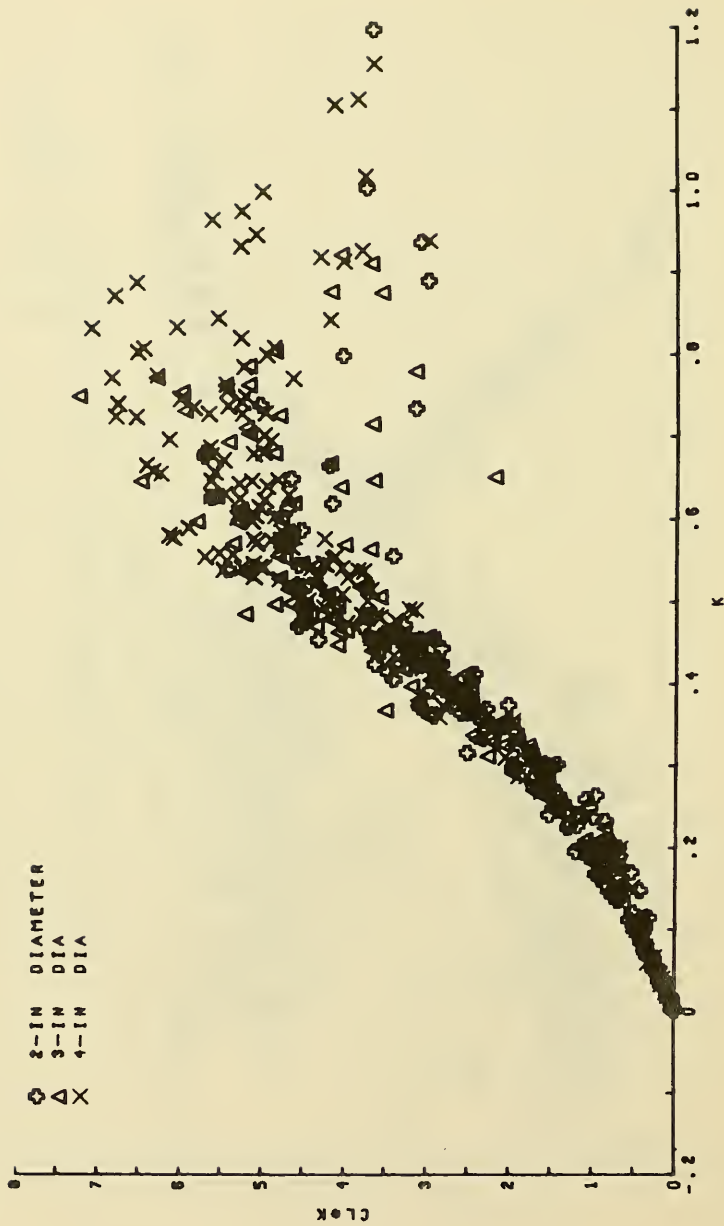


Figure 44. Effective negative coefficient of lift versus k.

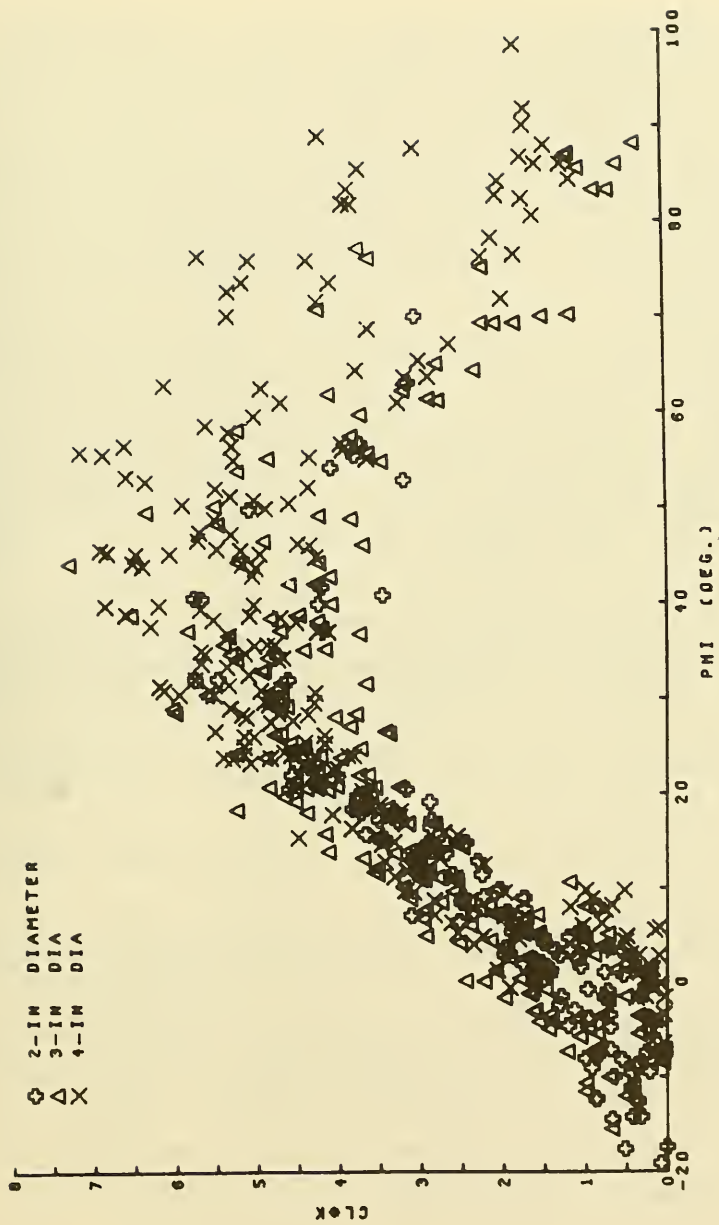


Figure 45. Effective negative coefficient of lift versus  $\phi$ .

The largest negative lift forces do not occur at clearances where the choking effect is absent (corresponding to  $k = 1$  and  $\phi = 90^\circ$ ). Rather, the largest values of the effective negative coefficient of lift correspond to values of  $\phi = 45^\circ$  and  $k = 0.75$ . Interestingly, when  $k = 1$  and  $\phi = 90^\circ$  where the positive lift forces have decreased to zero and the choking effect does not develop, the maximum effective negative coefficient of lift is approximately 4.5, the same magnitude as the potential flow solution for the positive coefficient of lift for zero bottom clearance. However, as the bottom clearance is increased further,  $k$  and  $\phi$  remain at 1 and  $90^\circ$ , respectively, while the effective negative coefficient of lift decreases to zero (with the diminishing lift forces).

The significance of these results is easily seen by following these relationships for a given pipe and wave as the pipeline is raised from the bottom, and  $k$  goes from 0 to 1. In the interval from  $k = 0$  to  $1/2$ , the magnitude of the maximum upward lift forces remains the same, which is approximately equal to the potential flow solution for a cylinder in contact with the bottom ( $C_L = 4.5$ ). However, at the same time, the negative lift forces increase continuously, reaching a magnitude equal to the positive lift forces at  $k = 1/2$  ( $C_L(1-k) = C_L(k) = 4.5$ ). Simultaneously, there is a shift in the positions of both the maximum positive and negative lift forces, since  $\phi$  increases from  $0^\circ$  to  $30^\circ$ .

In the interval  $k = 1/2$  to 1, the maximum positive lift forces continuously decrease to zero. At the same time, the maximum negative lift forces increase to reach a maximum value at  $k = 0.75$  (where  $C_L(k) = 6.0$  or  $7.0$ ), and then decrease back to a maximum corresponding to  $C_L(k) = 4.5$  at  $k = 1$ . The point of maximum negative lift corresponds to  $\phi = 45^\circ$ , the midpoint of the phase shift cycle.

The phase shift of the maximum lift forces is only half as much in the interval  $k = 0$  to  $1/2$  (where  $\phi$  goes from  $0^\circ$  to  $30^\circ$ ) as in the interval  $k = 1/2$  to 1 (where  $\phi$  goes from  $30^\circ$  to  $90^\circ$ ).

At  $k = 1$ , only negative lift forces exist, and these go to zero as the bottom clearance is increased further.

All of the above interrelationships between  $\phi$ ,  $k$ ,  $C_L$ ,  $C_L(1-k)$ , and  $C_L(k)$  were the same for all pipe diameters tested, regardless of the angle of orientation (provided that  $C_L$  was calculated considering only the component of the horizontal velocity perpendicular to the pipeline axis). Thus, for the range of conditions tested, these interrelationships were independent of the scale and configuration of the pipeline. Also, there is no mention of the wave conditions, which indicates the interrelationships are independent of the wave conditions as well.

The relationships between the parameters,  $C_L$ ,  $\phi$ , and  $k$ , defining the lift force equation are useful, since if either  $\phi$  or  $k$  is known, the other two parameters can be determined. All that is needed is a relationship between  $\phi$  or  $k$  and the wave and pipeline conditions.



There appears to be a better correlation between  $k$  and the parameters involving  $C_L$  ( $C_L$ ,  $C_L(1-k)$ , and  $C_L(k)$ ) than between the analogous relationships using  $\phi$ , so the former relationships should be used. Also, in comparing the plots of  $C_L(1-k)$  versus  $k$  (Fig. 42) and  $C_L(k)$  versus  $k$  (Fig. 44), the scatter appears minimal in the plot with  $C_L(k)$  for the interval of  $k$  between 0 and 1/2. For the interval of  $k$  between 1/2 and 1, the scatter is much less on the plot between  $C_L(1-k)$  and  $k$ . Therefore, it is suggested that when determining a value of  $C_L$  for a given value of  $k$ , the plot of  $C_L(k)$  versus  $k$  be used for values of  $k$  less than 1/2 (except for  $k$  close to 0), and the plot of  $C_L(1-k)$  versus  $k$  be used for values of  $k$  greater than 1/2 (except for  $k$  close to 1) (see Fig. 46). For  $k$  close to 0, it can be assumed that  $C_L = 4.5$ . However, for  $k \approx 1$ , the value of  $C_L$  can vary from about 4.5 to zero, since as the clearance is increased from the point where  $\phi = 90^\circ$  and  $k = 1$ , both  $\phi$  and  $k$  remain at their maximum values of  $90^\circ$  and 1, respectively, while the lift effect diminishes to zero.

When the above relationships between  $\phi$ ,  $k$ ,  $C_L$ ,  $C_L(1-k)$ , and  $C_L(k)$  are plotted for only the 4-inch-diameter pipe model, the scatter is reduced. Although the data for all three diameters completely overlap (showing the same relationships hold for all diameters), the amount of scatter increases with the smaller diameter models. This is because the data extend to higher relative clearances (clearance-diameter) for the smaller diameter models than the corresponding data for the 4-inch-diameter model, since all models were tested at the same actual clearances.

Since the lift effect diminishes at high values of the relative clearance, the lift forces on the smaller diameter models at the largest bottom clearances were very small in many cases. This is especially true for the smaller waves and higher orientation angles, where the horizontal velocities perpendicular to the pipeline were very low. In such cases, the lift forces were often insignificant, so the values of  $C_L$ ,  $\phi$ , and  $k$  calculated from the least squares analysis were not as accurate.

In addition, as the lift forces decrease with high relative clearances, eddy-induced forces may approach the magnitude of the lift forces, thus introducing further error in the calculated values of  $C_L$ ,  $\phi$ , and  $k$ .

The lift forces were generally significant for all clearances tested using the 4-inch-diameter pipe section, and since the measured forces were larger, the experimental error involved in measuring them was less than for the smaller diameter models.

Because of this, the data taken for very large bottom clearances were not included in the plotted relationships. For higher clearances, values of  $k$  and  $\phi$  equal to 1 and  $90^\circ$ , respectively, would be expected, since the choking phenomenon would not occur throughout the wave cycle. However, as the clearance is increased, the lift effect diminishes, resulting in decreasing values of the coefficient of lift.

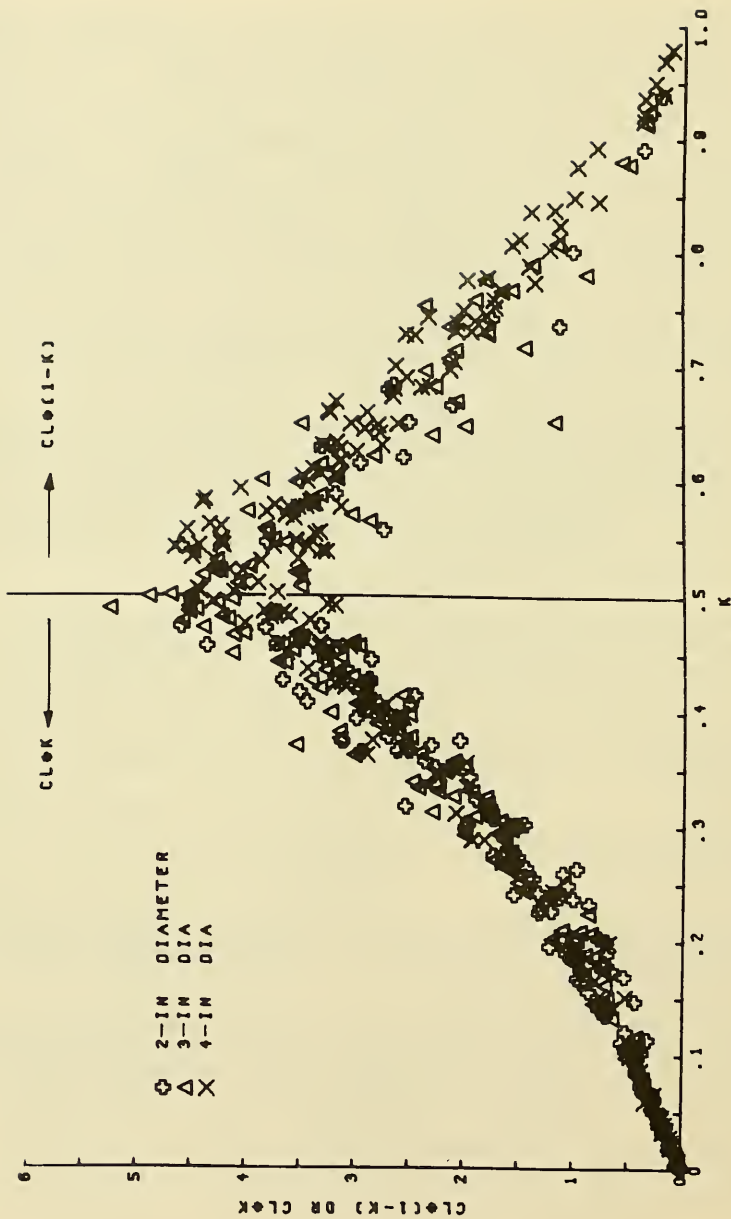


Figure 46.  $C_L(1-k)$  or  $C_L(k)$  versus  $k$ .

If such data were included in the plots of  $C_L$  versus  $k$  and  $\phi$ , values of  $C_L$  ranging from 0 to the maximum values shown in Figures 40 and 41 would be present in the vicinity of  $k = 1$  and  $\phi = 90^\circ$  in the respective plots. The same applies to the plots of  $C_L(k)$  versus  $k$  and  $\phi$ .

These trends were observed in the data taken for the largest bottom clearances (1 and 2 inches). However, since these lift forces were so small, a significant amount of error could be introduced into the calculated values of  $C_L$ ,  $\phi$ , and  $k$  because of the presence of eddy-induced forces, as discussed above. Therefore, these data were omitted from the plotted relationships, since errors in  $\phi$  or  $k$  corresponding to low values of  $C_L$  would produce considerable scatter, obscuring the valid relationships shown.

#### 4. Relationships Between $\phi$ and $k$ and Parameters Defining the Wave and Pipeline Conditions.

To use the above relationships between  $C_L$ ,  $\phi$ , and  $k$  to determine the wave-induced lift forces acting on a pipeline, either  $\phi$  or  $k$  must be known. Thus, a value of one of these parameters must be determined from relationships of  $\phi$  or  $k$  with the wave conditions and pipeline configuration.

The lift force phenomenon is a function of the following variables:

(a) Pipeline configuration

- (1) Diameter
- (2) Clearance
- (3) Orientation angle

(b) Fluid properties

- (1) Density
- (2) Viscosity

(c) Wave-induced flow conditions

- (1) Maximum horizontal water particle velocity perpendicular to the pipeline axis
- (2) Wave period, which represents the duration of the flow in one direction
- (3) Length of the horizontal excursions of the water particles perpendicular to the pipeline axis (this quantity is directly proportional to the product of the above two parameters)

Assuming that only water with a limited range of temperature is being dealt with, the fluid properties will be ignored for the present. The orientation angle of the pipeline can be handled as discussed above, considering only the components of the horizontal fluid motions

perpendicular to the pipeline axis. Since the length of the horizontal water particle excursions is directly proportional to the product of the wave period and the maximum horizontal water particle velocity, only four independent variables are left: diameter, clearance, horizontal water particle velocity, and wave period. Thus, any single parameter used to relate  $C_L$ ,  $\phi$ , or  $k$  to the wave and pipeline conditions must include these four variables. This constraint is necessary if the relationship is expected to be valid for general application under any set of wave and pipeline conditions.

The four variables can be arranged into several dimensionless parameters. The important parameters should include the following:

- (1) relative clearance,  $\text{clear}/\text{Dia}$

where  $\text{clear}$  = bottom clearance  
 $\text{Dia}$  = pipe diameter

- (2) Keulegan-Carpenter parameter,  $u_{\text{max}} T/\text{Dia}$

where  $T$  = wave period  
 $u_{\text{max}}$  = component of maximum horizontal water particle velocity perpendicular to the pipeline axis

- (3)  $\text{clear}/u_{\text{max}} T$

NOTE.--Not all of these parameters are necessary to describe the system since some are redundant, but some may be more useful than others.

Since viscosity is an important variable involved in the choking phenomenon, the Reynolds number,  $u_{\text{max}} \text{Dia}/\nu$ , and a Reynolds number for the clearance,  $u_{\text{max}} \text{clear}/\nu$ , are also important parameters (where  $\nu$  = kinematic viscosity).

The dimensionless parameters,  $\text{clear}/u_{\text{max}} T$ ,  $u_{\text{max}} T/\text{Dia}$ ,  $u_{\text{max}} \text{clear}/\nu$ , and  $u_{\text{max}} \text{Dia}/\nu$ , were plotted versus the lift force parameters,  $C_L$ ,  $\phi$ ,  $k$ ,  $C_L(1-k)$ , and  $C_L(k)$ , for constant values of the relative clearance,  $\text{clear}/\text{Dia}$ . The correlation was not good with the parameters involving the coefficient of lift ( $C_L$ ,  $C_L(1-k)$ , and  $C_L(k)$ ). However, good correlation was found between several of the dimensionless parameters and the quantities  $\phi$  and  $k$ .

The parameter,  $\text{clear}/u_{\text{max}} T$ , exhibited the best correlation with both  $\phi$  and  $k$  for each relative clearance, although there was some variation in these relationships for the data corresponding to the different pipe diameters (see Figs. 47 to 52). Although the differences are not large, the data do indicate the presence of a scale effect in these relationships.

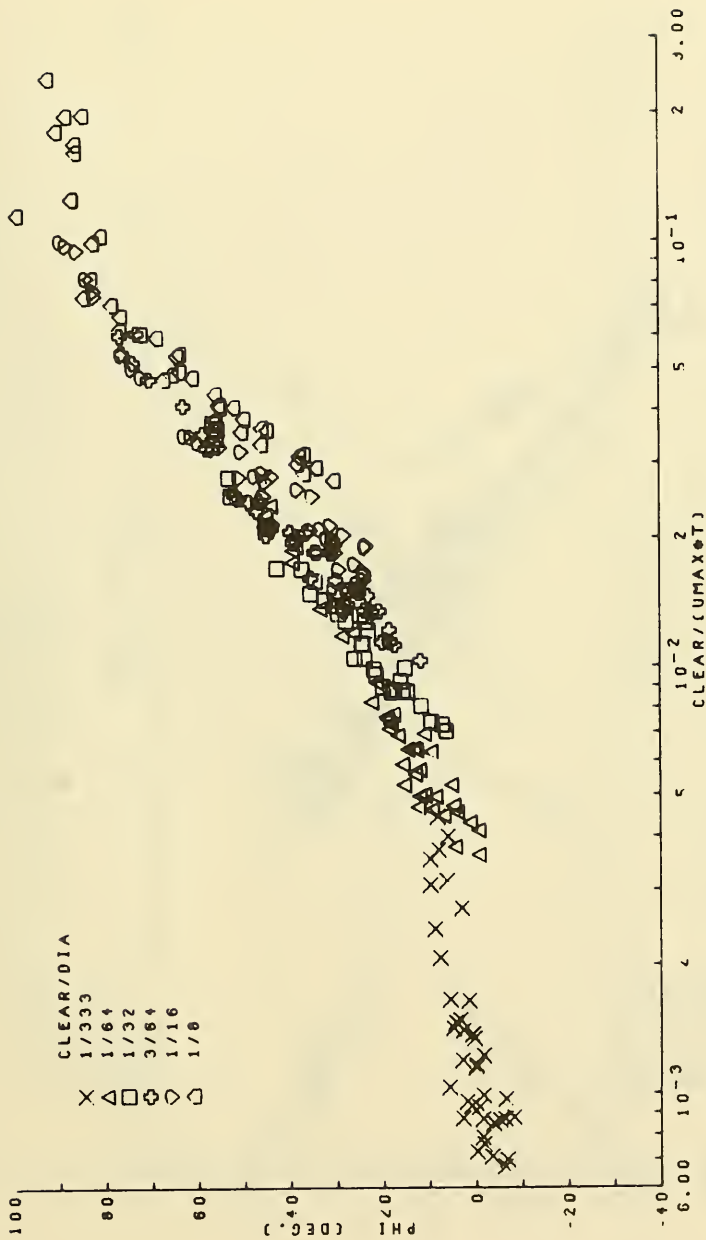


Figure 47.  $\phi$  versus  $\left(\frac{\text{clear}}{u_{\text{max}} \pi}\right)$  for 4-inch diameter.

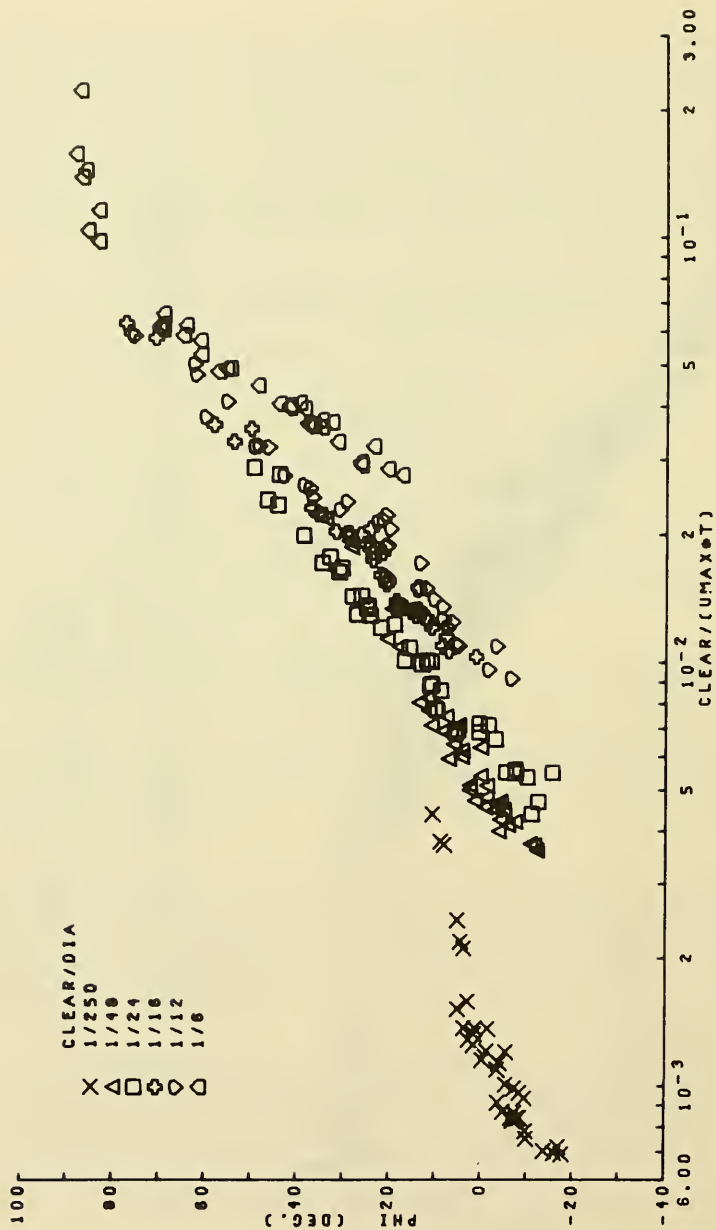


Figure 48.  $\phi$  versus  $\left(\frac{\text{clear}}{u_{\text{max}} T}\right)$  for 3-inch diameter.

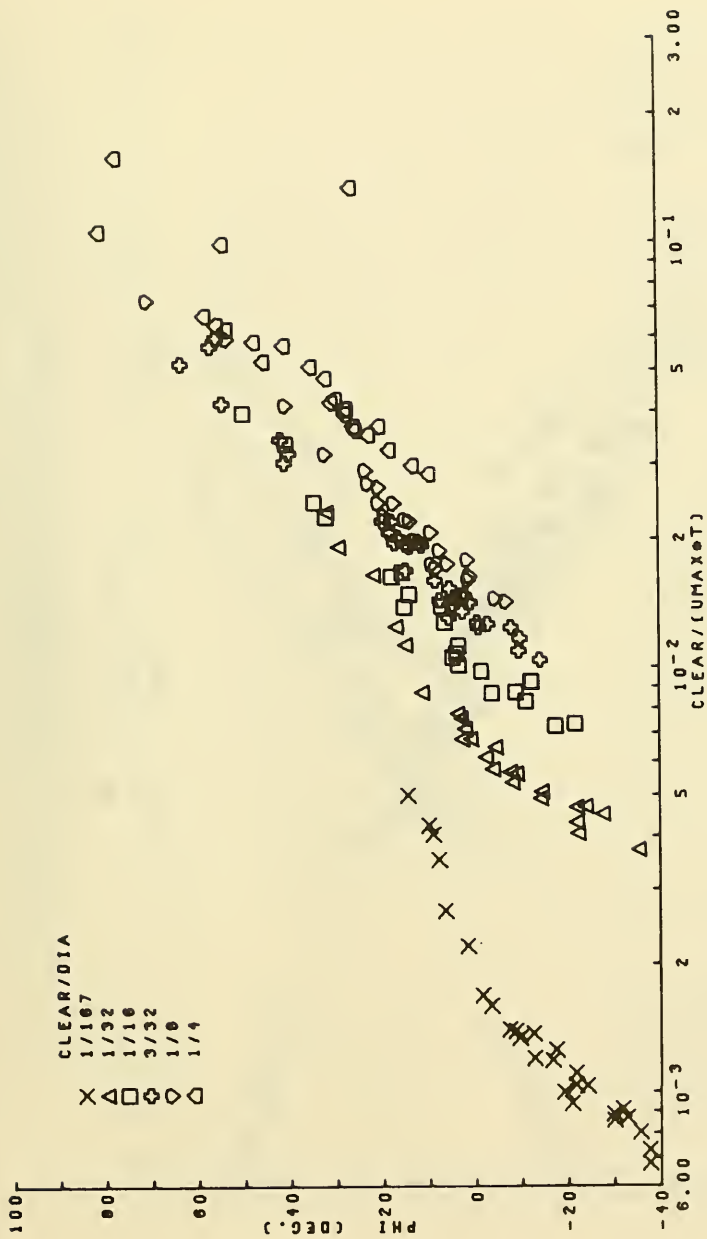


Figure 49.  $\phi$  versus  $\left\{ \frac{\text{clear}}{u_{\text{max}} T} \right\}$  for 2-inch diameter.

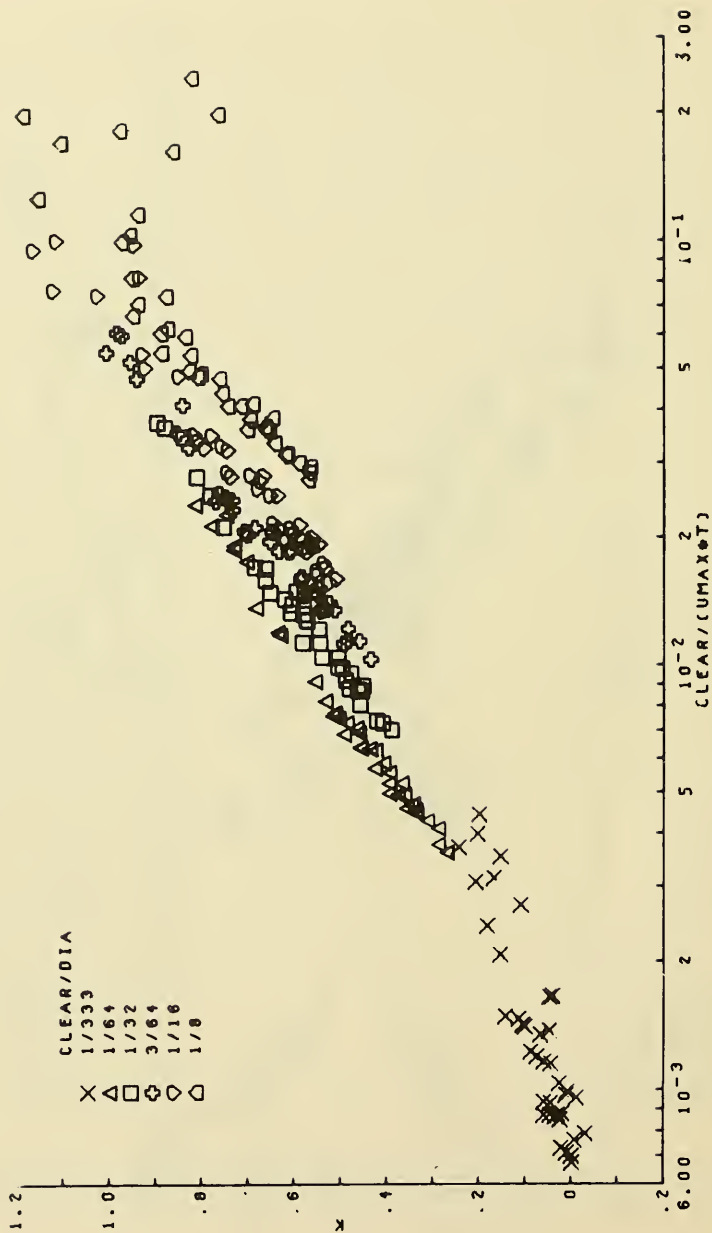


Figure 50.  $k$  versus  $\left(\frac{\text{clear}}{u_{\max} T}\right)$  for 4-inch diameter.



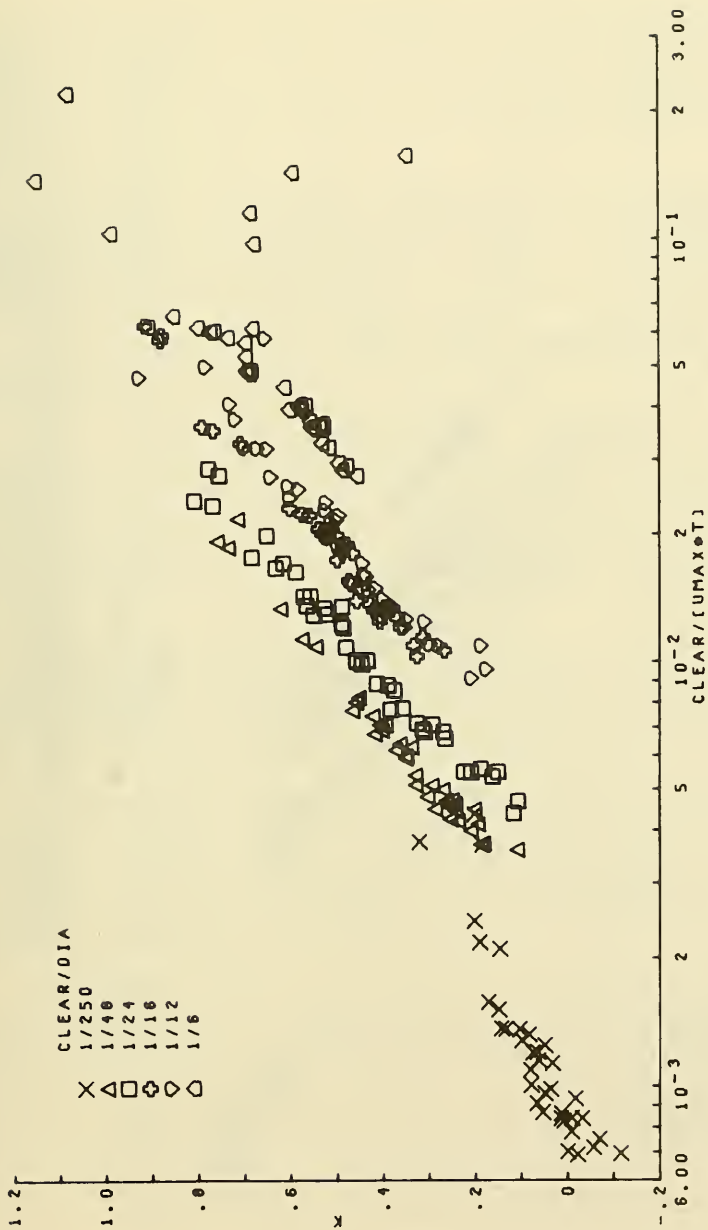


Figure 51.  $k$  versus  $\left(\frac{\text{clear}}{u_{\text{max}} T}\right)$  for 3-inch diameter.

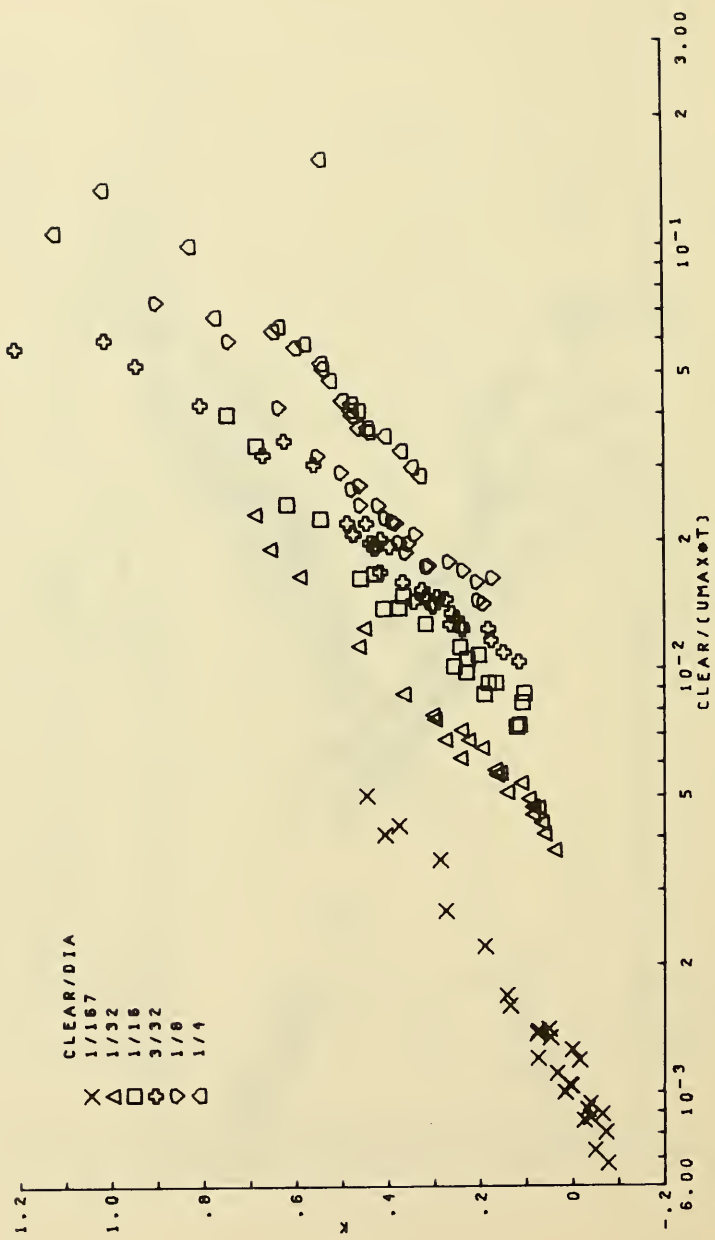


Figure 52.  $k$  versus  $\left(\frac{\text{clear}}{u_{\text{max}} T}\right)$  for 2-inch diameter.

$\phi$  and  $k$  were also correlated with the Keulegan-Carpenter parameter,  $u_{\max} T/\text{Dia}$ . However, these relationships were not the same when the data corresponding to a given relative clearance were compared for different pipe diameters. The relationships were the same for a given absolute clearance, rather than a relative clearance ( $\text{clear}/\text{Dia}$ ). These relationships are shown in Figures 53 and 54 for the combined data from all three pipe diameters.

The parameter,  $u_{\max} \text{clear}/v$ , demonstrated correlation with both  $\phi$  and  $k$ , but these relationships also exhibited a scale effect, such that the relationships for a given relative clearance were not the same when comparing the data for different pipe diameters. Figures 55 and 56 are examples of these relationships for the 4-inch-diameter pipeline.

Correlation between the Reynolds number,  $u_{\max} \text{Dia}/v$ , and the parameters,  $\phi$  and  $k$ , was not good, especially when comparing the data for the different pipe diameters.

Since none of the above dimensionless parameters alone could be used to determine a value of  $\phi$  or  $k$  for any given pipe diameter, clearance, and wave condition due to the presence of scale effects, several of the parameters were combined in various ways to form different dimensionless parameters containing all four of the important variables ( $\text{clear}$ ,  $\text{Dia}$ ,  $u_{\max}$ , and  $T$ ). An attempt was made to find a single parameter containing all of the important variables that was well correlated with  $\phi$  or  $k$  for all wave conditions, pipeline sizes, and configurations.

Several relationships were found that exhibited good correlation for all the wave and pipeline conditions tested. However, since this is a model study and, therefore, limited to lower values of the Keulegan-Carpenter parameter and Reynolds number than prototype design situations in the ocean, caution should be used in extrapolating these results.

The dimensionless combination,  $(\text{clear}/u_{\max} T)(\text{Dia}/u_{\max} T)$ , demonstrated the best correlation with both  $\phi$  and  $k$  for all conditions tested. These relationships are given in Figures 57 and 58. Since both  $k$  and  $\phi$  define the point at which choking occurs in the wave cycle, it appears that the choking phenomenon is directly dependent on the water particle excursions relative to both the pipe diameter,  $(\text{Dia}/u_{\max} T)$ , and the bottom clearance,  $(\text{clear}/u_{\max} T)$ .

Although the parameter,  $(\text{clear}/u_{\max} T)$ , is equivalent to the ratio of the bottom clearance to the horizontal excursion of the water particles (differing only by the constant  $1/\pi$ ), the quantity  $(u_{\max} T)$  should not be thought of only as defining the length of the water particle excursions. Both variables,  $u_{\max}$  and  $T$ , are independently important in defining the choking phenomenon. The larger  $u_{\max}$ , the sooner the choking conditions will develop in the wave cycle for a given clearance and pipe diameter. Similarly, since the wave period,  $T$ , defines the duration of the horizontal flow in one direction, the larger the wave period, the sooner choking will develop relative to the temporal length of the wave cycle.

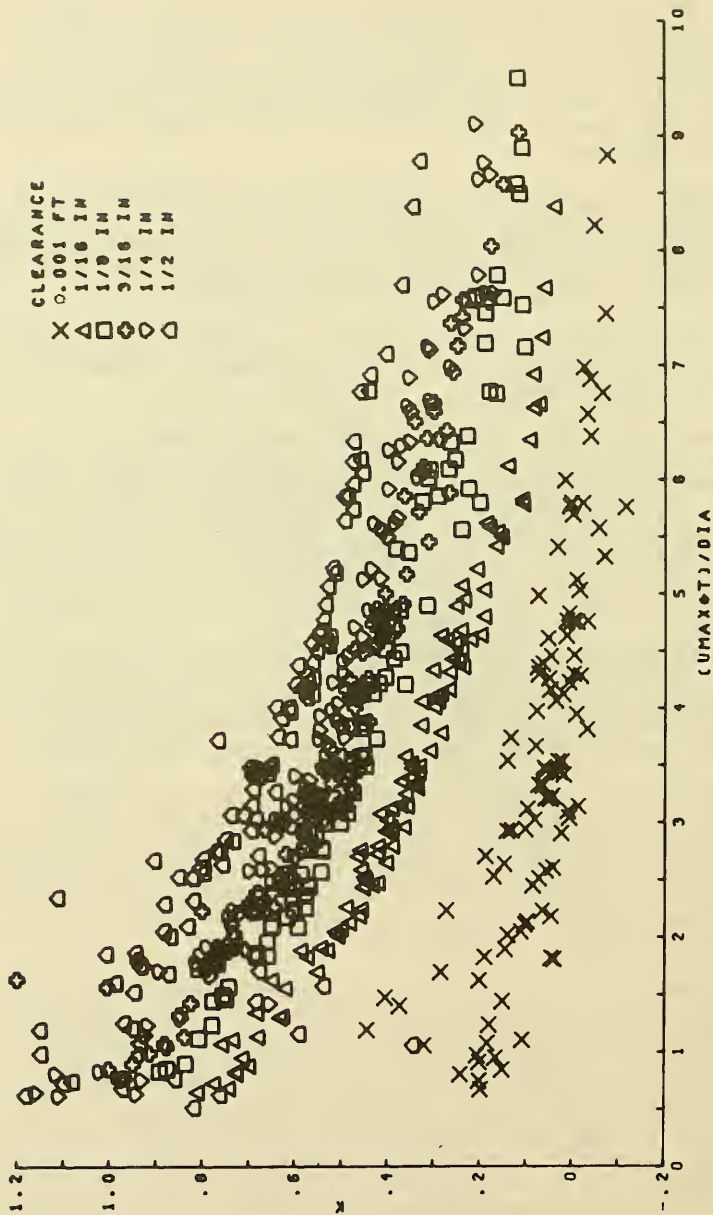


Figure 53.  $k$  versus  $\left( \frac{u_{\max}^T}{\text{Dia}} \right)$ .



Figure 54.  $\phi$  versus  $\left(\frac{u_{\max} T}{D_{ia}}\right)$ .

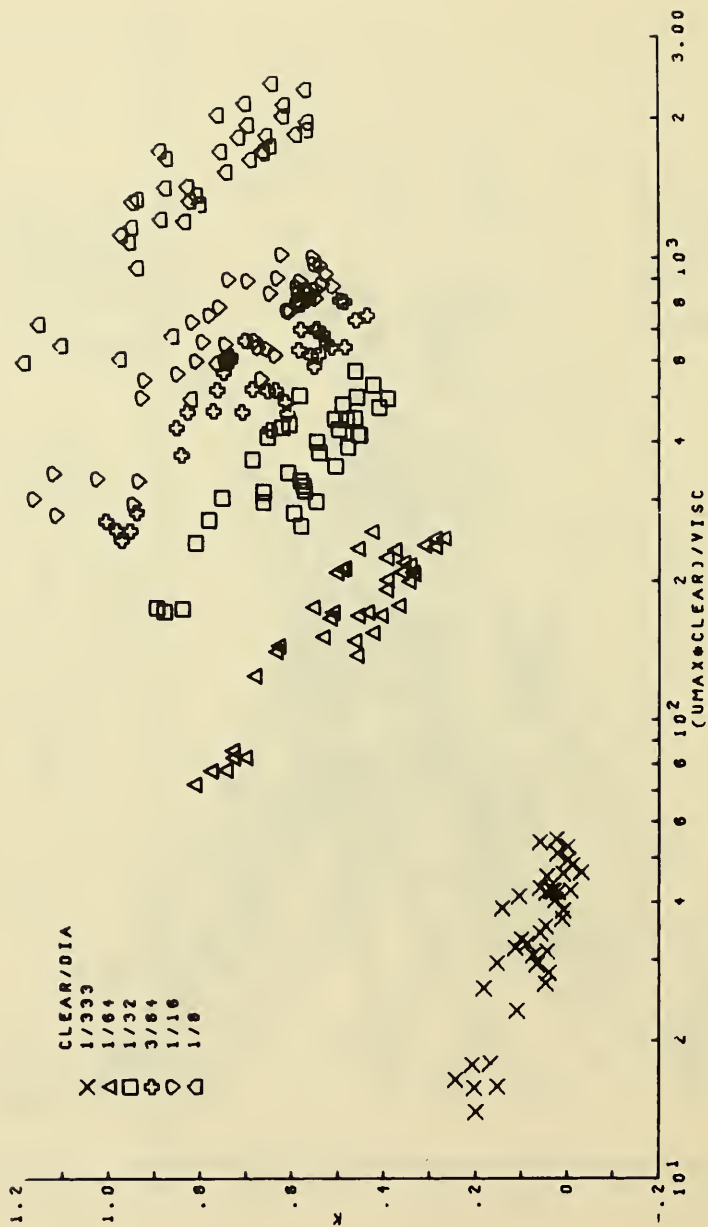


Figure 55. k versus  $\left[ \frac{U_{max}^{clear}}{v} \right]$  for 4-inch diameter.

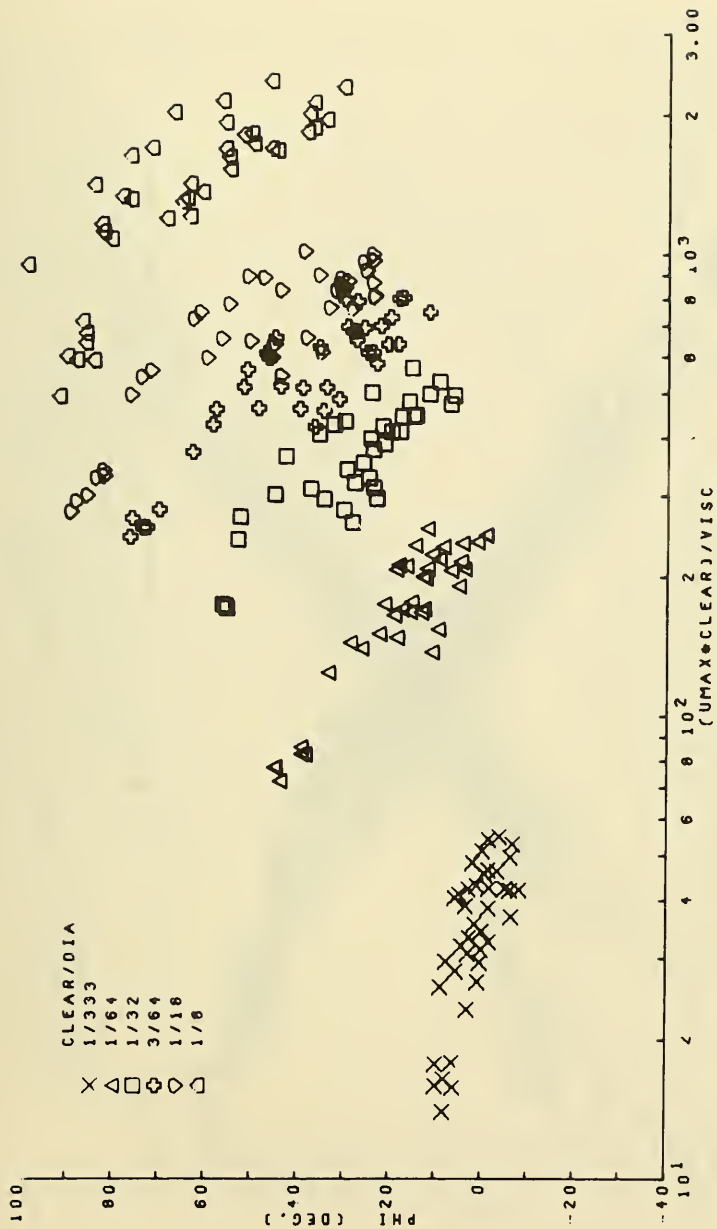


Figure 56.  $\phi$  versus  $\left\{ \frac{u_{\max} \text{ clear}}{v} \right\}$  for 4-inch diameter.

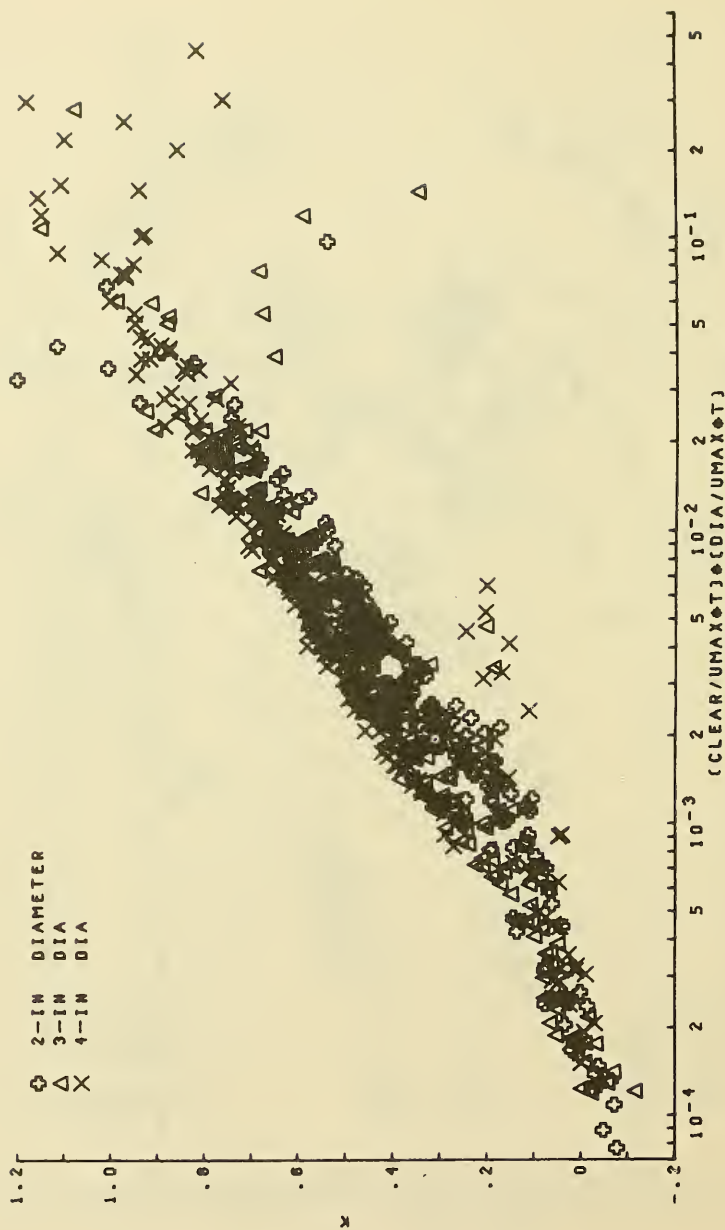


Figure 57.  $k$  versus  $\left(\frac{\text{clear}}{u_{\max}}\right) \left(\frac{\text{Dia}}{u_{\max}}\right)$ .



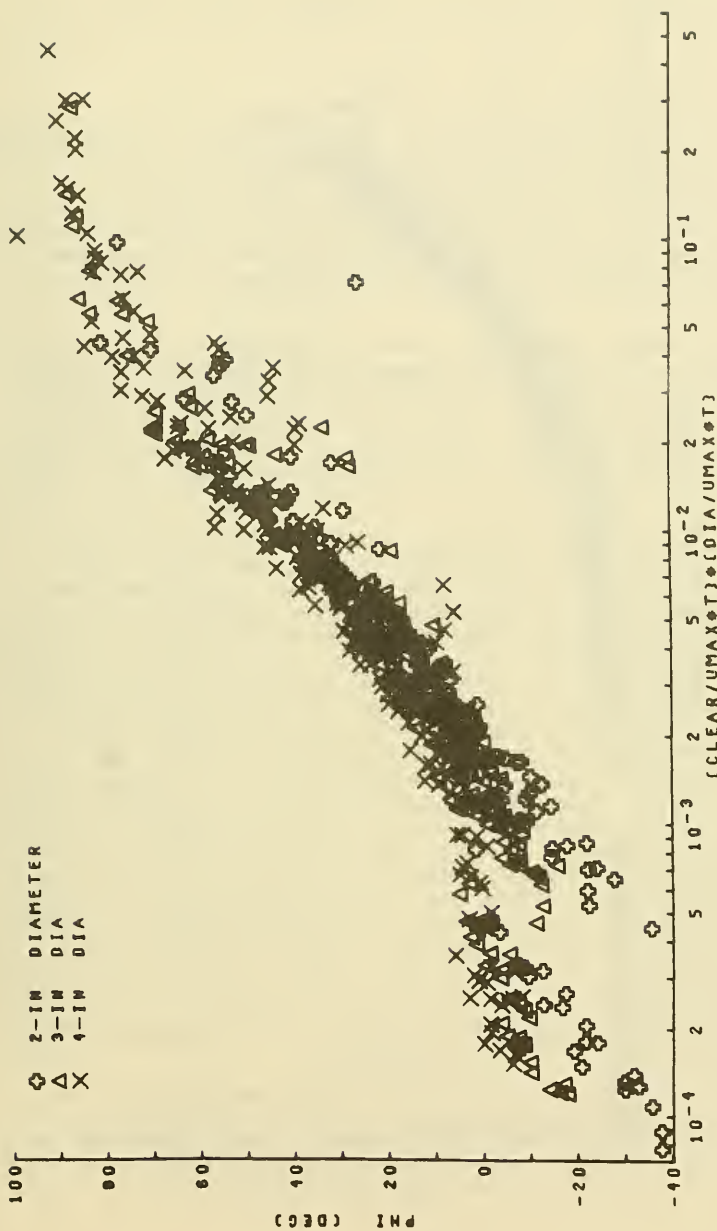


Figure 58.  $\phi$  versus  $\left(\frac{c_{\text{clear}}}{u_{\text{max}}}\right)^{0.5} \left(\frac{\text{Dia}}{u_{\text{max}}}\right)^{0.5}$ .

The slight amount of scatter in these plots in the vicinity of  $k = 1$  and  $\phi = 90^\circ$  is due to the error in calculated values of  $\phi$  and  $k$  for the largest bottom clearances where the lift effect was small (as discussed above).

Larger values of the dimensionless combination,  $(\text{clear}/u_{\text{max}} T)$  ( $\text{Dia}/u_{\text{max}} T$ ), than given in the plots would correspond to larger bottom clearances and pipe diameters relative to the maximum velocities, wave periods, and water particle excursions. For these conditions, the values of  $k$  and  $\phi$  would remain at 1 and  $90^\circ$ , respectively, while the lift effect would eventually diminish to zero with increasing values of this parameter. These trends are evident in the data taken at the largest bottom clearances (1 and 2 inches), although these data were not included in the above plots.

Similarly, lower values of the dimensionless parameter than given in the plots would correspond to higher maximum velocities, wave periods, and water particle excursions relative to the smallest bottom clearances and pipe diameters. So for lower values of this parameter, both  $k$  and  $\phi$  should remain at their defined minimum values of 0 and  $0^\circ$ , respectively, corresponding to lift forces acting in the upward direction only, with very little or no flow possible under the pipe section.

Although  $\phi$  was defined as varying from  $0^\circ$  to  $90^\circ$  only, negative values of  $\phi$  are exhibited in the data for the lowest values of the dimensionless parameters plotted. However, since most of these data points correspond to the smallest diameter pipeline model tested (2 inches), this could be partly due to experimental error, since the measured forces were smallest for the smallest model. Also, part of this discrepancy could be due to the difficulty of accurately defining the peak of the wave crest in the experimental wave records. This point was arbitrarily defined as the midpoint of the zero crossings on either side of the wave crest in the digitized data records. However, in some cases, the waves were not perfectly symmetrical, so the maximum elevation of the water surface did not coincide exactly with the midpoint of the zero crossings. This was especially true of the largest waves with the longest periods, which in the plotted relationships would correspond to the minimum values of the dimensionless parameters (at the lowest bottom clearance tested). Thus, the actual kinematics under these waves would be slightly out of phase with the calculated kinematics, resulting in an error in the calculated value of  $\phi$ . However, this source of error should be the same for the large-diameter models as for the smallest models.

##### 5. Relationships Between $\phi$ (clear/Dia) and $k$ (clear/Dia) and Parameters Defining the Wave and Pipeline Conditions.

Many other useful relationships were found by multiplying  $\phi$  and  $k$  by the relative clearance,  $(\text{clear}/\text{Dia})$ , and plotting these dimensionless products versus various dimensionless parameters defining the wave and pipe conditions. Figures 59 to 62 are examples, although several other parameters also showed good correlation with  $\phi$   $(\text{clear}/\text{Dia})$  and  $k$   $(\text{clear}/\text{Dia})$ .

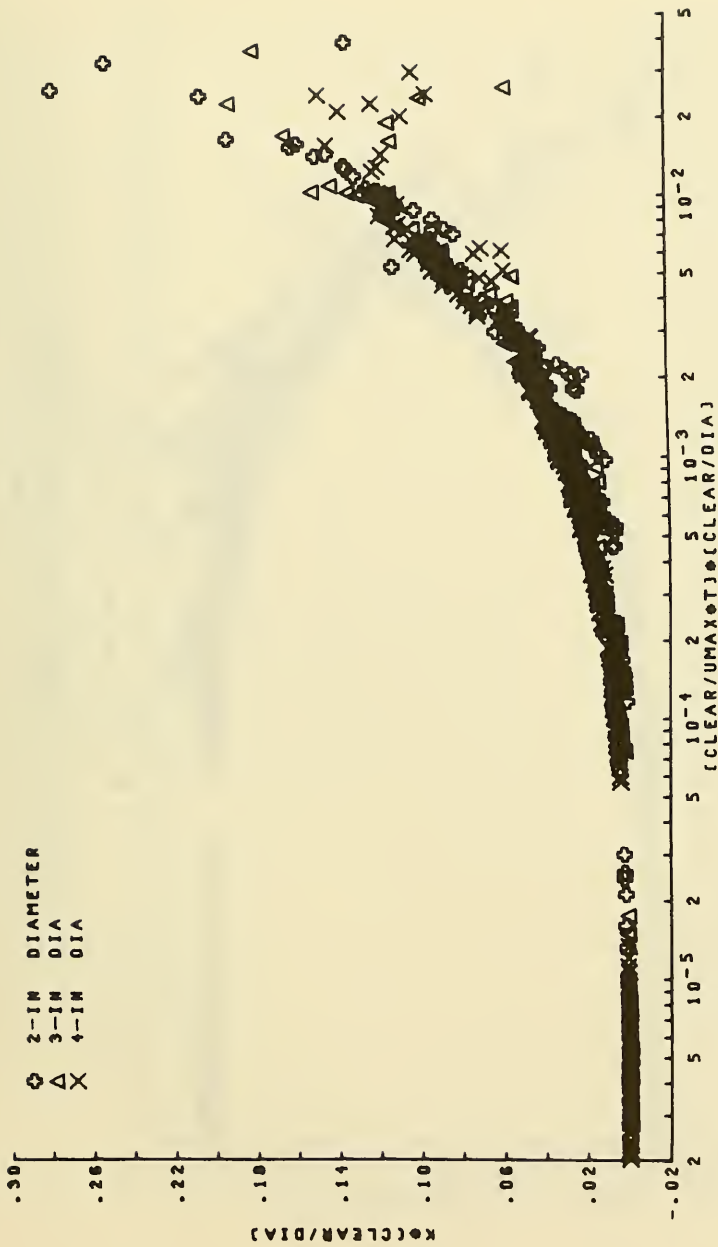


Figure 59.  $k \left( \frac{\text{clear}}{\text{Dia}} \right)$  versus  $\left( \frac{\text{clear}}{u_{\max}} \right) \left( \frac{\text{clear}}{\text{Dia}} \right)$ .

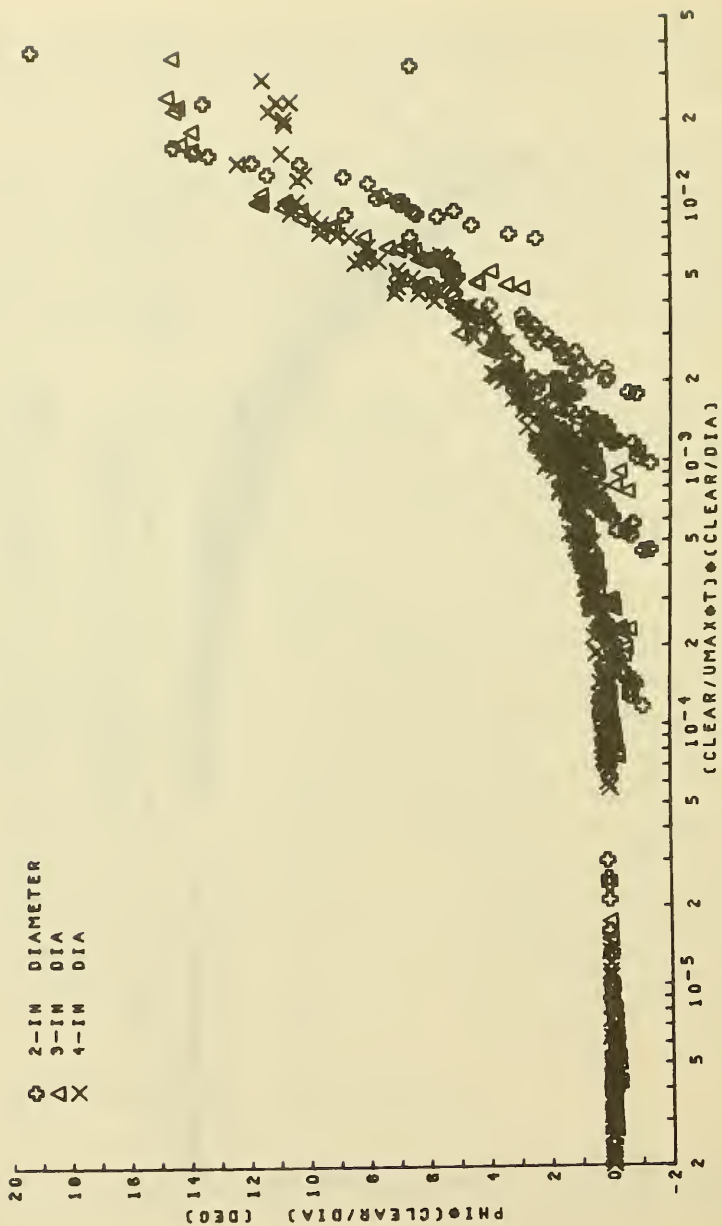


Figure 60.  $\phi \left( \frac{\text{clear}}{\text{Dia}} \right)$  versus  $\left( \frac{\text{clear}}{u_{\text{max}} T} \right) \left( \frac{\text{clear}}{\text{Dia}} \right)$ .

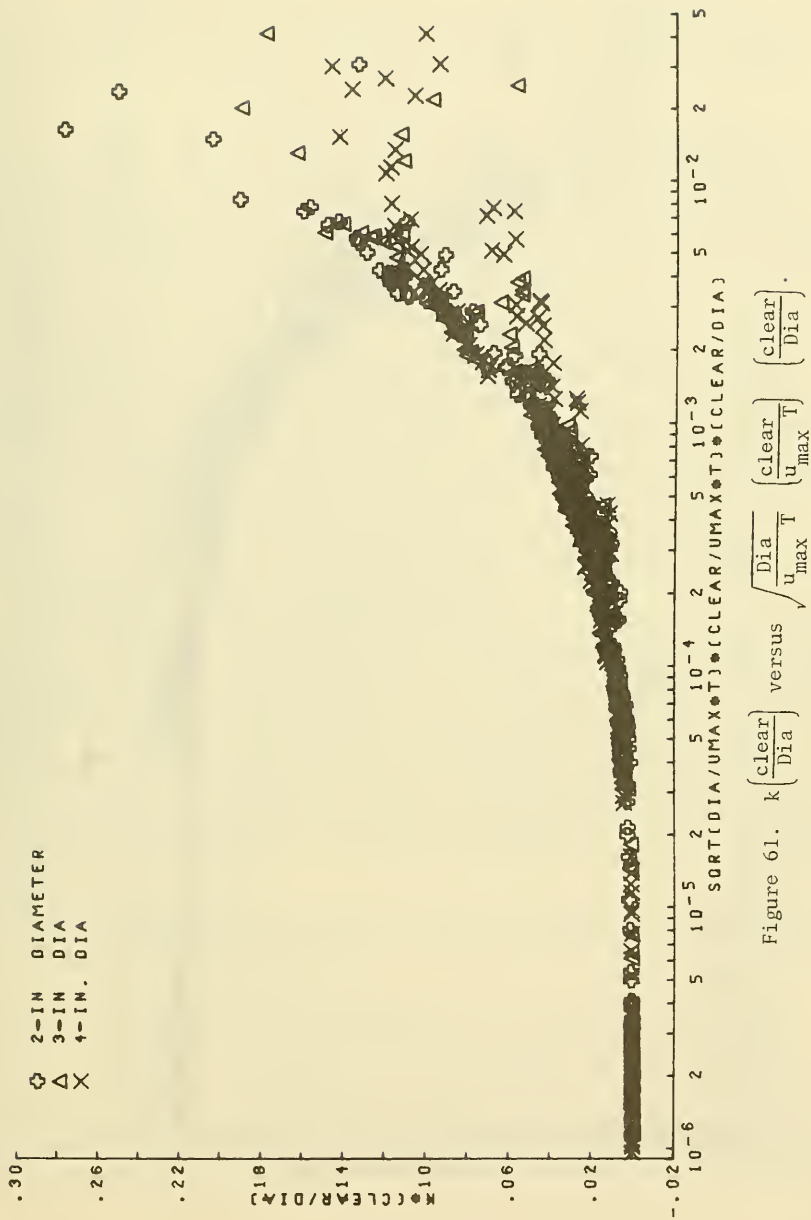


Figure 61.  $k \left( \frac{\text{clear}}{\text{Dia}} \right)$  versus  $\sqrt{\frac{\text{Dia}}{u_{\text{max}} T} \left( \frac{\text{clear}}{u_{\text{max}} T} \right) \left( \frac{\text{clear}}{\text{Dia}} \right)}$ .

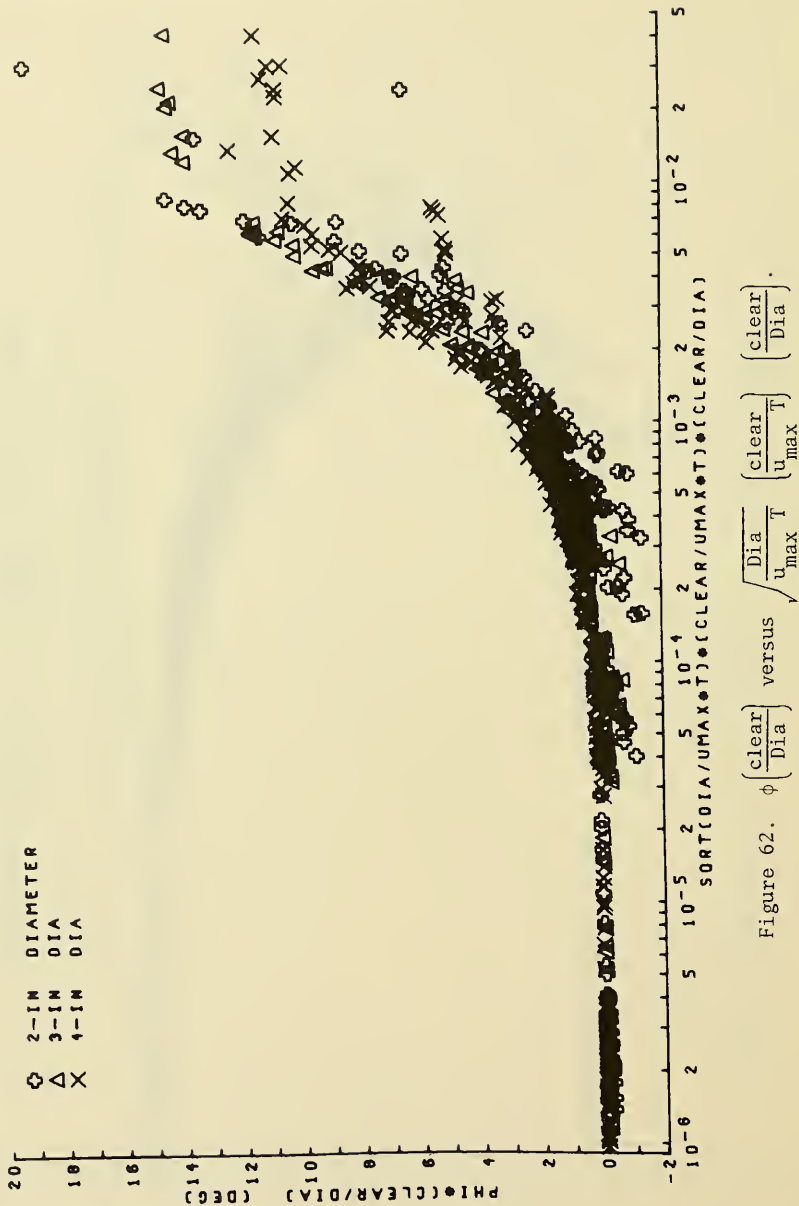


Figure 62.  $\phi \left( \frac{\text{clear}}{\text{Dia}} \right)$  versus  $\sqrt{\frac{\text{Dia}}{u_{\text{max}} T}}$

Both  $\phi$  (clear/Dia) and  $k$  (clear/Dia) are correlated with the dimensionless combinations (clear/ $u_{\max} T$ ) (clear/Dia) and  $\sqrt{\text{Dia}/u_{\max} T}$  (clear/ $u_{\max} T$ ) (clear/Dia). However,  $k$  (clear/Dia) appears to be better correlated with the first parameter, while  $\phi$  (clear/Dia) shows better correlation with the second parameter.

It is clear that for values of the dimensionless parameters lower than those shown on the plots, both  $\phi$  (clear/Dia) and  $k$  (clear/Dia) will remain at a value of zero. This would correspond to situations where the clearance was minimal relative to the horizontal velocities, wave periods, and horizontal excursions of the water particles. Thus, both  $k$  and  $\phi$  would be expected to equal zero and  $0^\circ$ , respectively, and the relative clearance would either equal or approach zero.

Large values of the dimensionless parameters correspond to situations where the clearance is large relative to the horizontal velocities, wave periods, and horizontal excursions of the water particles. For these cases,  $k$  and  $\phi$  will remain at maximum values of 1 and  $90^\circ$ , respectively, while the relative clearance, (clear/Dia), will increase with increasing values of the dimensionless parameters. But as the relative clearance is increased beyond this point, the lift forces will decrease to zero, so extension of the plotted relationships to much larger values of the dimensionless parameters is of little value.

#### 6. Relationships Between the Coefficients of Lift and Parameters Defining the Wave and Pipeline Conditions.

The coefficient of lift,  $C_L$ , the effective positive coefficient of lift,  $C_L(1-k)$ , the effective negative coefficient of lift,  $C_L(k)$ , and the maximum effective coefficient of lift (maximum of  $C_L(1-k)$  or  $C_L(k)$ ) were plotted against various combinations of the dimensionless parameters. The parameter, (clear/ $u_{\max} T$ )(Dia/ $u_{\max} T$ ), which previously gave the best correlations with  $\phi$  and  $k$  also demonstrated the best correlation with  $C_L$ ,  $C_L(1-k)$ , and  $C_L(k)$ . However, these relationships exhibited more scatter than the previously discussed interrelationships between the coefficients of lift and the parameters,  $k$  and  $\phi$ , so it is suggested that the previously discussed relationships be used for design purposes.

#### 7. Relationships Between the Lift Forces and Parameters Defining the Wave and Pipeline Conditions.

As with the coefficient of lift, the total lift force ( $F_L = 1/2 C_L \rho A u_{\max}^2$ ) can be partitioned into the maximum positive lift,  $F_L(1-k)$ , and the maximum negative lift,  $F_L(k)$  (Fig. 6). These three forces, as well as the maximum lift force (maximum of either  $F_L(1-k)$  or  $F_L(k)$ ) were plotted against various combinations of the dimensionless parameters. Only one relationship exhibited good correlations for the data from all three diameters plotted together. This was the Reynolds number,  $u_{\max} \text{Dia}/\nu$ , versus the maximum lift force (either  $F_L(1-k)$  or  $F_L(k)$ , whichever is greater) (Fig. 63).

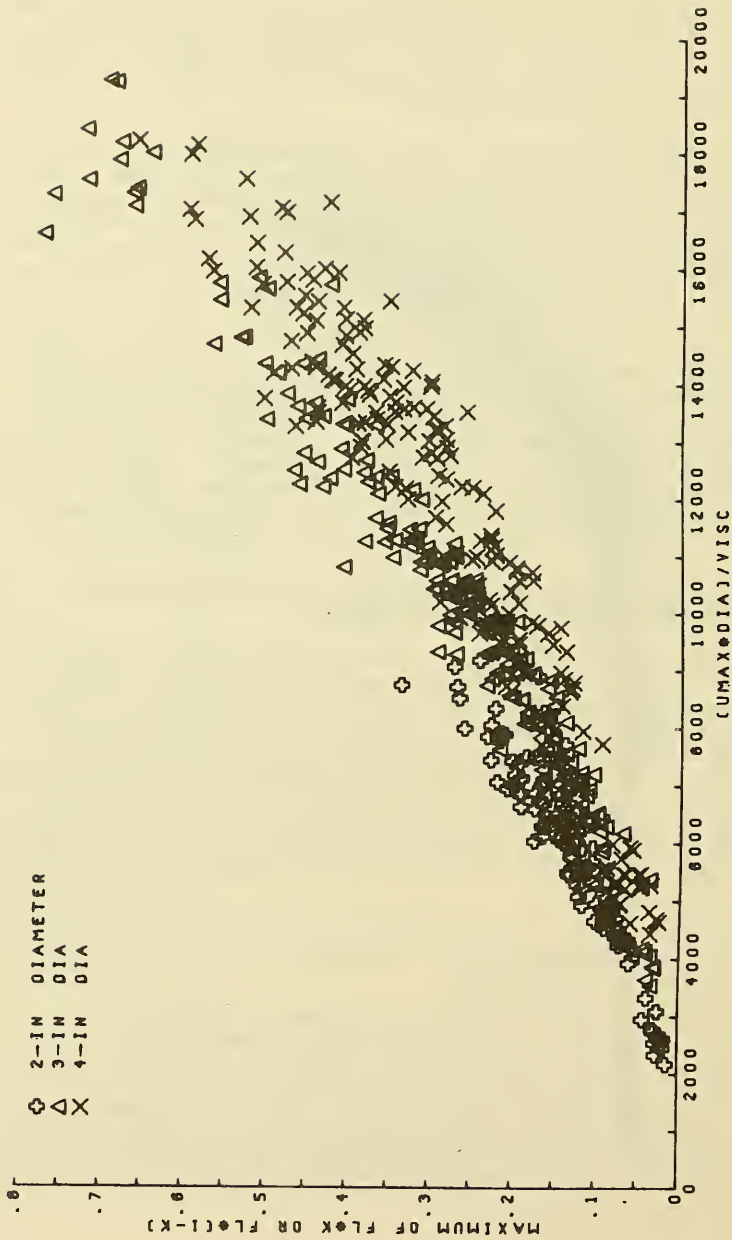


Figure 63. Maximum lift force (positive or negative) versus the Reynolds number.



This relationship shows that for any pipe diameter, orientation angle, or bottom clearance, the maximum lift force increases with the Reynolds number in a regular manner, at least over the range of the data in this investigation. The maximum lift force may occur in either the upward or downward direction, depending on the magnitude of the bottom clearance relative to the wave conditions and pipe size. This relationship does not hold for the maximum upward lift or maximum downward lift alone, but only for the largest of these two forces in any given situation.

#### 8. Relationships Involving the Vertical Coefficients of Mass and Drag and the Vertical Inertial and Drag Forces.

Both the vertical coefficient of mass and the vertical inertial forces were plotted against several dimensionless parameters defining the wave and pipeline conditions, but no useful relationships were found. This is not surprising when considering that the vertical inertial forces are relatively small, and thus subject to error from the transverse eddy-induced forces which were not accounted for in the least squares analysis.

No attempt was made to plot relationships involving the vertical drag forces or drag coefficients, since these forces were negligible.

#### 9. Relationships Between the Horizontal Coefficient of Mass and Parameters Describing the Wave and Pipeline Conditions.

A limited number of horizontal force data were taken using the 4-inch-diameter two-dimensional model. Values of  $C_M$  and  $C_D$  were calculated from the least squares analysis, and an attempt was made to relate these coefficients to various dimensionless parameters describing the wave and pipeline conditions.

Figure 64 shows the horizontal coefficient of mass plotted versus the relative clearance,  $clear/Dia$ , together with the potential flow solution for a circular cylinder in the vicinity of a plane wall subject to a uniform flow with constant acceleration (Grace, 1974). The data follow the potential flow solution reasonably well, although for a given relative clearance, there appears to be some variation in the value of  $C_M$  with varying wave conditions. Also, the wave force data give slightly higher values of the coefficient of mass for the highest bottom clearances tested. Although the experimental data are limited, they indicate that the potential flow solution may be very useful in determining a value for the horizontal coefficient of mass, at least for wave conditions where the inertial forces predominate over the drag forces.

However, since there was some variation in the values of  $C_M$  for different wave conditions for the same relative clearance, an attempt was made to determine relationships between the horizontal coefficient of mass and the various dimensionless parameters defining the wave and pipeline conditions. Reasonably good correlations were found between

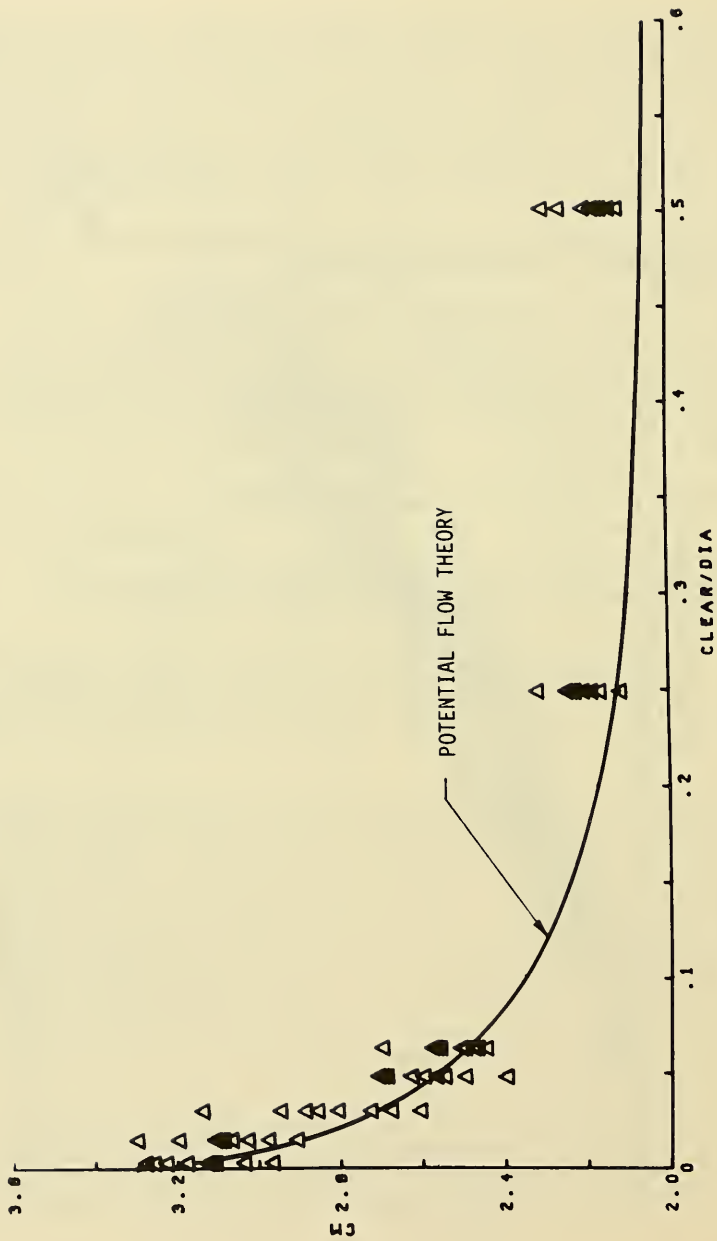


Figure 64. Comparison of the horizontal  $C_M$  with potential flow theory for a flow with constant acceleration.

several of the parameters. Figure 65 shows the relationship for  $C_M$  versus  $\text{clear}/u_{\max}T$ .

#### 10. Relationships Involving the Horizontal Coefficient of Drag.

The horizontal coefficient of drag was plotted against several dimensionless parameters, but no useful relationships were found. This was expected since the horizontal drag forces in this investigation were much smaller than the inertial forces, due to the limited horizontal excursions of the water particles relative to the diameter of the pipeline.

#### 11. Example Problems.

GIVEN: A design wave with height,  $H = 10$  feet and period,  $T = 10$  seconds acts on a pipeline with a diameter,  $\text{Dia} = 8$  feet in a water depth,  $d = 80$  feet. The pipeline is oriented at an angle of  $30^\circ$  with respect to the wave crests. Section A of the pipeline is in contact with the bottom; section B spans the bottom at a clearance,  $\text{clear} = 6$  inches.

FIND: For both sections A and B, find

- the values of the lift force parameters ( $C_L$ ,  $\phi$ , and  $k$ );
- the maximum positive and negative lift forces;
- the positions of these maximum lift forces in the wave cycle; and
- the lift force at  $\theta = 120^\circ$  in the wave cycle.

SOLUTION:

$$L_0 = \frac{g}{2} \frac{T^2}{\pi} = 5.12 (10)^2 = 512 \text{ feet}$$

$$\frac{d}{L_0} = \frac{80}{512} = 0.1562$$

Using tables,  $\frac{d}{L} = 0.1885$ , so  $L = \frac{80}{0.1885} = 424 \text{ feet}$

$$\sinh \frac{2\pi d}{L} = 1.481$$

$z =$  distance from bottom to center of pipe sections.

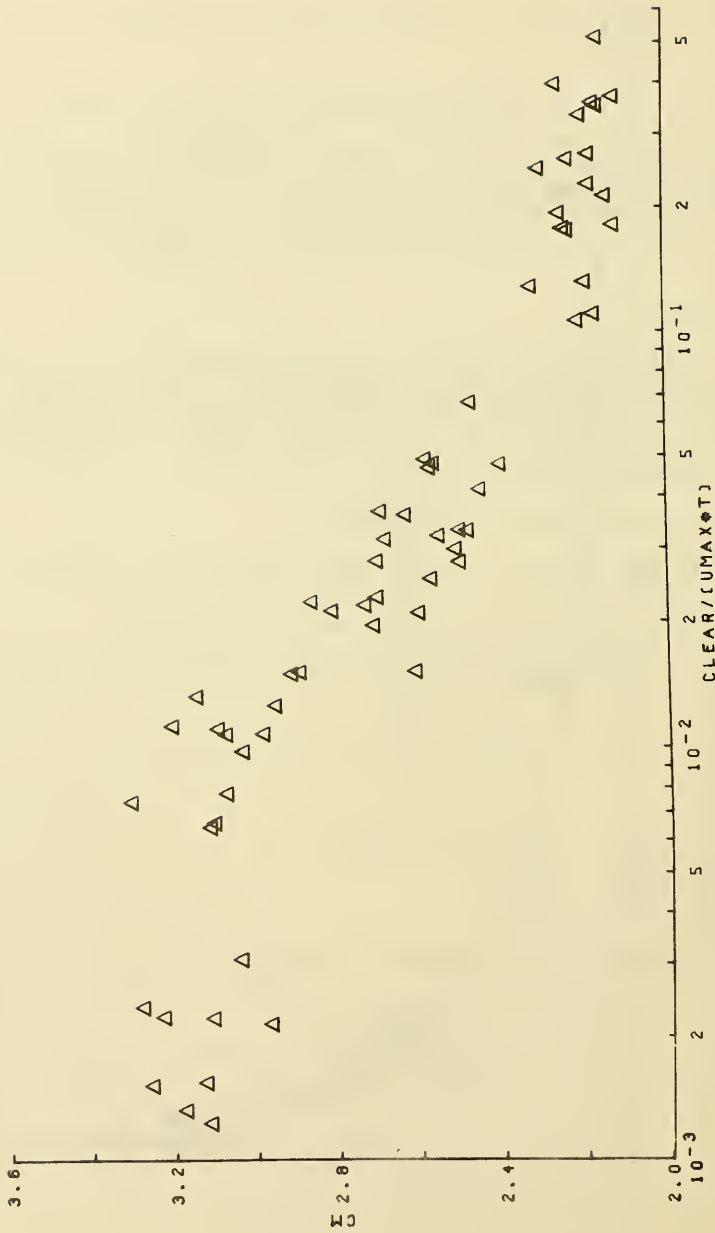


Figure 65. Horizontal  $C_M$  versus  $\left(\frac{\text{clear}}{u_{\text{max}}}\right)^2$ .

For section A (clear = 0)

$$z = 4 \text{ feet}$$

$$\frac{z}{L} = \frac{4}{424} = 0.00943$$

$$\text{From tables, } \cosh \frac{2\pi z}{L} = 1.0017$$

$$u_{\max} = \frac{\pi H}{T} \frac{\cosh\left(\frac{2\pi z}{L}\right)}{\sinh\left(\frac{2\pi d}{L}\right)} = \frac{\pi(10)(1.0017)}{(10)(1.481)} = 2.12 \text{ feet per second}$$

Component of  $u_{\max}$  perpendicular to the pipeline axis is

$$u_{\max} (\cos 30^\circ) = (2.12)(0.866) = 1.84 \text{ feet per second}$$

(a) Since the pipe is in contact with the bottom, (clear = 0),  $\phi = 0^\circ$  and  $k = 0$ . From Figure 40,  $C_L = 4.5$ .

(b) Maximum positive lift (per unit length)

$$\begin{aligned} F_L(1-k) &= \frac{1}{2} C_L \rho A u_{\max}^2 (1-k) \\ &= \frac{1}{2} (4.5)(2)(8)(1.84)^2 (1-0) \\ &= 121.9 \text{ pounds per foot.} \end{aligned}$$

Maximum negative lift (per unit length)

Since  $k = 0$ , there is no negative lift, and the lift force is positive throughout the wave cycle.

(c) Since  $\phi = 0^\circ$ , the positive lift forces are maximum at  $0^\circ$  and  $180^\circ$  in the wave cycle (under the crests and troughs), corresponding to the points of maximum horizontal velocities.

The lift does not become negative, but diminishes to zero at  $90^\circ$  and  $270^\circ$ , the positions of horizontal flow reversal in the wave cycle.

(d) At  $\theta = 120^\circ$

$$\begin{aligned} F_L &= \frac{1}{2} C_L \rho A u_{\max}^2 [\cos^2 (\theta - \phi) - k] \\ &= \frac{1}{2} (4.5)(2)(8)(1.84)^2 [\cos^2 (120^\circ - 0^\circ) - 0] \\ &= 30.5 \text{ pounds per foot} \end{aligned}$$

For section B (clear = 6 inches)

$$z = 4.5 \text{ feet}$$

$$\frac{z}{L} = \frac{4.5}{424} = 0.0106$$

$$\text{From tables, } \cosh \frac{2\pi z}{L} = 1.0022$$

$$u_{\max} = \frac{\pi H}{T} \frac{\cosh\left(\frac{2\pi z}{L}\right)}{\sinh\left(\frac{2\pi d}{L}\right)} = \frac{\pi(10)(1.0022)}{(10)(1.481)} = 2.13 \text{ feet per second}$$

component of  $u_{\max}$  perpendicular to the pipeline axis is

$$u_{\max} (\cos 30^\circ) = (2.13)(0.866) = 1.84 \text{ feet per second}$$

(a) Use Figure 57 to determine a value for  $k$

$$\left(\frac{\text{clear}}{u_{\max} T}\right) \left(\frac{\text{Dia}}{u_{\max} T}\right) = \frac{(0.5)(8)}{(1.84)(10)(1.84)(10)} = 0.0118$$

so from Figure 57,  $k = 0.67$

and from Figure 58,  $\phi = 45^\circ$ .

Alternatively, either  $\phi$  or  $k$  could be determined from Fig. 39, once the other is known.

From Figure 46, for  $k = 0.67$ ,

$$C_L(1-k) = 2.75$$

$$\text{so } C_L = \frac{2.75}{(1 - 0.67)} = 8.3.$$

(b) Maximum positive lift (per unit length)

$$\begin{aligned} F_L(1-k) &= \frac{1}{2} C_L \rho A u_{\max}^2 (1-k) \\ &= \frac{1}{2} (8.3)(2)(8)(1.84)^2 (1 - 0.67) \\ &= 74.2 \text{ pounds per foot} \end{aligned}$$

Maximum negative lift (per unit length)

$$\begin{aligned} - F_L(k) &= - \frac{1}{2} C_L \rho A u_{\max}^2 (k) \\ &= - \frac{1}{2} (8.3)(2)(8)(1.84)^2 (0.67) \\ &= - 150.6 \text{ pounds per foot} \end{aligned}$$

(c) Since  $\phi = 45^\circ$ , the positive lift forces are maximum at  $0^\circ + 45^\circ = 45^\circ$  and  $180^\circ + 45^\circ = 225^\circ$  in the wave cycle, and the negative lift forces are maximum at  $90^\circ + 45^\circ = 135^\circ$  and  $270^\circ + 45^\circ = 315^\circ$  in the wave cycle.

(d) At  $\theta = 120^\circ$

$$\begin{aligned} F_L &= \frac{1}{2} C_L \rho A u_{\max}^2 [\cos^2 (120^\circ - 45^\circ) - 0.67] \\ &= \frac{1}{2} (8.3)(2)(8)(1.84)^2 [\cos^2 (120^\circ - 45^\circ) - 0.67] \\ &= - 135.6 \text{ pounds per foot} \end{aligned}$$

Again, it should be stressed that the relationships involving the lift force parameters,  $C_L$ ,  $\phi$ , and  $k$ , were determined from model studies conducted at much lower values of the Keulegan-Carpenter parameter and Reynolds number than those encountered in full-scale situations in the ocean. Therefore, caution should be used in extrapolating these results to prototype designs.

Further studies using a larger scale facility are necessary to evaluate the importance of scale effects in these relationships, to determine their limitations, and possibly to extend or modify them so they are valid for any scale.

#### IV. CONCLUSIONS

1. The traditional steady-flow lift force model, expressed as  $F_L = 1/2 C_L \rho A u^2$ , is not a suitable model for the description of wave-induced lift forces. This model assumes that the lift force acts in one direction only (upward or downward) throughout the entire wave cycle.

2. For pipelines located at a small clearance above the bottom, a viscous choking effect limits the maximum velocities through the constriction formed by the bottom clearance. Correspondingly, the pressure drop on the bottom side of the pipe section is also limited.

In contrast, the flow velocities and corresponding pressure drop over the top side of the pipeline are not limited. As the choking effect develops and the flow becomes restricted through the bottom

clearance constriction, more of the flow must be diverted over the top of the pipe section, resulting in a downward shift in the stagnation point, as well as an increase in the flow velocities and associated pressure drop over the top side of the pipeline.

The induced changes in the flow pattern, velocities, and associated pressure distribution over the pipe section due to choking through the bottom clearance constriction result in an upward lift force, rather than the downward lift force predicted by potential flow theory.

3. Thus, for an oscillatory wave-induced flow, the lift force acts downward in those parts of the wave cycle where the horizontal water particle velocities are not high enough to produce choking through the bottom clearance. In this case, the unrestricted flow is faster through the bottom clearance constriction than over the top of the pipe section, so the corresponding pressure distribution results in a negative lift toward the bottom boundary.

However, in those parts of the wave cycle where the horizontal velocities are sufficient to induce choking through the bottom clearance constriction, the lift force acts in an upward direction.

4. For a given pipe diameter and wave condition, as the bottom clearance is increased, higher velocities are necessary to produce the choking effect. Thus, the negative lift force can reach a greater magnitude and occur later into the wave cycle before the choking condition is induced.

Correspondingly, the positive lift that occurs only after the choking condition develops is limited to a smaller part of the wave cycle, and the maximum magnitude of these forces decreases with increasing clearance. In addition, since there is a small timelag involved in the development of the choking phenomenon and the transition from negative to positive lift, the maximum positive lift occurs later into the wave cycle, although its magnitude is diminishing.

5. All major features of the wave-induced lift force phenomenon can be described adequately by a modified lift force equation,  $F_L = 1/2 C_L \rho A u_{max}^2 [\cos^2(\theta - \phi) - k]$ , where  $\phi$  represents a phase shift in the position of the maximum positive (upward) lift force relative to the point of maximum horizontal velocity at the center of the wave crest, and  $k$  represents the proportion of the total lift force cycle that acts in the negative (downward) direction. The values of  $\phi$  and  $k$  vary from  $0^\circ$  and  $0$ , respectively, for the case of a pipeline touching the bottom, and increase with increasing clearance (for a given pipeline and wave condition) to maximum values of  $90^\circ$  and  $1$ , respectively, when the pipeline is far enough from the bottom so that the choking condition does not develop.  $\phi = 0^\circ$  and  $k = 0$  correspond to lift forces that are positive throughout the wave cycle, with maximums occurring at the points of maximum horizontal velocity under the wave crests and troughs.  $\phi = 90^\circ$  and  $k = 1$  correspond to negative lift forces throughout the wave



cycle, with maximum downward forces occurring under the crests and troughs of the passing waves. These two cases represent the extreme conditions bounding the lift force phenomena. At any intermediate clearance between these limiting cases, both positive and negative lift forces will occur at different parts of the wave cycle, and the positions of the maximum upward and downward lift forces will not coincide with the positions of maximum horizontal velocities in the wave cycle.

In order to use this lift force model, values of the parameters,  $C_L$ ,  $\phi$ , and  $k$ , must be determined for the given set of wave and pipeline conditions. A model investigation was carried out to determine relationships between these parameters and various dimensionless parameters defining the wave and pipeline conditions.

6. A direct relationship was found between the lift force parameters,  $\phi$  and  $k$ . Relationships were also found between the coefficient of lift,  $C_L$ , and both  $\phi$  and  $k$ . In addition,  $C_L$  can be partitioned into the positive effective coefficient of lift,  $C_L(1-k)$ , and the effective negative coefficient of lift,  $C_L(k)$ . Both of these parameters are also related to both  $\phi$  and  $k$ . The correlation is better with  $k$  than  $\phi$  for the relationships involving  $C_L$ ,  $C_L(1-k)$ , and  $C_L(k)$ .

All of these relationships were the same for all pipe diameters, bottom clearances, and wave conditions tested.

7. The average value of  $C_L$  at  $k = 0$  and  $\phi = 0^\circ$  (which corresponds to a pipeline in contact with the bottom with no clearance) is 4.5. This is the same as the potential flow solution for the lift force on a circular cylinder against a plane wall subject to a steady, inviscid flow parallel to the wall.

8. Maximum values of  $C_L$  occur at  $k = 1/2$  and  $\phi = 30^\circ$ , where  $C_L = 9$ . In the interval from  $k = 0$  to  $1/2$  and  $\phi = 0^\circ$  to  $30^\circ$ , the effective positive coefficient of lift  $C_L(1-k)$  remains at approximately 4.5, while the effective negative coefficient of lift  $C_L(k)$  increases from 0 to 4.5. In the interval from  $k = 1/2$  to 1 and  $\phi = 30^\circ$  to  $90^\circ$ ,  $C_L(1-k)$  decreases to 0, while  $C_L(k)$  increases to reach a maximum of about 6 or 7 at  $k = 0.75$  and  $\phi = 45^\circ$ , and then decreases to a maximum of 4.5 at  $k = 1$  and  $\phi = 90^\circ$ .

9. Using the above relationships between  $C_L$ ,  $\phi$ , and  $k$ , if either  $\phi$  or  $k$  is known, the remaining two parameters can be determined. Therefore, an attempt was made to find relationships between  $\phi$  and  $k$  and various dimensionless parameters defining the wave and pipeline conditions.

The best correlation was found in the relationships between  $\phi$  and  $k$  and the parameter  $\text{clear}/u_{\max}T$  for constant values of the relative clearance,  $\text{clear}/\text{Dia}$ . However, comparison of the data corresponding to the different pipe diameters indicates a slight scale effect is present.

$\phi$  and  $k$  were also related to the parameter  $u_{\max} \text{clear}/v$  for constant values of  $\text{clear}/\text{Dia}$ , although the scale effect was worse for these relationships.  $\phi$  and  $k$  showed very good correlation with the Keulegan-Carpenter parameter,  $u_{\max} T/\text{Dia}$ , although these relationships were the same for a constant absolute clearance, rather than a constant relative clearance. Correlation between  $\phi$  and  $k$  and the Reynolds number was poor.

10. Because a scale effect was evident in the above relationships, several of the dimensionless parameters were combined to form new dimensionless parameters that contained all of the important variables ( $\text{clear}$ ,  $\text{Dia}$ ,  $u_{\max}$ , and  $T$ ). An attempt was made to find a single parameter that was related to either  $\phi$  or  $k$  for all wave and pipeline conditions tested in this investigation.

Both  $\phi$  and  $k$  showed very good correlation with the parameter  $(\text{clear}/u_{\max} T)(\text{Dia}/u_{\max} T)$ . These relationships were valid for all pipe diameters, bottom clearances, orientation angles, and wave conditions tested.

In addition, the relative clearance was combined with both  $\phi$  and  $k$  to form the quantities  $\phi(\text{clear}/\text{Dia})$  and  $k(\text{clear}/\text{Dia})$ , both of which exhibited very good correlation with more of the dimensionless combinations than either  $\phi$  or  $k$  alone.  $k(\text{clear}/\text{Dia})$  was best correlated with  $(\text{clear}/u_{\max} T)(\text{clear}/\text{Dia})$ .  $\phi(\text{clear}/\text{Dia})$  was also correlated with this parameter, but exhibited better correlation with the parameter  $\sqrt{\text{Dia}/u_{\max} T} (\text{clear}/u_{\max} T)(\text{clear}/\text{Dia})$ .

11.  $C_L$ ,  $C_L(1-k)$ , and  $C_L(k)$  were correlated with the same parameter as  $\phi$  and  $k$ ,  $(\text{clear}/u_{\max} T)(\text{Dia}/u_{\max} T)$ . However, these correlations were not as good as the previous correlations between the coefficients of lift and  $k$  or  $\phi$ .

12. For a pipeline that is not parallel to the wave crests, the lift forces are apparently due only to the components of the horizontal water particle velocities perpendicular to the axis of the pipeline. Using this convention, consistent values of the coefficient of lift,  $C_L$ , are obtained for all angles of orientation. In addition, the relationships between the lift force parameters  $C_L$ ,  $\phi$ , and  $k$ , as well as relationships between these parameters and various dimensionless parameters defining the wave and pipeline conditions, are identical for all angles of orientation.

13. The maximum lift force ( $F_L(1-k)$  or  $F_L(k)$ , whichever is greater) exhibited good correlation with the Reynolds number,  $(u_{\max} \text{Dia}/v)$ . This relationship did not hold for the maximum positive lift ( $F_L(1-k)$ ) or the maximum negative lift ( $F_L(k)$ ) alone, but only for the largest of these two forces in any situation. The relationship was the same for all diameters over the range of conditions tested.

14. The horizontal coefficient of mass,  $C_M$ , showed excellent agreement with the potential flow solution for a circular cylinder in the vicinity of a plane wall subject to a uniform flow with constant acceleration. These results indicate that the potential flow solution may be useful for selecting a value of  $C_M$  for wave-induced forces, at least for situations in which the inertial forces predominate over the drag forces. The horizontal  $C_M$  was also correlated with several of the dimensionless parameters defining the wave and pipeline conditions, such as the parameter  $clear/u_{max}T$ .

## V. RECOMMENDATIONS FOR FURTHER RESEARCH

1. Experiments similar to this investigation should be carried out in a larger wave tank facility. This would allow the testing of larger diameter pipeline models as well as experiments at higher Reynolds numbers and higher values of the Keulegan-Carpenter parameter. Such an investigation is necessary to determine the validity of extrapolating the results of the present study to design situations in the ocean, and to point out any weaknesses or limitations of the proposed lift force model due to scale effects.

2. It would be of interest to perform experiments to evaluate the magnitude, phase, and frequency spectra of the vertical transverse lift forces due to eddy shedding for a horizontal cylinder subject to oscillatory horizontal flow velocities. This could be done by oscillating a test cylinder horizontally in still water away from a boundary, or by using a pulsating flume facility. The horizontal flow patterns at the bottom could be simulated, but without the lift force phenomenon due to the boundary. Only the transverse lift forces due to eddy shedding would act in the vertical direction, so the magnitude and time history of these forces could be easily measured.

A thorough analysis of the eddy forces for different pipe diameters and flow conditions would allow an evaluation of their importance relative to the Bernoulli-type lift forces, and at the same time explain some of the variations in the vertical wave force parameters calculated from an analysis which neglected the eddy forces because they could not be separated analytically because of their random nature. Adequate knowledge of the eddy forces would allow the addition of the eddy lift force term,  $F_L^1 = 1/2 C_L^1 \rho A u_{max}^2$ , to the Morison equation with appropriate values of the coefficient  $C_L^1$  for any given set of wave and pipeline conditions.

It should be noted that evaluation of the eddy forces for a cylinder away from a boundary would only give an approximate estimate of the eddy release phenomenon for a pipe located near the bottom. The presence of the bottom boundary changes the flow pattern, velocities, and pressure distribution around the cylinder, and therefore would be expected to have some effect on the formation and release of eddies.

3. Since the restricted flow through the narrow bottom clearance constriction is the critical part of the lift force phenomenon, the effect of pipeline roughness and bottom roughness on the wave-induced lift forces should be studied. This has practical significance, since the ocean floor is not necessarily smooth, and pipelines installed in marine waters may soon become encrusted with marine organisms, thus increasing their surface roughness.

4. The effect on the lift force phenomenon of a horizontal bottom current superimposed on the oscillatory motions of the wave action should be investigated.

5. The effect of porosity of the bottom on lift forces should also be investigated.

LITERATURE CITED

- AL-KAZILY, M.F., "Forces on Submerged Pipelines Induced by Water Waves,"  
HEL 9-21, Hydraulic Engineering Laboratory, University of California,  
Berkeley, Calif., Oct. 1972.
- GRACE, R.A., "Wave Forces on Submerged Objects," Report No. 10, Look  
Laboratory, University of Hawaii, Honolulu, Hawaii, July 1974.
- MORISON, J.R., et al., "The Forces Exerted by Surface Waves on Piles,"  
*Petroleum Transactions*, Vol. 189, 1950, pp. 149-154.
- PAULLING, J.R., and SIBUL, O.J., "Instrumentation for Digital Recording,"  
*Proceedings of the 15th American Towing Tank Conference*, Ottawa,  
Canada, 1968.
- YAMAMOTO, T., NAIH, J.H., and SLOTTA, L.S., "Yet Another Report on  
Cylinder Drag or Wave Forces on Horizontal Submerged Cylinders,"  
Bulletin No. 47, Engineering Experiment Station, Oregon State  
University, Corvallis, Oreg., Apr. 1973.



APPENDIX A

LEAST SQUARES ANALYSIS OF EXPERIMENTAL DATA

Using Morison's method for the calculation of wave forces on a pipeline, the vertical component of the wave-induced force may be expressed as:

$$\begin{aligned}
 F_V &= (F_I)_V + (F_D)_V + F_L + F'_L \\
 &= C_M \rho V \frac{\partial v}{\partial t} + 1/2 C_D \rho A v |v| \\
 &\quad + 1/2 C_L \rho A u_{\max}^2 [\cos^2 (\theta - \phi) - k] \\
 &\quad + 1/2 C'_L \rho A u_{\max}^2.
 \end{aligned} \tag{A1}$$

Since the transverse lift force associated with eddy shedding ( $F'_L$ ) is a random phenomenon, there is no way to handle its time history in analyzing a wave force record with several other forces occurring simultaneously. Because the Bernoulli-type lift forces were much larger than the eddy-associated forces for a pipeline located close to the bottom, the eddy-associated lift force term was dropped from the analysis.

The vertical components of the water particle velocities and accelerations near the bottom are small in comparison with the corresponding horizontal components. As a result, the vertical lift forces due to the horizontal components of the water particle velocities are generally much larger than the vertical drag and inertial forces. The drag forces are especially insignificant since the vertical excursions of the water particles near the bottom are smaller than the diameter of the pipeline.

Using linear wave theory, the kinematics of the wave-induced water particle motions with respect to time can be expressed as:

$$u = \frac{\pi H}{T} \frac{\cosh \left( \frac{2\pi z}{L} \right)}{\sinh \left( \frac{2\pi d}{L} \right)} \cos \theta \tag{A2}$$

$$v = - \frac{\pi H}{T} \frac{\sinh \left( \frac{2\pi z}{L} \right)}{\sinh \left( \frac{2\pi d}{L} \right)} \sin \theta \tag{A3}$$

$$\frac{\partial v}{\partial t} = - \frac{2\pi^2 H}{T^2} \frac{\sinh\left(\frac{2\pi z}{L}\right)}{\sinh\left(\frac{2\pi d}{L}\right)} \cos \theta, \quad (\text{A4})$$

where

H = wave height

T = wave period

L = wavelength

d = stillwater depth

z = vertical distance above the bottom

$\theta = \frac{2\pi t}{T}$  = position of the wave cycle with respect to time.

Substituting these expressions into the vertical force equation yields:

$$\begin{aligned} F_V = & - C_M \left[ \frac{\rho V 2\pi^2 H}{T^2} \frac{\sinh\left(\frac{2\pi z}{L}\right)}{\sinh\left(\frac{2\pi d}{L}\right)} \right] \cos \theta \\ & - C_D \left[ \frac{\rho A \pi^2 H^2}{2T^2} \frac{\sinh^2\left(\frac{2\pi z}{L}\right)}{\sinh^2\left(\frac{2\pi d}{L}\right)} \right] \sin \theta \quad |\sin \theta| \\ & + C_L \left[ \frac{\rho A \pi^2 H^2}{2T^2} \frac{\cosh^2\left(\frac{2\pi z}{L}\right)}{\sinh^2\left(\frac{2\pi d}{L}\right)} \right] [\cos^2(\theta - \phi) - k] \end{aligned} \quad (\text{A5})$$

or

$$F_V = -C_M F_{Mv} \cos \theta - C_D F_{Dv} \sin \theta \quad |\sin \theta| + C_L F_{Lv} [\cos^2(\theta - \phi) - k], \quad (\text{A6})$$

where

$$F_{Mv} = \frac{\rho V 2\pi^2 H}{T^2} \frac{\sinh\left(\frac{2\pi z}{L}\right)}{\sinh\left(\frac{2\pi d}{L}\right)} \quad (\text{A7})$$

$$F_{Dv} = \frac{\rho A \pi^2 H^2}{2T^2} \frac{\sinh^2\left(\frac{2\pi z}{L}\right)}{\sinh^2\left(\frac{2\pi d}{L}\right)} \quad (\text{A8})$$



$$F_{LV} = \frac{\rho A \pi^2 H^2}{2T} \frac{\cosh^2 \left( \frac{2\pi z}{L} \right)}{\sinh^2 \left( \frac{2\pi d}{L} \right)} \quad (A9)$$

The expressions,  $F_{MV}$ ,  $F_{DV}$ , and  $F_{LV}$ , are constant for a given set of wave and pipeline conditions.

Linear wave theory was used in the analysis because, as discussed previously, there seems to be no obvious way of accurately describing the lift force phenomenon mathematically using higher order theories. Since the lift forces are much larger than the vertical drag or inertial forces, with the drag forces being almost completely insignificant, there was no point in using higher theories to express the vertical components of the drag and inertial forces.

For any vertical wave force record in which the corresponding wave and pipeline conditions are known, a least squares analysis can be performed on the data to determine the values of the unknown parameters  $C_L$ ,  $\phi$ ,  $k$ ,  $C_M$ , and  $C_D$  in the vertical wave force equation. The least squares analysis yields the values of these five parameters which best fit the force data throughout the entire wave cycle. This is accomplished by determining the values of these parameters which minimizes the sum of squares of the difference between the observed force data and the corresponding forces calculated with the mathematical model throughout a complete wave cycle.

Using the appropriate trigonometric identities,

$$\begin{aligned} \cos^2 (\theta - \phi) &= 1/2 + 1/2 \cos 2 (\theta - \phi) \\ &= 1/2 + 1/2 (\cos 2\theta \cos 2\phi + \sin 2\theta \sin 2\phi), \end{aligned} \quad (A10)$$

so the lift force equation can be expressed as:

$$F_L = 1/2 C_L \rho A u_{\max}^2 [1/2 \cos 2\phi \cos 2\theta + 1/2 \sin 2\phi \sin 2\theta + 1/2 - k] \quad (A11)$$

$$\text{or } F_L = A_1 \cos 2\theta + B_1 \sin 2\theta + C_1 \quad (A12)$$

$$\text{where } A_1 = 1/4 C_L \rho A u_{\max}^2 \cos 2\phi = 1/2 C_L F_{LV} \cos 2\phi \quad (A13)$$

$$B_1 = 1/4 C_L \rho A u_{\max}^2 \sin 2\phi = 1/2 C_L F_{LV} \sin 2\phi \quad (A14)$$

$$C_1 = 1/2 C_L \rho A u_{\max}^2 (1/2 - k) = C_L F_{L_V} (1/2 - k). \quad (A15)$$

In an analogous manner, the vertical components of the inertial and drag forces can be written as:

$$(F_I)_V = C_M \rho \left(\frac{\partial v}{\partial t}\right)_{\max} \cos \theta = D_1 \cos \theta \quad (A16)$$

$$\text{and } (F_D)_V = 1/2 C_D \rho A v_{\max} \sin \theta |v_{\max} \sin \theta| = E_1 \sin \theta |\sin \theta|, \quad (A17)$$

$$\text{where } D_1 = C_M \rho \left(\frac{\partial v}{\partial t}\right)_{\max} = - C_M F_{M_V} \quad (A18)$$

$$\left(\frac{\partial v}{\partial t}\right)_{\max} = - \frac{2\pi^2 H}{T^2} \frac{\sinh\left(\frac{2\pi z}{L}\right)}{\sinh\left(\frac{2\pi d}{L}\right)} \quad (A19)$$

$$E_1 = 1/2 C_D \rho A v_{\max} |v_{\max}| = - C_D F_{D_V} \quad (A20)$$

$$v_{\max} = - \frac{\pi H}{T} \frac{\sinh\left(\frac{2\pi z}{L}\right)}{\sinh\left(\frac{2\pi d}{L}\right)}. \quad (A21)$$

The total vertical wave force at any position  $\theta_i$  in the wave cycle can then be written as:

$$F_V(\theta_i) = F_L + (F_I)_V + (F_D)_V = A_1 \cos 2\theta_i + B_1 \sin 2\theta_i + C_1 + D_1 \cos \theta_i + E_1 \sin \theta_i |\sin \theta_i|. \quad (A22)$$

The parameters  $A_1$ ,  $B_1$ ,  $C_1$ ,  $D_1$ , and  $E_1$  are constant for any given values of  $C_L$ ,  $\phi$ ,  $k$ ,  $C_M$ , and  $C_D$ , corresponding to the particular wave and pipeline conditions under consideration.

The sum of squares of the differences between the observed vertical forces,  $F_{OV}(\theta_i)$ , and the corresponding calculated forces,  $F_V(\theta_i)$ , is written as:

$$\sum_{i=1}^n [F_V(\theta_i) - F_{OV}(\theta_i)]^2 = \sum_{i=1}^n [A_1 \cos 2\theta_i + B_1 \sin 2\theta_i + C_1 + D_1 \cos \theta_i + E_1 \sin \theta_i |\sin \theta_i| - F_{OV}(\theta_i)]^2. \quad (A23)$$

To minimize the sum of squares of the differences, the derivative of this expression is taken separately with respect to each of the five unknown parameters  $A_1$ ,  $B_1$ ,  $C_1$ ,  $D_1$ , and  $E_1$ , and the resulting expressions are set equal to zero, yielding a system of five simultaneous equations with five unknowns. The system of equations is then summed for each interval,  $i$ , over a complete wave cycle, and the resulting expressions are solved for the values of the unknown parameters  $A_1$ ,  $B_1$ ,  $C_1$ ,  $D_1$ , and  $E_1$  which thus minimize the sum of squares of the differences. The derivatives are:

$$\begin{aligned} \frac{\partial [F_V(\theta_i) - F_{OV}(\theta_i)]^2}{\partial A_1} &= 2A_1 \cos^2 2\theta_i + 2B_1 \sin 2\theta_i \cos 2\theta_i \\ &+ 2C_1 \cos 2\theta_i + 2D_1 \cos \theta_i \cos 2\theta_i \\ &+ 2E_1 \sin \theta_i |\sin \theta_i| \cos 2\theta_i \\ &- 2 F_{OV}(\theta_i) \cos 2\theta_i = 0 \end{aligned} \quad (A24)$$

$$\begin{aligned} \frac{\partial [F_V(\theta_i) - F_{OV}(\theta_i)]^2}{\partial B_1} &= 2A_1 \cos 2\theta_i \sin 2\theta_i + 2B_1 \sin^2 2\theta_i \\ &+ 2C_1 \sin 2\theta_i + 2D_1 \cos \theta_i \sin 2\theta_i \\ &+ 2E_1 \sin \theta_i |\sin \theta_i| \sin 2\theta_i \\ &- 2 F_{OV}(\theta_i) \sin 2\theta_i = 0 \end{aligned} \quad (A25)$$

$$\begin{aligned} \frac{\partial [F_V(\theta_i) - F_{OV}(\theta_i)]^2}{\partial C_1} &= 2A_1 \cos 2\theta_i + 2B_1 \sin 2\theta_i \\ &+ 2C_1 + 2D_1 \cos \theta_i \\ &+ 2E_1 \sin \theta_i |\sin \theta_i| \\ &- 2 F_{OV}(\theta_i) = 0 \end{aligned} \quad (A26)$$

$$\begin{aligned} \frac{\partial [F_v(\theta_i) - F_{ov}(\theta_i)]^2}{\partial D_1} &= 2A_1 \cos 2\theta_i \cos \theta_i \\ &+ 2B_1 \sin 2\theta_i \cos \theta_i + 2C_1 \cos \theta_i \\ &+ 2D_1 \cos^2 \theta_i + 2E_1 \sin \theta_i |\sin \theta_i| \cos \theta_i \\ &- 2F_{ov}(\theta_i) \cos \theta_i = 0 \end{aligned} \quad (A27)$$

$$\begin{aligned} \frac{\partial [F_v(\theta_i) - F_{ov}(\theta_i)]^2}{\partial E_1} &= 2A_1 \cos 2\theta_i \sin \theta_i |\sin \theta_i| \\ &+ 2B_1 \sin 2\theta_i \sin \theta_i |\sin \theta_i| \\ &+ 2C_1 \sin \theta_i |\sin \theta_i| \\ &+ 2D_1 \cos \theta_i \sin \theta_i |\sin \theta_i| \\ &+ 2E_1 (\sin \theta_i |\sin \theta_i|)^2 \\ &- 2F_{ov}(\theta_i) \sin \theta_i |\sin \theta_i| = 0 \end{aligned} \quad (A28)$$

For an even number of equally spaced time intervals,  $\theta_i$ , summed over a complete wave cycle, many of the terms cancel out due to the symmetry of these sinusoidal functions. Thus,

$$\sum_{i=1}^n \cos \theta_i = 0 \quad (A29)$$

$$\sum_{i=1}^n \cos 2\theta_i = 0 \quad (A30)$$

$$\sum_{i=1}^n \sin 2\theta_i = 0 \quad (A31)$$

$$\sum_{i=1}^n \sin \theta_i |\sin \theta_i| = 0 \quad (A32)$$

$$\sum_{i=1}^n \cos \theta_i \cos 2\theta_i = 0 \quad (A33)$$

$$\sum_{i=1}^n \cos \theta_i \sin 2\theta_i = 0 \quad (\text{A34})$$

$$\sum_{i=1}^n \cos \theta_i \sin \theta_i |\sin \theta_i| = 0 \quad (\text{A35})$$

$$\sum_{i=1}^n \cos 2\theta_i \sin 2\theta_i = 0 \quad (\text{A36})$$

$$\sum_{i=1}^n \cos 2\theta_i \sin \theta_i |\sin \theta_i| = 0 \quad (\text{A37})$$

$$\sum_{i=1}^n \sin 2\theta_i \sin \theta_i |\sin \theta_i| = 0 \quad (\text{A38})$$

when taken over a complete wave cycle, As a result, only the squared terms, and the terms involving the observed forces,  $F_o(\theta_i)$ , remain in these equations. The resulting expressions are:

$$A_1 \sum_{i=1}^n \cos^2 2\theta_i - \sum_{i=1}^n F_{ov}(\theta_i) \cos 2\theta_i = 0 \quad (\text{A39})$$

$$B_1 \sum_{i=1}^n \sin^2 2\theta_i - \sum_{i=1}^n F_{ov}(\theta_i) \sin 2\theta_i = 0 \quad (\text{A40})$$

$$C_1 \sum_{i=1}^n i - \sum_{i=1}^n F_{ov}(\theta_i) = nC_1 - \sum_{i=1}^n F_{ov}(\theta_i) = 0 \quad (\text{A41})$$

$$D_1 \sum_{i=1}^n \cos^2 \theta_i - \sum_{i=1}^n F_{ov}(\theta_i) \cos \theta_i = 0 \quad (\text{A42})$$

$$E_1 \sum_{i=1}^n (\sin \theta_i - |\sin \theta_i|)^2 - \sum_{i=1}^n F_{ov}(\theta_i) \sin \theta_i |\sin \theta_i| = 0 \quad (A43)$$

where  $n$  is the total number of values taken from the vertical wave force record (from an even number of equally spaced intervals per wave cycle, and over any number of complete wave cycles), and  $i$  is the number of the interval.

These expressions are easily solved for the unknown parameters  $A_1$ ,  $B_1$ ,  $C_1$ ,  $D_1$ , and  $E_1$ , yielding:

$$A_1 = \frac{\sum_{i=1}^n F_{ov}(\theta_i) \cos 2\theta_i}{\sum_{i=1}^n \cos^2 2\theta_i} \quad (A44)$$

$$B_1 = \frac{\sum_{i=1}^n F_{ov}(\theta_i) \sin 2\theta_i}{\sum_{i=1}^n \sin^2 2\theta_i} \quad (A45)$$

$$C_1 = \frac{\sum_{i=1}^n F_{ov}(\theta_i)}{n} \quad (A46)$$

$$D_1 = \frac{\sum_{i=1}^n F_{ov}(\theta_i) \cos \theta_i}{\sum_{i=1}^n \cos^2 \theta_i} \quad (A47)$$

$$E_1 = \frac{\sum_{i=1}^n F_{ov}(\theta_i) \sin \theta_i |\sin \theta_i|}{\sum_{i=1}^n (\sin \theta_i |\sin \theta_i|)^2} . \quad (A48)$$

With these relationships, the corresponding values of the parameters  $C_L$ ,  $\phi$ ,  $k$ ,  $C_M$ , and  $C_D$  in the vertical wave force equation which best fit the data throughout the complete wave cycle can be obtained.

The coefficients of mass and drag,  $C_M$  and  $C_D$ , are obtained directly from the parameters  $D_1$  and  $E_1$ , since

$$C_M = -\frac{D_1}{F_{Mv}} = -\frac{\sum_{i=1}^n F_{ov}(\theta_i) \cos \theta_i}{F_{Mv} \sum_{i=1}^n \cos^2 \theta_i} \quad (A49)$$

$$C_D = -\frac{E_1}{F_{Dv}} = -\frac{\sum_{i=1}^n F_{ov}(\theta_i) \sin \theta_i |\sin \theta_i|}{F_{Dv} \sum_{i=1}^n (\sin \theta_i |\sin \theta_i|)^2} . \quad (A50)$$

Since  $A_1 = 1/2 C_L F_{Lv} \cos 2\phi$  and  $B_1 = 1/2 C_L F_{Lv} \sin 2\phi$ , the phase shift parameter  $\phi$  can be obtained from:

$$\phi = 1/2 (2\phi) = 1/2 \tan^{-1} \left( \frac{\sin 2\phi}{\cos 2\phi} \right) = 1/2 \tan^{-1} \left( \frac{B_1}{A_1} \right) \quad (A51)$$

since  $1/2 C_L F_{Lv}$  cancels out of the expression  $\left( \frac{B_1}{A_1} \right)$ . Thus,

$$\phi = 1/2 \tan^{-1} \left( \frac{\sum_{i=1}^n F_{ov}(\theta_i) \sin 2\theta_i / \sum_{i=1}^n \sin^2 2\theta_i}{\sum_{i=1}^n F_{ov}(\theta_i) \cos 2\theta_i / \sum_{i=1}^n \cos^2 2\theta_i} \right) . \quad (A52)$$

After  $\phi$  is known, the coefficient of lift,  $C_L$ , can be obtained from either  $A_1$  or  $B_1$ , since

$$C_L = \frac{A_1}{1/2 F_{L_V} \cos 2\phi} = \frac{\sum_{i=1}^n F_{O_V}(\theta_i) \cos 2\theta_i}{1/2 F_{L_V} \cos 2\phi \sum_{i=1}^n \cos^2 2\theta_i} \quad (A53)$$

or

$$C_L = \frac{B_1}{1/2 F_{L_V} \sin 2\phi} = \frac{\sum_{i=1}^n F_{O_V}(\theta_i) \sin 2\theta_i}{1/2 F_{L_V} \sin 2\phi \sum_{i=1}^n \sin^2 2\theta_i} \quad (A54)$$

Alternatively,  $C_L$  could be obtained from  $A_1$  and  $B_1$  directly without first solving for  $\phi$ , since

$$\begin{aligned} \sqrt{A_1^2 + B_1^2} &= \sqrt{(1/2 C_L F_{L_V} \cos 2\phi)^2 + (1/2 C_L F_{L_V} \sin 2\phi)^2} \\ &= \sqrt{(1/2 C_L F_{L_V})^2 (\cos^2 2\phi + \sin^2 2\phi)} \\ &= 1/2 C_L F_{L_V} \end{aligned} \quad (A55)$$

Thus,

$$C_L = \frac{2 \sqrt{A_1^2 + B_1^2}}{F_{L_V}} = \frac{2 \sqrt{\left[ \frac{\sum_{i=1}^n F_{O_V}(\theta_i) \cos 2\theta_i}{\sum_{i=1}^n \cos^2 2\theta_i} \right]^2 + \left[ \frac{\sum_{i=1}^n F_{O_V}(\theta_i) \sin 2\theta_i}{\sum_{i=1}^n \sin^2 2\theta_i} \right]^2}}{F_{L_V}} \quad (A56)$$



Finally, the parameter  $k$  can be obtained from  $C_1$  knowing the value of  $C_L$ , since

$$k = 1/2 - \frac{C_1}{C_L F_{LV}} = 1/2 - \frac{\sum_{i=1}^n F_{ov}(\theta_i) / n}{C_L F_{LV}} \quad (A57)$$

Thus, once the vertical wave forces on a pipeline are measured experimentally, the values of the parameters  $C_L$ ,  $\phi$ ,  $k$ ,  $C_M$ , and  $C_D$  of the vertical wave force equation which best fit the data throughout the entire wave cycle can be determined for the particular set of wave and pipeline conditions tested.

In an analogous manner, the least squares analysis can be applied to the horizontal wave force data. Omitting the horizontal force associated with eddy shedding, the horizontal component of the wave-induced force can be expressed as equation (2):

$$F_h = (F_I)_h + (F_D)_h = C_M \rho V \frac{\partial u}{\partial t} + 1/2 C_D \rho A u |u| \quad (2)$$

The data from the horizontal force measurements show that the horizontal eddy forces are insignificant in comparison to the horizontal drag and inertial forces for the experimental conditions tested.

Using linear wave theory, the horizontal components of the wave kinematics with respect to time can be expressed as:

$$u = \frac{\pi H}{T} \frac{\cosh\left(\frac{2\pi z}{L}\right)}{\sinh\left(\frac{2\pi d}{L}\right)} \cos \theta$$

$$\frac{\partial u}{\partial t} = -\frac{2\pi^2 H}{T^2} \frac{\cosh\left(\frac{2\pi z}{L}\right)}{\sinh\left(\frac{2\pi d}{L}\right)} \sin \theta \quad (A58)$$

Substituting these expressions into the horizontal wave force equation yields:

$$F_h = C_D \left[ \frac{\rho A \pi^2 H^2}{2T^2} \frac{\cosh^2 \left( \frac{2\pi z}{L} \right)}{\sinh^2 \left( \frac{2\pi d}{L} \right)} \right] \cos \theta \left| \cos \theta \right| - C_M \left[ \frac{\rho V 2\pi^2 H}{T^2} \frac{\cosh \left( \frac{2\pi z}{L} \right)}{\sinh \left( \frac{2\pi d}{L} \right)} \right] \sin \theta \quad (A59)$$

$$\text{or } F_h = C_D F_{Dh} \cos \theta \left| \cos \theta \right| - C_M F_{Mh} \sin \theta \quad (A60)$$

where

$$F_{Dh} = \frac{\rho A \pi^2 H^2}{2T^2} \frac{\cosh^2 \left( \frac{2\pi z}{L} \right)}{\sinh^2 \left( \frac{2\pi d}{L} \right)} \quad (A61)$$

$$F_{Mh} = \frac{\rho V 2\pi^2 H}{T^2} \frac{\cosh \left( \frac{2\pi z}{L} \right)}{\sinh \left( \frac{2\pi d}{L} \right)} \quad (A62)$$

The expressions  $F_{Dh}$  and  $F_{Mh}$  are constant for a given set of wave and pipeline conditions.

The horizontal component of the wave-induced force can also be written as:

$$F_h = A_2 \cos \theta \left| \cos \theta \right| + B_2 \sin \theta \quad (A63)$$

where

$$A_2 = C_D F_{Dh} = 1/2 C_D \rho A u_{\max} \left| u_{\max} \right| \quad (A64)$$

$$u_{\max} = \frac{\pi H}{T} \frac{\cosh \left( \frac{2\pi z}{L} \right)}{\sinh \left( \frac{2\pi d}{L} \right)} \quad (\text{A65})$$

$$B_2 = - C_M F_{Mh} = C_M \rho V \left( \frac{\partial u}{\partial t} \right)_{\max} \quad (\text{A66})$$

$$\left( \frac{\partial u}{\partial t} \right)_{\max} = - \frac{2\pi^2 H}{T^2} \frac{\cosh \left( \frac{2\pi z}{L} \right)}{\sinh \left( \frac{2\pi d}{L} \right)} \quad (\text{A67})$$

Thus, the total horizontal wave force at any position  $\theta_i$  in the wave cycle can be expressed as:

$$\begin{aligned} F_h (\theta_i) &= (F_D)_h + (F_I)_h \\ &= A_2 \cos \theta_i |\cos \theta_i| + B_2 \sin \theta_i \end{aligned} \quad (\text{A68})$$

where the parameters  $A_2$  and  $B_2$  are constant for any given values of  $C_D$  and  $C_M$ , corresponding to the particular wave and pipeline conditions under consideration.

The sum of squares of the differences between the observed horizontal forces,  $F_{Oh} (\theta_i)$ , and the corresponding calculated forces,  $F_h (\theta_i)$ , is written as:

$$\begin{aligned} \sum_{i=1}^n [F_h (\theta_i) - F_{Oh} (\theta_i)]^2 &= \sum_{i=1}^n [A_2 \cos \theta_i |\cos \theta_i| \\ &+ B_2 \sin \theta_i - F_{Oh} (\theta_i)]^2. \end{aligned} \quad (\text{A69})$$

The derivatives of this expression taken with respect to the unknown parameters  $A_2$  and  $B_2$  and set equal to zero give the following equations:

$$\frac{\partial [F_h (\theta_i) - F_{Oh} (\theta_i)]^2}{\partial A_2} = 2 A_2 (\cos \theta_i |\cos \theta_i|)^2$$

$$\begin{aligned}
& + 2B_2 \sin \theta_i \cos \theta_i |\cos \theta_i| \\
& - 2 F_{oh} (\theta_i) \cos \theta_i |\cos \theta_i| \\
& = 0
\end{aligned} \tag{A70}$$

$$\begin{aligned}
\frac{\partial [F_h (\theta_i) - F_{oh} (\theta_i)]^2}{\partial B_2} & = 2 A_2 \cos \theta_i |\cos \theta_i| \sin \theta_i \\
& + 2 B_2 \sin^2 \theta_i \\
& - 2 F_{oh} (\theta_i) \sin \theta_i \\
& = 0.
\end{aligned} \tag{A71}$$

Since  $\sum_{i=1}^n \sin \theta_i \cos \theta_i |\cos \theta_i| = 0$  for an even number of equally spaced intervals  $\theta_i$  summed over a complete wave cycle, the resulting summed expressions for the derivatives set equal to zero are

$$A_2 \sum_{i=1}^n (\cos \theta_i |\cos \theta_i|)^2 - \sum_{i=1}^n F_{oh} (\theta_i) \cos \theta_i |\cos \theta_i| = 0 \tag{A72}$$

$$B_2 \sum_{i=1}^n \sin^2 \theta_i - \sum_{i=1}^n F_{oh} (\theta_i) \sin \theta_i = 0. \tag{A73}$$

These expressions are easily solved for the unknown parameters  $A_2$  and  $B_2$ , yielding:

$$A_2 = \frac{\sum_{i=1}^n F_{oh} (\theta_i) \cos \theta_i |\cos \theta_i|}{\sum_{i=1}^n (\cos \theta_i |\cos \theta_i|)^2} \tag{A74}$$

$$B_2 = \frac{\sum_{i=1}^n F_{oh}(\theta_i) \sin \theta_i}{\sum_{i=1}^n \sin^2 \theta_i} . \quad (A75)$$

The coefficients of mass and drag which best fit the horizontal wave force data throughout the entire wave cycle can thus be obtained directly from the parameters  $A_2$  and  $B_2$  since

$$C_D = \frac{A_2}{F_{Dh}} = \frac{\sum_{i=1}^n F_{oh}(\theta_i) \cos \theta_i |\cos \theta_i|}{F_{Dh} \sum_{i=1}^n (\cos \theta_i |\cos \theta_i|)^2} \quad (A76)$$

$$C_M = -\frac{B_2}{F_{Mh}} = -\frac{\sum_{i=1}^n F_{oh}(\theta_i) \sin \theta_i}{F_{Mh} \sum_{i=1}^n \sin^2 \theta_i} . \quad (A77)$$

APPENDIX B  
COMPUTER PROGRAM FOR VERTICAL LEAST SQUARES  
ANALYSIS (TWO-DIMENSIONAL DATA)

```

PROGRAM SMLDIA(INPUT,OUTPUT,PUNCH)
DIMENSION X(41),Y(41),Z(41),YS(41),YI(41),FI(41),FP(41),F(41),
IFV(41),RES(41),G(101),P(41),O(41),HI(41),HX(4)
C SET TEST CONDITIONS
ANGLE=0.
D=2.000
C READ IN DIGITIZED DATA
8 READ 1,UP,ON,UF,DF,DIA,XC
IF(UP)10,10,9
9 READ 2,CL,T,N,XW,XF,C,W,FD,(HI(I),I=1,4)
READ 3,(FI(I),I=1,40)
1 FORMAT(2F3.3,2F3.0,2F3.3)
2 FORMAT(F3.3,F3.2,I2,2F2.1,7F3.0)
3 FORMAT(24F3.0)
C DETERMINE WAVE HEIGHT
DO 11 I=1,4
IF(HI(I)-W)21,23,23
21 HX(I)=(W-HI(I))*(DN/C)*(1./XW)
GO TO 11
23 HX(I)=(HI(I)-W)*(UP/C)*(1./XW)
11 CONTINUE
H=(HX(1)+HX(2)-HX(3)-HX(4))/2.
C CALCULATE CONSTANTS IN FORCE EQUATION
PI=3.1415926536
R=1.938
CALL WAVE(L,T,D,XL)
ZV=CL+(.5*D/A)
A=EXP((2.*PI*ZV)/XL)
COSH=A+(1./A)
SINH=A-(1./A)
B=EXPI(2.*PI*D)/XL)
SINH=B-(1./B)
CS=COSH/SINH
SS=SINH/SINH
CF1=R*D/A*XC*H*PI*PI/(2.*T*T)
FLV=CF1*H*CS*CS
FDV=CF1*H*SS*SS
FMV=CF1*D/A*PI*SS
U=(H*CS*PI)/T
C DETERMINE AVERAGE, MAXIMUM, AND MINIMUM FORCES
FMAX=.5
FMIN=.5
SF=0.
DO 13 I=1,40
IF(FI(I)-FD)70,71,71
70 FP(I)=(FI(I)-FD)*(DF/C)*.002204/XF
GO TO 73
71 FP(I)=(FI(I)-FD)*(UF/C)*.002204/XF
73 CONTINUE
IF(FP(I)).GT.FMAX)902,901
902 FMAX=FP(I)
901 IF(FP(I)).LT.FMIN)903,12
903 FMIN=FP(I)
12 SF=SF+FP(I)
13 CONTINUE
SF=SF/40.

```

```

C   CALCULATE SUMS OF SQUARES AND PRODUCTS
    SFF=0.
    SFX=0.
    SFY=0.
    SFQ=0.
    SFZ=0.
    DT=.31415926536
    A=DT
    DO 15 I=1,40
    A=A+DT
    X(I)=COS(A)
    B=2.*A
    Y(I)=COS(B)
    Q(I)=SIN(B)
    C=SIN(A)
    Z(I)=C*ABS(C)
    F(I)=FP(I)-SF
    SFF=SFF+F(I)*F(I)
    SFX=SFX+F(I)*X(I)
    SFY=SFY+F(I)*Y(I)
    SFQ=SFQ+F(I)*Q(I)
    SFZ=SFZ+F(I)*Z(I)
15  CCNTINUE
    AX=SFX/20.
    AY=SFY/20.
    AQ=SFQ/20.
    AZ=SFZ/15.
    VX=AX*SFX
    VY=AY*SFY
    VQ=AQ*SFQ
    VZ=AZ*SFZ
    VR=SFF-VX-VY-VZ-VQ
C   CALCULATE COEFFICIENTS AND PARAMETERS PHI AND K
    PHI=28.64789*ATAN2(AQ,AY)
    IF(PHI,LT,-45.)7999,8999
7999 PHI=PHI+180.
8999 CONTINUE
    YA=SQRT(AQ*AQ+AY*AY)
    CLV=2.*YA/FLV
    ANG=(ANGLE*PI)/180.
    CLVA=CLV/COS(ANG)
    CLVU=CLVA/COS(ANG)
    CMV=-AX/FLV
    CDV=-AZ/FOV
    XK=.5-(SF/(CLV*FLV))
C   PRINT RESULTS OF ANALYSIS
    PRINT 200
200  FORMAT(IH1)
    PRINT 4
      4  FORMAT(10X,6HT(SEC),7X,6HHT(FT),5X,9HWAYEL(FT),6X,7HDEP(FT),4X,9HU
        1MAX(FPS),4X,9HCLEAR(FT),6X,7HDIA(FT),3X,12HCYL LGTH(FT),4X,8HANG(D
        2EG))
    PRINT 300,T,H,XL,D,U,CL,DIA,XC,ANGLE
300  FORMAT(2X,F13.2,F13.3,F13.2,SF13.3,F13.1////)
    PRINT 307
307  FORMAT(6X,12HTOTAL SUM SQ,6X,5HCOS2A,10X,5HSIN2A,11X,4HCOSA,8X,10H

```



```

1 SIN4/SIN4, 6X, 8HVARIANCF)
PRINT 301, SFF, VY, VO, VX, VZ, VR
301 FORMAT (6F15.6/)
PRINT 310
310 FORMAT (26X, 2HAY, 13X, 2HAQ, 13X, 2HAX, 13X, 2HAZ, 13X, 2HYA)
PRINT 302, AY, AQ, AX, AZ, YA
302 FORMAT (15X, 5F15.6/)
PRINT 303
303 FORMAT (41X, 3HFLV, 12X, 3HFMV, 12X, 3HFDV)
PRINT 303, FLV, FMV, FDV
303 FORMAT (30X, 3F15.6////)
PRINT 104
104 FORMAT (10X, 4H CLV, 10X, 5H CLVA, 10X, 5H CLVU, 11X, 5H CMV, 10X, 5H COV,
111X, 2H K, 12X, 4H PHI)
PRINT 305, CLV, CLVA, CLVU, CMV, COV, XK, PHI
305 FORMAT (15F15.3, F15.4, F15.2////)
PRINT 309
309 FORMAT (38X, 3HFAVG(LB), 7X, 3HFMAX(LB), 7X, 3HFMIN(LB))
PRINT 304, 5F, FMAX, FMIN
304 FORMAT (30X, F15.6, 2F15.5////)
3C4 PUNCH 387, CL, DIA, ANGLE, T, H, XL, U, CLV, CLVA, CLVU, PHI, XK, CMV, COV
387 FORMAT (F4.3, F5.3, F4.0, F5.2, F5.3, F6.2, F6.4, F5.2, 2F6.2, F7.2, F7.4, F6.
12, F5.2)
C PLGT ORIGINAL DATA AND RESULTS FOR COMPARISON
PRINT 26
26 FORMAT (4X, 7H FP(LB), 3X, 7H FV(LB), 2X, 8H RES(LB)/)
DO 31 L=1, 101
G(L)=1H
31 CONTINUE
DO 25 I=1, 40
FV(I)=AX*X(I)+AQ*Q(I)+AY*Y(I)+AZ*Z(I)+SF
RES(I)=FP(I)-FV(I)
25 CONTINUE
B=ABS(FP(1))
DO 59 I=2, 40
C=ABS(FV(I))
A=ABS(FP(I))
IF (C-B) 57, 57, 56
56 B=C
57 IF (A-B) 59, 59, 58
58 B=A
59 CONTINUE
BB=49./B
IF (BB-300.) 61, 43, 43
61 IF (BB-400.) 62, 44, 44
62 IF (BB-200.) 63, 45, 45
63 IF (BB-100.) 64, 46, 46
64 BB=50.
GO TO 47
43 BB=800.
GO TO 47
44 BB=400.
GO TO 47
45 BB=200.
GO TO 47
46 BB=100.
47 CONTINUE
DO 32 I=1, 40
G(S1)=1H
J=S1.+3B*FP(I)
K=S1.+8B*FV(I)
L=S1.+3B*RES(I)
G(J)=1H*
G(K)=1H*
G(L)=1H.
PRINT 100, FP(I), FV(I), RES(I), G
100 FORMAT (1H2, 3F10.5, 101A1/)
G(J)=1H
G(K)=1H
G(L)=1H
32 CONTINUE
GO TO 8
10 CONTINUE
END
SUBROUTINE WAVFL(T, D, XL)
B=32.2*T*T/6.283185
TPD=6.283185*D
IF (B-TPD) 2, 2, 3
C DEEP WATER INITIAL ESTIMATE FOR WAVELENGTH
2 XL=B
GC TO 4
C SHALLOW WATER INITIAL ESTIMATE FOR WAVELENGTH
3 XL=T*SQR(D*32.2)
4 XL=XL
XL=B*TANH(TPD/XL)
IF (ABS (XL-XL)-.005) 5, 4, 4
5 RETURN
END

```

APPENDIX C

COMPUTER PROGRAM FOR VERTICAL LEAST SQUARES  
ANALYSIS (THREE-DIMENSIONAL DATA)

```

PROGRAM WVFORC3(INPUT,TAPE1,OUTPUT,PUNCH)
DIMENSION X(150),Y(150),Z(150),Q(150),FI(380),HI(380),FP(150),FV(1
150),F(150),RES(150),G(101),HMAX(21),HMIN(2),T1(2),T2(2),HP(150),XTI
2(2),IDREC(2)
INTEGER LABEL(8)
C SET TEST CONDITIONS
CL=001
DIA=3333
XC=917
D=2.757
C READ IN DIGITIZED DATA
C WAVE DATA IS IN FT.
C FORCE DATA IS IN 10-GRAMS
CALL NOBLOK(1)
8 READ 1,ANGLE
1 FORMAT(F2.0)
IF(ANGLE.LT.0.)10,11
11 READ(1) LABEL
NRECS=LABEL(8)
PRINT 200
200 FORMAT(1H1)
PRINT 999,LABEL
999 FORMAT(1X,7A10,15//)
READ(1) NCHAN,IDREC,DELTA,NSAMP,FI
L=LENGTH(I)
READ(1) NCHAN,IDREC,DELTA,NSAMP,HI
L=LENGTH(I)
READ(1)
C DETERMINE WAVE HEIGHT
N=1
I=1
401 IF(HI(I).LT.0.)404,403
403 I=I+10
GO TO 401
402 IF(HI(I).GT.0.)416,404
404 I=I+1
GO TO 402
416 NI=I
425 HMAX(N)=0.
I=I+7
IF(HI(I).GT.0.)415,404
415 IF(HI(I).GT.HMAX(N))407,406
407 HMAX(N)=HI(I)
XTI(N)=I
406 I=I+1
IF(HI(I).GT.0.)415,430
430 GO TO (431,413),N
431 HMIN(N)=0.
I=I+7
411 IF(HI(I).LT.HMIN(N))432,410
432 HMIN(N)=HI(I)
410 I=I+1
IF(HI(I).LT.0.)411,433
433 N=N+1
GO TO 425

```

```

413 H=.5*(HMAX(1)+.5*(HMAX(2)-HMIN(1)
C DETERMINE WAVE PERIOD
I=M1-1
M3=1
801 I=I+1
IF(HI(1).GT.0.)810,801
810 T1(M3)=I
832 I=I+1
AI=I
IF(HI(1).GT.0.)811,801
811 IF((AI-T1(M3)).GT.10.)812,832
812 I=I+10
805 I=I+1
IF(HI(1).GT.0.)805,813
813 T2(M3)=I-1
GO TO (814,806),M3
814 M3=M3+1
XI=.3*(XTI(2)-XTI(1))
IX=XI
I=I+IX
GO TO 801
806 TM1=(T2(1)+T1(1))/2.
TM2=(T2(2)+T1(2))/2.
XTM1=TM1+.6
XTM2=TM2+.6
ITM1=XTM1
ITM2=XTM2
TT1=ITM1
TT2=ITM2
T=(TT2-TT1)*.02
XJ=50.*T
XJJ=XJ+.1
J=XJJ
C CALCULATE CONSTANTS IN FORCE EQUATION
PI=3.1415926536
R=.935
CALL WAVE1(T,O,XL)
ZV=CL+(.5*DIA)
A=EXP((2.*PI*ZV)/XL)
COSHA=A+(1./A)
SINHA=A-(1./A)
B=EXP((2.*PI*O)/XL)
SINHB=3-(1./B)
CS=COSHA/SINHB
SS=SINHA/SINHB
CF1=R*DIA*XC*H*PI*PI/(2.*T*T)
FLV=CF1*H*CS*CS
FOV=CF1*H*SS*SS
FMV=CF1*DIA*PI*SS
U=(H*CS*PI)/T
C DETERMINE AVERAGE, MAXIMUM, AND MINIMUM FORCES
FMAX=-.5
FMIN=.5
SF=0.
DO 13 I=1,J
FP(I)=F1(I+ITM1-1)*0.02204

```

```

      IF (FP(I).GT.FMAX)902,901
902  FMAX=FP(I)
901  IF (FP(I).LT.FMIN)903,12
903  FMIN=FP(I)
      SF=SF+FP(I)
      13  CONTINUE
      SF=SF/XJ
C   CALCULATE SUMS OF SQUARES AND PRODUCTS
      SFF=0.
      SFX=0.
      SFY=0.
      SFZ=0.
      SFQ=0.
      SFZ=0.
      DT=3.1415926536/(25.*T)
      A=-DT
      DO 15 I=1,J
      A=A+DT
      X(I)=COS (A)
      B=2.*A
      Y(I)=COS(B)
      Q(I)=SIN(B)
      C=SIN(A)
      Z(I)=C*ABS (C)
      F(I)=FP(I)-SF
      SFF=SFF+F(I)*F(I)
      SFX=SFX+F(I)*X(I)
      SFY=SFY+F(I)*Y(I)
      SFQ=SFQ+F(I)*Q(I)
      SFZ=SFZ+F(I)*Z(I)
      15  CONTINUE
      SXX=.5*XJ
      SYY=.5*YJ
      SQO=.5*XJ
      SZZ=.375*XJ
      AX=SFX/SXX
      AY=SFY/SYY
      AQ=SFQ/SQO
      AZ=SFZ/SZZ
      VX=AX*SFX
      VY=AY*SFY
      VQ=AQ*SFQ
      VZ=AZ*SFZ
      VR=SFF-VX-VY-VZ-VQ
C   CALCULATE COEFFICIENTS AND PARAMETERS PHI AND K
      PHI=28.64789*ATAN2(AQ,AY)
      7999  PHI=PHI+190.
      8999  CONTINUE
      YA=SQRT(AQ*AQ+AY*AY)
      CLV=2.*YA/FLV
      ANG=(ANGLE*PI)/180.
      CLVA=CLV/COS(ANG)
      CLVU=CLVA/COS(ANG)
      CMV=-AX/FLV
      CDV=-AZ/FLV
      XK=.5-(SF/(CLV*FLV))

```

```

C PRINT RESULTS OF ANALYSIS
PRINT 4
4 FORMAT(10X,6HT(SEC),7X,6HHT(FT),5X,9HWAVEL(FT),6X,7HOEP(FT),4X,9HU
1MAX(FPS),4X,9HCLEAR(FT),6X,7HOIA(FT),3X,12HCYL LGHT(FT),4X,8HANG(D
2EG))
PRINT 300,T,H,XL,D,U,CL,DIA,XC,ANGLE
300 FORMAT(2X,F13.2,F13.3,F13.2,5F13.3,F13.1////)
PRINT 307
307 FORMAT(6X,12HTOTAL SUM 50,6X,5HCOS2A,10X,5HSIN2A,11X,4HCOSA,8X,10H
ISINA/SINA,6X,8HVAR(ANCE))
PRINT 301,SFF,VY,VO,VX,VZ,VR
301 FORMAT(6F15.6/)
PRINT 310
310 FORMAT(26X,2HAY,13X,2HAQ,13X,2HAX,13X,2HAZ,13X,2HYA)
PRINT 302,VY,AD,AX,AZ,YA
302 FORMAT(15X,5F15.6/)
PRINT 308
308 FORMAT(4X,3HFLV,12X,3HFMV,12X,3HFDV)
PRINT 303,FLV,FMV,FDV
303 FORMAT(30X,3F15.6////)
PRINT 104
104 FORMAT(10X,4H CLV,10X,5H CLVA,10X,5H CLVU,11X,5H CMV,10X,5H COV,
111X,2H K,12X,4H PHI)
PRINT 305,CLV,CLVA,CLVU,CMV,COV,XK,PHI
305 FORMAT(5F15.3,F15.4,F15.2////)
PRINT 309
309 FORMAT(38X,8HFAVG(LB),7X,8HFMAX(LB),7X,8HFMIN(LB))
PRINT 304,SF,FMAX,FMIN
304 FORMAT(10X,F15.6,2F15.5////)
PUNCH 387,CL,DIA,ANGLE,T,H,XL,U,CLV,CLVA,CLVU,PHI,XK,CMV,COV
387 FORMAT(F4.3,F5.3,F4.0,F5.2,F5.3,F6.2,F6.4,F5.2,F6.2,F7.2,F7.4,F6.
12,F8.2)
C PLCT ORIGINAL DATA AND RESULTS FOR COMPARISON
IF(I.GT.1.8)601,600
601 IF(I.GT.2.4)603,602
600 JS=2
GO TO 606
E02 JS=3
GO TO 606
603 JS=4
606 C=ABS(FMAX)
A=ABS(FMIN)
B=MAX(A,C)
BB=35./B
CC=30./HMAX(1)
PRINT 26
26 FORMAT(4X,7H FP(LB),3X,7H FV(LB),2X,8H RES(LB)/)
DO 31 L=1,101
G(L)=1H
31 CONTINUE
DO 32 I=1,J,JS
G(I)=1HI
HP(I)=HI(I+ITM1-1)
FV(I)=AX*X(I)+AQ*Q(I)+AY*Y(I)+AZ*Z(I)+SF
RES(I)=FP(I)-FV(I)
JJ=51.+BB*FP(I)
KK=51.+BB*FV(I)
LL=51.+BB*RES(I)
MM=51.+CC*HP(I)
G(JJ)=1H*
G(KK)=1H*
G(LL)=1H.
G(MM)=1H$
PRINT 100,FP(I),FV(I),RES(I),G
100 FORMAT(1HZ,3F10.5,101A1/)
G(JJ)=1H
G(KK)=1H
G(LL)=1H
G(MM)=1H
32 CONTINUE
GO TO 8
10 CONTINUE
END
SUBROUTINE WAVEL(T,D,XL)
B=32.*T*T/6.283185
TPD=6.283185*D
IF(B-TPD) 2,2,3
C DEEP WATER INITIAL ESTIMATE FOR WAVELENGTH
2 XL=B
GO TO 4
C SHALLOW WATER INITIAL ESTIMATE FOR WAVELENGTH
3 XL=T*SQRT(D*32.2)
4 XLX=XL
XL=B*TANH(TPD/XLX)
IF(ABS(XLX-XL)-.00515,4,4)
5 RETURN
END

```

APPENDIX D

COMPUTER PROGRAM FOR HORIZONTAL LEAST SQUARES  
ANALYSIS (TWO-DIMENSIONAL DATA)

```

PROGRAM HORIZL (INPUT,OUTPUT,PUNCH)
DIMENSIONZ(41),P(41),YS(41),YI(41),FI(41),FP(41),F(41),FH(41),
IRES(41),G(101)
C SET TEST CONDITIONS
DIA=0.333
XC=0.917
ANGLE=0.
D=2.000
C READ IN DIGITIZED DATA
8 READ I,UP,DN,CFD,CFU
IF(UP)10,10,9
9 READ 2,CL,T,N,XW,XF,C,W0,F0
READ 3,(YI(I),FI(I),I=1,40)
1 FORMAT(2F3.3,2F3.0)
2 FORMAT(F3.3,F3.2,I2,2F2.1,3F3.0)
3 FORMAT(24F3.0)
C DETERMINE WAVE HEIGHT
DO 11 I=1,31,10
IF(YI(I)-W0)21,23,23
21 YS(I)=-{W0-YI(I)}*(DN/C)*(1./XW)
GO TO 11
23 YS(I)=(YI(I)-W0)*(UP/C)*(1./XW)
11 CONTINUE
C CALCULATE CONSTANTS IN FORCE EQUATION
PI=3.1415926536
R=1.938
CALL WAVEL(T,D,XL)
ZV=CL*(.5*DIA)
A=EXP((2.*PI*ZV)/XL)
COSHA=A*(1./A)
B=EXP((2.*PI*D)/XL)
SINHBB=B-(1./B)
CS=COSHA/SINHBB
CF1=R*DIA*XC*H*PI*PI/(2.*T*T)
FDH=CF1*H*CS*CS
FHM=CF1*DIA*PI*CS
U=(H*CS*PI)/T
C DETERMINE AVERAGE, MAXIMUM, AND MINIMUM FORCES
FMAX=-.5
FMIN=.5
SF=0.
DO 13 I=1,40
IF(FI(I)-FD)701,702,702
701 FP(I)=(FD-FI(I))*(CFD/C)*.002204/XF
GO TO 703
702 FP(I)=-{FI(I)-FD)*(CFU/C)*.002204/XF
703 CONTINUE
IF(FP(I).GT.FMAX)902,901
902 FMAX=FP(I)
901 IF(FP(I).LT.FMIN)903,12
903 FMIN=FP(I)
12 SF=SF+FP(I)
13 CONTINUE
SF=SF/40.
C CALCULATE SUMS OF SQUARES AND PRODUCTS

```



```

SFF=0.
SFP=0.
SFZ=0.
DT=.31415926536
A=-DT
DD IS I=1,40
A=A+DT
P(I)=SIN(A)
C=COS(A)
Z(I)=C*ABS (C)
F(I)=FP(I)
SFF=SFF+F(I)*F(I)
SFP=SFP+(I)*P(I)
SFZ=SFZ+F(I)*Z(I)
15 CONTINUE
AP=SFP/20.
AZ=SFZ/15.
VP=AP*SFP
VZ=AZ*SFZ
C CALCULATE COEFFICIENTS
CMH=-AP/FMH
CDH=AZ/FDH
C PRINT RESULTS OF ANALYSIS
PRINT 200
200 FORMAT(1H1)
PRINT 4
4 FORMAT(10X,6HT(SEC),7X,6HHT(FT),5X,9HWAVEL(FT),6X,7HDEP(FT),4X,9HU
IMAX(FPS),4X,9HCLEAR(FT),6X,7HDIA(FT),3X,12HCYL LGTH(FT),4X,8HANG(D
2EG))
PRINT 300,T,H,XL,D,U,CL,DIA,XC,ANGLE
300 FORMAT(2X,F13.2,F13.3,F13.2,SF13.3,F13.1////)
PRINT 330
330 FORMAT(26X,12HTOTAL SUM 50,7X,3HSIN,10X,8MCOS/COS/)
PRINT 331,SFF,VP,VZ
331 FORMAT(20X,3F15.6/)
PRINT 332
332 FORMAT(46X,2HAP,13X,2HAZ)
PRINT 333,AP,AZ
333 FORMAT(35X,2F15.6/)
PRINT 334
334 FORMAT(46X,3HFMH,12X,3HFDH)
PRINT 335,FMH,FDH
335 FORMAT(35X,2F15.6////)
PRINT 336
336 FORMAT(46X,3HCMH,12X,3HCDH)
PRINT 337,CMH,CDH
337 FORMAT(35X,2F15.3////)
PRINT 309
309 FORMAT(38X,8HF AVG(LB),7X,8HF MAX(LB),7X,8HF MIN(LB))
PRINT 304,SF,FMAX,FMIN
304 FORMAT(30X,F15.6,2F15.5////)
PUNCH 387,CL,DIA,ANGLE,T,H,XL,U,CMH,CDH,SF
387 FORMAT(F4.3,F5.3,F4.0,F5.2,F5.3,F6.2,F6.4,2F8.2,F10.6)
C PLOT ORIGINAL DATA AND RESULTS FOR COMPARISON
PRINT 26
26 FCFORMAT(4X,7H FP(LB),3X,7H FH(LB),2X,8H RES(LB)/)

```

```

A=ABS(FMIN)
C=ABS(FMAX)
B=AMAX1(A,C)
BB=35./B
DO 31 L=1,101
G(L)=1H
31 CONTINUE
DO 32 I=1,40
FH(I)=CDM*FDH*Z(I)-CNH*FMH*P(I)
RES(I)=FP(I)-FH(I)
G(51)=1HI
J=51.+BB*FP(I)
K=51.+BB*FH(I)
L=51.+BB*RES(I)
G(J)=1H*
G(K)=1H*
G(L)=1H*
PRINT 100,FP(I),FH(I),RES(I),G
100 FORMAT(1H2,3F10.5,101A1/)
G(J)=1H
G(K)=1H
G(L)=1H
32 CONTINUE
GO TO 8
10 CCONTINUE
END
SUBROUTINE WAVEL(T,D,XL)
B=32.*2*T*T/6.*283185
TPD=6.*283185*D
IF(B-TPD) 2,2,3
C DEEP WATER INITIAL ESTIMATE FOR WAVELENGTH
2 XL=B
GO TO 4
C SHALLOW WATER INITIAL ESTIMATE FOR WAVELENGTH
3 XL=T*SQRT(D*32.*2)
4 XLX=XL
XL=BB*TANH(TPD/XLX)
IF(ABS.(XLX-XL)-.00515,*,4
5 RETURN
END

```

APPENDIX E

TABULATED VERTICAL FORCE DATA  
FROM TWO-DIMENSIONAL EXPERIMENTS

	CLER	DIA	ANG	T	M	L	UMAX	CLV	CLVA	CLVU	PHI	K	CNV	CDV	
*001	*107	0	1	22	318	7.18	2991	3.56	3.86	3.86	4.90	2717	2.91	41.06	
*001	*107	0	1	22	342	7.06	2928	4.03	4.03	4.03	4.90	2717	2.91	41.06	
*001	*107	0	1	55	107	10.33	8908	3.17	3.17	3.17	-17.00	4035	1.32	30.62	
*001	*107	0	1	47	327	9.58	4063	4.59	4.59	4.59	-4.31	1590	2.84	36.88	
*001	*107	0	1	89	398	10.70	5385	3.90	3.90	3.90	-17.00	4035	1.32	30.62	
*001	*107	0	1	70	388	12.44	5755	3.50	3.50	3.50	-10.36	-0.194	2.24	14.70	
*001	*107	0	1	81	222	12.71	3325	4.45	4.45	4.45	-3.63	1002	1.29	21.78	
*001	*107	0	1	81	316	11.82	4929	3.41	3.41	3.41	-12.18	41.00	3.09	42.70	
*001	*107	0	2	00	259	13.01	5823	3.06	3.06	3.06	-21.71	-0.006	2.09	-06.29	
*001	*107	0	2	56	153	19.09	2676	4.14	4.14	4.14	-10.43	-0.479	1.61	-23.60	
*001	*107	0	2	56	187	18.35	5288	3.41	3.41	3.41	-3.35	2.71	1.81	27.18	
*001	*107	0	2	53	330	10.00	3774	2.88	2.88	2.88	-27.43	-0.039	2.01	11.50	
*010	*107	0	1	22	313	7.18	2902	7.06	7.06	7.06	36.78	6555	8.88	41.06	
*010	*107	0	1	22	342	7.06	2822	7.06	7.06	7.06	36.78	6555	8.88	41.06	
*010	*107	0	1	54	529	10.23	6929	4.57	4.57	4.57	5.20	34.50	3.33	30.08	
*010	*107	0	1	47	336	9.58	4180	6.57	6.57	6.57	18.33	4917	2.78	46.38	
*010	*107	0	1	89	406	11.31	5288	3.90	3.90	3.90	-17.00	4035	1.32	30.62	
*010	*107	0	1	73	432	11.90	6277	4.39	4.39	4.39	4.18	3122	0.41	47.93	
*010	*107	0	1	85	355	13.07	5402	4.91	4.91	4.91	4.96	3381	0.01	19.03	
*010	*107	0	1	85	388	11.18	6175	3.47	3.47	3.47	3.92	4.54	0.67	68.58	
*010	*107	0	2	52	101	18.91	2816	6.08	6.08	6.08	14.27	4901	-4.92	-96.33	
*010	*107	0	2	55	254	19.17	4457	3.48	3.48	3.48	-2.00	2437	3.60	-95.57	
*010	*107	0	2	55	327	19.17	5730	3.99	3.99	3.99	-11.17	3171	3.10	-44.23	
*021	*107	0	1	22	325	7.18	3014	2.57	2.57	2.57	62.56	8124	3.50	34.18	
*021	*107	0	1	20	322	6.99	2882	2.68	2.68	2.68	66.50	8709	-2.28	34.00	
*021	*107	0	1	24	406	7.37	391C	6.06	6.06	6.06	80.41	6637	1.71	-13.06	
*021	*107	0	1	57	507	10.51	6766	3.59	3.59	3.59	14.57	4456	3.90	50.58	
*021	*107	0	1	57	540	10.51	7286	3.59	3.59	3.59	62.02	3172	1.22	54.00	
*021	*107	0	1	59	401	10.70	5429	3.81	3.81	3.81	20.08	3180	-0.15	-5.87	
*021	*107	0	1	74	457	12.07	6568	4.07	4.07	4.07	20.19	4575	-0.91	50.86	
*021	*107	0	1	74	490	11.26	7318	3.17	3.17	3.17	-27.66	43.31	-0.74	-27.18	
*021	*107	0	1	86	349	13.16	5336	6.12	6.12	6.12	15.24	4417	1.73	50.52	
*021	*107	0	1	201	383	14.49	6119	6.00	6.00	6.00	12.36	3687	1.39	47.82	
*021	*107	0	1	201	416	13.68	6909	3.50	3.50	3.50	23.65	4355	-0.75	-27.18	
*021	*107	0	1	254	262	19.09	4579	4.24	4.24	4.24	0.08	3895	0.44	-13.08	
*021	*107	0	1	255	334	19.17	5953	3.37	3.37	3.37	4.26	2961	2.42	-29.21	
*001	*208	0	1	49	451	9.77	5701	4.19	4.19	4.19	0.19	4.85	1254	1.77	25.28
*001	*208	0	1	25	429	7.67	4174	5.72	5.72	5.72	12.35	2407	1.09	6.53	
*001	*208	0	1	48	466	9.81	5776	3.99	3.99	3.99	0.86	2.64	4.61	61.23	
*001	*208	0	1	48	322	9.67	4033	4.78	4.78	4.78	8.12	2153	1.51	-8.69	
*001	*208	0	1	58	379	10.60	5068	4.26	4.26	4.26	6.0	1882	1.48	4.65	
*001	*208	0	1	58	406	11.31	5776	3.99	3.99	3.99	0.86	2.64	4.61	61.23	
*001	*208	0	1	86	234	13.16	4568	4.57	4.57	4.57	4.87	1692	2.44	-3.14	
*001	*208	0	1	89	309	13.42	4770	4.23	4.23	4.23	12	1336	2.40	-62.18	
*001	*208	0	1	89	349	14.07	5546	3.66	3.66	3.66	-11.27	4913	1.76	37.08	
*001	*208	0	1	256	151	19.26	3173	4.22	4.22	4.22	-1.44	4046	-2.44	-11.373	
*001	*208	0	1	256	206	19.26	4488	3.81	3.81	3.81	-0.73	-0.369	2.26	-60.72	
*001	*208	0	1	256	304	19.45	6389	3.17	3.17	3.17	-18.66	6.31	-2.74	-23.19	
*011	*208	0	1	23	360	7.28	3395	6.13	6.13	6.13	46.08	7280	2.90	39.61	
*011	*208	0	1	23	368	7.28	3465	6.47	6.47	6.47	50.79	6989	1.34	33.96	
*011	*208	0	1	29	418	8.86	4622	3.92	3.92	3.92	34.04	622	3.66	42.82	
*011	*208	0	1	47	455	9.58	6687	6.49	6.49	6.49	21.11	8801	1.46	38.23	
*011	*208	0	1	48	324	9.48	3997	7.33	7.33	7.33	32.61	5930	-0.18	29.90	
*011	*208	0	1	48	361	11.31	5068	3.81	3.81	3.81	0.86	2.64	4.61	61.23	
*011	*208	0	1	69	421	11.62	6009	6.01	6.01	6.01	17.12	4559	5.59	21.59	
*011	*208	0	1	69	427	12.98	3447	7.42	7.42	7.42	20.89	6576	-2.99	10.93	
*011	*208	0	1	84	316	10.70	5385	3.90	3.90	3.90	-14.38	4035	1.32	30.62	
*011	*208	0	1	97	364	14.14	5810	5.88	5.88	5.88	9.67	3950	1.36	46.29	
*011	*208	0	1	248	197	18.57	3246	6.20	6.20	6.20	14.76	4827	6.69	62.04	
*011	*208	0	1	248	249	18.57	4366	3.50	3.50	3.50	-6.45	4.53	6.70	40.19	
*011	*208	0	1	256	306	19.26	5364	4.71	4.71	4.71	4.71	8.05	3040	1.0	220.55
*021	*208	0	1	23	346	7.28	3268	3.85	3.85	3.85	07.46	6866	2.50	27.46	
*021	*208	0	1	29	418	8.86	4622	3.92	3.92	3.92	34.04	622	3.66	42.82	
*021	*208	0	1	49	447	9.77	6552	6.88	6.88	6.88	33.21	5893	1.85	23.16	
*021	*208	0	1	48	325	9.48	4009	3.99	3.99	3.99	81.08	6699	-0.27	13.23	
*021	*208	0	1	58	383	10.60	5068	4.26	4.26	4.26	34.04	622	3.66	42.82	
*021	*208	0	1	69	405	11.62	5767	6.24	6.24	6.24	33.47	5254	-3.71	-13.46	
*021	*208	0	1	84	241	12.98	3615	5.96	5.96	5.96	43.07	6416	6.38	150.17	
*021	*208	0	1	86	348	13.16	5123	6.30	6.30	6.30	26.28	5848	2.10	61.10	
*021	*208	0	1	94	369	13.87	5764	5.99	5.99	5.99	22.01	5063	-0.63	55.51	
*021	*208	0	1	250	184	19.74	4200	3.98	3.98	3.98	32.98	6538	1.71	169.81	
*021	*208	0	1	255	264	19.17	4826	4.96	4.96	4.96	20.73	4466	13.29	174.88	
*021	*208	0	1	257	309	19.34	5416	5.25	5.25	5.25	14.67	3960	2.20	172.13	
*001	*250	0	1	24	355	7.37	3500	4.42	4.42	4.42	14.33	1688	2.96	42.90	
*001	*250	0	1	28	447	7.76	4951	4.36	4.36	4.36	9.66	1451	2.48	59.83	
*001	*250	0	1	44	463	9.29	5616	6.13	6.13	6.13	3.14	1618	4.09	49.15	
*001	*250	0	1	44	499	10.00	6389	3.17	3.17	3.17	-17.00	4035	1.32	30.62	
*001	*250	0	1	47	329	7.56	4032	4.34	4.34	4.34	6.89	1151	3.11	53.88	
*001	*250	0	1	55	402	10.33	5302	3.88	3.88	3.88	3.90	3860	3.27	43.34	
*001	*250	0	1	58	414	11.38	5829	3.82	3.82	3.82	72.73	6074	4.49	15.79	
*001	*250	0	1	85	328	13.07	3467	2.27	2.27	2.27	6.46	1923	2.50	-2.20	
*001	*250	0	1	85	366	13.25	5092	4.03	4.03	4.03	-1.61	953	3.15	31.57	
*001	*250	0	1	84	363	13.45	5252	4.22	4.22	4.22	4.22	4.22	4.22	34.46	
*001	*250	0	1	221	176	18.83	3078	3.70	3.70	3.70	2.88	4045	1.60	23.97	
*001	*250	0	1	252	262	19.30	3775	3.35	3.35	3.35	-17.00	4035	1.32	30.62	
*001	*250	0	1	252	307	19.25	5394	4.43	4.43	4.43	-0.60	-0.746	-5.72	-71.08	
*010	*250	0	1	24	365	7.37	3503	3.61	3.61	3.61	50.01	7201	2.74	34.92	
*010	*250	0	1	24	398	7.37	3661	4.03	4.03	4.03	7.41	4074	3.81	37.77	
*010	*250	0	1	44	446	9.39	5459	7.43	7.43	7.43	31.45	5553	7.6	41.43	
*010	*250	0	1	49	321	9.77	4065	7.43	7.43	7.43	40.34	6335	2.15	55.00	
*010	*250	0	1	49	359	10.51	5123	6.21	6.21	6.21	31.62	4781	3.96	41.19	
*010	*250	0	1	67	416	11.43	5888	6.83	6.83	6.83	24.19	5031	1.10	24.57	
*010	*250	0	1	83	225	12.80	3605	7.65	7.65	7.65	32.10	6032			

CLER	D14	ANG	T	H	L	UMAX	CLV	CLV4	CLVU	PHI	K	CMV	CDV
.001	.333	0.	1.23	.066	7.28	.0627	8.14	8.14	8.14	26.26	.6550	2.60	-518.75
.001	.333	0.	1.23	.117	7.28	.1107	7.60	7.60	7.60	25.83	.6574	2.59	-279.01
.001	.333	0.	1.22	.107	7.18	.1556	7.62	7.62	7.62	24.57	.6556	2.74	-189.35
.001	.333	0.	1.23	.077	7.37	.1909	8.26	8.26	8.26	35.37	.6425	2.66	-135.79
.001	.333	0.	1.24	.257	7.37	.2471	6.53	6.53	6.53	19.76	.5084	2.91	-117.97
.001	.333	0.	1.24	.277	7.37	.2667	6.62	6.62	6.62	19.27	.5174	2.49	-114.83
.001	.333	0.	1.82	.295	7.47	.2932	6.45	6.45	6.45	22.01	.4667	3.15	-70.13
.001	.333	0.	1.45	.004	9.39	.0783	3.64	3.64	3.64	22.67	.6122	2.59	-202.69
.001	.333	0.	1.45	.109	9.39	.1341	6.01	6.01	6.01	21.17	.4970	2.46	-127.40
.001	.333	0.	1.45	.164	9.39	.1857	5.74	5.74	5.74	18.09	.4488	2.46	-84.73
.001	.333	0.	1.45	.204	9.39	.2505	5.14	5.14	5.14	14.91	.4017	1.46	-51.31
.001	.333	0.	1.47	.206	9.58	.2577	4.94	4.94	4.94	14.83	.3672	3.25	-51.25
.001	.333	0.	1.47	.236	9.58	.2551	5.92	5.92	5.92	13.56	.3854	1.86	-58.12
.001	.333	0.	1.47	.268	9.58	.3368	5.13	5.13	5.13	13.16	.3510	1.31	-56.40
.001	.333	0.	1.46	.269	9.48	.3326	5.84	5.84	5.84	10.95	.3511	2.00	-56.40
.001	.333	0.	1.46	.283	9.77	.3584	5.75	5.75	5.75	14.97	.3030	2.90	-32.33
.001	.333	0.	1.82	.081	12.80	.0774	6.80	6.80	6.80	23.89	.5764	3.15	-205.19
.001	.333	0.	1.82	.086	12.60	.1330	5.80	5.80	5.80	19.37	.4687	4.23	-46.87
.001	.333	0.	1.82	.087	12.60	.1319	6.17	6.17	6.17	20.09	.5368	2.45	-520.12
.001	.333	0.	1.85	.127	12.71	.1918	6.06	6.06	6.06	13.76	.4214	2.74	-370.56
.001	.333	0.	1.82	.163	12.80	.2445	6.18	6.18	6.18	16.27	.4478	2.57	-270.80
.001	.333	0.	1.85	.190	13.07	.2896	5.41	5.41	5.41	14.61	.3324	3.42	-212.05
.001	.333	0.	1.85	.217	13.07	.3317	5.95	5.95	5.95	12.02	.3437	2.21	-209.74
.001	.333	0.	1.85	.241	13.07	.3663	5.55	5.55	5.55	9.94	.3191	.67	-203.48
.001	.333	0.	2.16	.139	15.98	.2314	6.42	6.42	6.42	20.84	.3609	3.11	-305.22
.001	.333	0.	2.20	.252	16.16	.3724	5.67	5.67	5.67	15.80	.2818	2.08	-252.57
.001	.333	0.	2.50	.399	18.74	.0668	6.13	6.13	6.13	17.15	.3136	1.91	-284.19
.001	.333	0.	2.51	.071	18.63	.1238	5.93	5.93	5.93	18.96	.4447	2.52	-866.16
.001	.333	0.	2.52	.104	18.91	.1822	5.09	5.09	5.09	16.52	.3532	3.25	-841.55
.001	.333	0.	2.53	.148	19.00	.2284	5.92	5.92	5.92	12.44	.3902	3.86	-678.17
.001	.333	0.	2.53	.157	19.00	.2755	4.95	4.95	4.95	10.53	.2854	1.17	-414.22
.001	.333	0.	2.53	.187	19.00	.3271	4.36	4.36	4.36	7.67	.2518	2.83	-313.75
.001	.333	0.	2.54	.214	19.09	.3680	4.67	4.67	4.67	8.00	.2210	1.72	-205.80
.005	.333	0.	1.22	.069	7.18	.0640	6.43	6.43	6.43	72.86	.9025	2.42	-86.76
.005	.333	0.	1.23	.124	7.18	.1159	7.85	7.85	7.85	59.68	.8249	2.30	-49.54
.005	.333	0.	1.23	.169	7.28	.1608	6.66	6.66	6.66	46.55	.8099	2.99	-39.79
.005	.333	0.	1.23	.222	7.28	.2166	7.79	7.79	7.79	49.84	.7558	2.62	3.41
.005	.333	0.	1.23	.260	7.28	.2663	8.10	8.10	8.10	38.69	.7137	1.92	-14.67
.005	.333	0.	1.48	.298	9.18	.2702	8.92	8.92	8.92	34.02	.7023	3.46	-92.56
.005	.333	0.	1.25	.285	7.47	.2790	7.91	7.91	7.91	38.04	.6993	2.66	3.23
.005	.333	0.	1.24	.302	7.37	.2908	7.95	7.95	7.95	43.15	.7031	2.94	11.30
.005	.333	0.	1.47	.307	9.48	.0728	6.42	6.42	6.42	69.39	.7728	3.14	-72.91
.005	.333	0.	1.45	.104	9.39	.1331	8.07	8.07	8.07	55.11	.6124	2.72	-77.46
.005	.333	0.	1.46	.160	9.48	.1996	7.65	7.65	7.65	42.13	.7447	2.66	-97.30
.005	.333	0.	1.81	.202	9.58	.0728	6.42	6.42	6.42	29.89	.6633	2.99	-96.19
.005	.333	0.	1.49	.213	9.67	.2528	8.47	8.47	8.47	34.78	.6250	2.11	-55.45
.005	.333	0.	1.49	.266	9.77	.3350	7.61	7.61	7.61	28.51	.5829	4.70	-12.02
.005	.333	0.	1.83	.265	9.86	.1633	6.54	6.54	6.54	35.68	.6120	2.86	-67.32
.005	.333	0.	1.83	.286	9.77	.1633	7.89	7.89	7.89	28.99	.5867	1.89	-41.88
.005	.333	0.	1.91	.052	12.71	.0786	7.00	7.00	7.00	50.50	.8128	1.71	-143.40
.005	.333	0.	1.83	.052	12.85	.0782	6.67	6.67	6.67	50.32	.8009	3.33	-160.01
.005	.333	0.	1.83	.096	12.85	.1464	6.32	6.32	6.32	38.12	.7927	3.16	-132.22
.005	.333	0.	1.83	.094	12.89	.1419	7.16	7.16	7.16	43.77	.7277	1.77	-92.42
.005	.333	0.	1.83	.131	12.89	.1583	7.19	7.19	7.19	36.24	.6602	2.57	-49.04
.005	.333	0.	1.83	.155	12.89	.2008	6.15	6.15	6.15	28.61	.6191	1.61	-59.56
.005	.333	0.	1.84	.199	12.98	.3016	6.37	6.37	6.37	22.67	.5760	1.84	-39.29
.005	.333	0.	1.83	.227	12.89	.3435	7.09	7.09	7.09	19.66	.5439	1.39	-28.58
.005	.333	0.	1.85	.245	13.07	.3735	7.03	7.03	7.03	19.86	.5234	1.51	-23.67
.005	.333	0.	2.20	.230	16.16	.3834	6.42	6.42	6.42	22.92	.4570	1.89	-8.10
.005	.333	0.	2.49	.041	18.66	.0717	6.67	6.67	6.67	52.39	.7707	2.84	-235.28
.005	.333	0.	2.51	.073	18.83	.1280	7.04	7.04	7.04	39.25	.6733	2.09	-131.05
.005	.333	0.	2.54	.103	19.09	.1401	6.57	6.57	6.57	31.67	.6078	1.69	-81.54
.005	.333	0.	2.45	.135	19.17	.2374	6.30	6.30	6.30	28.05	.5494	.83	-41.48
.005	.333	0.	2.45	.161	19.17	.2822	5.41	5.41	5.41	22.09	.4878	1.77	-116.55
.005	.333	0.	2.54	.161	19.09	.2820	6.08	6.08	6.08	20.98	.4981	3.29	21.72
.005	.333	0.	2.56	.190	19.26	.3329	5.21	5.21	5.21	17.89	.4319	.588	-102.53
.005	.333	0.	2.45	.206	19.17	.3612	5.73	5.73	5.73	17.48	.4293	2.53	45.06
.010	.333	0.	1.23	.074	7.28	.0643	3.90	3.90	3.90	64.95	1.0003	2.33	-92.55
.010	.333	0.	1.23	.121	7.28	.1150	5.43	5.43	5.43	74.26	.9447	2.36	-39.36
.010	.333	0.	1.23	.175	7.28	.1659	5.40	5.40	5.40	75.03	.9194	2.40	-25.08
.010	.333	0.	1.24	.223	7.37	.2149	5.83	5.83	5.83	65.11	.8594	2.39	-22.32
.010	.333	0.	1.24	.265	7.37	.2615	5.96	5.96	5.96	58.90	.8524	2.49	-13.22
.010	.331	0.	1.23	.281	7.28	.2668	6.47	6.47	6.47	58.10	.8572	1.59	-22.17
.010	.333	0.	1.26	.276	7.57	.2748	6.50	6.50	6.50	55.66	.8167	3.31	-4.43
.010	.331	0.	1.48	.064	9.67	.0773	5.22	5.22	5.22	66.57	.7820	2.47	-89.84
.010	.333	0.	1.48	.051	9.67	.0773	5.22	5.22	5.22	89.89	.9752	3.15	-103.68
.010	.333	0.	1.48	.109	9.67	.1372	6.34	6.34	6.34	73.27	.8764	2.45	-61.69
.010	.333	0.	1.49	.163	9.67	.1986	6.25	6.25	6.25	63.87	.8561	2.46	-35.52
.010	.333	0.	1.83	.194	9.77	.2485	5.92	5.92	5.92	48.12	.8197	1.92	-27.02
.010	.333	0.	1.50	.283	9.86	.3619	7.39	7.39	7.39	46.01	.7367	1.54	-27.07
.010	.333	0.	1.62	.272	12.80	.2597	7.15	7.15	7.15	43.14	.7609	2.38	-32.87
.010	.333	0.	1.62	.285	12.80	.3014	6.78	6.78	6.78	38.76	.7264	1.64	-32.87
.010	.333	0.	1.52	.265	10.05	.3441	6.99	6.99	6.99	59.01	.7305	3.47	13.61
.010	.333	0.	1.43	.267	9.67	.3359	7.23	7.23	7.23	49.01	.7600	1.43	-27.45
.010	.331	0.	1.83	.281	12.85	.0760	6.40	6.40	6.40	39.25	.6820	1.69	-58.74
.010	.333	0.	1.82	.073	12.60	.1407	6.18	6.18	6.18	64.55	.8601	3.35	-98.73
.010	.333	0.	1.83	.133	12.89	.2013	6.43	6.43	6.43	57.07	.8120	1.92	-62.83
.010	.333	0.	1.83	.185	12.89	.2604	6.13	6.13	6.13	38.13	.7344	2.94	-48.44
.010	.333	0.	1.97	.227	13.25	.3493	7.01	7.01	7.01	38.25	.6850	1.53	-8.00
.010	.333	0.	1.97	.252	13.25	.3973	7.14	7.14	7.14	36.34	.6430	1.21	-10.04
.010	.333	0.	1.97	.281	13.42	.4424	6.89	6.89	6.89	34.78	.6106	.703	-10.04
.010	.333	0.	2.21	.235	16.25	.3924	6.99	6.99	6.99	28.40	.5873	1.55	3.03
.010	.333	0.	2.52	.041	18.91	.0715	6.53	6.53	6.53	68.71	.8919	2.58	-225.86
.010	.333	0.	2.53	.089	19.00	.1286	6.91	6.91	6.91	35.75	.8014	3.25	-89.30
.010	.333	0.	2.51	.106	18.83	.1855	6.09	6.09	6.09	32.32	.7565	4.52	-39.30
.010	.333	0.	2.54	.140	19.09	.2458							

CLER	DIA	ANG	T	H	L	UMAX	CLV	CLV4	CLVU	PHI	K	GMV	COV
.013	.333	0	1.25	.226	7.47	.0218	5.42	5.42	5.42	68.91	.8536	2.97	47.95
.013	.333	0	1.28	.325	7.76	.3324	5.96	5.96	5.96	58.14	.8029	3.02	39.80
.013	.333	0	1.50	.302	10.14	.3944	7.34	7.34	7.34	46.17	.7311	1.96	52.06
.013	.333	0	1.81	.174	12.71	.2625	7.16	7.16	7.16	49.44	.7652	2.65	85.19
.013	.333	0	1.88	.258	13.33	.3577	7.34	7.34	7.34	41.90	.6607	3.72	118.13
.013	.333	0	2.21	.151	16.25	.2521	7.80	7.80	7.80	54.51	.7123	2.22	139.26
.013	.333	0	2.19	.237	16.07	.3915	7.74	7.74	7.74	45.08	.5815	2.10	156.89
.013	.333	0	2.57	.216	19.34	.3797	6.72	6.72	6.72	42.61	.5703	1.77	205.49
.013	.333	0	2.57	.216	19.34	.3797	6.71	6.71	6.71	29.34	.0562	1.77	257.36
.016	.333	0	1.24	.070	7.37	.0677	2.32	2.32	2.32	83.39	.9540	2.23	-74.44
.016	.333	0	1.23	.123	7.28	.1159	2.24	2.24	2.24	85.78	.9867	2.23	-40.12
.016	.333	0	1.22	.173	7.18	.1616	3.75	3.75	3.75	83.31	.9376	2.26	-21.26
.016	.333	0	1.25	.211	7.47	.2072	4.25	4.25	4.25	92.73	.9413	2.00	-5.17
.016	.333	0	1.24	.220	7.37	.2125	3.70	3.70	3.70	76.64	.8920	1.84	-3.37
.016	.333	0	1.23	.215	7.28	.2039	3.26	3.26	3.26	79.11	.8960	1.67	-6.87
.016	.333	0	1.24	.269	7.37	.2404	4.47	4.47	4.47	76.51	.8902	2.43	-10.07
.016	.333	0	1.24	.298	7.37	.2677	4.26	4.26	4.26	68.53	.8005	2.10	-1.57
.016	.333	0	1.25	.311	7.47	.3048	3.87	3.87	3.87	67.55	.8085	1.89	-9.84
.016	.333	0	1.26	.301	7.57	.2994	4.54	4.54	4.54	72.42	.8136	2.62	-5.54
.016	.333	0	1.24	.298	7.37	.2877	4.94	4.94	4.94	65.70	.8381	1.81	-2.87
.016	.333	0	1.25	.05	9.48	.0718	3.73	3.73	3.73	84.90	1.0210	2.43	-109.58
.016	.333	0	1.49	.108	9.67	.1357	4.09	4.09	4.09	91.57	.9268	2.09	-59.48
.016	.333	0	1.49	.156	9.77	.1985	4.57	4.57	4.57	75.78	.8638	1.81	-2.87
.016	.333	0	1.49	.199	9.77	.2432	4.64	4.64	4.64	75.03	.7921	4.21	35.73
.016	.333	0	1.46	.205	9.48	.2538	4.34	4.34	4.34	71.65	.8059	4.46	-42.99
.016	.333	0	1.48	.202	9.67	.2539	4.73	4.73	4.73	69.45	.8756	1.69	-29.22
.016	.333	0	1.48	.229	9.67	.2856	5.00	5.00	5.00	69.56	.8607	3.03	2.98
.016	.333	0	1.48	.229	9.67	.2884	5.60	5.60	5.60	65.36	.8392	1.56	-20.52
.016	.333	0	1.49	.263	9.77	.3334	5.45	5.45	5.45	69.52	.8768	2.16	-8.13
.016	.333	0	1.49	.263	9.77	.3581	5.68	5.68	5.68	79.19	.8769	2.85	-13.00
.016	.333	0	1.82	.091	12.80	.0768	3.92	3.92	3.92	87.21	1.0071	2.26	-163.53
.016	.333	0	1.82	.092	12.80	.1393	4.38	4.38	4.38	76.06	.8918	2.46	-58.56
.016	.333	0	1.81	.085	12.80	.1393	4.71	4.71	4.71	83.84	.8918	2.46	-32.79
.016	.333	0	1.86	.166	12.98	.2522	5.21	5.21	5.21	58.77	.8119	2.90	-28.09
.016	.333	0	1.86	.248	13.16	.3798	6.42	6.42	6.42	58.28	.7117	1.35	10.11
.016	.333	0	1.84	.202	12.98	.3070	5.68	5.68	5.68	61.81	.7904	1.94	-20.40
.016	.333	0	1.85	.226	13.07	.3452	6.25	6.25	6.25	47.07	.7321	1.24	-11.16
.016	.333	0	2.18	.143	15.98	.2375	6.51	6.51	6.51	58.99	.7686	1.60	-38.39
.016	.333	0	2.21	.223	16.25	.3325	6.83	6.83	6.83	67.23	.8116	1.64	-35.39
.016	.333	0	2.21	.223	16.25	.3325	6.83	6.83	6.83	76.88	1.0353	3.66	-266.77
.016	.333	0	2.56	.075	19.26	.1326	4.77	4.77	4.77	67.04	.8546	3.58	-73.83
.016	.333	0	2.56	.075	19.26	.1326	4.77	4.77	4.77	62.89	.8237	3.66	-32.79
.016	.333	0	2.55	.107	19.17	.1874	4.71	4.71	4.71	58.28	.7691	1.84	-16.35
.016	.333	0	2.57	.138	19.34	.2626	5.54	5.54	5.54	45.88	.6889	3.97	117.27
.016	.333	0	2.57	.138	19.34	.2626	5.70	5.70	5.70	39.52	.6562	3.43	146.49
.016	.333	0	2.57	.207	19.34	.3634	5.97	5.97	5.97	30.79	.6304	1.45	133.64
.021	.333	0	1.23	.066	7.28	.0630	2.17	2.17	2.17	84.45	.9808	2.34	-117.43
.021	.333	0	1.22	.126	7.18	.1175	2.31	2.31	2.31	86.47	.9824	2.50	-64.28
.021	.333	0	1.23	.226	7.28	.2148	2.67	2.67	2.67	85.51	.9371	2.68	-18.19
.021	.333	0	1.24	.220	7.37	.2123	2.81	2.81	2.81	81.70	.9836	2.12	-24.75
.021	.333	0	1.24	.261	7.37	.2517	2.76	2.76	2.76	78.05	.9584	2.82	-26.25
.021	.333	0	1.23	.265	7.28	.2519	2.66	2.66	2.66	75.17	.9710	1.74	-21.66
.021	.333	0	1.25	.291	7.47	.2651	2.73	2.73	2.73	74.40	.9046	2.56	-17.81
.021	.333	0	1.24	.291	7.37	.2807	2.82	2.82	2.82	79.65	.9609	1.92	-19.09
.021	.333	0	1.25	.313	7.47	.3073	2.98	2.98	2.98	81.36	.9056	2.89	-6.30
.021	.333	0	1.24	.309	7.37	.2987	3.21	3.21	3.21	77.88	.9423	2.31	-17.33
.021	.333	0	1.48	.041	9.49	.0721	3.99	3.99	3.99	76.88	1.0353	3.66	-266.77
.021	.333	0	1.46	.065	9.43	.0805	2.71	2.71	2.71	85.16	.9931	2.65	-156.24
.021	.333	0	1.46	.129	9.43	.1596	2.11	2.11	2.11	89.10	1.0066	2.57	-58.16
.021	.333	0	1.48	.176	9.67	.2218	3.47	3.47	3.47	79.81	.9653	1.84	-47.38
.021	.333	0	1.48	.222	9.67	.2753	3.56	3.56	3.56	75.29	.8828	2.12	-32.74
.021	.333	0	1.47	.302	9.59	.3778	4.57	4.57	4.57	65.94	.8417	1.12	-21.78
.021	.333	0	1.51	.325	9.65	.4190	5.38	5.08	5.08	65.94	.7984	2.33	-3.03
.021	.333	0	1.81	.054	12.71	.0818	2.61	2.61	2.61	85.23	.8335	3.26	-258.32
.021	.333	0	1.82	.051	12.80	.0777	3.10	3.10	3.10	84.26	.9182	2.25	-213.67
.021	.333	0	1.82	.095	12.80	.1435	3.34	3.34	3.34	84.36	.9695	2.72	-111.91
.021	.333	0	1.83	.135	13.07	.2021	3.49	3.49	3.49	77.95	.8449	4.47	-54.27
.021	.333	0	1.84	.134	12.98	.2044	3.67	3.67	3.67	75.72	.8092	4.47	-65.91
.021	.333	0	1.87	.172	13.25	.2638	3.88	3.88	3.88	73.81	.8984	2.11	-48.36
.021	.333	0	1.84	.204	12.98	.3096	4.54	4.54	4.54	64.71	.7969	2.95	-10.99
.021	.333	0	1.89	.239	13.16	.3599	4.93	4.93	4.93	60.46	.7847	3.01	-12.44
.021	.333	0	1.88	.261	13.33	.4026	4.99	4.99	4.99	55.89	.7469	3.26	-7.75
.021	.333	0	2.18	.149	15.98	.2472	5.01	5.01	5.01	67.72	.8310	3.76	-85.76
.021	.333	0	2.19	.239	16.07	.3378	4.83	4.83	4.83	62.90	.8090	1.90	-92.07
.021	.333	0	2.52	.041	18.91	.0717	2.94	2.94	2.94	84.29	1.0871	2.90	-392.99
.021	.333	0	2.54	.073	19.09	.1287	3.45	3.45	3.45	77.48	.9058	3.32	-154.30
.021	.333	0	2.54	.105	19.09	.1664	3.68	3.68	3.68	74.48	.8488	3.32	-112.44
.021	.333	0	2.53	.135	19.00	.2369	5.07	5.07	5.07	58.58	.6309	2.80	-29.39
.021	.333	0	2.54	.166	19.05	.2890	5.35	5.35	5.35	51.33	.7445	1.32	12.11
.021	.333	0	2.54	.195	19.17	.3419	5.43	5.43	5.43	45.89	.6599	1.51	20.82
.021	.333	0	2.57	.224	19.34	.3939	5.13	5.13	5.13	40.15	.6705	1.45	58.39

CLER	DIA	ANG	T	H	L	U4X4	CLV	CLV4	CLVU	PHI	K	CMV	CDV
.063	.333	0	1.21	.073	7.08	.0678	.60	.60	.60	85.06	.5902	2.02	-44.23
.083	.333	0	1.21	.128	7.08	.1192	.48	.48	.48	95.11	.6309	2.06	-24.81
.063	.333	0	1.22	.181	7.18	.1713	.63	.63	.63	86.80	.9474	2.03	-16.33
.083	.333	0	1.21	.239	7.08	.2223	.66	.66	.66	89.31	.6245	1.92	1.70
.083	.333	0	1.21	.295	7.08	.2739	.58	.58	.58	93.44	.6309	2.01	-4.82
.063	.333	0	1.24	.308	7.37	.3006	.58	.58	.58	92.08	.7767	1.86	-2.90
.083	.333	0	1.23	.340	7.28	.3264	.62	.62	.62	87.52	.7320	1.79	-.04
.083	.333	0	1.46	.060	9.48	.0746	1.13	1.13	1.13	87.28	.6597	2.06	-76.74
.083	.333	0	1.48	.110	9.67	.1366	.94	.94	.94	94.78	.5884	1.92	-34.11
.083	.333	0	1.47	.159	9.58	.1996	.82	.82	.82	90.08	.5192	1.72	-29.26
.083	.333	0	1.48	.197	9.67	.2500	.78	.78	.78	89.39	.6851	1.94	-13.82
.083	.333	0	1.48	.227	9.67	.2873	.76	.76	.76	91.22	.8698	1.91	-14.65
.083	.333	0	1.48	.256	9.67	.3276	.80	.80	.80	88.94	.8415	1.99	-9.46
.083	.333	0	1.47	.279	9.58	.3506	.70	.70	.70	92.03	.8466	1.83	-.10
.083	.333	0	1.82	.049	12.80	.0738	.88	.88	.88	87.03	.7884	1.86	-107.86
.083	.333	0	1.84	.090	12.96	.1376	1.18	1.18	1.18	86.35	.5980	1.94	-58.90
.083	.333	0	1.84	.131	12.98	.1992	.92	.92	.92	90.44	.8688	1.78	-39.66
.083	.333	0	1.87	.162	13.25	.2412	.79	.79	.79	90.39	.9872	1.52	-35.81
.083	.333	0	1.85	.198	13.07	.3037	1.01	1.01	1.01	95.77	.7748	1.11	-25.39
.083	.333	0	1.85	.227	13.07	.3471	.97	.97	.97	87.04	.7801	.92	-19.26
.083	.333	0	1.85	.224	13.07	.3436	.97	.97	.97	85.51	.6281	1.67	-14.31
.083	.333	0	1.87	.246	13.25	.3791	.98	.98	.98	84.55	.8059	.67	-18.62
.083	.333	0	1.87	.247	13.25	.3810	1.10	1.10	1.10	89.63	.7872	1.25	-10.39
.083	.333	0	2.18	.198	15.98	.2472	.96	.96	.96	79.84	.8674	1.52	-23.82
.083	.333	0	2.18	.242	15.98	.3049	1.03	1.03	1.03	78.64	.8535	1.22	-30.06
.083	.333	0	2.20	.226	16.16	.3770	1.30	1.30	1.30	81.48	.7789	1.51	-2.96
.083	.333	0	2.52	.005	18.91	.0786	.47	.47	.47	92.66	1.6169	2.04	-1.27
.083	.333	0	2.50	.080	19.74	.1402	.97	.97	.97	83.98	.9729	1.82	-91.26
.083	.333	0	2.50	.116	18.74	.2028	.99	.99	.99	86.58	.6067	1.62	-52.36
.083	.333	0	2.55	.153	19.17	.2692	1.00	1.00	1.00	83.31	.8293	1.29	-31.59
.083	.333	0	2.51	.190	19.83	.3153	1.18	1.18	1.18	84.57	.8007	1.20	-32.28
.083	.333	0	2.55	.207	19.00	.3638	1.13	1.13	1.13	77.25	.8531	.99	-18.70
.083	.333	0	2.53	.224	19.00	.3936	1.31	1.31	1.31	74.50	.8442	.88	-13.62

.167	.333	0	1.22	.073	7.18	.0665	.64	.64	.64	133.85	4.0404	1.91	-12.43
.167	.333	0	1.21	.133	7.08	.1262	.23	.23	.23	126.26	1.3436	1.83	-12.89
.167	.333	0	1.24	.190	7.37	.1884	.26	.26	.26	52.10	.7354	1.78	-6.56
.167	.333	0	1.22	.242	7.18	.2333	.23	.29	.29	87.88	-.2581	1.95	-14.96
.167	.333	0	1.23	.265	7.28	.2797	.22	.22	.22	90.47	.2232	1.75	-6.29
.167	.333	0	1.24	.314	7.37	.3115	.29	.29	.29	51.83	.0740	1.71	-.88
.167	.333	0	1.21	.344	7.28	.3359	.36	.36	.36	90.40	.2478	1.76	-.83
.167	.333	0	1.46	.043	9.48	.0755	.94	.94	.94	80.63	-.1263	1.86	-16.17
.167	.333	0	1.46	.112	9.48	.1408	.75	.75	.75	92.43	.3327	1.83	-15.98
.167	.333	0	1.46	.166	9.48	.2197	.51	.51	.51	95.83	.5207	1.80	-13.60
.167	.333	0	1.47	.206	9.58	.2813	.56	.56	.56	87.03	.6324	1.69	-7.57
.167	.333	0	1.48	.247	9.67	.3168	.50	.50	.50	90.62	.6018	1.56	-6.24
.167	.333	0	1.49	.265	9.77	.3417	.57	.57	.57	87.84	.5701	1.65	-4.50
.167	.333	0	1.51	.288	9.95	.3766	.41	.41	.41	87.71	.5582	1.32	-34.25
.167	.333	0	1.82	.091	12.80	.1391	.27	.27	.27	119.51	.8714	1.81	-23.66
.167	.333	0	1.83	.143	12.89	.2188	.90	.90	.90	99.39	.5701	1.50	-15.99
.167	.333	0	1.93	.168	12.89	.2568	.74	.74	.74	104.78	.3891	1.61	-16.77
.167	.333	0	1.84	.208	12.98	.3197	.65	.65	.65	94.40	.5671	1.34	-5.91
.167	.333	0	1.84	.240	12.98	.3676	.64	.64	.64	88.35	.5713	1.24	-5.60
.167	.333	0	1.86	.263	13.16	.4059	.71	.71	.71	90.47	.5226	.97	-2.73
.167	.333	0	2.17	.140	15.90	.2661	.89	.89	.89	72.48	.5391	1.39	-6.29
.167	.333	0	2.20	.236	16.16	.3558	.50	.50	.50	76.68	.6873	.37	-10.81
.167	.333	0	2.20	.236	16.16	.3486	.73	.73	.73	79.10	.5292	.71	-2.22
.167	.333	0	2.50	.039	18.74	.0689	.53	.53	.53	95.87	1.0978	1.97	-109.67
.167	.333	0	2.50	.070	18.74	.1222	.89	.89	.89	84.47	.9163	1.95	-56.74
.167	.333	0	2.51	.103	18.83	.1814	1.07	1.07	1.07	89.60	.9544	1.55	-38.27
.167	.333	0	2.53	.142	19.00	.2502	1.02	1.02	1.02	93.80	.8859	1.29	-25.68
.167	.333	0	2.54	.161	19.09	.2829	.94	.94	.94	94.19	.5919	1.39	-21.29
.167	.333	0	2.52	.198	19.09	.3474	.85	.85	.85	90.58	.5925	.85	-15.74
.167	.333	0	2.53	.220	19.00	.3771	.82	.82	.82	98.07	.5689	.43	-13.88

APPENDIX F

TABULATED VERTICAL FORCE DATA  
FROM THREE-DIMENSIONAL EXPERIMENTS



CLFP	DIA	ANG	T	H	L	UMAX	CLV	CLVA	CLVU	PHI	K	CMV	CDV
.001	.167	0	2.24	1.60	18.83	2.172	4.92	4.92	4.92	5.16	1.694	4.70	-252.67
.001	.167	0	1.74	2.23	13.41	2.343	5.42	5.42	5.42	2.87	1.890	6.0	211.71
.001	.167	0	1.38	2.90	7.92	2.522	4.05	4.05	4.05	-7.70	2.851	2.89	-87.75
.001	.167	0	1.26	3.36	7.94	1.953	5.41	5.41	5.41	9.83	3.749	4.26	-87.75
.001	.167	0	2.32	2.72	19.67	3.625	4.64	4.64	4.64	-16.70	-0.188	3.12	-398.58
.001	.167	0	2.06	3.13	16.91	3.862	5.14	5.14	5.14	-17.45	-0.733	5.0	-168.34
.001	.167	0	1.80	3.65	14.08	3.377	5.01	5.01	5.01	-8.70	3.08	2.82	-74.05
.001	.167	0	1.32	5.41	8.63	3.425	5.58	5.58	5.58	1.63	1.899	5.29	-32.56
.001	.167	0	2.32	3.20	21.51	4.859	4.9	4.9	4.9	-23.88	-0.248	21.6	-60.32
.001	.167	0	2.24	3.93	18.83	5.130	4.56	4.56	4.56	-32.78	-0.391	5.35	-389.23
.001	.167	0	1.98	4.77	16.05	5.700	3.89	3.89	3.89	-29.78	-0.643	3.41	-88.67
.001	.167	0	1.86	5.27	15.83	5.461	3.99	3.99	3.99	-29.78	-0.42	3.47	-88.67
.001	.167	0	2.50	4.27	21.54	5.899	3.76	3.76	3.76	-37.61	-0.717	16.26	-202.38
.001	.167	0	2.20	4.83	18.81	6.241	4.04	4.04	4.04	-37.62	-0.492	8.56	-604.02
.001	.167	0	1.85	6.63	12.55	6.977	4.88	4.88	4.88	-20.81	-0.87	4.9	-338.82
.001	.167	30	1.25	1.11	11.75	5.702	3.01	3.01	3.01	-0.9	-0.272	5.56	69.27
.001	.167	30	2.18	1.85	18.19	5.814	3.42	3.55	4.57	-31.76	-0.322	3.31	213.19
.001	.167	30	1.58	6.60	11.61	6.079	3.60	4.16	4.81	-12.70	0.753	1.86	72.50
.001	.167	30	2.38	3.00	20.30	4.856	3.46	3.99	4.61	-19.17	-0.170	7.0	-34.32
.001	.167	30	2.16	4.05	17.98	5.172	3.86	4.46	5.15	-24.10	0.030	4.14	228.36
.001	.167	30	2.18	3.98	18.19	5.102	4.19	4.64	5.53	-21.67	0.061	5.08	233.82
.001	.167	30	1.96	4.49	15.83	5.320	3.75	4.33	5.01	-21.70	0.334	1.04	60.68
.001	.167	30	1.42	6.72	9.78	5.078	3.90	4.51	5.21	-3.45	1.355	-1.5	32.23
.001	.167	30	2.32	2.78	19.67	3.702	3.41	3.94	4.55	-9.50	0.478	-1.57	-91.15
.001	.167	30	2.04	3.36	16.70	4.119	3.56	4.12	4.75	-12.54	0.763	1.96	31.98
.001	.167	30	1.70	3.93	12.97	4.012	4.04	4.66	5.38	-1.61	1.421	1.14	20.15
.001	.167	30	1.50	5.45	8.40	3.310	4.69	5.62	6.26	0.63	2.747	2.14	60.48
.001	.167	30	2.05	1.75	17.13	2.181	4.58	5.28	6.10	1.60	-0.239	3.47	155.65
.001	.167	30	1.80	2.14	14.08	2.332	4.16	4.81	5.55	5.97	2.628	-3.4	4.01
.001	.167	30	1.38	2.91	9.32	2.062	4.57	5.28	6.10	8.99	0.458	2.27	-12.52
.001	.167	30	1.30	3.30	9.78	1.827	4.78	5.52	6.37	14.72	4.445	2.16	-34.56
.001	.167	60	2.30	2.63	19.46	3.163	3.69	3.39	3.77	8.41	4.383	-9.08	-642.93
.001	.167	60	1.88	2.15	14.96	2.452	1.73	3.46	6.92	20.88	3.838	-6.69	-788.71
.001	.167	60	1.48	2.74	10.47	2.255	4.95	1.90	3.80	21.62	2.785	-2.00	-834.71
.001	.167	60	1.36	3.24	8.86	3.137	7.49	4.9	3.88	3.61	-0.170	12.5	75.59
.001	.167	60	2.34	2.76	19.88	3.699	1.70	3.40	6.60	1.16	1.528	-2.75	-300.64
.001	.167	60	2.08	3.29	17.13	4.085	1.67	3.33	6.67	8.2	1.668	-12.10	-335.37
.001	.167	60	1.62	3.93	12.97	3.313	1.12	3.43	6.10	12.12	3.289	-8.2	-150.11
.001	.167	60	1.32	5.41	8.63	3.427	1.17	2.35	4.70	2.81	1.404	-1.6	-332.12
.001	.167	60	2.38	3.73	20.30	5.039	1.61	3.21	6.42	-3.10	0.513	-13.10	-155.47
.001	.167	60	1.98	4.77	16.05	5.427	1.73	3.10	6.19	1.25	-1.85	-9.2	-129.38
.001	.167	60	1.98	4.78	16.05	5.715	1.55	3.10	6.19	1.95	0.364	-7.43	-199.66
.001	.167	60	1.42	6.61	9.78	4.993	1.49	2.97	5.95	8.81	0.286	-2.01	-224.73
.001	.167	60	1.22	6.61	9.78	4.869	1.49	2.97	5.95	8.81	-0.79	-9.08	-37.9
.001	.167	60	2.20	4.87	18.81	6.286	1.47	2.94	5.89	-6.17	-0.033	12.71	-175.85
.001	.167	60	1.68	6.78	12.74	6.819	1.49	2.97	5.94	0.9	-0.272	-4.36	-156.25
.005	.167	0	2.56	3.92	22.17	5.472	3.58	3.58	3.58	-35.43	0.395	1.81	-1002.86
.005	.167	0	2.22	4.45	18.62	5.775	4.19	4.19	4.19	-22.29	0.614	18.78	-153.42
.005	.167	0	1.58	6.36	11.61	5.859	5.62	5.62	5.62	-9.04	1.646	5.35	-39.32
.005	.167	0	2.36	3.51	20.09	4.716	4.82	4.82	4.82	-22.02	0.739	20.28	-244.35
.005	.167	0	2.20	3.90	18.41	5.031	4.66	4.66	4.66	-24.01	0.867	8.16	-415.49
.005	.167	0	1.95	4.56	15.83	5.410	4.53	4.53	4.53	-14.26	0.984	5.15	-98.03
.005	.167	0	2.02	6.39	9.78	4.830	3.61	6.51	6.51	2.85	2.983	3.56	-25.51
.005	.167	0	2.35	2.57	20.09	3.589	5.42	5.42	5.42	-8.41	2.423	8.70	-146.46
.005	.167	0	2.10	3.05	17.34	3.820	6.19	6.19	6.19	-4.64	1.953	8.93	-94.87
.005	.167	0	1.88	3.57	14.96	4.080	5.88	5.88	5.88	7.2	2.760	2.43	-124.62
.005	.167	0	1.34	3.24	8.86	3.137	7.49	4.9	4.9	3.61	1.625	3.13	-24.67
.005	.167	0	2.40	1.51	20.51	2.052	7.47	7.47	7.47	14.02	4.431	-3.73	-560.56
.005	.167	0	1.95	2.01	15.93	2.387	7.47	7.47	7.47	10.65	4.325	-2.8	-287.54
.005	.167	0	1.64	2.18	12.29	2.318	7.49	7.48	7.48	20.70	5.289	-8.2	-150.11
.005	.167	0	1.34	3.37	8.86	2.025	7.15	7.15	7.15	29.25	6.521	2.70	-99.97
.005	.167	30	2.34	1.53	19.88	2.047	5.79	6.68	7.2	17.99	5.067	0.6	398.94
.005	.167	30	1.95	1.95	15.83	2.315	6.13	7.14	8.24	15.60	5.077	-11.27	221.20
.005	.167	30	1.53	2.00	11.61	2.307	5.78	6.67	7.70	21.70	5.894	-1.7	75.12
.005	.167	30	1.32	3.11	8.63	1.968	6.26	7.22	8.34	31.74	5.849	1.52	62.21
.005	.167	30	2.44	2.62	20.92	3.368	4.79	5.63	5.81	2.70	-2.248	2.9	-359.67
.005	.167	30	2.14	3.10	17.77	3.932	4.79	5.54	6.39	2.60	2.401	-1.72	233.26
.005	.167	30	1.88	3.60	14.96	4.116	4.85	5.60	6.47	3.60	3.023	-2.02	150.33
.005	.167	30	1.98	4.48	16.05	5.360	4.13	4.77	5.81	2.70	-2.248	2.9	-359.67
.005	.167	30	2.42	3.41	23.72	4.644	3.74	4.32	4.99	-8.21	1.115	9.79	422.33
.005	.167	30	2.22	4.10	18.62	5.320	3.57	4.12	4.76	-14.88	1.419	-2.27	66.05
.005	.167	30	1.66	2.42	12.51	4.254	4.26	4.58	5.50	-7.71	1.561	-1.67	182.76
.005	.167	30	2.42	6.43	9.78	4.859	5.33	6.15	7.10	11.34	3.653	8.88	3.25
.005	.167	30	2.54	3.95	21.96	5.500	3.25	3.76	4.34	-21.94	0.066	11.72	227.90
.005	.167	30	2.22	4.43	18.62	6.012	3.61	4.17	4.82	-27.62	0.863	-5.5	-6.66
.005	.167	30	1.66	2.42	12.51	4.254	4.26	4.58	5.50	-7.71	1.561	-1.67	182.76
.005	.167	60	2.54	3.89	22.37	5.454	2.13	4.27	8.53	4.8	2.187	-22.97	-95.73
.005	.167	60	2.24	4.42	18.83	6.027	2.16	4.32	8.64	3.28	2.343	-19.37	-173.31
.005	.167	60	1.60	6.42	12.29	6.150	2.11	4.23	8.46	14.40	2.478	-9.9	-25.55
.005	.167	60	2.40	3.23	20.51	4.782	2.46	4.93	9.66	7.83	3.090	-10.83	-213.86
.005	.167	60	2.22	4.02	18.62	5.217	2.40	4.80	9.60	6.68	2.837	-21.04	-223.98
.005	.167	60	2.02	4.82	16.06	5.326	2.53	6.13	12.13	6.65	2.714	-13.9	-286.69
.005	.167	60	1.46	3.62	10.24	3.057	1.98	3.96	7.92	2.63	3.257	-4.72	-332.49
.005	.167	60	2.42	2.65	20.72	3.609	2.64	5.28	10.56	13.99	4.075	-23.39	-486.08
.005	.167	60	2.22	4.42	18.62	5.217	2.40	4.80	9.60	6.68	2.837	-21.04	-223.98
.005	.167	60	1.92	3.92	15.40	4.067	2.73	5.47	10.93	2.150	3.894	-7.14	-580.02
.005	.167	60	1.30	5.22	9.09	3.572	2.46	4.93	9.86	4.526	4.42	-2.61	-519.00
.005	.167	60	1.92	3.92	15.40	4.067	2.73	5.47	10.93	2.150	3.894	-7.14	-580.02
.005	.167	60	1.92	3.95	15.40	2.271	3.28	6.56	13.13	36.37	5.509	-9.74	-1416.64
.005	.167	60	1.66	2.32	12.51	2.295	3.60	7.20	14.40	46.71	6.225	-2.05	-1163.30
.005	.167	60	1.34	3.02	8.86	1.991	3.30	6.60	13.19	60.95	6.225	-2.05	-1163.30

CLER	D14	ANG	T	H	L	UMAX	CLV	CLVA	CLVU	PHI	K	CMV	COV
010	167	0	2.76	.361	24.22	.5192	4.30	4.30	4.30	-17.63	1208	13.67	418.68
010	167	0	2.36	.447	20.09	.6012	3.56	3.56	3.56	-21.77	1136	5.73	-28.70
010	167	0	1.89	.559	14.96	.6387	5.04	5.04	5.04	-3.81	1900	0.50	106.29
010	167	0	2.72	.32	32.11	.404	5.2	5.2	5.2	-25.27	162	18.05	25.92
010	167	0	2.40	.347	20.51	.4710	4.83	4.83	4.83	-12.38	1800	11.0	106.79
010	167	0	2.04	.426	16.70	.5223	5.66	5.66	5.66	-1.50	2286	5.13	238.06
010	167	0	1.97	.44	16.88	.516	5.9	5.9	5.9	15.18	397	15.18	39.7
010	167	0	2.50	.244	21.54	.3373	7.20	7.20	7.20	7.26	3021	-1.29	603.11
010	167	0	2.20	.288	18.41	.3718	7.96	7.96	7.96	6.37	3168	8.18	530.24
010	167	0	1.93	.34	14.96	.4394	8.1	8.1	8.1	5.95	276	14.53	27.44
010	167	0	2.36	.497	.009	34001.0	10.00	10.00	10.00	61.83	5304	5.06	144.00
010	167	0	2.42	.150	20.72	.2044	9.26	9.26	9.26	21.75	4294	-11.89	83.46
010	167	0	2.06	.187	16.91	.2305	9.76	9.76	9.76	23.39	4826	6.22	491.04
010	167	0	1.76	.23	13.64	.237	9.9	9.9	9.9	23.7	6.22	491.04	
010	167	0	1.44	.277	10.01	.2157	8.40	8.40	8.40	40.35	5811	2.84	190.55
010	167	30	2.38	.151	20.30	.2036	9.39	7.38	8.52	31.12	5097	-3.40	-307.03
010	167	30	2.02	1.40	.206	.82	10.0	10.0	10.0	32.00	40.0	10.0	10.0
010	167	30	1.74	.225	13.41	.2363	5.64	6.51	7.52	41.52	6261	3.23	-193.97
010	167	30	1.42	.283	9.78	.2138	5.08	5.87	6.78	49.66	7432	5.65	-70.37
010	167	30	2.46	.248	21.13	.3408	5.61	6.48	7.48	11.39	3587	6.74	-104.68
010	167	30	2.12	.304	17.85	.3826	6.42	6.95	8.03	13.97	3640	5.24	-227.61
010	167	30	1.84	.350	14.52	.3910	6.42	7.41	8.56	15.51	4258	5.89	-170.43
010	167	30	1.38	.504	9.32	.3573	7.3	6.65	7.64	34.37	6162	4.84	-154.38
010	167	30	2.42	.347	20.72	.4720	3.97	4.55	5.29	4.74	2264	10.53	-185.58
010	167	30	2.24	.383	18.83	.4994	3.69	4.28	4.91	3.89	2016	20.27	-193.10
010	167	30	2.49	.429	16.70	.5259	3.61	4.28	4.89	3.41	2616	16.53	-137.40
010	167	30	1.46	.630	10.24	.5046	6.07	7.00	8.09	17.81	4574	9.21	23.57
010	167	30	2.60	.397	22.58	.5583	3.07	3.55	4.09	-11.18	1072	13.29	-326.29
010	167	30	2.36	.435	20.09	.5899	2.72	3.14	3.63	-8.98	1028	17.23	-232.87
010	167	60	1.73	.629	11.4	.6689	4.01	4.11	4.22	26.85	6030	-9.00	2315.99
010	167	60	2.32	.470	19.67	.6262	2.08	4.16	8.33	20.45	6177	19.2	1680.98
010	167	60	2.66	.386	23.20	.5474	2.06	4.16	8.33	20.45	6177	19.2	1680.98
010	167	60	2.32	.470	19.67	.6262	2.08	4.16	8.33	20.45	6177	19.2	1680.98
010	167	60	2.48	.441	16.70	.5403	2.55	5.01	10.19	35.68	7273	3.1	3395.69
010	167	60	2.24	.386	19.83	.5061	2.91	5.81	11.62	25.35	6890	1.11	1891.70
010	167	60	2.24	.386	19.83	.5061	2.91	5.81	11.62	25.35	6890	1.11	1891.70
010	167	60	1.46	.645	10.24	.5166	2.20	4.40	8.80	37.71	11075	7.60	814.13
010	167	60	2.60	.241	22.58	.3384	2.77	5.55	11.09	31.18	5127	-4.81	2510.95
010	167	60	2.60	.241	22.58	.3384	2.77	5.55	11.09	31.18	5127	-4.81	2510.95
010	167	60	1.94	.355	15.61	.4170	2.42	4.23	9.67	38.59	7020	1.25	1419.33
010	167	60	1.38	.498	9.32	.3531	1.91	3.83	7.66	38.59	10534	5.66	994.16
010	167	60	2.60	.147	22.58	.1880	2.80	3.60	2.80	4.0	4713	5.32	293.99
010	167	60	1.85	.173	18.14	.2221	2.03	3.16	8.11	49.98	4983	4.61	2098.46
010	167	60	1.86	.214	14.74	.2423	1.55	3.10	6.20	56.97	7517	9.31	1881.51
010	167	60	1.84	.257	11.16	.2273	.57	1.14	2.29	60.39	12004	8.59	1944.51

016	167	0	2.46	.447	21.13	.4131	2.80	2.90	2.90	-14.28	1142	20.03	-479.66
016	167	0	2.20	.504	13.41	.6512	2.96	2.96	2.96	-9.63	1474	19.06	-563.74
016	167	0	1.64	.60	12.29	.6720	4.76	4.76	4.76	.82	3022	10.34	-284.74
016	167	0	2.34	.38	19.88	.5114	4.20	5.3	5.3	2.0	2909	19.22	-645.97
016	167	0	2.18	.440	18.19	.5642	3.67	3.67	3.67	-7.6	2625	16.34	-569.52
016	167	0	1.92	.518	15.40	.6034	4.20	4.20	4.20	2.51	2595	11.44	-433.56
016	167	0	2.42	.34	24.22	.404	5.2	5.2	5.2	-25.27	162	18.05	25.92
016	167	0	2.6	.248	23.20	.3355	5.94	5.94	5.94	10.36	3738	-5.24	-1349.30
016	167	0	2.14	.342	17.77	.4351	5.89	5.89	5.89	14.71	4134	7.51	-202.63
016	167	0	2.4	.38	19.88	.418	5.8	5.8	5.8	15.8	4134	7.51	-202.63
016	167	0	1.36	.55	9.09	.3799	6.14	6.14	6.14	40.72	5575	6.21	-163.76
016	167	0	2.30	.171	19.46	.2262	7.82	7.82	7.82	30.61	8930	12.23	-102.67
016	167	0	1.9	.40	15.40	.425	7.8	7.8	7.8	35.03	6218	2.30	302.86
016	167	0	1.54	.275	11.16	.2427	5.04	5.04	5.04	5.11	939	19.9	-510.74
016	167	0	1.34	.342	8.86	.2254	3.30	3.30	3.30	63.00	9387	2.45	-421.74
016	167	30	2.56	.143	22.17	.2003	6.47	7.47	8.62	38.52	6666	3.62	27.88
016	167	30	2.4	.198	15.70	.2439	4.73	5.67	6.31	43.46	5698	4.84	-124.21
016	167	30	1.70	.244	12.97	.2495	3.25	3.75	4.33	47.78	10927	-2.12	-192.22
016	167	30	1.40	.310	9.55	.2269	2.30	2.66	3.07	56.58	11993	9.88	3.45
016	167	30	2.52	.263	21.75	.3656	5.03	5.81	6.70	17.09	8288	3.40	21.89
016	167	30	2.20	.315	18.41	.4070	5.19	5.99	6.92	16.26	4120	1.94	-110.75
016	167	30	1.90	.375	15.18	.4326	5.50	6.35	7.33	17.62	4443	-1.06	-180.21
016	167	30	1.38	.537	9.32	.3909	5.03	6.01	6.71	41.55	6216	1.53	77.55
016	167	30	2.44	.372	20.92	.5081	4.11	4.75	5.48	4.16	2732	2.3	-61.73
016	167	30	2.26	.413	19.04	.5420	4.18	4.82	5.57	2.40	2911	3.56	-98.79
016	167	30	2.06	.483	15.91	.5956	4.17	4.81	5.56	1.91	3158	-9.5	-115.11
016	167	30	1.54	.640	11.16	.5657	5.21	6.02	6.95	17.95	316	1.62	-90.88
016	167	30	2.22	.394	22.78	.5560	3.00	3.47	4.00	-9.6	1811	2.11	-157.16
016	167	30	2.26	.452	19.08	.6461	3.16	3.65	4.22	-5.07	4271	9.58	-122.42
016	167	30	1.76	.53	13.86	.7053	4.23	4.99	5.74	7.36	3431	-6.68	70.38
016	167	60	2.50	.428	21.54	.5916	2.77	5.55	11.10	7.69	3647	41.72	-182.20
016	167	60	2.22	.479	18.62	.6216	3.17	6.34	12.68	12.62	4297	-33.26	-326.68
016	167	60	1.64	.676	12.29	.6578	2.69	5.28	10.76	38.81	2083	-19.62	-645.97
016	167	60	2.38	.390	20.30	.5260	2.90	5.80	11.61	13.04	2986	47.89	-482.45
016	167	60	2.24	.418	18.83	.5621	2.90	5.80	11.60	20.51	3182	-41.35	-602.37
016	167	60	1.98	.485	16.05	.606	3.10	6.24	12.48	24.0	4297	-33.26	-326.68
016	167	60	1.44	.674	10.01	.5250	2.10	4.21	6.41	54.10	1945	-10.60	-559.16
016	167	60	2.40	.285	20.51	.3627	2.64	5.28	10.55	21.92	4307	-37.42	-846.45
016	167	60	2.15	.327	17.34	.4053	3.30	6.23	12.46	22.0	4297	-33.26	-326.68
016	167	60	1.88	.376	14.96	.4296	2.79	5.59	11.18	37.07	3429	-25.51	-925.98
016	167	60	1.34	.542	8.86	.3759	3.07	6.13	12.26	68.47	3327	-4.86	856.45
016	167	60	1.98	.427	16.05	.4948	2.82	5.8	11.93	6.85	4134	7.51	-202.63
016	167	60	1.94	.217	15.61	.2548	2.84	5.68	11.36	38.25	6451	-25.74	-1020.28
016	167	60	1.56	.266	11.38	.2399	4.62	9.29	18.48	60.60	4118	-13.58	-2097.88
016	167	60	1.32	.333	8.6	.2112	4.8	9.68	19.36	78.37	4158	-0.6	-1693.98
016	167	60	2.38	.161	22.06	.2159	5.4	5.6	5.6	3.71	259	2.1	-221.10
016	167	60	1.96	.203	15.93	.2405	5.25	6.06	7.00	43.77	6517	3.5	-264.34
016	167	60	1.64	.247	12.29	.2405	3.46	4.00	4.62	51.56	7508	-1.56	-207.56
016	167	60	2.38	.148	21.13	.3408	5.61	6.48	7.48	11.39	3587	6.74	-104.68
016	167	60	2.52	.267	21.75	.3701							

CLER	DIA	4NG	T	H	L	U44X	CLV	CLVA	CLVU	PHI	K	CHV	COV
*021	*167	0	2.40	*151	20.51	*2043	7.88	7.88	8.04	*6375	2.02	377.60	
*021	*167	0	2.18	*170	18.19	*2181	8.44	8.44	8.59	*5761	3.81	202.96	
*021	*167	0	1.86	*250	11.38	*2261	4.28	4.28	5.27	*7368	3.81	144.05	
*021	*167	0	2.58	*237	22.37	*3129	8.24	8.24	8.24	*4062	3.27	390.09	
*021	*167	0	2.24	*298	18.63	*3813	8.38	8.38	8.10	*4010	6.75	251.88	
*021	*167	0	1.92	*345	15.40	*4022	9.11	9.11	9.51	*22.57	4.58	92.96	
*021	*167	0	1.40	*491	9.55	*3601	8.92	8.92	8.92	*40.28	6.31	2.60	
*021	*167	0	2.37	*317	21.54	*4022	8.92	8.92	9.13	*1.33	3.58	-21.86	
*021	*167	0	2.32	*386	19.67	*5136	5.64	5.64	5.55	*3069	13.53	2.65	
*021	*167	0	2.04	*444	16.70	*5439	6.58	6.58	6.58	*7.24	3.56	5.53	
*021	*167	0	2.56	*399	23.17	*4022	8.92	8.92	9.06	*20.26	4.72	6.80	
*021	*167	0	2.68	*384	23.40	*5467	3.67	3.67	3.67	*1.18	8.89	10.02	
*021	*167	0	2.38	*448	20.30	*605.3	4.49	4.49	-4.75	*2005	16.12	-28.12	
*021	*167	0	2.24	*413	19.63	*6645	5.56	5.56	5.56	*8.93	31.29	9.21	
*021	*167	30	1.78	*374	24.42	*5463	8.33	8.33	8.33	*2.81	11.97	-203.50	
*021	*167	30	2.70	*382	23.61	*5450	2.38	2.75	3.17	*7.3	1695	20.44	
*021	*167	30	2.36	*488	20.09	*5984	2.76	3.18	3.67	8.06	*2326	19.87	
*021	*167	30	2.44	*593	19.52	*6435	4.79	5.48	6.39	11.30	3815	11.97	
*021	*167	30	2.48	*440	21.34	*6482	4.96	5.73	6.61	9.01	*3359	19.33	
*021	*167	30	2.30	*398	19.46	*5270	6.63	5.34	6.17	12.77	*3707	7.47	
*021	*167	30	2.04	*437	16.70	*5359	5.32	6.4	7.09	13.57	*3778	18.59	
*021	*167	30	1.48	*623	10.47	*5127	6.28	7.25	8.37	31.82	*5470	10.85	
*021	*167	30	2.65	*287	23.20	*4076	5.18	5.25	6.91	14.59	*3968	15.18	
*021	*167	30	2.36	*334	20.09	*4948	3.67	6.20	7.16	19.00	*4004	17.22	
*021	*167	30	2.05	*389	16.91	*4800	5.20	6.01	6.94	20.33	*4540	12.41	
*021	*167	30	1.70	*478	12.97	*4883	6.77	7.81	9.02	23.06	*4962	10.06	
*021	*167	30	2.20	*349	20.51	*4666	7.59	8.45	9.56	31.77	*6668	4.78	
*021	*167	30	2.08	*179	17.13	*2221	4.60	5.31	6.13	55.77	*6687	6.67	
*021	*167	30	1.78	*219	13.86	*2365	3.24	3.74	4.31	58.95	*7688	5.60	
*021	*167	30	2.20	*308	18.41	*2245	2.52	2.92	3.37	70.01	*8920	6.44	
*021	*167	60	2.58	*134	22.37	*1874	4.76	5.92	6.85	80.65	*3190	6.77	
*021	*167	60	2.30	*157	19.46	*2083	1.22	2.44	4.89	84.15	*6049	11.32	
*021	*167	60	1.84	*212	14.52	*2368	9.1	1.82	3.63	91.79	*4280	10.37	
*021	*167	60	1.54	*261	10.70	*2216	5.60	1.11	1.16	109.78	*8755	12.76	
*021	*167	60	2.52	*260	21.75	*3614	2.48	4.95	9.90	56.97	*6043	-8.24	
*021	*167	60	2.18	*310	18.19	*3976	2.42	4.84	9.68	54.33	*7722	4.34	
*021	*167	60	2.04	*437	16.70	*5359	5.32	7.8	9.78	27.42	*8422	13.30	
*021	*167	60	1.40	*506	9.55	*3711	8.92	1.37	2.75	67.97	*2.240	6.87	
*021	*167	60	2.36	*375	20.09	*5037	3.72	7.44	14.89	47.13	*6971	-0.43	
*021	*167	60	2.24	*448	20.30	*6053	4.49	7.44	14.89	47.13	*6971	0.43	
*021	*167	60	2.02	*445	16.48	*5413	2.98	5.97	11.93	55.59	*8234	-4.40	
*021	*167	60	1.46	*638	10.24	*5109	1.75	3.50	7.00	71.01	*14171	10.76	
*021	*167	60	2.29	*454	19.25	*5985	3.46	6.93	13.86	36.95	*7348	3.12	
*021	*167	60	1.74	*620	13.41	*6517	3.36	6.72	13.43	52.07	*9384	16.36	
*042	*167	0	2.56	*410	22.17	*5731	3.57	3.97	4.97	9.73	*3.23	13.17	
*042	*167	0	1.70	*650	12.97	*6195	3.50	3.80	3.50	13.30	*3463	9.43	
*042	*167	0	2.33	*379	19.46	*5022	5.62	5.62	5.62	25.53	*4401	7.62	
*042	*167	0	2.20	*308	18.41	*2143	6.78	6.78	5.78	20.49	*4422	3.53	
*042	*167	0	1.94	*455	15.61	*5100	7.70	7.70	7.70	27.45	*4773	9.40	
*042	*167	0	1.40	*652	9.55	*4782	4.52	4.52	4.52	53.29	*4.65	5.13	
*042	*167	0	2.24	*298	18.63	*3817	8.07	8.07	8.07	31.93	*5225	8.58	
*042	*167	0	2.03	*317	17.13	*3538	7.18	7.18	7.18	35.25	*5387	4.82	
*042	*167	0	1.82	*363	14.30	*4014	6.92	6.92	6.92	41.00	*5989	5.54	
*042	*167	0	1.30	*534	8.40	*3247	1.88	1.88	1.88	54.01	*6237	1.55	
*042	*167	0	2.23	*169	19.25	*2232	1.34	1.34	1.34	60.38	*2785	-5.59	
*042	*167	0	2.00	*196	16.26	*2370	1.45	1.45	1.45	53.64	*7170	1.54	
*042	*167	0	1.45	*235	12.74	*2364	6.82	6.82	6.82	45.44	*1.0054	1.19	
*042	*167	0	1.42	*289	9.78	*2190	6.88	6.88	6.88	26.25	*1.0131	3.41	
*042	*167	30	2.20	*170	14.41	*2108	3.91	3.91	4.62	65.78	*8109	6.01	
*042	*167	30	1.99	*203	16.05	*2428	9.3	1.08	1.24	54.60	*1.0148	3.95	
*042	*167	30	1.62	*248	12.06	*2371	9.88	1.02	1.18	66.26	*1.81	4.91	
*042	*167	30	2.43	*233	19.55	*2178	1.11	1.11	1.29	34.48	*77.09	5.48	
*042	*167	30	2.44	*276	20.92	*3771	4.58	5.29	6.11	45.43	*5424	2.13	
*042	*167	30	2.10	*315	17.34	*3944	4.40	4.98	5.87	47.46	*5785	8.35	
*042	*167	30	1.86	*353	14.74	*4059	3.40	3.81	4.40	55.36	*6337	4.83	
*042	*167	30	1.34	*514	8.86	*3393	7.5	8.6	9.9	80.69	*1.153	5.86	
*042	*167	30	2.42	*361	20.72	*4923	5.08	5.87	6.77	27.87	*6.06	12.05	
*042	*167	30	2.24	*391	18.83	*5134	5.32	6.14	7.09	30.77	*4.76	15.42	
*042	*167	30	2.02	*453	16.48	*5587	4.95	5.72	6.61	29.77	*7709	11.72	
*042	*167	30	1.44	*640	10.01	*4986	2.51	2.90	3.35	58.03	*7707	4.29	
*042	*167	30	2.62	*402	22.78	*5670	3.37	3.89	4.50	18.22	*37.05	10.42	
*042	*167	30	2.26	*461	19.04	*6058	4.25	4.90	5.66	22.73	*4050	17.11	
*042	*167	30	1.80	*621	14.08	*6787	4.39	5.07	5.85	27.85	*4764	9.09	
*042	*167	60	2.70	*300	23.61	*5573	2.71	3.42	4.08	55.26	*6971	-2.02	
*042	*167	60	2.32	*454	19.67	*6043	2.86	3.42	4.08	13.84	*8.75	1.99	
*042	*167	60	1.80	*612	14.08	*6086	2.42	3.03	3.66	65.90	*1.0243	4.79	
*042	*167	60	2.40	*359	20.51	*4874	2.11	2.22	2.44	62.31	*9200	-1.68	
*042	*167	60	2.44	*368	21.96	*5448	2.34	2.54	2.74	64.48	*1.81	2.11	
*042	*167	60	2.02	*446	16.48	*5448	1.71	1.92	2.13	68.94	*69.96	3.01	
*042	*167	60	1.50	*630	10.70	*5318	9.3	1.86	3.71	80.92	*17.325	7.47	
*042	*167	60	2.44	*368	21.96	*5448	2.34	2.54	2.74	64.48	*1.81	2.11	
*042	*167	60	2.18	*305	18.19	*3916	4.81	1.63	3.25	70.68	*9881	2.52	
*042	*167	60	1.90	*354	15.18	*4090	9.5	1.70	3.40	68.11	*1.0721	6.08	
*042	*167	60	2.44	*368	21.96	*5448	2.34	2.54	2.74	64.48	*1.81	2.11	
*042	*167	60	2.46	*149	21.13	*2046	1.10	1.20	1.49	70.97	*9.07	12.22	
*042	*167	60	2.10	*179	17.34	*2236	3.37	3.74	4.49	84.78	*1972	10.52	
*042	*167	60	1.54	*264	11.16	*2333	1.36	1.49	1.63	143.2	*24.17	14.17	
*042	*167	60	1.54	*264	11.16	*2333	1.36	2.72	5.44	-3.86	*1598	9.86	

	CLLR	EIA	ANG	T	H	L	UNMAX	CLV	CLVA	CLVU	PHI	K3	CMV	CDV
•001	250	0	1.32	322	9.63	2041	5.44	5.44	5.44	8.03	1.843	3.90	40.27	
•001	250	0	1.36	509	7.09	2447	5.63	5.63	5.63	3.78	1.458	4.72	26.12	
•001	250	0	1.44	640	10.47	5268	5.21	5.21	5.21	2.67	0.985	-0.79	-0.84	
•001	250	0	1.74	231	13.41	2432	5.34	5.34	5.34	4.87	1.694	3.13	17.42	
•001	250	0	1.84	494	14.82	5154	5.03	5.03	5.03	3.19	0.752	3.52	30.31	
•001	250	0	1.84	494	14.82	5154	4.86	4.86	4.86	-7.35	0.361	5.18	23.74	
•001	250	0	1.76	635	13.64	6771	4.37	4.37	4.37	-8.45	0.140	4.31	47.63	
•001	250	0	1.46	647	10.24	5190	4.43	4.43	4.43	5.08	2.23	0.681	2.53	40.13
•001	250	0	2.10	316	17.34	3556	5.25	5.25	5.25	-1.34	0.654	5.46	25.09	
•001	250	0	2.24	407	18.83	5310	4.22	4.22	4.22	-0.73	0.093	2.08	56.65	
•001	250	0	2.28	444	19.25	6113	4.90	4.90	4.90	-0.32	1.49	-25.00		
•001	250	0	2.46	619	21.13	2040	5.05	5.05	5.05	0.61	0.750	1.56	97.70	
•001	250	0	2.40	271	20.51	3681	4.69	4.69	4.69	-4.01	0.329	-3.59	-140.72	
•001	250	0	2.40	366	23.51	4962	4.05	4.05	4.05	-8.03	-0.32	1.99	-25.00	
•001	250	0	2.46	619	21.13	2040	5.05	5.05	5.05	-16.14	11.58	3.37	220.61	
•001	250	15	1.34	310	8.86	2043	5.17	5.17	5.17	3.70	1.433	3.17	20.90	
•001	250	15	1.34	335	3.86	3531	4.93	5.10	5.29	4.52	1.904	4.79	28.72	
•001	250	15	1.46	511	14.30	5622	4.33	4.48	4.62	-5.46	0.781	4.91	27.94	
•001	250	15	1.74	232	13.41	2443	4.68	4.84	5.01	5.26	2.249	2.27	-1.34	
•001	250	15	1.84	369	14.52	4125	4.54	4.70	4.86	1.29	1.330	2.44	-5.90	
•001	250	15	1.84	369	14.52	4125	4.54	4.70	4.86	1.29	1.330	2.44	-5.90	
•001	250	15	1.76	536	13.64	6784	4.77	4.94	5.12	-4.96	0.534	2.88	21.61	
•001	250	15	2.06	184	16.91	2269	4.76	4.93	5.11	5.14	1.553	1.47	-21.89	
•001	250	15	2.18	308	18.19	3943	4.34	4.54	4.70	-5.44	0.743	5.42	55.54	
•001	250	15	2.44	410	19.53	352	3.93	3.97	4.11	-7.38	0.134	3.33	104.07	
•001	250	15	2.26	457	19.04	6525	4.00	4.14	4.28	-13.84	-0.011	4.40	61.72	
•001	250	15	2.44	410	19.53	352	3.93	3.97	4.11	-7.38	0.134	3.33	104.07	
•001	250	15	2.40	261	20.51	3681	4.69	4.83	4.97	-5.5	0.203	6.29	6.94	
•001	250	15	2.40	261	20.51	3681	4.69	4.83	4.97	-5.5	0.203	6.29	6.94	
•001	250	15	2.54	353	21.96	4920	4.04	4.18	4.33	-7.10	0.080	5.69	68.27	
•001	250	15	2.62	405	22.78	5722	4.03	4.17	4.32	-17.74	-0.217	1.25	-175.86	
•001	250	30	1.32	315	8.63	1957	4.65	5.14	5.93	10.59	0.818	3.52	74.09	
•001	250	30	1.34	331	8.86	3504	4.04	4.17	4.32	-17.74	-0.217	1.25	-175.86	
•001	250	30	1.42	680	9.78	5148	3.95	4.26	5.27	2.82	1.708	3.63	25.09	
•001	250	30	1.73	232	12.97	2377	3.71	3.89	4.49	6.86	1.864	3.20	-23.50	
•001	250	30	1.82	378	14.30	4186	3.69	4.26	4.92	5.14	1.462	2.10	-0.20	
•001	250	30	1.84	514	14.52	5755	3.37	3.89	4.49	-3.57	0.801	5.29	4.58	
•001	250	30	1.84	514	14.52	5755	3.37	3.89	4.49	-3.57	0.801	5.29	4.58	
•001	250	30	2.02	199	16.48	2258	4.19	4.83	5.58	4.41	1.312	5.94	12.34	
•001	250	30	2.10	323	17.34	4041	3.76	4.35	5.02	-1.52	1.030	5.20	10.09	
•001	250	30	2.28	491	19.25	6493	3.20	3.70	4.27	-9.60	-0.090	3.97	-48.09	
•001	250	30	2.33	159	20.30	2151	3.64	4.20	4.85	3.32	0.930	3.10	-74.02	
•001	250	30	2.40	284	20.51	3687	3.33	3.64	4.44	4.81	0.887	4.97	-60.85	
•001	250	30	2.40	284	20.51	3687	3.33	3.64	4.44	4.81	0.887	4.97	-60.85	
•001	250	30	2.65	407	23.20	5784	2.58	3.34	3.80	-9.95	-0.695	-2.29	-71.29	
•001	250	45	1.40	297	7.55	2176	2.62	3.1	3.5	5.25	7.0	2.79	33.32	
•001	250	45	1.18	509	7.09	2447	2.32	2.8	3.2	4.25	8.229	1.9	58.26	
•001	250	45	1.50	637	10.70	5340	2.58	3.64	5.15	2.12	1.481	1.91	30.89	
•001	250	45	1.78	221	13.66	2386	2.38	3.37	4.77	5.19	0.158	3.13	120.21	
•001	250	45	1.88	308	14.96	3943	2.33	3.30	4.66	4.77	0.95	4.03	-27.97	
•001	250	45	1.88	308	14.96	3943	2.33	3.30	4.66	4.77	0.95	4.03	-27.97	
•001	250	45	1.94	567	15.61	6667	2.70	3.82	5.40	-4.66	0.418	2.74	63.00	
•001	250	45	2.12	181	17.55	2281	2.81	3.86	5.62	7.78	0.72	2.61	148.40	
•001	250	45	2.20	312	18.41	4028	2.80	3.39	4.79	-6.67	1.008	1.93	35.18	
•001	250	45	2.26	383	19.04	5034	2.72	3.85	5.45	-4.48	0.360	3.30	80.90	
•001	250	45	2.26	470	19.04	6170	2.65	3.75	5.30	-9.09	0.042	4.72	122.24	
•001	250	45	2.52	140	21.75	1945	2.86	3.5	5.2	8.40	0.436	3.67	155.07	
•001	250	45	2.58	244	22.37	3425	2.36	3.34	4.72	-1.53	0.728	1.6	25.34	
•001	250	45	2.46	355	21.13	4872	2.31	3.27	4.62	2.52	0.251	2.56	116.81	
•001	250	60	2.38	158	20.30	2131	1.8	2.39	4.77	-10.59	-0.101	-1.2	-20.24	
•001	250	60	1.36	309	9.32	2192	1.77	2.35	3.70	2.95	2.863	3.34	321.59	
•001	250	60	1.33	520	9.09	3567	1.44	2.88	3.77	-2.53	1.537	4.29	150.70	
•001	250	60	1.82	509	14.30	5628	1.85	1.71	3.42	3.75	1.035	3.31	138.98	
•001	250	60	1.82	509	14.30	5628	1.85	1.71	3.42	3.75	1.035	3.31	138.98	
•001	250	60	2.06	188	16.31	2321	1.24	2.29	4.57	2.31	-0.880	3.69	267.05	
•001	250	60	2.14	314	17.77	3984	1.15	2.49	4.59	-1.15	0.004	3.83	221.22	
•001	250	60	2.32	404	21.40	5758	1.18	3.09	4.37	-3.43	0.727	1.86	220.01	
•001	250	60	2.22	393	13.62	5103	1.95	1.69	3.39	14.92	-0.936	4.30	274.57	
•001	250	60	2.30	459	19.46	6080	1.99	1.68	3.96	7.79	-0.143	1.58	240.59	
•001	250	60	2.38	158	20.30	2131	1.8	2.39	4.77	-10.59	-0.101	-1.2	-20.24	
•001	250	60	2.44	268	20.92	3669	1.85	1.70	3.39	9.8	-0.091	2.27	224.12	
•001	250	60	2.70	385	23.61	6502	1.86	1.77	3.54	12.52	-1.629	1.03	36.52	
•001	250	75	1.80	334	14.08	2560	1.45	1.72	3.65	-30.43	-0.749	4.0	350.79	
•001	250	75	1.48	370	14.06	4223	1.10	1.40	1.55	-62.78	-0.075	2.97	140.40	
•001	250	75	1.52	621	10.93	5371	1.10	1.39	1.50	-4.56	8.005	4.44	108.02	
•001	250	75	1.80	334	14.08	2560	1.45	1.72	3.65	-30.43	-0.749	4.0	350.79	
•001	250	75	1.88	370	14.06	4223	1.10	1.40	1.55	-62.78	-0.075	2.97	140.40	
•001	250	75	1.86	699	14.74	6548	1.13	1.50	1.94	70.17	4.788	3.93	120.63	
•001	250	75	1.80	621	10.93	5371	1.10	1.39	1.50	-4.56	8.005	4.44	108.02	
•001	250	75	2.10	184	17.34	3505	1.18	1.71	2.73	-27.89	-1.6262	4.49	334.06	
•001	250	75	2.20	312	18.41	4024	1.16	1.60	2.32	-64.23	-3.588	3.24	231.46	
•001	250	75	2.26	414	19.04	5431	1.21	1.82	3.18	71.25	3.96	1.18	181.25	
•001	250	75	2.32	668	13.67	6235	1.21	1.82	3.18	71.25	3.96	1.18	181.25	
•001	250	75	2.34	158	19.88	2109	1.21	1.81	3.14	26.10	-1.4207	4.00	360.64	
•001	250	75	2.20	245	22.58	3448	1.06	1.22	1.83	56.57	-3.46	2.62	305.99	
•001	250	75	2.50	365	21.54	474	1.3	1.49	1.99	79.0	1.952	4.26	322.37	
•001	250	75	2.24	477	18.83	6489	1.27	1.04	4.00	31.19	5.139	4.36	134.91	



CLER	CIA	ANG	T	H	L	UMAX	LV2	CLV4	CLVU	PHI	K	CMV	COV		
*010	*250	0	1.38	218	9.32	1550	5.74	5.74	5.74	64.01	1.3744	2.46	-19.91		
*010	*250	0	1.38	852	3.32	1210	6.75	6.75	6.75	11.768	1.768	3.01	11.01		
*010	*250	0	1.40	620	9.55	4549	8.03	8.03	8.03	30.83	5885	4.10	25.62		
*010	*250	0	1.42	801	9.78	6067	7.67	7.67	7.67	21.73	4857	2.61	23.75		
*010	*250	0	1.42	1632	10.64	1158	8.82	8.82	8.82	11.10	8626	6.02	17.85		
*010	*250	0	1.78	417	13.86	4503	7.36	7.36	7.36	26.91	5207	1.01	02		
*010	*250	0	1.80	690	14.08	4557	7.15	7.15	7.15	11.06	3894	1.76	9.07		
*010	*250	0	1.82	1632	10.64	1158	8.82	8.82	8.82	9.30	8626	6.02	17.85		
*010	*250	0	2.12	177	15.75	2429	7.15	7.15	7.15	35.38	7579	7.03	181.55		
*010	*250	0	2.14	380	17.77	4821	7.23	7.23	7.23	16.73	4339	2.19	19.35		
*010	*250	0	2.18	776	17.77	7025	5.60	5.60	5.60	5.12	3132	1.81	20.26		
*010	*250	0	2.16	706	17.94	9014	4.90	4.90	4.90	-10.64	1018	2.16	44.88		
*010	*250	0	2.42	154	20.72	2103	5.97	5.97	5.97	32.26	9385	1.76	-88.41		
*010	*250	0	2.40	323	20.51	4378	6.97	6.97	6.97	12.87	4466	5.04	126.54		
*010	*250	0	2.42	584	20.02	6436	6.83	6.83	6.83	9.23	8483	3.67	7.57		
*010	*250	0	2.44	556	21.34	7661	4.48	4.48	4.48	-7.40	2059	2.69	28.52		
*010	*250	0	2.52	679	21.75	9429	3.67	3.67	3.67	-10.98	1165	1.11	88.60		
*010	*250	0	1.38	213	9.32	1511	9.44	9.44	9.44	66.36	8626	2.41	62.07		
*010	*250	15	1.38	397	9.32	2816	8.96	8.96	8.96	9.27	9.60	43.87	7550	2.60	104.57
*010	*250	15	1.38	455	9.32	3233	8.61	8.61	8.61	6.02	46.38	8089	4.84	98.37	
*010	*250	15	1.42	585	9.78	4427	8.72	8.72	8.72	9.59	9.27	24.08	5435	2.93	76.65
*010	*250	15	1.40	591	9.55	4338	6.85	6.85	6.85	6.99	7.13	32.74	6841	1.17	20.96
*010	*250	15	1.42	699	9.78	5294	6.56	6.56	6.56	6.79	7.03	27.88	5713	3.47	65.81
*010	*250	15	1.40	776	9.78	5674	7.74	7.74	7.74	8.30	8.59	34.44	4158	2.93	76.65
*010	*250	15	1.40	781	9.55	5731	7.78	7.78	7.78	8.05	8.44	24.77	5263	1.99	44.81
*010	*250	15	1.72	172	13.19	1787	6.17	6.17	6.17	6.39	6.62	45.03	11.57	-98	55.58
*010	*250	15	1.80	402	14.08	4400	6.11	6.32	6.55	24.59	5656	4.73	104.32	10.42	39.75
*010	*250	15	1.80	418	14.08	4586	6.11	6.32	6.55	24.59	5656	4.73	104.32	10.42	39.75
*010	*250	15	1.82	782	14.40	8657	5.32	5.32	5.32	7.00	5.69	31.02	3.03	55.18	55.18
*010	*250	15	2.08	170	17.13	2116	7.56	7.82	8.10	37.46	8929	-8.7	77.68	66.66	66.66
*010	*250	15	2.12	361	18.08	4586	6.11	6.32	6.55	24.59	5656	4.73	104.32	10.42	39.75
*010	*250	15	2.16	545	17.68	6962	5.13	5.31	5.50	.35	3.25	15.01	49.75	49.75	49.75
*010	*250	15	2.20	679	18.41	8773	4.41	4.57	4.73	-7.54	1884	8.57	38.16	38.16	38.16
*010	*250	15	2.20	686	18.41	8830	4.41	4.57	4.73	-7.54	1884	8.57	38.16	38.16	38.16
*010	*250	15	2.40	330	20.51	4472	6.02	6.23	6.45	10.84	4570	1.15	141.81	141.81	141.81
*010	*250	15	2.46	580	21.13	7568	3.58	3.71	3.84	-5.44	2244	6.64	74.04	74.04	74.04
*010	*250	15	2.50	666	21.55	9244	3.72	3.85	3.99	-9.26	1083	99.00	17.17	18.01	18.01
*010	*250	15	2.40	330	20.51	4472	6.02	6.23	6.45	10.84	4570	1.15	141.81	141.81	141.81
*010	*250	30	1.40	407	9.55	2988	6.08	7.02	8.11	49.38	7775	4.89	6.96	6.96	6.96
*010	*250	30	1.40	587	9.55	4310	7.47	8.63	9.97	38.45	6514	3.55	43.33	43.33	43.33
*010	*250	30	1.42	778	9.78	4584	6.02	6.39	6.84	54.68	6175	2.62	29.98	29.98	29.98
*010	*250	30	1.78	170	13.86	1640	4.52	5.22	6.03	56.08	7467	3.56	-19.28	-19.28	-19.28
*010	*250	30	1.78	373	13.86	4035	6.62	7.64	8.82	30.17	6326	3.56	73.67	73.67	73.67
*010	*250	30	2.12	393	17.77	4586	6.11	6.32	6.55	24.59	5656	4.73	104.32	104.32	104.32
*010	*250	30	1.86	740	14.74	8370	5.08	5.86	6.77	9.54	3830	2.56	5.91	5.91	5.91
*010	*250	30	2.16	159	17.98	2025	6.80	9.53	11.47	37.83	6778	7.25	120.13	120.13	120.13
*010	*250	30	2.18	393	17.77	4586	6.11	6.32	6.55	24.59	5656	4.73	104.32	104.32	104.32
*010	*250	30	2.20	493	18.41	4368	6.24	7.20	8.32	8.80	3752	1.48	-10.91	-10.91	-10.91
*010	*250	30	2.20	643	18.41	4803	6.23	5.35	6.17	-3.14	2650	6.70	46.66	46.66	46.66
*010	*250	30	2.40	330	20.51	4472	6.02	6.23	6.45	10.84	4570	1.15	141.81	141.81	141.81
*010	*250	30	2.40	300	20.51	4067	6.89	7.96	9.19	18.91	4902	1.40	46.74	46.74	46.74
*010	*250	30	2.42	513	20.72	6987	5.09	5.88	6.79	-1.65	2922	5.38	56.84	56.84	56.84
*010	*250	30	2.46	648	21.13	8902	3.45	3.98	4.59	-15.50	1900	7.45	-87.41	-87.41	-87.41
*010	*250	45	1.42	585	9.32	4586	6.11	6.32	6.55	24.59	5656	4.73	104.32	104.32	104.32
*010	*250	45	1.38	405	9.32	2893	3.64	4.57	5.78	55.25	6800	2.66	65.85	65.85	65.85
*010	*250	45	1.40	213	9.55	1563	2.90	4.10	5.80	68.88	4170	2.65	59.18	59.18	59.18
*010	*250	45	1.38	283	9.32	2009	2.55	4.61	5.91	63.35	4170	2.65	59.18	59.18	59.18
*010	*250	45	1.40	213	9.55	1563	2.90	4.10	5.80	68.88	4170	2.65	59.18	59.18	59.18
*010	*250	45	1.42	779	9.78	5903	4.48	6.34	8.96	35.27	6392	1.65	83.85	83.85	83.85
*010	*250	45	1.82	160	14.30	1765	3.21	4.24	6.42	67.03	8294	2.65	89.09	89.09	89.09
*010	*250	45	1.82	342	14.30	3785	4.81	6.80	9.62	39.66	6825	1.64	125.91	125.91	125.91
*010	*250	45	1.84	552	14.52	6175	4.39	6.21	8.79	22.44	4288	-9.3	68.99	68.99	68.99
*010	*250	45	1.88	708	14.96	8093	4.30	6.08	8.60	14.43	4208	-8.57	55.52	55.52	55.52
*010	*250	45	2.12	173	17.55	2181	3.85	5.17	7.31	48.22	7067	2.14	125.63	125.63	125.63
*010	*250	45	2.14	351	17.77	4451	3.79	5.36	7.58	27.00	5761	-1.09	163.70	163.70	163.70
*010	*250	45	2.16	478	18.41	6178	4.39	6.21	8.78	15.32	4444	-7.6	147.23	147.23	147.23
*010	*250	45	2.18	631	18.62	8198	3.72	5.26	7.43	7.69	3482	2.37	76.49	76.49	76.49
*010	*250	45	2.22	631	18.62	8198	3.72	5.26	7.43	7.69	3482	2.37	76.49	76.49	76.49
*010	*250	45	2.24	156	20.51	2110	3.95	5.58	7.90	43.67	6661	1.50	154.94	154.94	154.94
*010	*250	45	2.34	295	19.88	3943	4.42	6.24	8.83	25.41	5408	1.11	267.01	267.01	267.01
*010	*250	45	2.42	522	20.72	7110	3.86	5.38	8.08	10.83	4483	1.66	175.74	175.74	175.74
*010	*250	60	1.40	400	9.32	4344	4.82	6.56	9.58	10.83	33.57	3.57	68.99	68.99	68.99
*010	*250	60	1.42	210	9.78	1588	1.47	2.94	5.87	80.25	5174	2.33	156.10	156.10	156.10
*010	*250	60	1.40	400	9.32	4344	4.82	6.56	9.58	10.83	33.57	3.57	68.99	68.99	68.99
*010	*250	60	1.44	776	10.01	6054	1.86	3.72	7.43	45.15	7310	2.23	28.38	28.38	28.38
*010	*250	60	1.78	170	13.86	1834	1.09	2.18	4.36	66.99	5343	2.28	48.90	48.90	48.90
*010	*250	60	1.82	361	14.30	3957	1.75	3.50	7.00	51.27	7780	1.88	294.77	294.77	294.77
*010	*250	60	1.82	546	14.30	6045	2.31	4.62	9.25	35.53	6276	1.72	92.14	92.14	92.14
*010	*250	60	1.86	728	14.74	8231	2.33	4.66	9.31	24.10	5288	1.79	73.36	73.36	73.36
*010	*250	60	1.88	913	15.18	10523	1.85	3.69	7.37	34.29	6415	-2.3	105.94	105.94	105.94
*010	*250	60	2.00	118	19.88	4265	1.84	3.69	7.37	34.29	6415	-2.3	105.94	105.94	105.94
*010	*250	60	2.20	492	18.41	4357	2.17	4.34	8.68	23.56	5239	-1.19	79.90	79.90	79.90
*010	*250	60	2.22	362	14.30	6003	2.02	4.24	8.46	58.02	8034	2.16	24.70	24.70	24.70
*010	*250	60	2.24	149	19.88	1990	1.32	2.65	5.30	61.01	11.342	5.1	-27.34	-27.34	-27.34
*010	*250	60	2.46	284	21.13	3897	2.02	4.03	8.07	35.08					

CLER	DIA	ANG	T	H	L	U44x	CLV	CLVA	CLVU	PH1	K	CNV	CDV
*316	250	0	1.34	306	8.96	2019	4.76	4.76	4.76	70.73	*8808	3.15	55.72
*016	250	0	1.32	527	8.63	1349	7.13	7.13	7.13	50.00	*7876	1.18	18.81
*016	250	0	1.46	425	10.01	4884	8.64	8.64	8.64	38.13	*5591	3.03	106.29
*316	250	0	1.72	227	13.41	2387	6.04	6.04	6.04	50.43	*8280	2.86	44.44
*016	250	0	1.86	1369	14.74	4170	9.08	9.08	9.08	29.17	*5314	-7.39	-11.34
*016	250	0	1.82	499	14.33	3528	9.25	9.25	9.25	31.23	*7424	3.07	52.77
*016	250	0	1.86	635	14.08	6547	7.08	7.08	7.08	11.57	*4078	2.95	48.01
*016	250	0	2.02	181	16.48	2200	8.06	8.06	8.06	47.26	*6920	4.54	199.37
*016	250	0	2.03	318	19.13	3952	9.56	9.56	9.56	25.12	*4730	11.85	274.73
*016	250	0	2.20	401	18.41	5177	7.93	7.93	7.93	18.41	*4264	5.71	225.09
*016	250	0	2.28	475	19.25	6269	7.22	7.22	7.22	8.45	*3334	8.39	152.57
*016	250	0	2.26	156	9.01	2008	9.35	9.35	9.35	48.78	*6855	5.99	285.40
*016	250	0	2.30	427	19.46	4740	9.09	9.09	9.09	23.58	*4880	7.01	280.42
*016	250	0	2.34	376	13.83	5039	7.87	7.87	7.87	13.55	*4198	-1.72	144.03
*016	250	0	2.56	424	22.17	5924	6.41	6.41	6.41	11.17	*3262	3.86	45.96
*016	250	15	1.32	308	9.63	1357	7.78	7.91	4.05	77.16	*9142	2.89	88.13
*016	250	15	1.38	501	9.32	3558	6.83	7.07	7.32	53.73	*7088	1.90	68.39
*016	250	15	1.52	610	10.93	5281	8.48	8.77	9.08	28.62	*5181	1.86	49.28
*016	250	15	1.74	24	11.41	2361	4.92	5.09	5.27	58.27	*8044	2.56	30.28
*016	250	15	1.82	363	15.18	4190	8.35	8.65	9.05	31.54	*5220	1.22	100.48
*016	250	15	1.82	499	14.30	5528	7.64	7.91	8.19	21.83	*4419	6.43	132.03
*016	250	15	1.92	323	16.30	6899	6.82	7.06	7.31	14.40	*4053	-7.3	57.21
*016	250	15	2.04	181	16.70	2215	6.93	7.18	7.43	51.74	*7352	2.44	152.52
*016	250	15	2.12	320	17.55	4037	8.14	8.42	8.72	23.77	*4817	5.43	162.27
*016	250	15	2.14	10	13.83	5308	6.53	6.88	7.10	16.75	*3959	7.60	257.08
*016	250	15	2.28	446	19.25	6193	6.81	7.05	7.30	7.62	*3122	6.12	99.10
*016	250	15	2.32	155	19.67	2070	7.28	7.44	7.80	48.55	*6964	3.42	202.66
*016	250	15	2.38	328	20.30	3752	8.20	8.49	8.79	21.44	*4656	5.51	147.80
*016	250	15	2.48	485	21.34	4899	7.64	7.91	8.19	13.83	*3815	3.28	74.93
*016	250	15	2.66	403	23.20	5727	5.52	5.72	5.92	7.16	*2878	2.99	25.23
*016	250	30	1.44	296	9.35	2170	3.55	3.81	4.07	68.10	*8783	3.62	38.49
*016	250	30	1.39	09	9.22	3616	4.92	5.18	5.44	65.56	*7909	3.06	57.65
*016	250	30	1.48	640	10.47	5273	7.24	8.36	9.55	36.88	*6021	-1.06	10.43
*016	250	30	1.80	223	14.08	4234	4.32	4.99	5.76	59.88	*8371	2.54	39.49
*016	250	30	1.92	361	15.48	4204	7.01	8.09	9.34	38.47	*5748	-6.14	31.81
*016	250	30	1.86	442	14.74	5563	7.30	8.43	9.74	23.56	*4995	-2.93	-15.61
*016	250	30	1.86	615	14.74	6956	5.97	6.90	7.97	18.45	*4371	4.61	102.13
*016	250	30	2.12	192	17.55	4256	5.77	6.43	7.43	31.03	*7418	1.89	72.09
*016	250	30	2.20	308	18.41	3975	7.26	8.39	9.69	23.98	*5389	4.63	82.69
*016	250	30	2.24	403	18.83	5260	6.42	7.42	8.56	20.63	*4672	3.72	200.92
*016	250	30	2.40	157	20.51	2134	5.22	6.03	6.96	51.12	*7395	2.54	242.63
*016	250	30	2.40	277	20.51	3764	7.01	9.10	9.35	26.11	*5007	-8.50	186.97
*016	250	30	2.40	361	15.48	4204	7.01	8.09	9.34	38.47	*5748	-6.14	31.81
*016	250	30	2.70	387	23.61	5531	6.21	7.17	8.29	10.80	*3612	2.28	104.86
*016	250	45	1.48	278	10.47	2289	2.16	3.08	4.33	78.86	*7412	3.28	63.61
*016	250	45	1.48	508	9.55	3182	7.14	8.24	9.51	13.47	*6451	5.82	75.16
*016	250	45	1.72	214	11.41	2361	4.78	5.76	6.96	36.12	*5684	2.91	100.88
*316	250	45	1.64	213	14.52	2382	2.81	3.98	5.62	70.66	*7375	3.47	98.41
*016	250	45	1.98	347	16.05	4149	4.86	6.17	8.71	38.02	*5936	-1.33	73.57
*016	250	45	1.98	463	15.61	5842	5.35	7.62	10.78	30.01	*4971	1.17	51.83
*016	250	45	1.82	612	14.30	6771	4.54	6.43	9.09	29.78	*4974	-7.51	60.32
*016	250	45	2.42	150	20.72	2039	3.94	5.57	7.88	59.38	*6364	4.37	206.82
*016	250	45	2.24	254	19.25	1874	4.45	6.30	8.90	38.64	*5700	1.66	193.96
*016	250	45	2.38	355	20.10	4889	5.17	7.31	10.38	25.94	*4635	-1.19	18.19
*016	250	45	2.29	473	19.25	6110	4.96	7.01	9.91	18.07	*4198	6.14	184.29
*016	250	45	2.80	129	24.63	1863	3.32	4.70	8.65	51.72	*6773	4.22	50.88
*016	250	45	2.68	248	22.99	3509	4.64	6.31	8.92	29.47	*5460	1.45	165.77
*016	250	45	2.44	311	21.34	4833	5.29	7.48	10.58	19.34	*4645	1.99	89.50
*016	250	45	2.62	413	22.78	5825	4.57	6.46	9.13	21.19	*3909	-4.44	76.50
*016	250	60	1.44	306	9.55	2248	4.71	1.81	2.62	62.70	*7369	2.44	137.74
*016	250	60	1.39	519	9.32	3680	1.20	2.39	4.78	58.62	*904	2.05	72.91
*016	250	60	1.56	609	11.38	5510	1.61	3.22	6.44	50.72	*7994	2.33	92.15
*016	250	60	1.86	221	14.74	2499	1.09	2.19	4.38	76.59	*7590	2.54	157.24
*016	250	60	1.92	365	15.40	4254	1.87	3.44	6.67	38.02	*7453	2.03	31.07
*016	250	60	1.90	500	15.18	5771	1.84	3.67	7.34	45.22	*7149	2.07	113.25
*016	250	60	1.84	640	14.52	7163	1.65	3.30	6.60	42.16	*6902	2.31	106.55
*016	250	60	2.12	181	17.55	4256	1.43	2.87	5.74	63.99	*5877	1.80	69.51
*016	250	60	2.30	307	18.41	3965	1.78	3.57	7.14	50.48	*8714	1.70	162.86
*016	250	60	2.20	398	19.46	5278	2.05	4.10	8.19	37.34	*6237	-5.52	136.08
*016	250	60	2.40	481	20.51	6066	1.55	3.15	6.24	45.55	*7180	1.85	121.50
*016	250	60	2.44	150	21.13	2054	1.33	2.67	5.33	68.63	*6683	7.7	151.58
*016	250	60	2.48	266	21.34	3666	1.77	3.64	7.08	45.54	*6488	1.51	191.05
*016	250	60	2.68	348	22.99	4889	1.64	3.41	6.92	39.78	*5929	1.85	106.29
*016	250	60	2.66	400	23.20	5688	1.62	3.64	7.28	31.60	*5500	-1.41	273.74
*016	250	75	1.46	297	10.24	2384	0.63	2.42	4.96	6.80	*4693	2.80	207.34
*016	250	75	1.44	521	9.55	3283	1.17	1.87	3.65	25.93	*6183	2.89	99.87
*016	250	75	1.80	139	11.41	2361	0.44	1.70	3.39	61.81	*858	1.45	97.66
*016	250	75	1.84	229	14.52	2561	1.20	1.79	3.06	86.30	*1028	3.19	205.41
*016	250	75	1.49	360	15.61	4238	0.49	1.88	3.28	85.07	*7465	2.05	131.90
*016	250	75	1.42	501	15.40	5835	0.32	2.05	3.91	73.77	*6882	2.44	96.17
*016	250	75	1.86	618	14.74	4985	0.58	2.24	3.85	57.65	*8967	3.02	88.96
*016	250	75	2.22	176	13.62	2287	0.62	2.40	4.26	89.16	*7477	2.93	213.51
*016	250	75	2.12	318	14.52	4256	0.40	1.91	3.52	91.02	*7552	2.40	186.02
*016	250	75	2.36	376	20.09	4980	0.68	2.64	4.26	10.20	*7450	1.27	156.66
*016	250	75	2.34	452	14.88	6045	0.61	2.15	3.98	66.93	*7475	1.41	147.09
*016	250	75	2.42	613	15.40	6066	0.40	2.31	4.16	73.16	*8161	1.80	106.29
*016	250	75	2.40	251	22.58	1530	0.55	2.11	3.84	82.68	*5463	1.78	194.88
*016	250	75	2.44	352	21.34	4854	0.65	2.50	4.66	57.91	*6825	0.93	162.48
*016	250	75	2.76	380	24.22	5469	0.67	2.60	4.66	63.28	*7547	1.11	208.20





CLFEP	DTA	ANS	T	H	L	JMAK	CLVJ	CLVA	CLVU	PHI	K	CMV	COV
042	250	0	1	20	0.31	7.26	1.371	1.36	1.05	87.05	1.0815	2.58	25.70
042	250	0	1	18	0.23	6.51	1.212	1.04	1.02	86.77	1.1515	2.17	21.20
042	250	0	1	14	0.40	4.17	1.151	1.04	1.04	85.54	0.9885	3.13	36.94
042	250	0	1	10	0.67	2.55	1.009	1.04	1.04	84.92	0.7646	3.51	45.59
042	250	0	1	8	0.85	2.15	1.874	1.26	1.27	82.94	1.215	1.85	11.93
042	250	0	1	6	1.25	1.29	1.021	1.27	1.27	81.20	0.9073	0.69	17.43
042	250	0	1	4	1.65	0.50	1.174	1.06	1.06	81.89	0.6033	1.57	-0.01
042	250	0	1	2	1.72	0.54	1.319	1.09	1.09	81.93	0.5437	4.58	13.03
042	250	0	1	24	0.04	1.31	1.073	1.02	1.05	87.69	1.0332	1.25	32.25
042	250	0	2	22	0.25	1.86	1.062	1.03	1.03	85.59	0.957	3.11	63.14
042	250	0	2	24	0.26	1.88	1.065	1.03	1.03	85.38	0.959	1.44	-25.01
042	250	0	2	26	0.27	1.90	1.068	1.03	1.03	85.17	0.962	3.02	93.37
042	250	0	2	28	0.28	1.92	1.071	1.03	1.03	84.96	0.965	3.63	175.93
042	250	0	2	30	0.29	1.94	1.074	1.03	1.03	84.75	0.968	4.24	268.49
042	250	0	2	32	0.30	1.96	1.077	1.03	1.03	84.54	0.971	4.85	361.05
042	250	0	2	34	0.31	1.98	1.080	1.03	1.03	84.33	0.974	5.46	453.61
042	250	0	2	36	0.32	2.00	1.083	1.03	1.03	84.12	0.977	6.07	546.17
042	250	0	2	38	0.33	2.02	1.086	1.03	1.03	83.91	0.980	6.68	638.73
042	250	0	2	40	0.34	2.04	1.089	1.03	1.03	83.70	0.983	7.29	731.29
042	250	0	2	42	0.35	2.06	1.092	1.03	1.03	83.49	0.986	7.90	823.85
042	250	0	2	44	0.36	2.08	1.095	1.03	1.03	83.28	0.989	8.51	916.41
042	250	0	2	46	0.37	2.10	1.098	1.03	1.03	83.07	0.992	9.12	1008.97
042	250	0	2	48	0.38	2.12	1.101	1.03	1.03	82.86	0.995	9.73	1101.53
042	250	0	2	50	0.39	2.14	1.104	1.03	1.03	82.65	0.998	10.34	1194.09
042	250	0	2	52	0.40	2.16	1.107	1.03	1.03	82.44	1.001	10.95	1286.65
042	250	0	2	54	0.41	2.18	1.110	1.03	1.03	82.23	1.004	11.56	1379.21
042	250	0	2	56	0.42	2.20	1.113	1.03	1.03	82.02	1.007	12.17	1471.77
042	250	0	2	58	0.43	2.22	1.116	1.03	1.03	81.81	1.010	12.78	1564.33
042	250	0	2	60	0.44	2.24	1.119	1.03	1.03	81.60	1.013	13.39	1656.89
042	250	0	2	62	0.45	2.26	1.122	1.03	1.03	81.39	1.016	14.00	1749.45
042	250	0	2	64	0.46	2.28	1.125	1.03	1.03	81.18	1.019	14.61	1842.01
042	250	0	2	66	0.47	2.30	1.128	1.03	1.03	80.97	1.022	15.22	1934.57
042	250	0	2	68	0.48	2.32	1.131	1.03	1.03	80.76	1.025	15.83	2027.13
042	250	0	2	70	0.49	2.34	1.134	1.03	1.03	80.55	1.028	16.44	2119.69
042	250	0	2	72	0.50	2.36	1.137	1.03	1.03	80.34	1.031	17.05	2212.25
042	250	0	2	74	0.51	2.38	1.140	1.03	1.03	80.13	1.034	17.66	2304.81
042	250	0	2	76	0.52	2.40	1.143	1.03	1.03	79.92	1.037	18.27	2397.37
042	250	0	2	78	0.53	2.42	1.146	1.03	1.03	79.71	1.040	18.88	2489.93
042	250	0	2	80	0.54	2.44	1.149	1.03	1.03	79.50	1.043	19.49	2582.49
042	250	0	2	82	0.55	2.46	1.152	1.03	1.03	79.29	1.046	20.10	2675.05
042	250	0	2	84	0.56	2.48	1.155	1.03	1.03	79.08	1.049	20.71	2767.61
042	250	0	2	86	0.57	2.50	1.158	1.03	1.03	78.87	1.052	21.32	2860.17
042	250	0	2	88	0.58	2.52	1.161	1.03	1.03	78.66	1.055	21.93	2952.73
042	250	0	2	90	0.59	2.54	1.164	1.03	1.03	78.45	1.058	22.54	3045.29
042	250	0	2	92	0.60	2.56	1.167	1.03	1.03	78.24	1.061	23.15	3137.85
042	250	0	2	94	0.61	2.58	1.170	1.03	1.03	78.03	1.064	23.76	3230.41
042	250	0	2	96	0.62	2.60	1.173	1.03	1.03	77.82	1.067	24.37	3322.97
042	250	0	2	98	0.63	2.62	1.176	1.03	1.03	77.61	1.070	24.98	3415.53
042	250	0	2	100	0.64	2.64	1.179	1.03	1.03	77.40	1.073	25.59	3508.09
042	250	0	2	102	0.65	2.66	1.182	1.03	1.03	77.19	1.076	26.20	3600.65
042	250	0	2	104	0.66	2.68	1.185	1.03	1.03	76.98	1.079	26.81	3693.21
042	250	0	2	106	0.67	2.70	1.188	1.03	1.03	76.77	1.082	27.42	3785.77
042	250	0	2	108	0.68	2.72	1.191	1.03	1.03	76.56	1.085	28.03	3878.33
042	250	0	2	110	0.69	2.74	1.194	1.03	1.03	76.35	1.088	28.64	3970.89
042	250	0	2	112	0.70	2.76	1.197	1.03	1.03	76.14	1.091	29.25	4063.45
042	250	0	2	114	0.71	2.78	1.200	1.03	1.03	75.93	1.094	29.86	4156.01
042	250	0	2	116	0.72	2.80	1.203	1.03	1.03	75.72	1.097	30.47	4248.57
042	250	0	2	118	0.73	2.82	1.206	1.03	1.03	75.51	1.100	31.08	4341.13
042	250	0	2	120	0.74	2.84	1.209	1.03	1.03	75.30	1.103	31.69	4433.69
042	250	0	2	122	0.75	2.86	1.212	1.03	1.03	75.09	1.106	32.30	4526.25
042	250	0	2	124	0.76	2.88	1.215	1.03	1.03	74.88	1.109	32.91	4618.81
042	250	0	2	126	0.77	2.90	1.218	1.03	1.03	74.67	1.112	33.52	4711.37
042	250	0	2	128	0.78	2.92	1.221	1.03	1.03	74.46	1.115	34.13	4803.93
042	250	0	2	130	0.79	2.94	1.224	1.03	1.03	74.25	1.118	34.74	4896.49
042	250	0	2	132	0.80	2.96	1.227	1.03	1.03	74.04	1.121	35.35	4989.05
042	250	0	2	134	0.81	2.98	1.230	1.03	1.03	73.83	1.124	35.96	5081.61
042	250	0	2	136	0.82	3.00	1.233	1.03	1.03	73.62	1.127	36.57	5174.17
042	250	0	2	138	0.83	3.02	1.236	1.03	1.03	73.41	1.130	37.18	5266.73
042	250	0	2	140	0.84	3.04	1.239	1.03	1.03	73.20	1.133	37.79	5359.29
042	250	0	2	142	0.85	3.06	1.242	1.03	1.03	72.99	1.136	38.40	5451.85
042	250	0	2	144	0.86	3.08	1.245	1.03	1.03	72.78	1.139	39.01	5544.41
042	250	0	2	146	0.87	3.10	1.248	1.03	1.03	72.57	1.142	39.62	5636.97
042	250	0	2	148	0.88	3.12	1.251	1.03	1.03	72.36	1.145	40.23	5729.53
042	250	0	2	150	0.89	3.14	1.254	1.03	1.03	72.15	1.148	40.84	5822.09
042	250	0	2	152	0.90	3.16	1.257	1.03	1.03	71.94	1.151	41.45	5914.65
042	250	0	2	154	0.91	3.18	1.260	1.03	1.03	71.73	1.154	42.06	6007.21
042	250	0	2	156	0.92	3.20	1.263	1.03	1.03	71.52	1.157	42.67	6099.77
042	250	0	2	158	0.93	3.22	1.266	1.03	1.03	71.31	1.160	43.28	6192.33
042	250	0	2	160	0.94	3.24	1.269	1.03	1.03	71.10	1.163	43.89	6284.89
042	250	0	2	162	0.95	3.26	1.272	1.03	1.03	70.89	1.166	44.50	6377.45
042	250	0	2	164	0.96	3.28	1.275	1.03	1.03	70.68	1.169	45.11	6470.01
042	250	0	2	166	0.97	3.30	1.278	1.03	1.03	70.47	1.172	45.72	6562.57
042	250	0	2	168	0.98	3.32	1.281	1.03	1.03	70.26	1.175	46.33	6655.13
042	250	0	2	170	0.99	3.34	1.284	1.03	1.03	70.05	1.178	46.94	6747.69
042	250	0	2	172	1.00	3.36	1.287	1.03	1.03	69.84	1.181	47.55	6840.25
042	250	0	2	174	1.01	3.38	1.290	1.03	1.03	69.63	1.184	48.16	6932.81
042	250	0	2	176	1.02	3.40	1.293	1.03	1.03	69.42	1.187	48.77	7025.37
042	250	0	2	178	1.03	3.42	1.296	1.03	1.03	69.21	1.190	49.38	7117.93
042	250	0	2	180	1.04	3.44	1.299	1.03	1.03	69.00	1.193	49.99	7210.49
042	250	0	2	182	1.05	3.46	1.302	1.03	1.03	68.79	1.196	50.60	7303.05
042	250	0	2	184	1.06	3.48	1.305	1.03	1.03	68.58	1.199	51.21	7395.61
042	250	0	2	186	1.07	3.50	1.308	1.03	1.03	68.37	1.202	51.82	7488.17
042	250	0	2	188	1.08	3.52	1.311	1.03	1.03	68.16	1.205	52.43	7580.73
042	250	0	2	190	1.09	3.54	1.314	1.03	1.03	67.95	1.208	53.04	7673.29
042	250	0	2	192	1.10	3.56	1.317	1.03	1.03	67.74	1.211	53.65	7765.85
042	250	0	2	194	1.11	3.58	1.320	1.03					

CLF#	CL#	AN.	T	H	L	UMAX	CLV	CLVA	CLVO	PHI	K	CMV	CDV
083	250	0	1.36	298	9.09	2055	33	33	33	85.83	8219	2.18	-10.71
083	250	0	1.32	298	8.63	3176	46	46	46	78.44	5476	1.94	2.55
083	250	0	1.32	299	8.78	4791	53	53	53	81.73	5718	2.04	2.97
083	250	0	1.60	239	11.84	2256	31	31	31	82.96	9330	1.93	-8.52
083	250	0	1.82	398	14.30	4415	54	54	54	68.34	9459	-31	-17.22
083	250	0	1.82	397	14.30	4415	71	71	71	68.34	9459	-31	-17.22
083	250	0	1.94	450	15.61	5306	83	83	83	63.61	7880	-56	-17.55
083	250	0	1.78	624	13.86	6760	230	230	230	57.93	6826	-33	-3.77
083	250	0	1.98	1185	16.05	2216	50	50	50	81.20	5842	1.69	-5.58
083	253	C	2.08	318	17.13	3965	102	102	102	73.39	7981	1.61	23.39
083	250	0	2.22	402	18.62	5224	375	375	375	55.19	6535	1.12	21.35
083	250	0	2.22	402	18.62	5224	47	47	47	75.84	9558	1.19	-20.31
083	250	0	2.36	273	20.09	3681	100	100	100	72.43	8157	2.52	18.05
083	253	C	2.34	379	19.88	5086	330	330	330	54.41	8657	5.2	28.21
083	253	C	2.64	407	22.99	5768	600	600	600	36.34	9263	5.37	43.22
083	253	15	1.32	299	8.63	1913	42	43	45	86.63	14715	2.06	-10.31
083	250	15	1.32	532	8.63	3403	49	51	53	83.63	8820	2.06	0.18
083	250	15	1.38	689	9.32	4918	85	87	88	83.44	8313	2.61	1.96
083	250	15	1.38	697	9.32	4979	40	41	43	95.38	8799	7.4	1.96
083	250	15	1.52	258	10.93	2245	47	48	50	90.84	10488	1.92	-11.71
083	250	15	1.78	374	13.86	4038	64	66	69	83.09	8895	2.00	1.56
083	250	15	1.92	467	15.40	5455	124	128	133	63.18	8443	-53	15.72
083	250	15	1.72	671	13.19	6989	173	179	186	58.79	7396	0.4	-4.23
083	250	15	1.90	1194	15.18	2249	37	39	40	89.44	8188	1.21	-23.45
083	250	15	2.06	333	16.91	4119	63	65	67	74.96	10796	1.25	10.76
083	250	15	2.18	423	18.19	5434	219	226	234	59.82	7475	-141	-6.54
083	250	15	2.24	506	19.83	6623	482	484	495	46.32	6073	4.32	33.42
083	250	15	2.22	506	19.83	6623	51	52	54	91.89	11597	1.46	-22.49
083	250	15	2.24	285	18.83	3730	104	108	112	64.56	10027	2.29	-3.2
083	250	15	2.40	373	20.51	5084	267	276	286	58.51	7236	-2.08	-1.66
083	250	15	2.44	430	21.96	5903	34	40	46	90.24	9263	1.22	13.81
083	250	30	1.38	301	9.32	2147	43	43	50	58.87	8703	10.27	-7.89
083	250	30	1.32	533	8.63	3407	38	44	51	93.64	8044	2.01	-8.28
083	250	30	1.46	688	10.24	4305	34	40	46	90.24	9263	1.22	8.0
083	250	30	1.64	237	12.29	2322	45	52	60	85.65	11173	1.91	-20.83
083	250	30	1.80	378	14.08	4146	40	47	54	86.81	9711	1.88	3.46
083	250	30	1.98	478	16.05	5737	100	115	133	65.14	8150	1.77	-9.95
083	250	30	1.76	658	13.64	7041	100	115	133	68.98	7325	1.07	1.64
083	250	30	1.98	1198	16.05	2371	29	33	38	83.46	11391	1.64	-20.69
083	250	30	2.24	1111	18.52	3348	163	189	218	61.38	7354	4.0	4.39
083	250	30	2.28	491	19.25	6489	340	393	454	51.82	6204	2.95	-30.49
083	250	30	2.26	1169	19.04	2150	48	55	66	72.30	7603	1.59	-16.65
083	250	30	2.42	1200	25	3504	64	74	85	68.28	8993	1.35	-8.01
083	250	30	2.42	367	20.72	5010	144	166	192	61.81	7882	-3.79	-35.16
083	250	30	2.68	401	23.40	5712	369	449	519	51.59	8160	2.22	50.09
083	250	45	1.46	290	9.78	3259	61	62	67	89.12	9794	1.2	11.18
083	250	45	1.34	523	8.86	3476	22	31	44	84.91	11405	1.12	9.29
083	250	45	1.50	620	10.70	5257	22	31	44	88.26	11948	1.26	9.46
083	250	45	1.70	236	12.97	2419	24	35	49	77.37	10925	1.89	13.50

083	250	45	1.89	359	14.96	4111	31	44	62	82.13	11363	1.97	14.87
083	250	45	2.00	469	16.26	5672	43	61	87	66.14	10431	-414	17.06
083	250	45	1.82	612	14.30	6787	28	40	56	80.74	9877	0.4	14.75
083	250	45	2.04	182	16.70	2239	27	38	53	78.01	11062	1.65	11.56
083	250	45	2.20	302	18.41	3912	44	62	88	77.72	11960	-31	9.23
083	250	45	2.26	403	19.04	5296	48	68	97	66.86	10269	-12	18.30
083	250	45	2.30	450	19.46	6108	119	168	238	58.58	8344	1.06	18.11
083	250	45	2.26	157	14.04	2063	18	25	35	88.75	29880	1.49	17.09
083	250	45	2.50	265	21.54	3667	46	65	92	81.44	11244	-0.2	22.10
083	250	45	2.44	353	20.92	4839	64	91	129	63.53	9474	-5.4	32.65
083	250	45	2.66	381	23.20	5423	77	180	254	58.71	7295	-1.85	52.49
083	250	60	1.52	270	10.93	2344	04	07	15	101.85	24655	2.30	36.45
083	250	60	1.36	512	9.09	3532	12	24	48	99.32	16900	2.24	19.00
083	250	60	1.46	624	10.94	5030	23	45	91	83.91	10309	2.23	15.06
083	250	60	1.82	225	14.30	2498	20	40	81	89.66	11892	2.25	26.61
083	250	60	1.86	355	14.74	4019	27	44	109	90.86	8545	1.84	16.33
083	250	60	1.86	355	14.74	4019	27	44	109	90.86	8545	1.84	16.33
083	250	60	1.82	620	14.30	6871	28	56	112	75.05	11231	1.26	19.39
083	250	60	2.08	185	17.13	2302	26	42	104	89.65	8784	2.21	25.25
083	250	60	1.98	489	16.05	5618	28	46	112	80.15	10444	2.25	24.90
083	250	60	2.24	413	18.83	5399	35	70	140	78.43	8930	1.27	31.06
083	250	60	2.34	464	19.88	6223	42	64	168	77.18	9949	-2.22	32.04
083	250	60	2.42	539	21.16	3929	58	91	162	64.04	8578	2.24	24.21
083	250	60	2.42	273	20.72	3723	29	57	114	84.59	7625	1.08	23.04
083	250	60	2.39	368	20.30	4976	26	51	103	76.41	10582	1.35	39.97
083	250	60	2.72	393	23.81	5636	48	96	192	62.30	8531	-9.2	33.05
083	250	75	1.38	420	12.06	2397	31	119	459	175.97	9578	2.51	62.90
083	250	75	1.34	505	9.32	3607	19	49	267	7.27	10243	2.44	27.20
083	250	75	1.42	607	10.78	3929	24	67	113	63.05	3337	2.47	24.97
083	250	75	1.98	212	14.96	2429	12	48	146	141.41	19036	2.59	53.38
083	250	75	1.92	342	15.40	3994	07	25	98	118.30	24758	2.15	39.91
083	250	75	1.64	614	14.52	6083	23	89	344	2.67	36.11	1.8	1.84
083	250	75	2.22	164	18.62	2180	12	46	177	127.96	18086	2.42	56.57
083	250	75	2.22	298	18.02	3878	26	100	385	84.56	8284	1.93	41.95
083	250	75	2.30	385	19.46	5114	10	40	155	84.90	10680	1.56	28.00
083	250	75	2.42	444	17.13	5529	24	91	343	90.19	10503	1.75	25.68
083	250	75	2.34	451	19.88	6065	32	123	475	85.57	9213	1.59	35.13
083	250	75	2.60	136	22.58	1909	17	67	258	177.74	14883	2.31	54.15
083	250	75	2.44	219	20.72	3189	11	43	166	139.68	10323	1.84	52.03
083	250	75	2.54	240	21.96	4745	26	101	390	70.84	7893	1.47	45.50
083	250	75	2.70	344	23.61	5638	22	64	324	85.39	8707	1.46	44.47

CLER	DIA	ANG	T	H	L	UMAX	CLV	CLVA	CLVU	PHI	K	CMV	CDV
*167	250	0	1.60	.236	11.84	*2245	.19	.19	.19	-82.35	-1.7103	1.92	-8.01
*167	250	0	1.442	.479	9.78	*3679	.20	.20	.20	62.35	-5598	2.01	.20
*167	250	0	1.46	.662	10.24	*5179	.23	.23	.23	-86.44	-0391	1.20	5.44
*167	250	0	1.448	.652	10.47	*5431	.28	.28	.28	65.47	*5340	.52	-1.09
*167	250	0	1.90	1.198	15.18	*2300	.21	.21	.21	-66.57	*0711	1.77	-5.37
*167	250	0	1.95	1.340	15.83	*4056	.37	.37	.37	75.32	*3371	.41	.16
*167	250	0	2.04	1.440	16.70	*5423	1.65	1.65	1.65	-47.25	*042	2.52	22.04
*167	250	0	1.78	1.624	13.86	*6790	.69	.69	.69	127.37	*5753	-1.2	10.92
*167	250	0	2.26	1.57	19.04	*2072	.17	.17	.17	32.24	*2362	1.41	-17.56
*167	250	0	2.24	.288	18.83	*3770	.18	.18	.18	70.36	*3781	.27	-.68
*167	250	0	2.442	.367	20.72	*5010	.61	.61	.61	70.36	*6616	.09	15.85
*167	250	0	2.28	.460	19.25	*5093	.28	.28	.28	71.70	*1825	-1.36	3.94
*167	250	0	2.74	1.22	24.01	*17.62	.63	.63	.63	-87.81	*-0840	1.24	-32.70
*167	250	0	2.66	.229	23.20	*3261	.21	.21	.21	64.45	*1016	-1.77	-4.01
*167	250	0	2.22	.390	18.62	*5079	.56	.56	.56	44.57	*8539	-1.70	1.17
*167	250	0	2.64	.397	22.99	*5635	3.02	3.02	3.02	49.20	*6195	-1.78	48.01
*167	250	30	1.56	.248	11.38	*22.2	.25	.29	.34	76.14	*-2500	2.06	-0.98
*167	250	30	1.38	.502	9.32	*3618	.37	.43	.49	-88.78	*0016	1.74	-2.76
*167	250	30	1.50	.619	10.70	*52.86	.24	.28	.32	80.90	*2850	.74	-.07
*167	250	30	1.54	.601	11.16	*5378	.23	.27	.31	69.04	*.683	.51	-2.67
*167	250	30	1.88	.207	14.96	*2377	.21	.24	.28	70.68	*-0064	1.87	-18.84
*167	250	30	1.96	.343	15.83	*4089	.18	.21	.25	72.47	*2044	.90	-5.59
*167	250	30	2.04	.431	16.70	*5306	.23	.26	.30	57.00	*2603	.81	-1.10
*167	250	30	2.02	.444	16.48	*5425	.50	.58	.67	-83.76	*5170	.83	-1.00
*167	250	30	2.02	.444	16.48	*5426	.70	.81	.94	-48.18	*3495	1.18	8.13
*167	250	30	1.86	.607	14.74	*6905	.82	.94	1.09	52.70	*3680	1.58	2.86
*167	250	30	2.26	.153	19.04	*2012	.29	.33	.38	87.22	*3498	1.62	-24.85
*167	250	30	2.16	.301	17.98	*3855	.19	.20	.23	-62.66	*-0164	.09	-3.68
*167	250	30	2.34	.393	19.88	*5274	.28	.32	.37	68.30	*7214	-1.12	-3.73
*167	250	30	2.26	.400	19.04	*5265	.43	.49	.57	65.00	*6101	.29	4.85
*167	250	30	2.32	.453	19.67	*6060	1.14	1.32	1.52	46.19	*6585	.13	-3.71
*167	250	30	2.58	1.135	22.37	*1897	.44	.55	.68	78.07	*-3773	1.33	-31.91
*167	250	30	2.56	.226	22.17	*3454	.18	.20	.24	77.55	*5149	-.0	-22.59
*167	250	30	2.40	.365	20.51	*4663	1.03	1.19	1.38	59.69	*6727	.22	3.28
*167	250	30	2.66	.387	23.20	*5509	.58	.67	.77	64.58	*7028	-1.45	-3.35
*167	250	60	1.50	.260	10.70	*2224	.26	.33	1.06	-15.51	-1.5137	2.58	43.52
*167	250	60	1.36	.502	9.09	*3498	.07	.14	.27	-38.84	*-36890	2.48	25.29
*167	250	60	1.52	.602	10.93	*5260	.19	.36	.72	97.59	*6513	2.11	16.13
*167	250	60	1.92	.213	14.30	*2375	.26	.25	1.03	-80.92	*-3378	2.62	39.23
*167	250	60	1.94	.359	15.61	*4235	.23	.46	.91	-78.43	*3170	1.72	22.63
*167	250	60	2.02	.452	16.48	*5520	.23	.46	.93	102.31	*6396	.86	20.15
*167	250	60	1.84	.606	14.52	*6818	.45	.90	1.79	75.85	*9407	.70	17.89
*167	250	60	2.14	.169	17.77	*2158	.43	.96	1.72	-80.09	*-6832	2.33	31.39
*167	250	60	2.22	.310	18.62	*4042	.07	.15	.30	-60.43	*-3055	1.45	29.25
*167	250	60	2.30	.374	19.46	*4980	.12	.24	.49	55.73	*9503	.14	32.39
*167	250	60	2.34	.455	19.88	*6114	.45	.91	1.81	90.78	*5667	-.56	25.15
*167	250	60	2.48	1.12	21.34	*1969	.54	1.09	2.18	-73.99	*-4836	2.02	28.11
*167	250	60	2.67	.248	22.58	*3502	.10	.19	.38	19.72	*-2964	1.06	37.89
*167	250	60	2.44	.357	20.92	*4957	.38	.76	1.52	80.23	*5674	.16	32.07
*167	250	60	2.64	.397	22.99	*5641	.24	.47	.75	67.34	*9112	-1.33	37.97

CLER	O14	ANG	T	H	L	JMAX	CLV	CLV4	CLVU	P41	K	CMV	COV		
*001	*333	0	2.00	1.78	16.91	*2200	5.25	5.25	5.25	8.60	*0780	4.24	290.19		
*001	*303	0	1.76	2.27	13.65	*2387	4.63	4.63	4.63	4.77	*1223	3.11	150.50		
*001	*333	0	1.40	2.70	10.24	*2172	4.82	4.82	4.82	5.20	*1560	2.96	102.64		
*001	*333	0	1.30	3.15	8.40	*1922	5.10	5.10	5.10	5.98	*2018	2.76	96.38		
*001	*333	0	2.28	2.89	19.25	*3811	4.59	4.59	4.59	-0.03	*0432	5.19	162.18		
*001	*333	0	2.06	3.38	16.91	*4172	4.35	4.35	4.35	-0.08	*0582	3.50	134.39		
*001	*333	0	1.76	3.79	13.64	*4048	4.70	4.70	4.70	2.73	*0308	3.43	103.24		
*001	*333	0	1.34	4.42	8.86	*3591	4.95	4.95	4.95	7.69	*1525	3.52	74.83		
*001	*333	0	2.24	3.96	18.83	*5269	5.03	5.03	5.03	-5.19	*1432	2.52	100.14		
*001	*333	0	2.22	3.95	18.62	*5130	4.62	4.62	4.62	-8.19	*0193	3.64	147.76		
*001	*333	0	2.04	4.28	16.70	*5244	5.66	5.66	5.66	.99	*0593	2.99	138.46		
*001	*333	0	1.40	4.68	9.55	*5026	4.75	4.75	4.75	4.90	*1040	2.57	62.54		
*001	*333	0	2.46	4.40	21.13	*6040	4.38	4.38	4.38	-6.25	*0023	3.66	202.4		
*001	*333	0	2.22	4.96	18.62	*6450	3.95	3.95	3.95	-6.73	*0013	3.28	106.40		
*001	*333	0	1.76	6.26	13.64	*6690	4.64	4.64	4.64	-3.82	*0234	3.68	105.38		
*001	*333	15	2.50	4.21	21.54	*5830	4.31	4.31	4.31	-3.43	*0083	3.56	168.25		
*001	*333	15	2.20	5.00	18.41	*6458	3.64	3.64	3.64	3.77	3.90	-1.17	65.92		
*001	*333	15	2.74	6.49	13.41	*6837	4.21	4.21	4.21	-1.49	*0590	1.19	67.83		
*001	*331	15	2.24	4.06	18.83	*5302	3.89	3.89	3.89	-6.23	*0449	1.55	78.48		
*001	*333	15	2.22	4.11	18.62	*5341	3.38	3.38	3.38	3.62	*0284	1.97	122.03		
*001	*333	15	1.42	6.66	9.78	*4905	4.27	4.27	4.27	3.37	*1417	1.79	50.89		
*001	*333	15	1.94	4.88	15.61	*5747	3.80	3.80	3.80	-4.07	-4.70	*0443	2.93	62.47	
*001	*333	15	2.24	2.96	18.83	*3866	4.39	4.39	4.39	4.55	4.71	2.90	127.44		
*001	*333	15	2.06	3.32	16.91	*4102	4.02	4.02	4.02	-1.67	*0872	1.48	89.44		
*001	*333	15	1.76	3.76	13.64	*4016	4.25	4.25	4.25	4.38	*1227	2.72	81.27		
*001	*333	15	1.30	5.37	8.40	*3279	4.74	4.74	4.74	.91	*508	8.68	151.3	72.54	
*001	*333	15	2.08	1.86	17.13	*2316	4.30	4.30	4.30	4.45	4.60	.62	*0899	2.74	164.88
*001	*333	15	1.82	2.19	14.30	*2421	4.26	4.26	4.26	4.41	4.57	7.90	*1513	2.45	148.20
*001	*333	15	1.50	2.64	10.70	*2236	4.46	4.46	4.46	4.61	4.78	9.78	*2071	2.01	111.32
*001	*333	15	1.34	3.13	8.86	*2074	4.53	4.53	4.53	4.69	4.85	7.97	*2437	2.42	94.66
*001	*333	30	2.05	1.92	16.91	*2369	3.51	3.51	3.51	4.05	4.68	6.19	*1254	4.47	-80.72
*001	*333	30	1.74	4.25	13.41	*3209	3.06	3.06	3.06	3.07	8.68	12.16	3.76	-45.14	
*001	*333	30	1.46	2.78	10.24	*2234	2.61	2.61	2.61	3.01	3.48	9.76	*1512	3.64	-18.45
*001	*333	30	1.32	3.09	8.83	*1995	2.55	2.55	2.55	3.40	8.18	*1992	3.44	27.67	
*001	*333	30	2.24	2.87	18.83	*3748	3.28	3.28	3.28	3.79	4.38	.77	*0468	5.01	-94.54
*001	*333	30	2.08	3.37	17.13	*4127	2.85	2.85	2.85	3.30	3.80	.31	*0661	4.41	-45.53
*001	*333	30	1.76	3.70	13.64	*3953	2.88	2.88	2.88	3.33	3.84	5.54	*0399	4.78	-44.82
*001	*333	30	1.30	4.56	8.40	*3270	3.09	3.09	3.09	3.56	4.11	3.03	*1091	1.14	28.43
*001	*333	30	2.30	3.91	19.46	*5181	3.09	3.09	3.09	3.57	4.12	-6.44	*0103	5.97	-83.10
*001	*333	30	2.16	4.24	17.98	*5413	2.98	2.98	2.98	3.44	3.97	-1.56	*0078	6.33	-36.62
*001	*333	30	1.96	4.40	15.83	*5701	2.94	2.94	2.94	3.97	5.82	6.27	4.42	3.34	
*001	*333	30	1.40	4.79	9.55	*4996	3.93	3.93	3.93	4.07	4.63	1.43	*0465	4.04	25.44
*001	*333	30	2.54	4.29	21.96	*5576	3.11	3.11	3.11	3.60	4.15	-1.75	*0081	4.07	-11.09
*001	*333	30	2.24	5.01	18.83	*6552	2.48	2.48	2.48	2.97	3.31	-1.49	*0313	1.91	-29.52
*001	*333	30	1.78	6.28	13.86	*6787	2.88	2.88	2.88	3.32	3.84	1.21	-0.121	4.58	21.57
*001	*333	45	2.56	3.77	22.17	*5272	1.92	1.92	1.92	2.71	3.24	-5.50	*0484	7.15	-15.77
*001	*333	45	2.24	4.40	18.83	*5752	1.55	1.55	1.55	2.75	3.89	1.65	*0161	6.15	-10.15
*001	*333	45	1.62	6.35	12.06	*5089	2.25	2.25	2.25	3.18	4.50	.18	*1299	5.08	14.93
*001	*333	45	2.38	3.58	20.30	*4936	1.67	1.67	1.67	2.36	3.34	3.05	*0936	5.53	6.36
*001	*333	45	2.22	4.07	18.62	*5296	1.77	1.77	1.77	2.50	3.54	5.60	*0302	6.04	26.16
*001	*333	45	1.98	4.48	16.05	*5368	2.56	2.56	2.56	3.42	5.12	1.97	*0736	4.81	-4.75
*001	*333	45	1.42	6.52	9.78	*4949	2.53	2.53	2.53	3.58	5.07	2.46	*1721	4.94	34.72
*001	*333	45	2.38	2.61	20.30	*3530	2.20	2.20	2.20	3.11	4.37	7.19	*0171	5.56	56.12
*001	*333	45	2.08	3.13	17.13	*3893	1.92	1.92	1.92	2.81	3.97	-2.20	*0231	4.77	41.50
*001	*333	45	1.87	3.57	14.30	*3922	1.94	1.94	1.94	2.74	3.87	.72	*0524	4.32	147.76
*001	*333	45	1.30	4.27	8.40	*3215	2.59	2.59	2.59	3.68	5.17	1.17	*1338	3.89	41.50
*001	*333	45	1.30	5.28	8.40	*3222	2.70	2.70	2.70	3.82	5.40	2.21	*1885	3.77	56.69
*001	*333	45	2.22	1.85	18.62	*2084	2.37	2.37	2.37	3.35	4.74	2.35	*0520	4.24	26.84
*001	*333	45	1.90	2.10	15.18	*2426	1.97	1.97	1.97	2.78	3.90	1.84	*0962	3.39	29.09
*001	*333	45	1.66	2.38	12.51	*2363	2.11	2.11	2.11	2.93	4.21	1.60	*1425	3.48	38.91
*001	*333	45	1.40	2.90	9.55	*2131	2.08	2.08	2.08	2.94	4.15	-4.42	*2663	3.35	62.94
*001	*333	60	7.46	1.44	21.13	*1993	5.6	5.6	5.6	1.13	2.25	34.40	-2.841	12.13	402.83
*001	*333	60	1.96	1.99	15.83	*2358	1.32	1.32	1.32	2.65	5.30	-35.48	*3175	10.32	608.09
*001	*333	60	1.84	2.11	14.52	*2398	2.27	2.27	2.27	3.06	4.36	4.77	*5332	9.88	632.61
*001	*333	60	1.50	2.56	10.70	*2133	5.70	5.70	5.70	11.40	22.81	157.63	5.814	64.46	815.07
*001	*333	60	2.58	2.42	22.37	*3389	.27	.27	.27	5.4	1.07	59.29	*3901	14.98	248.52
*001	*333	60	2.20	2.93	18.41	*3788	.77	.77	.77	1.33	3.06	128.72	*6384	12.81	312.29
*001	*333	60	1.50	3.60	10.70	*2133	5.70	5.70	5.70	11.40	22.81	157.63	5.814	64.46	815.07
*001	*333	60	1.40	5.05	9.55	*3719	3.53	3.53	3.53	7.06	14.12	167.59	*6824	5.56	374.75
*001	*333	60	2.46	3.50	21.13	*4808	.45	.45	.45	1.81	8.82	87.54	*8794	15.62	217.67
*001	*333	60	1.50	3.60	10.70	*2133	5.70	5.70	5.70	11.40	22.81	157.63	5.814	64.46	815.07
*001	*333	60	2.04	4.33	16.0	*5317	.53	.53	.53	1.06	2.2	133.09	*12685	12.49	480.64
*001	*333	60	1.50	6.13	10.70	*5185	2.02	2.02	2.02	4.03	8.07	158.38	*8878	7.45	278.81
*001	*333	60	2.66	3.81	23.40	*5424	.39	.39	.39	1.94	3.89	82.77	*6865	15.33	161.42
*001	*333	60	2.30	4.72	19.62	*6266	.39	.39	.39	1.94	3.89	82.77	*6865	15.33	161.42
*001	*333	60	1.86	6.00	14.74	*6790	.07	.07	.07	1.5	2.9	11.861	1.711	10.54	104.61

CLEP	DIA	ANG	T	H	L	UMAX	CLV	CLVA	CLVU	PHI	K	CMV	COV
001	33.3	0	2.48	4.20	21.34	3793	0.07	8.07	0.07	-0.69	2688	2.11	128.75
001	33.3	0	2.18	4.50	18.19	3740	6.54	6.64	6.64	-0.61	2880	5.38	231.47
001	33.3	0	1.52	4.90	10.93	3520	7.28	7.28	7.28	0.03	2920	7.28	309.05
005	33.3	0	2.34	3.65	19.88	4486	6.97	6.97	6.97	3.97	3359	2.44	178.33
005	33.3	0	2.13	3.94	18.19	5066	6.51	6.51	6.51	4.82	3424	3.60	217.86
005	33.3	0	1.52	4.50	15.20	3846	7.53	7.53	7.53	0.61	3461	6.62	308.91
005	33.3	0	1.42	4.57	9.78	4388	7.48	7.48	7.48	0.27	3856	3.64	84.64
005	33.3	0	2.24	3.02	18.83	3944	6.65	6.65	6.65	15.80	4057	2.90	240.03
005	33.3	0	2.04	3.27	16.74	4037	7.82	7.82	7.82	12.65	4384	2.24	180.34
005	33.3	0	1.68	3.96	12.74	3094	9.11	9.11	9.11	11.03	5112	4.09	145.11
005	33.3	0	1.30	4.54	8.40	3392	8.40	8.40	8.40	20.78	6291	2.95	79.30
005	33.3	0	2.04	1.76	16.70	2154	9.07	9.07	9.07	25.02	6332	3.19	367.27
005	33.3	0	1.64	4.24	12.51	2223	9.04	9.04	9.04	29.05	6311	2.83	197.78
005	33.3	0	1.34	2.82	9.32	2006	7.32	9.32	9.32	39.45	7297	2.14	136.60
005	33.3	0	1.26	1.26	7.94	1818	7.09	9.09	9.09	45.03	7450	2.52	115.27
005	33.3	15	2.02	1.78	18.44	2132	8.70	9.21	9.33	26.50	6717	3.50	180.97
005	33.3	15	1.88	2.11	12.74	2129	8.26	8.55	8.85	31.55	6570	2.20	243.65
005	33.3	15	1.40	2.72	9.55	2005	8.38	8.68	8.98	38.54	7258	2.56	180.01
005	33.3	15	1.28	3.00	8.17	1795	8.42	7.95	43.97	8129	2.96	84.88	
005	33.3	15	2.28	2.83	19.25	3741	6.97	7.21	7.47	9.59	4234	3.91	255.36
005	33.3	15	2.06	3.30	18.91	4072	6.20	6.42	6.64	13.34	4564	4.89	227.63
005	33.3	15	1.76	3.76	13.64	4015	6.67	6.91	7.15	19.29	5164	3.50	169.07
005	33.3	15	1.32	5.34	8.63	3402	8.04	8.33	8.62	26.30	6367	3.47	103.72
005	33.3	15	2.38	3.58	20.30	4836	3.98	6.19	6.41	12.43	3452	3.12	293.60
005	33.3	15	2.20	4.11	18.41	5313	5.17	5.35	5.54	7.48	3558	4.98	225.47
005	33.3	15	1.99	4.54	16.05	5441	6.99	6.31	6.53	11.02	3943	1.62	162.70
005	33.3	15	1.42	4.65	9.78	5047	6.93	7.18	7.43	18.87	5031	4.60	110.80
005	33.3	15	2.48	4.17	21.34	5701	6.18	6.40	6.62	4.52	2878	1.40	175.98
005	33.3	15	2.16	4.53	17.88	5744	5.85	6.08	6.31	14.26	3108	4.64	199.36
005	33.3	15	1.44	4.90	10.47	4695	6.76	7.00	7.25	14.71	4557	3.57	101.02
005	33.3	10	2.40	4.13	20.51	5800	4.41	5.10	5.89	6.97	3340	1.30	9.52
005	33.3	10	2.14	4.85	17.77	5650	5.96	6.08	7.94	12.03	3615	6.61	17.67
005	33.3	10	1.52	4.61	10.93	5731	4.82	5.56	6.43	16.69	4917	4.57	24.94
005	33.3	10	2.38	3.56	20.30	4784	5.18	5.49	6.91	15.44	3672	4.60	35.94
005	33.3	10	2.20	4.00	18.41	5174	4.83	5.57	6.48	8.16	3948	3.54	1.27
005	33.3	10	1.99	4.53	16.05	5430	5.25	6.06	7.00	13.08	3937	4.45	30.67
005	33.3	10	1.31	4.65	9.32	4738	5.63	6.50	7.51	21.39	5844	4.67	39.03
005	33.3	10	1.52	4.79	19.67	3723	5.39	6.23	7.19	11.06	4587	4.06	92.03
005	33.3	10	2.10	1.19	17.34	4004	5.42	6.49	7.49	18.65	6633	4.19	28.76
005	33.3	10	1.78	3.78	13.86	4087	5.61	6.48	7.48	22.42	5321	3.92	21.72
005	33.3	10	1.52	4.10	10.93	3386	6.20	7.16	8.12	3.60	6212	3.50	121.04
005	33.3	10	2.16	1.75	17.98	2238	6.35	7.33	8.47	23.81	5593	3.44	-14.31
005	33.3	10	1.82	2.14	14.30	2374	6.62	7.67	8.69	29.86	6171	3.77	-1.63
005	33.3	10	1.52	2.59	10.93	2281	6.57	7.56	8.56	39.51	7018	3.50	25.91
005	33.3	10	1.34	3.16	8.86	2094	6.62	7.64	8.62	45.33	7373	3.74	39.34
005	33.3	45	2.10	1.70	19.19	2188	4.53	6.41	9.06	30.52	5567	5.00	96.99
005	33.3	45	1.84	2.16	14.32	2414	3.91	5.3	7.82	36.60	6919	4.67	92.03
005	33.3	45	1.52	2.65	10.93	3255	3.45	4.88	6.90	35.57	8300	4.06	70.73
005	33.3	45	1.36	3.01	9.09	2067	4.36	6.17	8.72	45.22	7494	3.52	99.02
005	33.3	45	2.36	2.63	20.09	3542	3.71	5.25	7.42	19.38	4791	5.66	95.76
005	33.3	45	2.14	3.15	17.77	3696	3.60	5.09	7.20	17.15	5252	4.60	4.60
005	33.3	45	1.82	3.61	14.30	3909	3.79	5.37	7.59	21.92	5914	5.60	54.69
005	33.3	45	1.32	5.22	8.63	3327	4.45	6.29	8.90	29.16	6582	4.19	49.56
005	33.3	45	2.39	3.69	20.30	4986	2.96	4.18	5.91	13.46	4178	5.85	43.86
005	33.3	45	2.22	4.04	18.62	5266	3.23	4.57	6.46	14.77	4335	7.71	68.46
005	33.3	45	2.00	4.57	16.26	5523	3.45	4.88	6.90	10.13	4501	7.14	24.51
005	33.3	45	1.44	4.49	10.01	5074	3.85	5.45	7.70	24.28	6221	4.90	29.34
005	33.3	45	1.30	5.91	8.40	3386	6.20	7.16	8.12	3.60	6212	3.50	121.04
005	33.3	45	2.22	4.68	18.62	6087	3.20	4.52	6.40	13.77	4185	6.48	7.84
005	33.3	45	1.70	6.27	12.97	5423	3.84	5.44	7.69	13.26	4937	4.44	-0.85
005	33.3	60	2.60	3.91	22.58	5504	4.7	7.94	1.88	16.69	4519	3.52	134.25
005	33.3	60	2.40	4.60	14.83	6007	1.36	2.72	5.43	18.68	9948	15.04	139.15
005	33.3	60	1.74	5.83	13.41	6139	1.56	3.13	6.26	9.79	11334	10.33	149.87
005	33.3	60	2.39	3.60	20.30	4872	3.9	5.77	1.55	24.68	17748	12.15	198.33
005	33.3	60	2.00	3.99	18.41	5160	8.3	1.66	3.62	17.67	12300	13.02	183.88
005	33.3	60	2.00	4.32	16.26	5218	1.51	3.01	6.03	14.94	10495	11.64	197.73
005	33.3	60	1.46	6.03	10.24	4848	2.08	4.16	8.32	8.80	1121	6.87	183.48
005	33.3	60	2.40	4.61	20.51	3572	1.19	2.36	4.77	30.74	8502	11.86	34.35
005	33.3	60	2.14	3.06	10.77	3884	1.24	2.7	4.94	15.95	9291	11.87	271.88
005	33.3	60	1.88	3.53	14.96	4040	1.16	2.33	4.66	34.29	11719	9.52	282.78
005	33.3	60	1.36	4.90	8.86	3339	6.00	5.19	10.39	16.17	9249	4.9	23.11
005	33.3	60	2.34	1.55	19.88	2078	1.65	3.31	6.62	45.07	5355	10.95	511.42
005	33.3	60	1.92	2.05	15.40	2387	1.56	1.11	2.23	50.97	10309	8.54	574.10
005	33.3	60	1.72	2.24	13.19	2328	1.67	3.36	6.67	15.88	7820	6.84	66.93
005	33.3	60	1.42	2.83	9.78	2148	4.53	9.67	18.14	26.70	6412	4.17	515.19

CLER	DIA	4ND	T	H	L	UMAX	CLV	CLVA	CLVU	PHI	K	CMV	COV	
•010	•333	0	•2	•54	•417	21.96	•5810	6.72	6.72	6.26	•3885	3.36	259.56	
•010	•333	0	•2	•26	•473	19.04	•6211	7.29	7.29	9.44	•4203	•73	139.97	
•010	•333	0	•1	•78	•616	13.86	•6666	7.63	7.63	15.45	•4605	1.69	116.36	
•010	•333	0	•2	•0	•616	20.51	•4833	8.00	8.00	32.31	•4109	-1.84	178.33	
•010	•333	0	•2	•26	•401	19.04	•3267	7.47	7.47	14.50	•4612	•17	150.94	
•010	•333	0	•2	•00	•466	16.26	•5631	7.83	7.83	16.10	•4865	•42	133.50	
•010	•333	0	•1	•44	•642	10.01	•5024	8.17	8.17	32.31	•6192	2.52	81.57	
•010	•333	0	•2	•72	•282	18.62	•3668	8.41	8.41	21.59	•5708	•86	259.52	
•010	•333	0	•2	•04	•314	16.70	•3851	8.84	8.84	24.72	•5794	1.25	151.35	
•010	•333	0	•1	•68	•364	12.74	•3645	9.46	9.46	37.33	•6605	2.57	177.58	
•010	•333	0	•1	•30	•519	8.40	•3174	8.08	8.08	5.03	•5236	•79	98.34	
•010	•333	0	•2	•22	•167	18.62	•2175	8.68	8.68	39.98	•6723	1.70	281.45	
•010	•333	0	•1	•90	•207	15.18	•2396	8.27	8.27	42.77	•7511	2.70	182.13	
•010	•333	0	•1	•64	•240	12.29	•2345	8.00	8.00	50.15	•8073	2.31	162.35	
•010	•333	0	•1	•36	•297	9.09	•2045	7.34	7.34	56.35	•8928	2.71	105.90	
•010	•333	15	•2	•26	•160	19.04	•2099	8.71	9.02	9.34	41.67	•7047	3.38	167.46
•010	•333	15	•1	•42	•204	15.80	•2176	7.56	7.83	8.11	46.78	•7755	•84	214.90
•010	•333	15	•1	•72	•223	13.19	•2319	7.63	7.90	8.17	46.45	•6165	2.65	176.05
•010	•333	15	•1	•42	•274	9.78	•2081	7.26	7.41	7.78	55.40	•8761	2.85	132.12
•010	•333	15	•2	•16	•262	21.13	•3597	8.63	8.93	9.25	22.97	•5452	•95	145.30
•010	•333	15	•2	•16	•305	17.58	•3891	8.28	8.58	8.88	27.81	•5733	1.46	197.17
•010	•333	15	•1	•94	•353	1.61	•4157	7.48	7.75	8.02	29.47	•6065	3.88	164.19
•010	•333	15	•1	•38	•515	9.32	•3670	7.48	7.74	8.01	44.99	•7436	•35	249.48
•010	•333	15	•2	•46	•366	11.13	•5025	6.62	6.85	7.09	17.97	•4736	•35	242.18
•010	•333	15	•2	•26	•412	19.04	•5415	6.62	6.85	7.09	17.55	•4787	•98	132.51
•010	•333	15	•2	•60	•449	16.26	•5423	8.26	8.55	8.66	15.09	•5037	1.78	112.94
•010	•333	15	•1	•46	•57	10.24	•5283	7.41	7.67	7.94	29.01	•6038	•41	189.58
•010	•333	15	•2	•56	•411	22.17	•5753	6.45	6.68	6.92	7.04	•4072	2.34	216.17
•010	•333	15	•2	•20	•469	18.41	•6058	6.46	6.69	6.92	11.66	•4561	•53	164.36
•010	•333	15	•1	•46	•688	10.24	•5531	5.57	5.83	7.42	35.49	•6510	•40	40.48
•010	•333	30	•2	•38	•389	20.30	•5263	6.28	7.26	4.39	21.37	•4757	4.29	45.54
•010	•333	30	•2	•12	•455	17.95	•5737	6.48	7.48	8.63	21.75	•4951	4.07	32.63
•010	•333	30	•1	•96	•455	9.32	•5403	6.11	7.06	8.15	24.30	•5942	3.52	93.79
•010	•333	30	•2	•40	•353	20.51	•4789	6.17	7.12	9.23	25.97	•5030	4.77	135.64
•010	•333	30	•2	•24	•392	18.83	•5126	5.26	6.08	7.02	23.79	•5389	5.30	101.61
•010	•333	30	•1	•96	•455	9.32	•5403	6.11	7.06	8.15	24.30	•5942	3.52	93.79
•010	•333	30	•1	•42	•653	9.78	•4955	5.48	6.33	7.31	42.74	•6445	4.91	66.18
•010	•333	30	•2	•44	•260	20.92	•3553	6.10	7.04	8.13	28.27	•5785	3.76	67.79
•010	•333	30	•2	•12	•300	17.55	•3767	7.46	8.61	9.94	30.18	•5942	4.39	71.54
•010	•333	30	•1	•88	•350	16.36	•4009	6.38	7.32	8.46	34.44	•6409	2.91	33.26
•010	•333	30	•1	•32	•513	8.63	•3268	6.07	7.01	8.09	53.07	•8079	4.75	54.56
•010	•333	30	•2	•30	•150	19.46	•1995	7.12	8.22	9.49	42.47	•7331	2.48	12.27
•010	•333	30	•1	•92	•198	10.40	•2309	6.70	7.74	8.94	50.12	•7855	3.10	5.18
•010	•333	30	•1	•74	•215	13.41	•2265	6.67	7.70	8.89	43.88	•7767	3.78	36.24
•010	•333	30	•1	•48	•285	10.47	•2349	6.36	7.34	8.48	55.65	•8369	3.68	35.79
•010	•333	45	•2	•36	•150	20.09	•2016	4.31	6.10	8.63	46.41	•7325	5.19	93.26
•010	•333	45	•1	•96	•195	15.83	•2310	4.43	6.26	8.86	58.44	•7846	4.79	104.05
•010	•333	45	•1	•76	•209	13.64	•2234	5.12	7.24	10.23	53.51	•7970	4.39	132.21
•010	•333	45	•1	•49	•264	10.47	•2183	2.97	4.19	5.93	58.89	•9974	4.08	112.25
•010	•333	45	•2	•52	•253	21.75	•3518	6.00	7.22	8.39	28.59	•4402	4.43	106.03
•010	•333	45	•2	•18	•293	18.19	•3766	4.44	6.28	8.89	35.79	•6595	5.58	109.91
•010	•333	45	•1	•94	•348	15.61	•4098	4.10	5.79	8.19	40.89	•7005	5.13	88.39
•010	•333	45	•1	•36	•503	9.32	•3582	3.26	4.62	6.53	53.66	•8753	3.36	72.04
•010	•333	45	•2	•44	•350	20.32	•4795	4.63	6.54	9.25	23.12	•5446	6.59	2.08
•010	•333	45	•2	•30	•376	19.46	•4993	4.41	6.24	8.82	22.12	•5690	7.28	18.19
•010	•333	45	•2	•02	•427	16.48	•5197	4.66	6.59	9.32	26.94	•6039	6.12	55.38
•010	•333	45	•1	•80	•607	10.70	•5136	3.88	5.49	7.76	36.35	•7508	6.91	44.33
•010	•333	45	•2	•64	•389	22.59	•5511	3.22	4.55	6.43	22.23	•5102	4.59	132.95
•010	•333	45	•2	•30	•461	19.46	•6122	3.89	5.21	7.79	19.56	•5329	1.75	1.23
•010	•333	60	•1	•84	•592	14.52	•6635	3.60	5.09	7.20	26.05	•5973	4.75	9.00
•010	•333	60	•2	•60	•402	22.58	•5714	1.13	2.25	4.50	38.00	•10606	12.19	131.34
•010	•333	60	•2	•32	•434	19.67	•5793	2.20	4.40	8.80	31.74	•9196	11.77	57.74
•010	•333	60	•1	•82	•614	14.30	•6807	1.45	2.91	5.82	44.08	•11289	8.60	90.00
•010	•333	60	•2	•22	•359	18.62	•4668	1.39	2.77	5.55	40.17	•11150	11.36	155.33
•010	•333	60	•2	•14	•378	17.77	•4903	1.84	3.68	7.36	35.24	•11389	9.49	149.77
•010	•333	60	•1	•92	•247	15.40	•4983	1.55	3.10	6.19	46.03	•12150	8.59	146.81
•010	•333	60	•1	•34	•339	8.86	•4232	1.37	2.74	5.47	44.67	•15428	4.32	131.45
•010	•333	60	•2	•44	•263	20.92	•3602	1.56	3.12	6.24	52.72	•9912	10.02	240.63
•010	•333	60	•2	•46	•311	18.13	•3930	1.23	2.53	4.91	47.39	•11954	9.39	229.57
•010	•333	60	•1	•90	•486	15.19	•4021	1.43	3.66	6.12	51.21	•11304	8.56	208.96
•010	•333	60	•1	•34	•514	4.86	•3406	1.59	3.18	6.36	43.23	•12631	4.05	181.50
•010	•333	60	•2	•36	•117	20.30	•1165	2.21	4.51	8.84	42.06	•15844	8.84	386.74
•010	•333	60	•1	•96	•198	15.83	•2356	1.09	2.98	5.97	61.92	•9715	7.38	431.20
•010	•333	60	•1	•40	•216	14.08	•2364	1.07	2.14	4.28	79.32	•12538	6.09	495.05
•010	•333	60	•1	•44	•264	10.47	•2180	1.68	1.37	2.74	19.37	•14552	4.45	445.38

CLER	O14	ANG	T	H	L	UM4X	CLV	CLV4	CLVJ	PHI	K	CMV	COV
016	333	0	2.40	4.20	20.51	5705	8.05	8.05	8.05	20.16	+582	4.23	266.71
016	333	0	2.18	4.68	18.19	6268	7.42	7.42	7.42	18.41	4826	4.11	184.47
016	333	0	1.56	6.00	11.38	6255	5.13	8.13	8.13	29.99	5949	3.20	72.38
016	333	0	2.32	3.74	19.67	4984	8.20	8.20	8.20	20.66	5114	4.68	253.00
016	333	0	2.16	4.18	17.98	5137	8.18	8.18	8.18	28.15	5104	2.71	85.63
016	333	0	1.90	4.69	15.18	5418	9.19	9.19	9.19	25.79	4443	2.65	109.05
016	333	0	1.36	6.79	5.09	4673	7.73	7.73	7.73	46.46	7329	2.93	70.56
016	333	0	2.22	3.92	18.02	3794	8.97	8.97	8.97	11.24	5115	2.89	159.03
016	333	0	1.99	3.35	16.05	4017	8.66	8.66	8.66	39.19	6512	-63	103.45
016	333	0	1.52	4.66	10.93	4039	7.17	7.17	7.17	51.89	7601	1.86	59.51
016	333	0	1.12	5.68	8.53	3619	6.40	6.40	6.40	77.77	8248	3.07	18.60
016	333	0	1.76	2.22	13.64	2370	6.20	6.20	6.20	61.64	8789	2.53	92.74
016	333	0	2.08	1.76	17.13	2185	3.53	9.53	9.53	49.45	7891	3.45	146.90
016	333	0	1.50	2.59	10.70	2193	5.05	5.45	5.65	70.02	9361	2.52	65.43
016	333	0	1.28	3.43	8.17	7004	5.39	5.39	5.39	72.67	9721	2.85	56.71
016	333	15	2.16	1.66	17.98	2118	7.42	7.68	7.95	50.82	8169	4.10	94.44
016	333	15	1.86	2.06	14.74	2328	6.53	7.76	7.03	57.21	8614	2.60	53.15
016	333	15	1.88	2.42	11.61	2235	6.21	5.40	5.50	65.95	9407	2.69	41.56
016	333	15	1.36	3.16	9.09	2175	4.67	4.84	5.01	75.69	10026	3.01	57.63
016	333	15	2.30	2.77	19.88	3714	7.84	8.11	8.40	34.57	6075	2.71	185.09
016	333	15	2.09	3.36	17.13	4177	6.94	7.18	7.43	33.94	6321	4.25	149.25
016	333	15	1.82	3.79	14.30	4201	7.00	7.24	7.50	43.93	6834	2.61	67.80
016	333	15	1.32	5.44	8.63	3866	6.11	6.33	6.55	58.49	8490	3.25	42.25
016	333	15	2.40	3.65	20.51	4959	6.66	6.90	7.14	23.85	5398	3.20	220.16
016	333	15	2.19	4.11	18.19	6284	8.08	9.36	9.66	27.52	5226	1.05	60.94
016	333	15	1.96	4.75	15.83	5842	6.87	7.11	7.37	29.40	5781	1.30	100.46
016	333	15	1.40	6.72	9.55	4949	6.71	6.95	7.19	47.07	7321	3.25	54.87
016	333	15	2.56	4.32	22.37	6057	6.79	7.02	7.27	11.73	4334	.02	176.04
016	333	15	2.20	5.05	18.41	6524	6.12	6.34	6.56	17.43	4925	2.06	139.63
016	333	15	1.68	4.45	12.51	2409	7.75	8.02	8.30	27.27	5778	1.24	48.64
016	333	30	2.56	4.12	22.17	5767	5.85	6.75	7.79	18.48	4418	.77	110.39
016	333	30	2.12	5.01	17.55	3318	5.59	6.46	7.46	22.32	5430	3.16	65.87
016	333	30	1.48	7.23	10.47	4971	5.27	6.09	7.03	45.03	8889	3.30	55.10
016	333	30	2.34	3.91	19.68	5239	5.85	6.75	7.80	23.05	5487	1.36	74.70
016	333	30	2.18	4.30	18.19	5522	5.58	6.45	7.44	25.07	5558	5.50	105.07
016	333	30	1.96	4.78	15.83	5688	5.16	7.04	8.13	35.42	5825	2.42	76.50
016	333	30	1.42	6.70	8.78	5089	5.30	6.11	7.06	51.06	7463	3.98	35.74
016	333	30	2.28	2.90	19.25	3823	6.14	7.09	8.19	36.43	6465	4.54	91.87
016	333	30	2.09	3.36	17.13	4178	5.30	6.12	7.07	39.71	7051	1.35	15.22
016	333	30	1.82	3.93	13.64	4197	5.33	6.15	7.11	46.65	7690	2.68	101.18
016	333	30	1.30	5.52	8.40	3375	5.42	6.26	7.23	62.78	8384	3.27	34.66
016	333	30	2.12	1.76	17.55	2216	5.71	6.59	7.61	53.66	8242	2.89	-32.57
016	333	30	1.82	2.17	14.30	2401	5.00	5.77	6.66	62.70	8777	2.82	-11.36
016	333	30	1.50	2.73	10.70	2312	4.03	4.85	5.37	73.59	9501	3.00	8.53
016	333	30	1.36	3.21	9.09	2207	4.36	5.04	5.82	76.35	9691	2.77	16.93
016	333	45	2.40	2.11	20.51	2869	3.92	5.85	7.84	50.89	7825	4.16	56.70
016	333	45	2.02	2.68	16.44	3267	3.98	5.83	7.96	51.40	8504	3.42	61.29
016	333	45	1.90	2.89	15.16	3341	3.12	4.41	6.24	60.02	9152	2.83	11.80
016	333	45	1.58	3.48	11.61	3214	2.78	3.93	5.55	65.87	9241	3.15	36.44
016	333	45	2.40	2.74	20.51	3725	4.10	5.80	8.20	44.62	7163	3.08	85.44
015	333	45	2.12	3.17	17.55	4005	4.38	6.20	8.77	44.25	7246	3.75	104.84
016	333	45	1.88	3.66	14.96	4184	3.38	4.78	6.77	52.34	7775	5.11	36.36
016	333	45	1.34	5.32	8.86	3531	2.65	3.75	5.31	69.66	8550	3.66	36.97
016	333	45	2.38	3.67	20.30	4958	4.13	5.85	8.27	35.09	6265	2.62	111.73
016	333	45	2.18	4.04	16.19	5196	4.27	6.05	8.55	33.37	6515	2.37	136.77
016	333	45	1.94	4.65	15.61	5481	4.13	5.84	8.26	42.17	6835	2.31	71.46
016	333	45	1.76	3.93	13.64	4197	5.33	6.15	7.11	46.65	7690	2.68	101.18
016	333	45	2.60	4.10	22.58	5777	3.69	5.22	7.18	26.84	5605	1.88	175.26
016	333	45	2.32	4.47	19.67	5966	5.47	7.73	10.93	23.08	5844	3.26	165.95
016	333	45	1.78	6.48	13.66	47014	3.65	5.17	7.31	39.98	6689	2.88	41.46
016	333	60	2.54	4.37	21.96	6089	1.85	3.70	7.39	45.19	9210	7.30	185.93
016	333	60	2.24	4.75	18.83	6204	2.87	5.75	11.50	47.19	8535	7.75	154.86
016	333	60	1.78	6.44	13.66	6971	1.85	3.69	7.38	58.37	11104	4.09	108.46
016	333	60	2.32	3.92	19.67	5222	1.78	3.55	7.10	52.84	10024	6.71	140.67
016	333	60	2.22	4.15	18.62	5401	2.24	4.49	8.97	54.20	8729	6.57	144.90
016	333	60	2.00	4.73	16.28	5720	2.25	4.50	9.00	51.59	9207	5.98	122.24
016	333	60	1.42	6.78	9.78	5148	1.29	2.98	5.16	67.16	13868	4.55	101.13
016	333	60	2.40	2.81	20.51	3821	2.01	4.02	8.04	64.51	9404	7.02	144.71
016	333	60	2.08	3.29	17.13	4102	2.30	4.60	9.20	66.18	9339	6.73	194.79
016	333	60	1.48	5.57	10.01	5136	3.48	4.92	9.00	75.00	10722	5.15	105.22
016	333	60	1.32	5.48	8.63	3492	3.94	1.89	3.78	67.29	16041	3.42	125.37
016	333	60	2.24	1.68	18.83	2197	1.85	3.71	7.41	83.61	10053	7.81	275.62
016	333	60	1.45	6.38	14.96	4184	3.38	4.78	6.77	52.34	7775	5.11	36.36
016	333	60	1.60	2.43	11.84	2289	1.40	2.79	5.59	119.43	11802	4.72	365.00
016	333	60	1.36	3.10	9.09	2132	6.6	1.23	2.66	6.65	129023	3.23	70.53

CLEF	CLV	ANG	T	H	L	UMAX	CLV	CLVA	CLVU	QHI	K	CMV	COV
.021	.333	0	2.00	1.78	16.41	2107	5.08	6.04	6.08	6.29	.9534	3.17	141.96
.021	.333	0	1.75	1.64	15.41	2107	4.72	5.67	5.71	5.92	.9534	3.17	141.96
.021	.333	0	1.32	3.02	8.63	1926	4.10	4.10	4.10	4.10	.9534	3.17	141.96
.021	.333	0	1.24	3.23	7.72	1717	3.19	3.19	3.19	3.19	.9407	3.20	83.85
.021	.333	0	1.24	3.23	7.72	3632	8.99	8.92	8.92	8.92	.9407	3.20	83.85
.021	.333	0	2.06	3.13	10.91	3874	8.12	8.12	8.12	8.12	.9407	3.20	83.85
.021	.333	0	1.77	3.72	12.97	3810	7.91	7.91	7.91	7.91	.9407	3.20	83.85
.021	.333	0	1.32	5.15	8.63	3287	4.96	4.96	4.96	4.96	.9407	3.20	83.85
.021	.333	0	1.12	3.63	10.04	4326	9.67	9.67	9.67	9.67	.9407	3.20	83.85
.021	.333	0	2.30	3.57	19.46	4744	9.58	9.58	9.58	9.58	.9407	3.20	83.85
.021	.333	0	2.12	3.69	17.55	4504	10.23	10.23	10.23	10.23	.9407	3.20	83.85
.021	.333	0	2.16	3.84	17.77	4876	10.47	10.47	10.47	10.47	.9407	3.20	83.85
.021	.333	0	1.92	4.33	15.40	5024	10.50	10.50	10.50	10.50	.9407	3.20	83.85
.021	.333	0	2.16	3.91	17.99	4992	10.11	10.11	10.11	10.11	.9407	3.20	83.85
.021	.333	0	2.14	3.91	17.77	4565	9.65	9.65	9.65	9.65	.9407	3.20	83.85
.021	.333	0	1.38	6.43	7.22	4586	6.93	6.93	6.93	6.93	.9407	3.20	83.85
.021	.333	0	2.46	3.93	21.13	6239	8.39	8.39	8.39	8.39	.9407	3.20	83.85
.021	.333	15	2.12	4.65	17.55	5865	9.33	9.33	9.33	9.33	.9407	3.20	83.85
.021	.333	0	1.42	6.96	9.78	5216	8.16	8.16	8.16	8.16	.9407	3.20	83.85
.021	.333	15	2.40	3.91	20.51	5309	8.46	8.46	8.46	8.46	.9407	3.20	83.85
.021	.333	15	2.12	4.62	17.55	5830	8.55	8.55	8.55	8.55	.9407	3.20	83.85
.021	.333	15	1.82	7.17	9.73	5839	6.84	6.84	6.84	6.84	.9407	3.20	83.85
.021	.333	15	2.20	3.51	19.04	5138	7.65	7.65	7.65	7.65	.9407	3.20	83.85
.021	.333	15	2.12	4.62	17.55	5386	7.93	8.21	8.50	9.07	.9407	3.20	83.85
.021	.333	15	1.89	4.78	18.96	5971	7.41	7.57	7.95	8.40	.9407	3.20	83.85
.021	.333	15	1.36	6.61	9.09	4550	5.59	5.79	5.99	6.02	.9407	3.20	83.85
.021	.333	15	2.22	2.96	13.62	3854	7.39	7.65	7.92	8.45	.9407	3.20	83.85
.021	.333	15	2.04	3.16	16.70	3878	8.94	9.26	9.58	9.90	.9407	3.20	83.85
.021	.333	15	1.66	4.02	12.51	3989	6.19	6.41	6.64	6.64	.9407	3.20	83.85
.021	.333	15	1.30	5.39	8.40	3297	4.11	4.25	4.40	4.52	.9407	3.20	83.85
.021	.333	15	2.22	1.67	18.62	2173	5.23	5.42	5.61	6.01	.9407	3.20	83.85
.021	.333	15	1.78	2.19	18.61	2366	3.77	4.42	4.74	5.07	.9407	3.20	83.85
.021	.333	15	1.36	3.01	9.09	2072	3.24	3.35	3.47	3.81	.9407	3.20	83.85
.021	.333	15	1.24	3.34	7.72	1827	2.96	3.06	3.17	3.59	.9407	3.20	83.85
.021	.333	30	2.18	1.72	18.33	2210	4.31	4.97	5.74	6.25	.9407	3.20	83.85
.021	.333	30	1.84	2.16	14.52	2416	3.54	4.09	4.73	5.17	.9407	3.20	83.85
.021	.333	30	1.84	2.87	10.01	2247	2.77	3.20	3.70	4.17	.9407	3.20	83.85
.021	.333	30	1.28	3.21	8.17	1877	2.81	3.25	3.75	4.18	.9407	3.20	83.85
.021	.333	30	2.32	2.78	19.07	3701	7.18	8.29	9.57	10.63	.9407	3.20	83.85
.021	.333	30	2.08	3.25	17.13	4047	5.50	6.35	7.33	8.52	.9407	3.20	83.85
.021	.333	30	1.76	3.78	13.64	4042	4.64	5.16	5.68	6.18	.9407	3.20	83.85
.021	.333	30	1.32	5.28	8.63	3365	3.51	4.05	4.68	5.09	.9407	3.20	83.85
.021	.333	30	2.28	3.92	19.25	5173	6.42	7.41	8.56	9.63	.9407	3.20	83.85
.021	.333	45	1.96	4.86	15.83	5777	3.79	5.36	7.58	8.78	.9407	3.20	83.85
.021	.333	0	1.96	4.76	15.83	5659	5.78	6.67	7.71	8.85	.9407	3.20	83.85
.021	.333	30	1.40	6.66	9.55	4905	4.50	5.20	6.00	6.24	.9407	3.20	83.85
.021	.333	30	2.56	4.19	22.17	5864	6.73	7.77	8.97	10.08	.9407	3.20	83.85
.021	.333	30	2.44	4.72	25.04	1748	2.88	4.07	5.76	6.94	.9407	3.20	83.85
.021	.333	30	1.76	6.42	13.64	5861	6.13	7.08	8.17	9.38	.9407	3.20	83.85
.021	.333	45	2.58	4.21	22.37	5924	4.21	5.96	8.43	10.97	.9407	3.20	83.85
.021	.333	45	2.18	4.60	18.19	6427	4.07	5.75	8.16	10.34	.9407	3.20	83.85

.021	.333	45	1.68	6.55	12.74	6614	3.51	4.57	7.03	51.87	7.724	3.70	35.30
.021	.333	45	2.34	3.81	19.88	5101	3.74	5.29	7.48	41.74	6.843	3.50	102.42
.021	.333	45	2.30	3.98	18.41	5148	4.29	6.06	8.57	48.59	6.682	4.27	119.43
.021	.333	45	1.96	4.86	15.83	5777	3.79	5.36	7.58	48.78	6.936	3.47	57.24
.021	.333	45	1.44	4.44	10.01	5041	2.55	3.60	5.09	60.09	6.663	4.02	24.38
.021	.333	45	2.32	2.82	19.67	3762	3.67	5.20	7.35	52.11	7.532	2.15	65.27
.021	.333	45	2.10	3.17	17.34	3969	3.84	5.01	7.08	53.37	7.857	3.42	26.34
.021	.333	45	1.82	3.73	14.30	4139	2.85	4.02	5.69	63.45	6.856	3.33	33.37
.021	.333	45	1.32	5.40	8.63	3443	1.82	2.57	3.64	83.48	6.986	3.16	23.81
.021	.333	45	2.14	1.62	17.77	2054	3.03	4.28	6.05	72.28	6.913	3.46	40.88
.021	.333	45	2.84	1.20	25.04	1748	2.88	4.07	5.76	69.74	6.9207	2.98	29.91
.021	.333	45	1.64	6.16	12.29	2307	1.78	2.51	3.56	83.26	1.0451	3.09	29.73
.021	.333	45	1.30	3.19	8.40	1950	1.08	1.53	2.16	92.92	1.1463	2.85	47.97
.021	.333	60	2.40	1.45	20.51	1973	1.51	3.02	6.05	83.44	6.817	6.84	203.53
.021	.333	60	1.96	1.91	15.83	2274	1.58	3.17	6.34	102.57	1.0182	8.75	279.97
.021	.333	60	1.56	2.45	11.38	2224	1.05	2.10	4.20	144.94	1.0595	4.21	279.47
.021	.333	60	1.32	3.04	8.63	3338	94	1.49	3.77	174.94	1.1121	3.03	203.68
.021	.333	60	2.52	2.57	21.75	3569	1.79	3.57	7.15	69.33	6.930	8.63	99.60
.021	.333	60	2.14	3.26	17.77	4146	1.24	2.49	4.97	81.21	1.0812	6.88	121.87
.021	.333	60	1.90	3.52	15.18	4141	1.41	2.83	5.66	82.09	1.2639	6.64	133.71
.021	.333	60	1.36	5.17	9.09	3560	2.6	3.52	1.04	107.91	4.1993	3.92	107.60
.021	.333	60	2.42	3.63	20.72	4944	2.34	4.67	9.35	63.51	6.8546	8.36	72.41
.021	.333	60	2.24	3.88	18.83	5071	2.40	4.59	9.97	63.35	6.8716	8.13	85.58
.021	.333	60	1.82	4.49	16.70	5515	1.66	3.32	6.64	68.04	1.0260	7.15	70.46
.021	.333	60	1.52	5.94	10.93	5152	1.87	1.73	3.47	76.48	1.5463	5.13	65.51
.021	.333	60	2.66	1.96	23.20	5626	2.65	5.30	10.61	54.83	7.534	7.49	62.04
.021	.333	60	2.24	4.68	16.83	4120	2.31	4.63	9.26	52.18	6.837	3.70	54.37
.021	.333	60	1.74	5.84	13.41	6162	1.64	3.28	6.56	65.50	1.1103	5.77	63.48



CLER	DI4	ANG	T	H	L	U4X	CLV	CLV4	CLVU	PH1	K	CMV	CDV	
*042	*333	0	2.44	2.49	21.34	*5723	3.20	3.20	3.20	3.20	*5654	6.50	60.66	
*042	*333	0	2.42	2.49	17.55	*6236	6.64	6.64	6.64	6.64	*6149	3.97	119.84	
*042	*333	0	1.48	1.71	10.47	*5541	3.41	3.41	3.41	3.41	*7594	2.77	82.30	
*042	*333	0	2.36	2.36	20.05	*4930	6.42	6.42	6.42	6.42	*44.71	*6593	5.25	106.65
*042	*333	0	1.42	1.42	18.19	*5351	6.98	6.98	6.98	6.98	50.36	*6529	2.45	17.56
*042	*333	0	1.94	1.94	15.61	*5648	5.60	5.60	5.60	5.60	55.97	*6184	3.3	39.84
*042	*333	0	1.38	1.69	9.32	*4972	2.20	2.20	2.20	2.20	71.83	*8959	2.33	23.06
*042	*333	0	1.02	1.34	18.19	*3993	1.99	1.99	1.99	1.99	60.87	*8065	3.03	90.61
*042	*333	0	1.02	1.34	18.19	*3993	1.99	1.99	1.99	1.99	60.87	*8065	2.65	47.34
*042	*333	0	1.50	1.50	10.70	*1909	2.22	2.22	2.22	2.22	78.26	*8251	2.65	31.09
*042	*333	0	1.29	1.59	8.17	*3278	1.75	1.75	1.75	1.75	82.30	*9705	2.85	23.57
*042	*333	0	1.62	1.62	19.00	*2294	2.21	2.21	2.21	2.21	80.81	*10635	1.80	59.59
*042	*333	0	1.74	2.31	13.41	*2439	1.38	1.38	1.38	1.38	90.11	*1036	3.03	31.72
*042	*333	0	1.30	1.32	8.40	*1979	1.42	1.42	1.42	1.42	85.93	*8601	2.64	35.98
*042	*333	0	1.20	1.20	16.26	*4168	3.90	3.90	3.90	3.90	84.32	*7631	2.53	33.30
*042	*333	15	2.04	1.91	16.70	*2341	1.73	1.73	1.73	1.73	70.53	*11942	2.74	54.02
*042	*333	15	1.60	2.47	11.64	*2329	1.42	1.42	1.42	1.42	88.60	*12130	2.77	40.51
*042	*333	15	2.00	2.32	16.26	*4011	4.22	4.22	4.22	4.22	85.99	*10102	2.76	35.63
*042	*333	15	1.22	1.35	7.49	*1757	1.12	1.12	1.12	1.12	87.97	*11828	2.70	41.72
*042	*333	15	2.24	3.02	18.83	*3952	3.46	3.46	3.46	3.46	65.27	*7984	3.60	52.16
*042	*333	15	1.62	1.41	12.69	*4168	2.22	2.22	2.22	2.22	64.26	*8215	1.83	43.28
*042	*333	15	1.28	1.58	8.17	*3272	1.53	1.53	1.53	1.53	80.54	*9525	3.06	32.78
*042	*333	15	2.30	3.37	19.46	*5143	6.08	6.08	6.08	6.08	45.91	*6607	4.00	112.23
*042	*333	15	2.14	1.41	17.77	*2665	6.99	7.24	7.50	49.80	*6454	2.60	44.69	
*042	*333	15	1.92	1.47	15.40	*5504	5.63	5.83	6.04	5.20	102	*7142	2.60	44.69
*042	*333	15	1.40	1.67	9.55	*4965	1.92	1.99	2.06	76.45	*8708	3.21	29.78	
*042	*333	15	2.26	2.50	19.04	*5702	6.95	7.19	7.45	36.86	*5663	1.73	237.41	
*042	*333	15	2.26	2.50	19.04	*5702	6.95	7.19	7.45	36.86	*5663	4.81	12.08	
*042	*333	15	1.80	1.65	14.08	*7191	6.46	6.46	6.46	6.46	48.12	*6418	2.42	34.30
*042	*333	15	2.58	4.43	22.37	*6222	5.94	6.36	7.92	38.34	*5891	*452	-36.84	
*042	*333	15	2.25	1.18	19.04	*6816	5.44	6.29	7.25	37.88	*6178	3.76	27.30	
*042	*333	15	1.84	1.68	14.52	*7267	4.19	4.84	5.58	56.63	*7007	2.26	58.81	
*042	*333	15	2.28	1.36	19.25	*5170	3.64	4.20	4.95	56.99	*7421	-1.37	3.24	
*042	*333	15	2.12	1.45	17.55	*5492	4.68	5.40	6.24	64.19	*6884	3.50	25.24	
*042	*333	15	1.92	1.40	15.40	*5724	3.69	4.26	4.92	55.94	*7539	1.62	-3.22	
*042	*333	15	1.36	1.63	9.55	*4782	1.70	1.96	2.26	84.19	*8751	3.32	17.37	
*042	*333	15	2.16	1.30	17.98	*6889	2.42	2.79	3.22	64.59	*9846	2.89	30.37	
*042	*333	15	2.00	1.34	16.26	*4043	3.22	3.71	4.20	68.60	*8332	1.89	7.00	
*042	*333	15	1.84	1.68	14.52	*7267	4.19	4.84	5.58	56.63	*7007	2.26	58.81	
*042	*333	15	1.98	2.07	15.83	*2460	1.22	1.41	1.62	82.60	*11516	3.01	-13.56	
*042	*333	15	1.58	2.62	11.61	*2425	1.11	1.29	1.48	66.70	*11504	2.84	2.20	
*042	*333	15	1.30	1.33	8.40	*2039	1.28	1.48	1.71	90.03	*9734	2.67	16.12	
*042	*333	15	2.00	1.30	17.98	*6889	2.42	2.79	3.22	64.59	*9846	2.89	30.37	
*042	*333	15	1.84	1.68	14.52	*7267	4.19	4.84	5.58	56.63	*7007	2.26	58.81	
*042	*333	15	1.74	2.33	13.41	*2458	1.05	1.24	1.43	81.76	*8194	2.63	7.33	
*042	*333	15	1.20	1.35	7.26	*1669	1.51	1.74	1.98	84.16	*11449	3.23	17.04	
*042	*333	15	1.74	2.33	13.41	*2458	1.05	1.24	1.43	81.76	*8194	2.63	7.33	
*042	*333	15	1.34	1.37	8.86	*2105	1.72	1.89	2.11	92.71	*11084	2.97	16.98	
*042	*333	15	1.24	1.64	7.72	*1831	1.42	1.61	1.83	107.22	*14053	2.59	30.37	
*042	*333	15	2.24	3.09	18.83	*4040	1.41	1.59	1.83	106.52	*23445	2.49	27.40	
*042	*333	15	2.04	1.35	16.70	*1120	1.67	2.36	2.81	72.85	*9756	3.52	12.48	
*042	*333	15	2.04	1.35	16.70	*1120	1.67	2.36	2.81	72.85	*9756	3.47	25.29	
*042	*333	45	1.72	1.39	13.19	*4083	1.19	1.68	2.37	89.30	*10331	2.66	18.07	
*042	*333	45	1.32	1.54	9.63	*3514	1.59	1.83	1.18	93.42	*12294	3.07	20.02	
*042	*333	45	2.32	1.05	19.67	*5402	2.15	3.04	4.30	64.75	*8333	2.17	23.03	
*042	*333	45	1.18	1.26	18.19	*5886	2.00	2.83	4.10	67.59	*8005	2.55	27.76	
*042	*333	45	1.94	1.94	15.61	*5921	2.00	2.83	4.10	67.59	*8005	2.55	27.76	
*042	*333	45	1.42	1.60	9.78	*5178	1.06	1.43	2.00	122	*8551	1.0094	3.20	19.80
*042	*333	45	2.18	1.82	18.19	*6074	1.15	1.46	1.67	23.55	*7181	2.08	3.90	
*042	*333	45	1.52	1.79	10.93	*6420	1.08	1.52	2.16	82.31	*1.0092	3.35	13.83	
*042	*333	45	2.50	1.40	11.64	*5560	1.45	2.90	5.80	86.95	*8696	6.13	45.91	
*042	*333	45	2.10	1.74	17.34	*5940	0.11	1.82	1.64	119.75	*1.8713	3.97	53.60	
*042	*333	45	1.42	1.76	7.78	*5373	1.41	1.15	2.30	44.59	95.55	*9861	5.89	52.96
*042	*333	45	2.18	1.16	18.19	*5348	1.00	1.41	1.80	51.21	90.20	*9583	5.62	46.52
*042	*333	45	1.46	1.65	10.24	*5261	1.38	1.70	3.40	90.75	*9583	5.62	46.52	
*042	*333	45	2.34	2.98	19.68	*1863	1.90	1.77	1.54	114.24	*2.1749	6.07	52.30	
*042	*333	45	2.10	1.32	17.34	*4039	1.97	1.94	3.38	98.32	*1.0913	4.00	98.14	
*042	*333	45	1.82	1.71	14.30	*4153	1.60	1.40	2.39	117.04	*1.4973	5.07	88.98	
*042	*333	45	1.37	1.45	8.33	*4187	1.40	1.77	3.59	117.55	*1.9385	3.14	75.41	
*042	*333	45	1.14	1.44	17.68	*2152	1.88	1.77	3.59	117.55	*1.9385	3.14	75.41	
*042	*333	45	1.42	1.16	14.30	*2197	1.06	2.12	4.24	121.09	*8532	4.40	172.34	
*042	*333	45	1.62	1.02	10.93	*2237	1.40	1.41	3.78	175.18	*9833	3.10	132.45	
*042	*333	45	1.24	1.35	7.72	*1545	1.57	1.15	2.29	119.96	*1.1699	2.49	116.53	

APPENDIX G

TABULATED HORIZONTAL FORCE DATA  
FROM TWO-DIMENSIONAL EXPERIMENTS

CLER	DIA	ANG	T	H	L	UMAX	CMH	CDH	FAVG
*021	*333	0	1.25	366	7.47	3579	3.23	9.30	-0.40139
*001	*333	0	1.25	272	7.37	2623	3.04	12.50	-0.32582
*001	*333	0	1.49	341	9.77	4323	3.13	6.77	-0.061342
*001	*333	0	1.47	254	9.58	3168	2.97	7.08	-0.025974
*001	*333	0	1.86	231	13.16	3529	3.26	5.53	-0.31721
*001	*333	0	1.82	154	12.80	2329	3.08	11.80	-0.10542
*01	*333	0	2.25	199	16.59	3345	3.18	4.15	-0.155226
*001	*333	0	2.22	121	16.33	2032	3.11	6.82	-0.170550
*001	*333	0	2.56	180	19.24	3169	3.12	2.82	-0.162336
*031	*333	0	2.50	108	18.74	1882	3.30	6.05	-0.026190
*005	*333	0	1.24	277	7.37	2672	2.91	12.73	-0.028429
*005	*333	0	1.25	379	7.47	3708	3.07	8.44	-0.029782
*005	*333	0	1.51	332	9.95	4272	3.07	0.95	-0.579994
*005	*333	0	1.49	245	9.77	3105	2.98	7.29	-0.026295
*005	*333	0	1.47	236	13.25	3419	3.30	4.93	-0.34043
*005	*333	0	1.87	154	13.25	2365	3.20	9.32	-0.024890
*025	*333	0	2.25	200	16.69	3367	3.10	5.25	-0.021022
*005	*333	0	2.24	120	16.50	2026	3.09	7.84	-0.104462
*005	*333	0	2.57	173	19.34	3040	3.11	4.91	-0.029217
*005	*333	0	2.56	114	19.26	1995	3.03	4.33	-0.144776
*010	*333	0	1.25	382	7.47	3741	2.81	7.84	-0.052314
*010	*333	0	1.23	270	7.28	2541	2.68	13.59	-0.018002
*010	*333	0	1.50	341	9.85	4354	2.61	7.63	-0.027555
*010	*333	0	1.48	243	9.67	3063	2.73	6.97	-0.021852
*010	*333	0	1.83	237	12.89	3584	2.89	7.71	-0.024153
*010	*333	0	1.82	161	12.80	2438	2.66	7.62	-0.129485
*010	*333	0	2.26	197	18.68	3321	3.14	8.30	-0.02481
*010	*333	0	2.58	174	19.43	3082	2.95	4.18	-0.020582
*016	*333	0	1.25	391	7.47	3832	2.80	6.75	-0.058444
*016	*333	0	1.24	278	7.37	2687	2.40	9.08	-0.158226
*016	*333	0	1.49	332	9.77	4210	2.57	7.09	-0.30375
*016	*333	0	1.47	240	9.58	2924	2.83	7.29	-0.025250
*016	*333	0	1.85	246	13.07	3750	2.70	3.88	-0.11948
*016	*333	0	1.83	155	12.89	2356	2.69	8.18	-0.195500
*016	*333	0	2.26	195	18.68	3347	2.80	5.01	-0.125224
*016	*333	0	2.56	180	19.26	3165	2.71	3.25	-0.140055
*016	*333	0	2.55	111	19.17	1940	2.55	6.45	-0.111226
*021	*333	0	1.24	372	7.37	3557	2.57	6.85	-0.36861
*021	*333	0	1.22	271	7.18	2534	2.17	10.34	-0.020785
*021	*333	0	1.50	329	9.86	4213	2.48	5.73	-0.30647
*021	*333	0	1.45	238	9.39	2927	2.58	6.03	-0.025318
*021	*333	0	1.84	250	13.98	3601	2.41	3.06	-0.029043
*021	*333	0	1.81	159	12.71	2401	2.56	5.85	-0.028431
*021	*333	0	2.25	198	18.59	3336	2.50	4.88	-0.152121
*021	*333	0	2.11	170	18.63	2966	2.70	5.45	-0.020077
*021	*333	0	2.55	112	19.17	1970	2.45	3.72	-0.135224
*031	*333	0	1.25	382	7.47	3782	2.23	4.00	-0.33437
*031	*333	0	1.23	268	7.28	2576	2.23	7.88	-0.021391
*031	*333	0	1.50	327	9.86	4204	2.19	4.23	-0.33330
*031	*333	0	1.48	245	9.87	3104	2.12	3.44	-0.192250
*031	*333	0	1.85	228	13.07	3489	2.32	2.40	-0.352527

*031	*333	0	1.50	158	12.82	2381	2.25	3.85	-0.022253
*031	*333	0	2.24	124	16.50	2088	2.17	2.40	-0.022005
*031	*333	0	2.24	124	16.50	2088	2.24	3.03	-0.107050
*031	*333	0	2.56	174	19.26	3093	2.21	1.88	-0.021499
*17	*333	0	1.24	385	7.37	3824	2.4	4.52	-0.16353
*167	*333	0	1.23	269	7.28	2632	2.16	7.70	-0.027366
*147	*333	0	1.51	314	9.95	4107	2.18	3.77	-0.029137
*157	*333	0	1.49	238	9.77	3623	2.12	4.72	-0.023058
*157	*333	0	1.85	235	13.07	3623	2.30	2.04	-0.30318
*157	*333	0	1.54	148	12.98	2277	2.26	3.78	-0.009391
*157	*333	0	2.25	193	16.50	3264	2.18	1.88	-0.178005
*157	*333	0	2.22	124	16.33	2094	2.17	1.37	-0.006528
*157	*333	0	2.55	175	19.17	3081	2.14	1.49	-0.10830
*147	*333	0	2.56	111	19.26	1951	2.20	1.77	-0.112886
*01	*333	0	9.4	712	4.49	0891	2.94	28.61	-0.00608
*01	*333	0	9.6	241	4.68	1108	2.87	34.50	-0.023344
*005	*333	0	9.5	218	4.59	0962	2.87	27.72	-0.111029
*005	*333	0	9.5	250	4.59	1101	2.95	25.24	-0.021214
*010	*333	0	9.5	213	4.59	0940	2.49	31.52	-0.047255
*010	*333	0	9.5	250	4.59	1103	2.63	23.85	-0.10414
*01	*333	0	9.5	219	4.59	0970	2.30	28.27	-0.008339
*C16	*333	0	9.5	251	4.59	1111	2.54	23.00	-0.11360
*021	*333	0	9.4	210	4.49	0892	2.39	28.91	-0.18517
*C21	*333	0	9.4	252	4.49	1059	2.42	31.69	-0.18473
*031	*333	0	9.4	207	4.49	0890	2.24	21.48	-0.026694
*033	*333	0	9.5	246	4.59	1117	2.15	19.89	-0.026303
*147	*333	0	9.5	208	4.59	0940	2.05	19.43	-0.008509
*147	*333	0	9.5	242	4.59	1150	1.95	23.69	-0.003568



Bowie, George L.  
Forces exerted by waves on a pipeline at or near the ocean bottom /  
by George L. Bowie. - Fort Belvoir, Va. : U.S. Coastal Engineering  
Research Center ; Springfield, Va. : available from National Tech-  
nical Information Service, 1977.

177 p. : ill. (Technical paper - U.S. Coastal Engineering Research  
Center ; no. 77-11) Also (Contract - U.S. Coastal Engineering Research  
Center ; DACW72-74-C-0004)

Bibliography: p. 123.

This report presents an analysis of wave-induced forces on a sub-  
marine pipeline near the ocean floor. The wave-induced forces consist  
of several components-inertial forces, drag forces, lift forces, and  
under some conditions, eddy-induced forces.

1. Wave forces. 2. Underwater pipelines. I. Title. II. Series:  
U.S. Coastal Engineering Research Center. Technical paper no. 77-11)  
III. Series: U.S. Coastal Engineering Research Center. Contract  
DACW72-74-C-0004.

TC203

.U581tp

no. 77-11

627

Bowie, George L.

Forces exerted by waves on a pipeline at or near the ocean bottom /  
by George L. Bowie. - Fort Belvoir, Va. : U.S. Coastal Engineering  
Research Center ; Springfield, Va. : available from National Tech-  
nical Information Service, 1977.

177 p. : ill. (Technical paper - U.S. Coastal Engineering Research  
Center ; no. 77-11) Also (Contract - U.S. Coastal Engineering Research  
Center ; DACW72-74-C-0004)

Bibliography: p. 123.

This report presents an analysis of wave-induced forces on a sub-  
marine pipeline near the ocean floor. The wave-induced forces consist  
of several components-inertial forces, drag forces, lift forces, and  
under some conditions, eddy-induced forces.

1. Wave forces. 2. Underwater pipelines. I. Title. II. Series:  
U.S. Coastal Engineering Research Center. Technical paper no. 77-11)  
III. Series: U.S. Coastal Engineering Research Center. Contract  
DACW72-74-C-0004.

TC203

.U581tp

no. 77-11

627

Bowie, George L.  
Forces exerted by waves on a pipeline at or near the ocean bottom /  
by George L. Bowie. - Fort Belvoir, Va. : U.S. Coastal Engineering  
Research Center ; Springfield, Va. : available from National Tech-  
nical Information Service, 1977.

177 p. : ill. (Technical paper - U.S. Coastal Engineering Research  
Center ; no. 77-11) Also (Contract - U.S. Coastal Engineering Research  
Center ; DACW72-74-C-0004)

Bibliography: p. 123.

This report presents an analysis of wave-induced forces on a sub-  
marine pipeline near the ocean floor. The wave-induced forces consist  
of several components-inertial forces, drag forces, lift forces, and  
under some conditions, eddy-induced forces.

1. Wave forces. 2. Underwater pipelines. I. Title. II. Series:  
U.S. Coastal Engineering Research Center. Technical paper no. 77-11)  
III. Series: U.S. Coastal Engineering Research Center. Contract  
DACW72-74-C-0004.

TC203

.U581tp

no. 77-11

627

Bowie, George L.

Forces exerted by waves on a pipeline at or near the ocean bottom /  
by George L. Bowie. - Fort Belvoir, Va. : U.S. Coastal Engineering  
Research Center ; Springfield, Va. : available from National Tech-  
nical Information Service, 1977.

177 p. : ill. (Technical paper - U.S. Coastal Engineering Research  
Center ; no. 77-11) Also (Contract - U.S. Coastal Engineering Research  
Center ; DACW72-74-C-0004)

Bibliography: p. 123.

This report presents an analysis of wave-induced forces on a sub-  
marine pipeline near the ocean floor. The wave-induced forces consist  
of several components-inertial forces, drag forces, lift forces, and  
under some conditions, eddy-induced forces.

1. Wave forces. 2. Underwater pipelines. I. Title. II. Series:  
U.S. Coastal Engineering Research Center. Technical paper no. 77-11)  
III. Series: U.S. Coastal Engineering Research Center. Contract  
DACW72-74-C-0004.

TC203

.U581tp

no. 77-11

627



Bowie, George L.  
 Forces exerted by waves on a pipeline at or near the ocean bottom /  
 by George L. Bowie. - Fort Belvoir, Va. : U.S. Coastal Engineering  
 Research Center ; Springfield, Va. : available from National Tech-  
 nical Information Service, 1977.  
 177 p. : ill. (Technical paper - U.S. Coastal Engineering Research  
 Center ; no. 77-11) Also (Contract - U.S. Coastal Engineering Research  
 Center ; DACM72-74-C-0004)  
 Bibliography: p. 123.  
 This report presents an analysis of wave-induced forces on a sub-  
 marine pipeline near the ocean floor. The wave-induced forces consist  
 of several components--inertial forces, drag forces, lift forces, and  
 under some conditions, eddy-induced forces.  
 I. Wave forces. 2. Underwater pipelines. I. Title. II. Series:  
 U.S. Coastal Engineering Research Center. Technical paper no. 77-11)  
 III. Series: U.S. Coastal Engineering Research Center. Contract  
 DACM72-74-C-0004.

TC203 .U581tp no. 77-11 627

Bowie, George L.  
 Forces exerted by waves on a pipeline at or near the ocean bottom /  
 by George L. Bowie. - Fort Belvoir, Va. : U.S. Coastal Engineering  
 Research Center ; Springfield, Va. : available from National Tech-  
 nical Information Service, 1977.  
 177 p. : ill. (Technical paper - U.S. Coastal Engineering Research  
 Center ; no. 77-11) Also (Contract - U.S. Coastal Engineering Research  
 Center ; DACM72-74-C-0004)  
 Bibliography: p. 123.  
 This report presents an analysis of wave-induced forces on a sub-  
 marine pipeline near the ocean floor. The wave-induced forces consist  
 of several components--inertial forces, drag forces, lift forces, and  
 under some conditions, eddy-induced forces.  
 I. Wave forces. 2. Underwater pipelines. I. Title. II. Series:  
 U.S. Coastal Engineering Research Center. Technical paper no. 77-11)  
 III. Series: U.S. Coastal Engineering Research Center. Contract  
 DACM72-74-C-0004.

TC203 .U581tp no. 77-11 627

Bowie, George L.  
 Forces exerted by waves on a pipeline at or near the ocean bottom /  
 by George L. Bowie. - Fort Belvoir, Va. : U.S. Coastal Engineering  
 Research Center ; Springfield, Va. : available from National Tech-  
 nical Information Service, 1977.  
 177 p. : ill. (Technical paper - U.S. Coastal Engineering Research  
 Center ; no. 77-11) Also (Contract - U.S. Coastal Engineering Research  
 Center ; DACM72-74-C-0004)  
 Bibliography: p. 123.  
 This report presents an analysis of wave-induced forces on a sub-  
 marine pipeline near the ocean floor. The wave-induced forces consist  
 of several components--inertial forces, drag forces, lift forces, and  
 under some conditions, eddy-induced forces.  
 I. Wave forces. 2. Underwater pipelines. I. Title. II. Series:  
 U.S. Coastal Engineering Research Center. Technical paper no. 77-11)  
 III. Series: U.S. Coastal Engineering Research Center. Contract  
 DACM72-74-C-0004.

TC203 .U581tp no. 77-11 627

Bowie, George L.  
 Forces exerted by waves on a pipeline at or near the ocean bottom /  
 by George L. Bowie. - Fort Belvoir, Va. : U.S. Coastal Engineering  
 Research Center ; Springfield, Va. : available from National Tech-  
 nical Information Service, 1977.  
 177 p. : ill. (Technical paper - U.S. Coastal Engineering Research  
 Center ; no. 77-11) Also (Contract - U.S. Coastal Engineering Research  
 Center ; DACM72-74-C-0004)  
 Bibliography: p. 123.  
 This report presents an analysis of wave-induced forces on a sub-  
 marine pipeline near the ocean floor. The wave-induced forces consist  
 of several components--inertial forces, drag forces, lift forces, and  
 under some conditions, eddy-induced forces.  
 I. Wave forces. 2. Underwater pipelines. I. Title. II. Series:  
 U.S. Coastal Engineering Research Center. Technical paper no. 77-11)  
 III. Series: U.S. Coastal Engineering Research Center. Contract  
 DACM72-74-C-0004.

TC203 .U581tp no. 77-11 627







